Master's thesis

NTNU
Norwegian University of Science and Technology
Faculty of Natural Sciences
Department of Chemical Engineering

Ine Mariell Fagerbakk Haugli

Reactivity of silicomanganese slag towards cabon materials

A comparison of coke and charcoal as reducing agents

Master's thesis in Chemical Engineering
Supervisor: Magnus Rønning, Merete Tangstad and Leif Storlien
June 2019

NTNU
Norwegian University of
Science and Technology

Ine Mariell Fagerbakk Haugli

Reactivity of silicomanganese slag towards cabon materials

A comparison of coke and charcoal as reducing agents

Master's thesis in Chemical Engineering
Supervisor: Magnus Rønning, Merete Tangstad and Leif Storlien
June 2019

Norwegian University of Science and Technology
Faculty of Natural Sciences
Department of Chemical Engineering

NTNU
Norwegian University of
Science and Technology

Abstract

Silicomanganese is produced by carbothermic reduction with coke as a reducing agent. While coke is made from coal and is a fossil carbon source, charcoal is made from biocarbon, usually wood, and is a renewable carbon source that does not emit any excess CO_2 when used for metal production. If the coke could be substituted with charcoal, the emissions of CO_2 from silicomanganese production would be significantly reduced. This project therefore compares coke and charcoal as reducing agents for silicomanganese.

Two synthetic silicomanganese slags, where slag 2 had higher content of manganese oxide and silicon oxide than slag 1, were tested towards an industrial coke and a charcoal made from hardwood in a sessile drop furnace. The tests were performed in CO atmosphere at 1600°C, and with reduction times of 5, 15 and 30 minutes. In total 22 tests were performed, where the two slags were tested with both carbon materials at all three reduction times. Pictures captured from the furnace were analysed to find the development of contact angle and relative volume during tests. The samples were weighed and casted in epoxy after the tests, before being analysed by SEM and EPMA to find chemical composition of slag and metal. The manganese oxide content of the slag, the calculated silicon content of the metal and the calculated reduction degrees for manganese and silicon were assessed for all tests.

The results showed that the tests run with charcoal had better wetting of both slags, and higher decrease in relative volume for both slags than tests run with coke. The results also showed that the content of manganese oxide in the slag was higher for tests run with charcoal than for tests run with coke, and that the silicon content in the metal was generally higher for tests run with charcoal than for tests run with coke. The silicon content was a bit higher for tests run with slag 2 than for tests run with slag 1. Further, the reduction degrees of manganese and silicon were higher for tests run with charcoal than for tests run with coke.

The main conclusions were that the silicon content in the metal did not reach the desired 18% in any of the tests, and that charcoal was a better reducing agent than coke.

Sammendrag

Silikomangan produseres ved karbotermisk reduksjon med koks som reduksjonsmiddel. Mens koks er laget av kull og er en fossil karbonkilde, er trekull laget av trær og er en fornybar karbonkilde som ikke slipper ut ekstra CO_2 når den brukes til metallproduksjon. Dersom koks kan byttes ut med trekull vil utslippene av CO_2 fra produksjon av silikomangan reduseres betydelig. I denne oppgaven sammenlignes derfor koks og trekull som reduksjonsmiddel for silikomangan.

To syntetiske silikomangan-slagger, hvor den ene hadde et høyere innhold av manganoksid og silisiumoksid enn den andre, ble testet mot en industriell koks og trekull av løvtre i en fuktningsovn. Testene ble utført i CO-gass med ovnstemperatur på 1600°C, og hadde varigheter på 5, 15 og 30 minutter. Totalt 22 tester ble utført, og de to slaggene ble testet med begge karbonmaterialene og med alle tre varighetene. Bilder tatt i ovnen under testene ble brukt til å finne endring i volumet av slaggdråpen, og utviklingen kontaktvinkelen hadde i løpet av testene. Prøvene ble veid og støpt inn i epoxy etter testene, før de ble analysert i elektronmikroskop og mikrosonde for å finne sammensetningen av slagg og metall. Innholdet av manganoksid i slaggen, beregnet innhold av silisium i metallet, og beregnede reduksjonsgrader for mangan og silisium ble vurdert for alle tester.

Resultatene viste at testene med trekull hadde bedre fukting og høyere endring i relativt volum med begge slaggene enn testene med koks. Resultatene viste også at innholdet av manganoksid var lavere for tester med trekull enn for tester med koks, og at silisiuminnholdet i metallet var høyere for tester med trekull enn for tester med koks. Innholdet av silisium var noe høyere for tester med slagg 2 enn tester med slagg 1. Videre viste resultatene at reduksjonsgradene for både mangan og silisium var høyere når trekull ble brukt enn når koks ble brukt.

Hovedkonklusjonene er at innholdet av silisium i metallet var lavere enn de ønskede 18% i alle tester, og at trekull var et bedre reduksjonsmiddel enn koks.

Acknowledgements

I would like to express great appreciation to professor Merete Tangstad, who gave me the opportunity to write my master thesis and specialisation project in her research group at the Department of Materials Science and Engineering. This allowed me to work further with metal production and manganese ferroalloys, which I developed an interest in while working on my bachelor thesis in the spring of 2016.

I would further offer my thanks to my supervisors; Leif Sigurd Storlien, Merete Tangstad and Magnus Rønning for their patient guidance, useful feedback and advice during the work with this thesis. I would also like to thank Sarina Bao, Berit Vinje Kramer and Yingda Yu for giving me guidance in safe operation of the equipment I have used, and for offering assistance when issues occurred during the project.

Finally, I would like to thank my family and my fiancé for their endless support and encouragement during all my years as a student, and especially during the work with this master thesis.

Table of contents

Figures

Tables

Introduction

The general focus on environment and reducing the impacts on the climate from human activities is increasing. An example of this is the Sustainable Development Goals set forward by the European Commission in 2015. This includes 17 goals and 169 associated targets for more sustainable development [1]. Goals 12 (Responsible consumption and production) and 13 (Climate action) are the goals that are most relevant for the Norwegian metal production and processing industry. Another example of increasing focus on the climate is the Paris agreement from 2015, where 195 countries adopted an agreement and a global action plan to limit the global warming to 2°C in order to avoid dangerous climate change [2]. Along with the European Commission, Norway has set a goal to reduce the emissions by 40% compared to the emissions in 1990, by 2030 [3].

A big part of the norwegian emissions is from the industries, and from the metal production and processing industry. For the norwegian emissions to decrease, this industry needs to contribute by reducing their emissions. In the production of manganese ferroalloys in Norway, fossil coke is used for thermal reduction of manganese in electrical furnaces, which results in large emissions of CO_2. In order to reduce these emissions and attempt to meet the reduction goals set by the Norwegian Government, green carbon materials that are not from fossil sources needs to be introduced to the production. Charcoal is made from non-fossil sources like wood adn is CO_2 neutral, as it emits no excess CO_2 when used in metal production. If the coke used in today's production of manganese ferroalloys can be substituted with charcoal, the emissions of CO_2 will be significantly reduced.

The main objective of this thesis is to compare the reactivity of silicomanganese slag towards coke with the reactivity towards charcoal, and thus get more information about the ability charcoal has of reducing manganese oxide and silicon oxide from silicomanganese slag. Comparing the content of silicon in the metal that is produced by the two slags with charcoal and coke is also an objective, to see if a standard silicomanganese alloy can be produced under these conditions. The overall goal is to gain some knowledge of the interaction between charcoal and silicomanganese slag, and in that way contribute to the comprehensive research puzzle that needs to be solved in order to hopefully substitute coke with charcoal in the production of manganese ferroalloys.

1. Production of silicomanganese

This chapter gives an introduction to manganese ferroalloys and production of silicomanganese, in addition to the carbon materials coke and charcoal.

1.1 Manganese and manganese ferroalloys

1.1.1 Manganese

Manganese is a metal, element number 25 in the periodic table, is solid in room temperature and has a melting temperature of 1245°C [4]. It is the fifth most abundant metal in earth's crust and is rare in pure form in nature, but is found as manganese oxides and manganese carbonates in ores and minerals. Manganese metal is very brittle, and is therefore not very useful as a pure metal, but is useful in steel as it can eliminate the effect of sulphur by combining with it, and it is useful in aluminium as it can decrease corrosion [4]. The most common use of manganese is as an alloying element in steel, as it increases the strength, toughness and hardness of steel. About 90% of the manganese that is produced is produced as manganese ferroalloys and is used by the steel industry. The rest is produced as manganese dioxide which can be used in dry cell batteries, and as manganese metal which can be used as an alloying element in production of aluminium and copper [5].

1.1.2 Manganese ferroalloys

Manganese ferroalloys are alloys that contains mainly manganese and iron, in addition to silicon and carbon. The alloys are first divided into groups based on the silicon content, where ferromanganese contains small amounts of silicon, and silicomanganese contains 17-20 percent of silicon. The alloys are further divided based on the carbon content. High carbon ferromanganese (HC FeMn) contains about 7 percent carbon, medium carbon ferromanganese (MC FeMn) contains 1-2 percent carbon, while low carbon ferromanganese (LC FeMn) contains less than 0,5 percent carbon. Standard silicomanganese (SiMn) contains 1,5-2 percent carbon while low carbon silicomanganese (LC SiMn) contains 0,05-0,5 percent carbon. Figure 1.1 shows an overview of the different manganese ferroalloys [5].

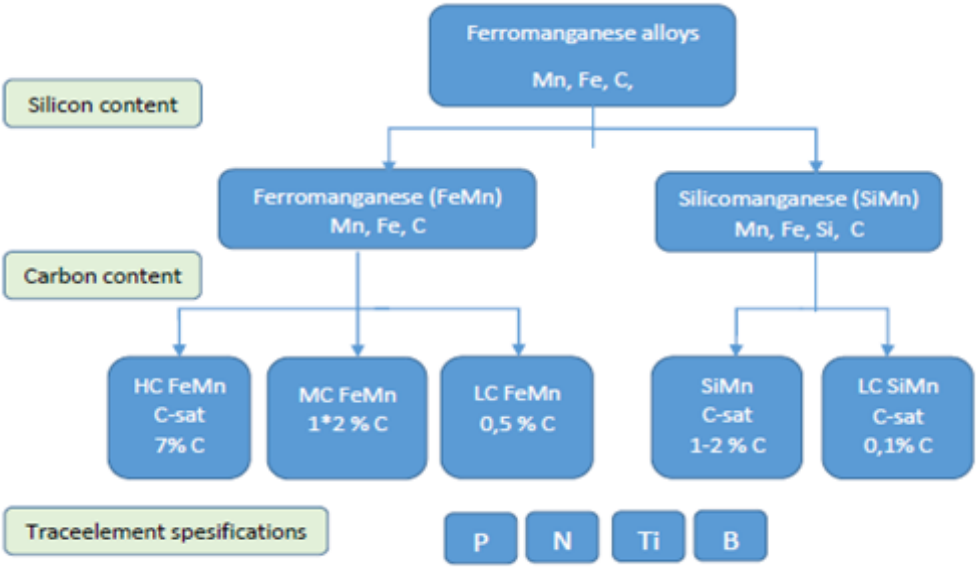

Figure 1.1: Overview of manganese ferroalloys [5]

1.2 Production of manganese ferroalloys

1.2.1 Raw materials

The raw materials needed to produce manganese ferroalloys are manganese ores, a carbon reducing agent, additives, and if silicomanganese is to be produced, quartz. There is usually a close sizing control of the raw materials to ensure good permeability permitting a good gas flow giving a smooth and efficient operation in the furnace. Fines are unwanted, as they lead to higher energy consumption, dust losses and low productivity [6].

Manganese ores are the main manganese source and an important raw material. The ores contain different manganese oxides, the main oxides are MnO, MnO_2, Mn_2O_3 and Mn_3O_4. In addition, the ores contain varying amounts of other oxides whereas the most important are iron oxide, silicon oxide, aluminum oxide, calcium oxide and magnesium oxide. The ores also contain several minor elements. Ores are divided into different types based on the manganese content. Metallurgical ores have more than 35 percent and up to 50 percent manganese, ferruginous ores have 15 to 35 percent manganese, while manganinferous ores are iron ores that contain 5-10 percent manganese [6]. The main producers of manganese ores are China, Africa, Australia, Brazil and Gabon. There are also found nodules on the ocean floor containing up to 24 percent manganese [4]. Metallurgical ores are used in production of manganese ferroalloys, and the Mn/Fe ratio is an important parameter, in addition to number of volatiles and excess oxygen. Phosphorous is unwanted in manganese ferroalloys due to the negative effect phosphorus have on steel, and ores that contain less than 0,1 percent phosphorus are marked high-grade.

Slag from ferromanganese production can be used as a manganese source in production of silicomanganese, as the slag is rich in MnO and contains 35-40 percent [7]. This is common for plants that produce both ferromanganese and silicomanganese. Using ferromanganese slag as a raw material also introduces less phosphorus to the silicomanganese, as the phosphorus enters the metal instead of the slag in the ferromanganese production. The main components of the ferromanganese slag in addition to MnO are the oxides SiO_2, CaO, MgO and Al_2O_3. There are also some minor components like K_2O, Na_2O, TiO_2 and ZnO. Slag from silicomanganese production has a rather low MnO content, 5-10 percent, and is not remelted but can rather be sold for usages as e.g. filler material [7].

A reducing agent in the form of a carbon material needs to be present in order to produce manganese ferroalloys. Norwegian producers use metallurgical coke as a reducing agent, but producers elsewhere in the world has used or are using other carbon sources such as anthracite and charcoal. The carbon material is responsible for reducing the oxides in the raw materials, both solid carbon and gaseous carbon monoxide are reductants of importance in the production.

When producing silicomanganese, a silicon oxide containing raw material is necessary to get enough silicon in the production. Quartz is used for this purpose, and it contains mainly SiO_2 and a small amount of other oxides.

In addition to these raw materials, additives can be used in the production. Dolomite ($CaMg(CO_3)_2$) and limestone ($CaCO_3$) are commonly used as basic fluxes to give the slag suitable chemical properties, to ensure good furnace operation and a high manganese yield.

1.1.2 Production of Silicomanganese

In this project, silicomanganese slag is used and the production process will therefore be described for silicomanganese. Production of ferromanganese is similar, but the furnace temperature is lower, about 1400°C, and the production does not need quartz as a raw material. Ferromanganese can be produced in a blast furnace, but silicomanganese cannot because of the high temperature required, and they are therefore not so common to use.

1.1.2.1 Electric arc furnace

Silicomanganese is produced in an submerged arc furnace. This furnace can produce both silicomanganese and ferromanganese, at temperatures of 1600°C and 1400°C respectively. A submerged arc furnace is normally circular with diameters up to 16 meters and heights up to 8 meters [5], see figure 1.2. The furnace consists of a steel shell with lining material on the inside. There are two concepts of lining, the lining material can either have low or high heat conductivity, which causes the lining to have high or low temperature, respectively. The first concept causes the lining to have high inner temperature, and keeps the heat inside the furnace. The second is called freeze lining, as the low temperature of the lining causes slag to freeze at the lining and protect the furnace walls from high temperatures. The lifespan of the lining affects the furnace performance, as a bad refractory can lead to burnouts with costly repairs, downtime and loss of production. It is common to use chamotte (Al_2O_3) in the sides and carbon blocks in the bottom as lining material [6]. There is often a layer of refractory brickwork in addition to the lining on the inside of the furnace. All Norwegian furnaces are closed with a pressure-controlled lid, and all off-gases and dust from the furnace are collected and treated. The raw materials enter the furnace through hoops in the hood, usually placed around each electrode. The furnace has a tap hole where the metal and slag is tapped, and are separated after tapping. If the furnace has two tap holes, the tapping can be alternated between them, to decrease the wear of the tap hole. This also makes maintenance and repairs of one of the tap holes easier.

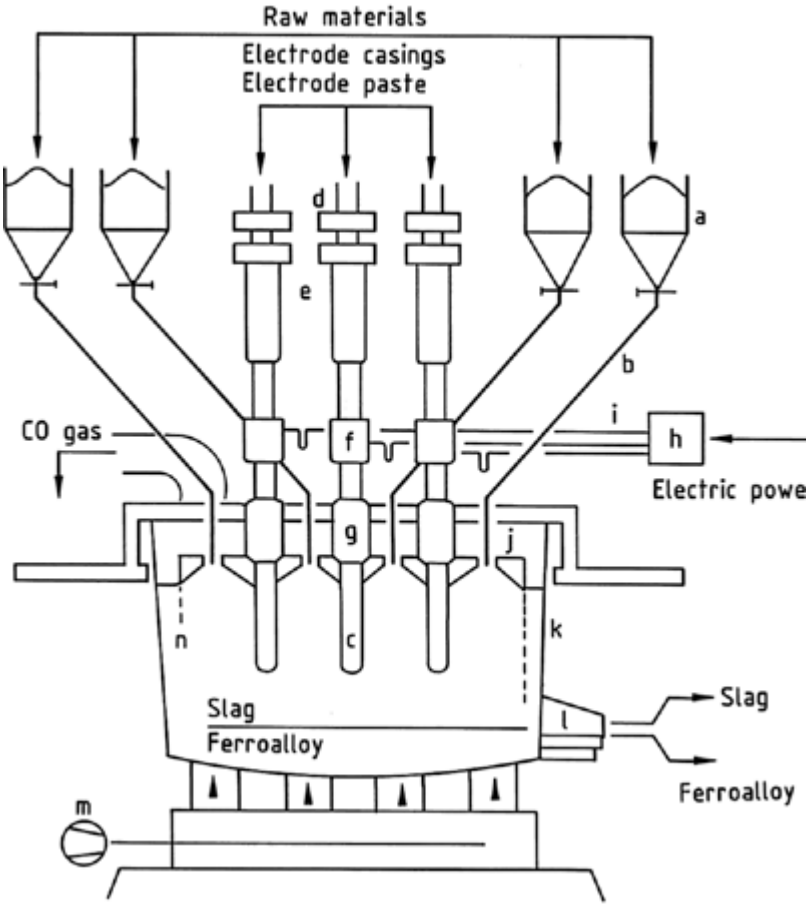

Figure 1.2: Schematic of a submerged arc furnace [8] a: Charging bins; b: Charging tubes; c: Electrodes; d: Electrode slipping device; e: Electrode positioning device; f: Current transmission to electrodes; g: Electrodes sealing; h: Furnace Transformer; i: Current bus bar system; j: Furnace cover; k: Furnace shell; l: Tap hole; m: Furnace bottom cooling; n: Refractory material

The submerged arc furnace usually has three electrodes, placed in a triangle evenly distributed inside the furnace, as shown on figure 1.2. Sødeberg electrodes are commonly used, they are constantly baked as new electrode mass melts and is baked on its way down into the furnace. When the electrode enters the melt the electrode mass is solid, and the iron casing around it melts and enters the metal. Furnace capacity is measured by the electric power it uses. The furnaces in Norway are relatively large as they operate at 25-40 MW.

1.1.2.2 Zones in the furnace

The activity of the furnace is usually divided into two zones, the prereduction zone from the top of the furnace down to the melt, and the coke bed zone from the melt to the bottom of the furnace. Figure 1.3 shows a sketch of the area around an electrode, and lists the most important reactions in the furnace. The prereduction zone is above the green line and the cokebed zone is below the green line in figure 1.3. The black and red arrows indicate how the raw materials and off-gases move in the furnace, and that there is highest movement and activity close to the electrodes.

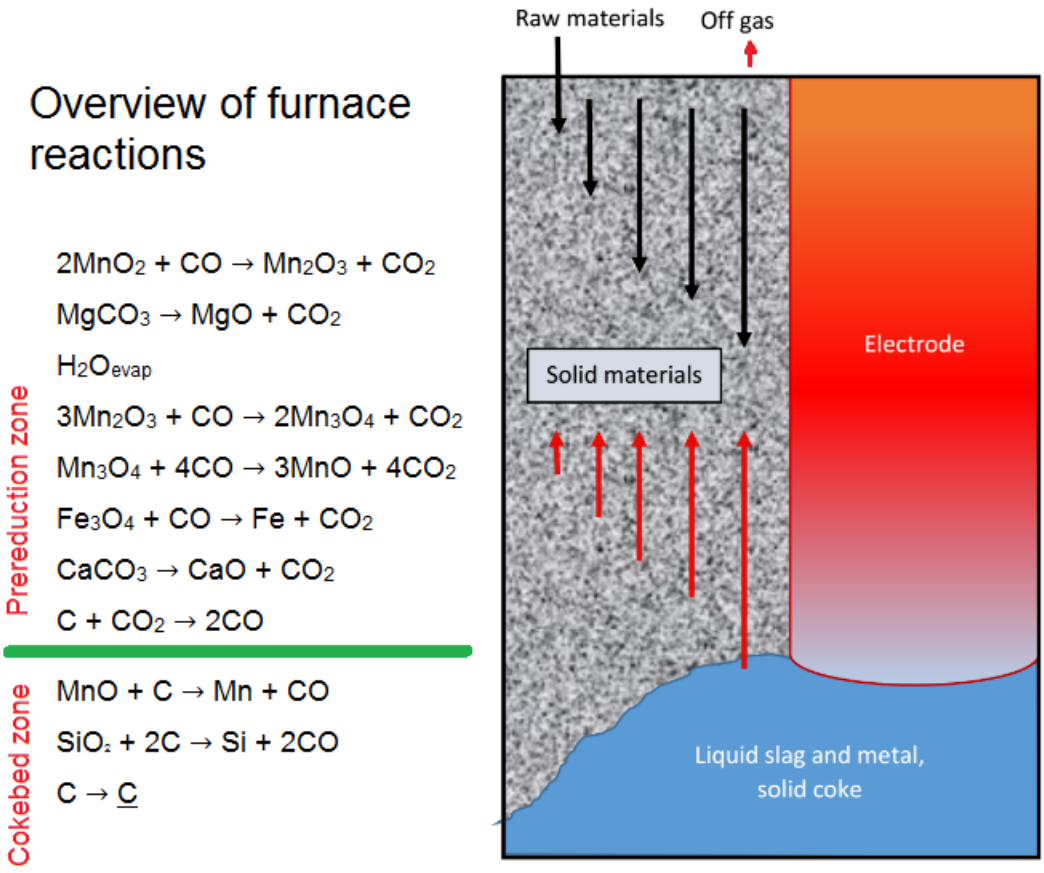

Figure 1.3: overview of furnace reactions

The raw materials enter at the top of the furnace, in the prereduction zone. Temperatures are here about 200°C. The most important reactions that occur in the prereduction zone are listed below, sorted by where the reactions occur in the prereduction zone, from top to bottom. As the raw materials move downwards in the furnace, they are heated by the off-gases that rise from the cokebed zone. This is mainly CO-gas, and as the raw materials are heated, the CO-gas also reduce higher oxides in the ores and the gas is converted to CO_2-gas, as equations 1.1 and 1.4-1.7 show. Moisture that may be in the raw materials evaporate to steam (equation 1.3), and iron oxides will reduce into metallic iron in the prereduction zone (equation 1.6). Near the coke bed, the Boudouard reaction will occur, where CO_2 reacts with carbon and produces CO (equation 1.8). At the bottom of the prereduction zone, at temperatures of about 1250°C, the remaining oxide mix from the raw materials starts to melt into a liquid slag.

$2MnO_2 + CO \rightarrow Mn_2O_3 + CO_2$	1.1
$MgCO_3 \rightarrow MgO + CO_2$	1.2
H_2O_{evap}	1.3
$3Mn_2O_3 + CO \rightarrow 2Mn_3O_4 + CO_2$	1.4
$Mn_3O_4 + CO \rightarrow 3MnO + CO_2$	1.5
$Fe_3O_4 + CO \rightarrow Fe + CO_2$	1.6
$CaCO_3 \rightarrow CaO + CO_2$	1.7
$C + CO_2 \rightarrow 2CO$	1.8

The cokebed zone is the high temperature area of the furnace, and the temperature is about 1600°C. There is liquid slag, liquid metal and solid carbon (coke) in this area, the metal is in the bottom of the furnace, while the slag and coke is a mixed layer above the metal, with some dry coke that makes the cokebed at the top of this zone. The cokebed is near and around the electrodes, and it is desired that the cokebed is bell shaped around each electrode for good electrode tip position. When the amount of coke in the furnace increase, the cokebed will get pointier, and when the amount of coke decrease in the furnace, the coke bed will get wider. Coke and slag is mixed in the furnace, but directly beneath the electrodes there is little coke and mostly slag.

The most important reactions that occur in the cokebed zone are listed below. At around 1400°C manganese oxide is reduced by solid carbon in the coke and some carbon in the electrode to manganese metal and CO-gas (equation 1.9). Manganese is also known to be reduced by metallic iron as shown in equation 1.10, before the produced iron oxide is reduced by solid carbon and produces iron and CO-gas as shown in equation 1.11. At around 1600°C silicon oxide is reduced by solid carbon to metallic silicon and CO-gas (equation 1.12). Some carbon also enters the metal, until the metal phase is saturated (equation 1.13). The activity in the cokebed zone is highest close to and around each electrode. All elements with lower melting temperatures, like phosphorus and iron will enter the metal phase. Elements with high melting temperatures, like calcium, magnesium, aluminium will stay in the slag phase as oxides. Silicon and Manganese will be divided between the metal phase as metallic Mn and metallic Si, and the slag phase as manganese oxide and silicon oxide.

$$MnO + C \rightarrow Mn + CO \quad (1.9)$$
$$MnO + Fe \rightarrow FeO + Mn \quad (1.10)$$
$$FeO + C \rightarrow Fe + CO \quad (1.11)$$
$$SiO_2 + 2C \rightarrow Si + 2CO \quad (1.12)$$
$$C \rightarrow \underline{C} \quad (1.13)$$

The distribution of manganese and silicon between the metal and slag phase depends on temperature and slag composition. The slag is a good source of information, as it contains everything that the metal does not contain. The main oxides in the slag are MnO, SiO_2, MgO, CaO and Al_2O_3. Of these, MnO, CaO and MgO are basic oxides which give oxygen ions to the slag and are network breaking, while SiO_2 and Al_2O_3 are acid oxides which take oxygen up from the slag and are network forming. Al_2O_3 can both give and take an oxygen ion and can therefore act as both an acid and a basic oxide. In silicomanganese production Al_2O_3 acts as an acidic oxide. Similar oxides enhance each other and increase the chemical activity, while different oxides weaken each other and decrease the chemical activity, as well as lowering the melting point of the slag. Basicity and lime basicity give the ratio of basic oxides over acid oxides and is given by equation 1.14 and 1.15 respectively [6].

$$B = (MgO + CaO)/(SiO_2 + Al_2O_3) \quad (1.14)$$
$$LB = (MgO + CaO)/SiO_2 \quad (1.15)$$

The manganese oxide content in the slag decrease with increasing lime basicity, which is desirable with regard to manganese yield. The R-ratio is given in equation 1.16 and describes the ratio between the acid and basic oxides that are considered to be irreducible during production. These oxides keep the same mutual ratio throughout reduction, and the R-ratio is therefore useful.

$$R = (MgO + CaO)/Al_2O_3 \quad 1.16$$

The viscosity in the slag increase when the amount of acid oxides increase. When the slag consists of more than 67 mole% basic oxides, hence low amount of acid oxides, the network in the slag will have broken down to only simple SiO_4^- anions. There is then few chains and little network in the slag, which gives low viscosity. If the slag contains less basic and more acid oxides, there will be longer chains of ions which forms a network, and higher viscosity.

Some properties of the slag that is important are viscosity, chemical equilibrium, liquidus composition and electrical resistivity. Studies found that the effect of temperature on the metal/slag equilibrium is relatively small, whereas the temperature plays an important role for the slag/metal/gas equilibrium. Increasing temperature shifts the equilibrium to lower contents of MnO in slag, which gives more manganese in the metal. Increasing slag basicity ratio and decreasing the CO partial pressure will also reduce the manganese oxide content in the slag considerably, and hence increasing the manganese content of the metal.

The furnace is regularly tapped, usually every 2-3 hours [6], and the metal and slag is usually tapped from the same tap hole and is separated after tapping. Most of the slag is separated from the metal during tapping, e.g. by using cascade tapping where the metal and slag is tapped in a ladle, and the slag flows into slag pots as the ladle is filled with metal since the metal is heavier than the slag. The remaining slag in the ladle after tapping can be removed by tilting the ladle to make it flow out, and mechanically by using a scrape. The metal can be refined after tapping, to fine-tune the composition of the metal by e.g. adding more silicon. The metal is then casted into a bed of fines, and the same is done with the slag. After cooling, the metal is crushed into appropriate size before it is stored and sold. The same is done with the slag.

1.1.3 Thermodynamics

In the previous chapters, the production of silicomanganese was described, and the equations of reactions occurring in the two zones of the furnace were listed. In this chapter, the thermodynamics of the process will be briefly described, and the most important phase diagrams that help describe the process will be shown.

Manganese forms stable carbides and oxides, not unlike iron. In manganese ores, the higher manganese oxides MnO_2, Mn_2O_3 and Mn_3O_4 predominate. Figure 1.4 shows the phase diagram for the system Mn-O, where these oxides are found along with MnO and liquid manganese.

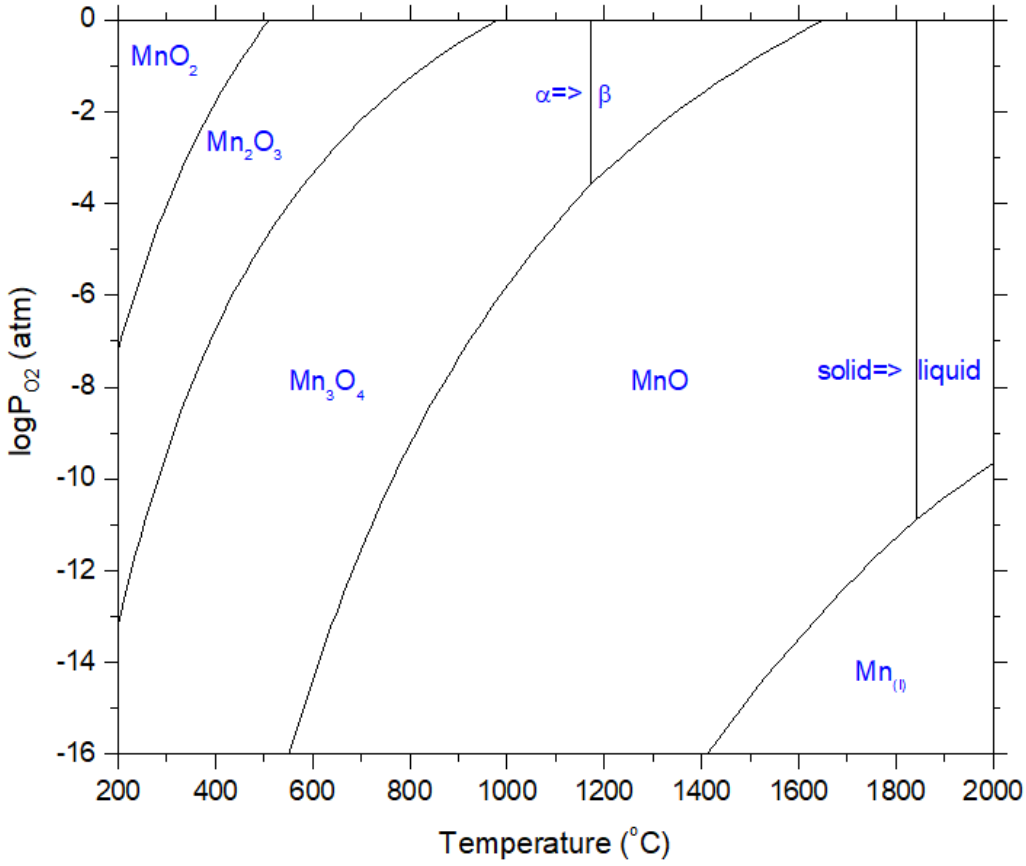

Figure 1.4: Phase diagram for the Mn-O system [6]

The higher manganese oxides thermally dissociate as they are heated. As can be seen from figure 1.4 at 1 atm pressure, MnO_2 dissociates to Mn_2O_3 at 510°C, with further heating Mn_2O_3 dissociate to Mn_3O_4 at 981°C, while Mn_3O_4 needs to be heated to 1652°C for it to dissociate to MnO at 1652°C. The equations for these three reactions are given by equations 1.1, 1.4 and 1.5 in section 1.1.2.

As mentioned, carbon materials is an important part of manganese alloy production, as it is used as a reducing agent. When taking this into consideration, a system describing the process should contain carbon in addition to manganese and oxygen. Figure 1.5 shows the calculated equilibrium relations for the system Mn-O-C with mol ratio Mn/C = 1.

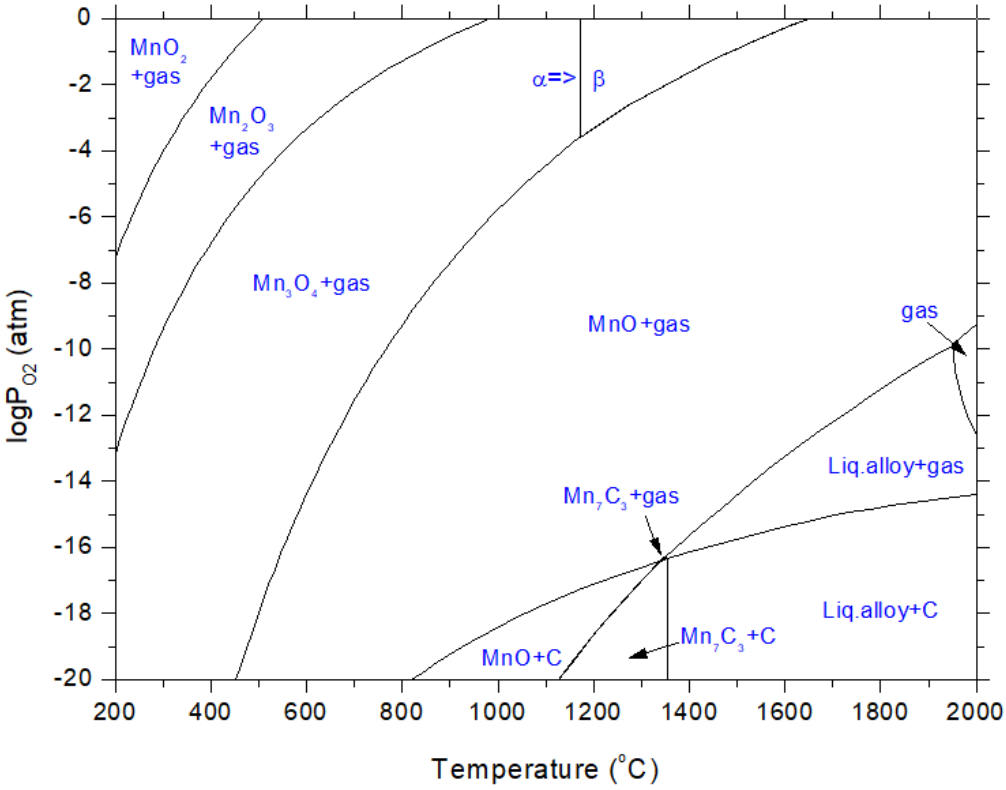

Figure 1.5: Calculated equilibrium diagram for Mn-O-C [6]

As figure 1.5 shows, the presence of carbon in the manganese oxygen system has no significant effect on the relations between MnO_2, Mn_2O_3, Mn_3O_4 and MnO, but the carbon slightly stabilizes the liquid phase. Formation of liquid manganese metal saturated with carbon is close to 1370°C, at an oxygen potential that is attainable at 1 atm in the presence of carbon and CO-gas. The extent of gas reduction is reflected by the furnace off-gas ratio between CO and CO_2.

When a mixture of manganese oxides and carbon is heated in the presence of CO-gas above 981°C the higher manganese oxides are converted to Mn_3O_4 by thermal decomposition as equations 1.17 and 1.18 shows, and by CO-gas reduction shown in equations 1.19 and 1.20. At this temperature, the reaction on carbon surface is sufficiently rapid to cause Mn_3O_4 reduction (equation 1.21), and Boudouard reaction (equation 1.8) to occur simultaneously. The CO_2 formed by reduction of Mn_3O_4 may give the overall reaction shown in equation 1.22.

$$MnO_2 \rightarrow \tfrac{1}{2}\, Mn_2O_3 + \tfrac{1}{4}\, O_2 \qquad 1.17$$

$$\tfrac{1}{2}\, Mn_2O_3 \rightarrow \tfrac{1}{3}\, Mn_3O_4 + 1/12\, O_2 \qquad 1.18$$

$$MnO_2 + \tfrac{1}{2}\, CO \rightarrow \tfrac{1}{2}\, Mn_2O_3 + \tfrac{1}{2}\, CO_2 \qquad 1.19$$

$$\tfrac{1}{2}\, Mn_2O_3 + \tfrac{1}{6}\, CO \rightarrow \tfrac{1}{3}\, Mn_3O_4 + \tfrac{1}{6}\, CO_2 \qquad 1.20$$

$$\tfrac{1}{3}\, Mn_2O_4 + \tfrac{1}{3}\, CO \rightarrow MnO + \tfrac{1}{3}\, CO_2 \qquad 1.21$$

$$\tfrac{1}{3}\, Mn_3O_4 + \tfrac{1}{3}\, C \rightarrow MnO + \tfrac{1}{3}\, CO \qquad 1.22$$

The raw materials also contain iron oxides, and a normal weight ratio of manganese and iron in manganese ores may be Mn/Fe = 7. The system that is closest to describing the prereduction zone is therefore the system Mn7Fe-C-O with a surplus of carbon. Most of the iron oxides will have reduced to metallic iron when the temperature reaches 1200°C. The result is a carbon-saturated iron alloy that has increasing content of manganese with increasing temperature. The last reduction step where manganese oxide is reduced to manganese metal (equation 1.9 in section 1.1.2) takes place in liquid state where manganese oxide is dissolved in the oxide melt, and where the produced manganese metal is continuously dissolved in the liquid carbon saturated iron-manganese alloy.

The basic system for silicomanganese is Mn-Si-C-O. Gibbs phase rule is useful for describing systems, and it is listed in equation 1.24, where F is degrees of freedom, C is number of components, P is number of phases and R is number of active restrictions.

$$F = C - P + 2 - R \qquad 1.24$$

The Mn-Si-C-O system has four components. The system has one gaseous phase and six possible condensed phases if the temperature is so high that manganese and silicon is completely melted. At this temperature there is a carbon-saturated liquid solution and molten slag, and the six possible condensed phases are liquid binary manganese oxide and silicon oxide slag, liquid metal alloy, graphite, silicon carbide, solid manganese oxide and solid silicon oxide. Gibbs rule states that with four components and no active restrictions, there are six phases and no degrees of freedom, which gives the possibility of one gaseous phase and five condensed phases. If both pressure and temperature are fixed, this gives two active restrictions and the number of possible phases are according to Gibbs rule reduced to four. The system made of the four phases liquid slag, metal, graphite and gas is therefore invariant at fixed temperature and pressure, which means that the final composition of the slag and metal are defined regardless of the starting composition, and that the system is uniquely defined. The Mn-Si-C-O system consists of four three-component systems, and the phase tetrahedron is shown in figure 1.6.

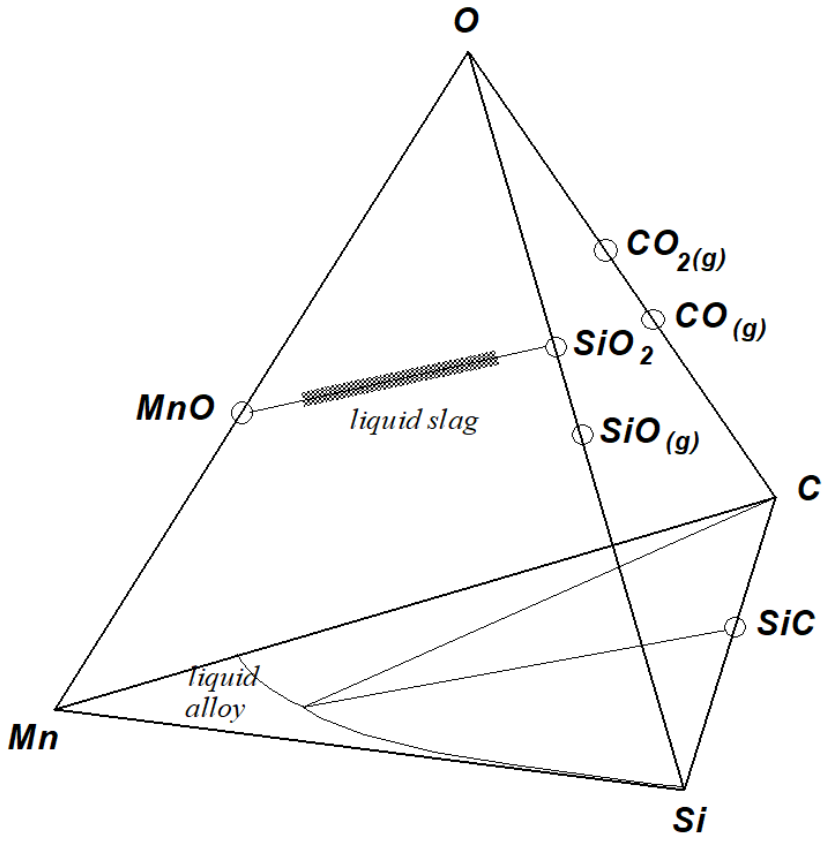

Figure 1.6: Phase tetrahedron for the system Mn-Si-C-O at a fixed temperature. Ding (1993) [6]

The Mn-Si-C subsystem is shown on one of the sides in the tetrahedron in figure 1.6. The liquid boundary represents the carbon solubility line, which is temperature dependent. When the silicon content is low, graphite is the stable carbon phase. When the silicon content is increased to a certain value at fixed temperature, a coexistence point is reached, where both graphite and silicon carbide coexists with liquid alloy. At higher silicon contents silicon carbide is the stable phase, and there is no graphite.

The subsystem Mn-C-O was shown in figure 1.4. The two other subsystems in the phase tetrahedron are the subsystem Mn-C-O and Mn-Si-O. In the Mn-C-O system the saturation point of carbon is found on the manganese-carbon axis, the manganese-carbon alloy is saturated with 7,79 wt% carbon at this point, if the temperature and pressure are fixed to 1500°C and 1 atm [6]. The three-phase equilibrium point is also found on the manganese-carbon axis of this subsystem, at this point the gas phase contains mainly CO gas and only little (1%) manganese gas, while the condensed phase is manganese-carbon alloy that contains 5.24 wt% carbon, and the solid phase is manganese oxide [6]. In the Mn-Si-O subsystem at 1500°C and 1 atm, the silicon content of the manganese oxide saturated slag is 20,5% and the lowest content of silicon in the manganese-silicon alloy is 0,6%. The highest silicon content is 17,5%, which correspond to silicon oxide saturated slag.

The system Mn-Fe-Si-C is an important metal system in manganese metallurgy. Iron and manganese are completely miscible in liquid state, and the Mn-Fe system shows very little deviation from ideal behaviour. Manganese and iron are not known to form any stable

intermetallic components. Carbon and manganese are completely miscible in liquid state and the liquidus temperature increases with increasing carbon content. Stable carbides forms during solidification, e.g. $Mn_{23}C_6$, Mn_3C, Mn_2C_3. Silicon and manganese are completely miscible in liquid state. Several silicides are formed during solidification.

The Mn-Fe-Si-C system is the basic system describing the commercially important silicomanganese alloys. Figure 1.7 shows calculated equilibrium phase diagram for Mn7Fe-Si-C system.

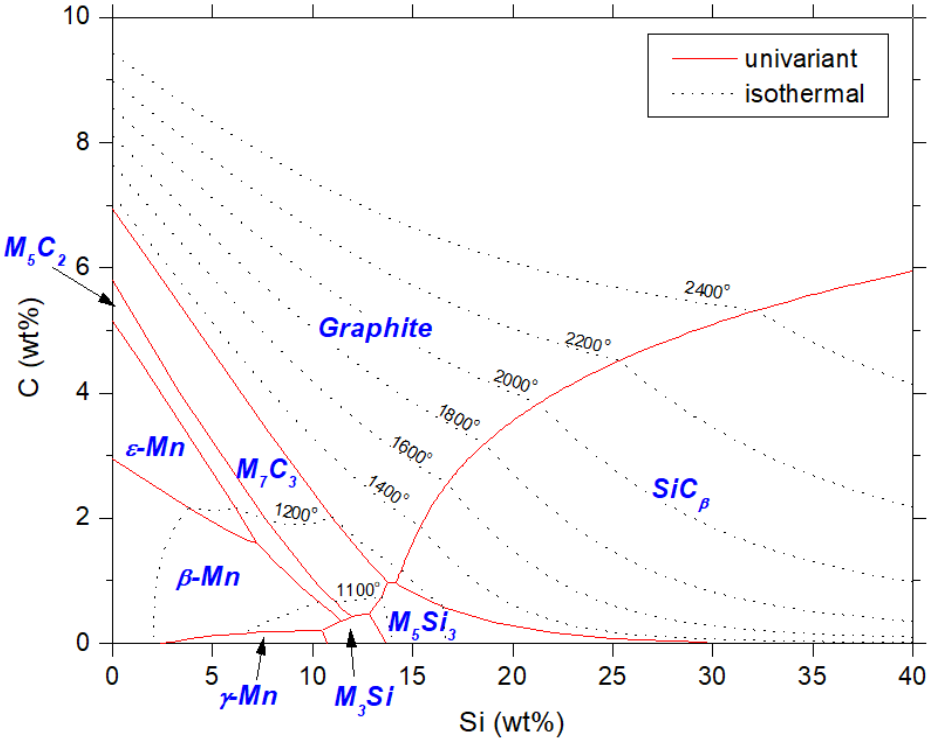

Figure 1.7: Calculated equilibrium phase diagram for the Mn7Fe-Si-C system [6]

Figure 1.7 shows equilibrium phase relations and carbon solubility at various temperatures, and silicon carbide stable areas. At low silicon content graphite is the stable carbon phase, until a certain value, about 17% for a manganese/iron ratio of 7 at 1600°C. At higher silicon contents graphite is replaced by silicon carbide as the stable carbon containing phase. The activities of manganese and silicon determine their distribution between slag and alloy phases. The activities of manganese and silicon at 1400°C and 1600°C are shown in figure 1.8 as a function of silicon content.

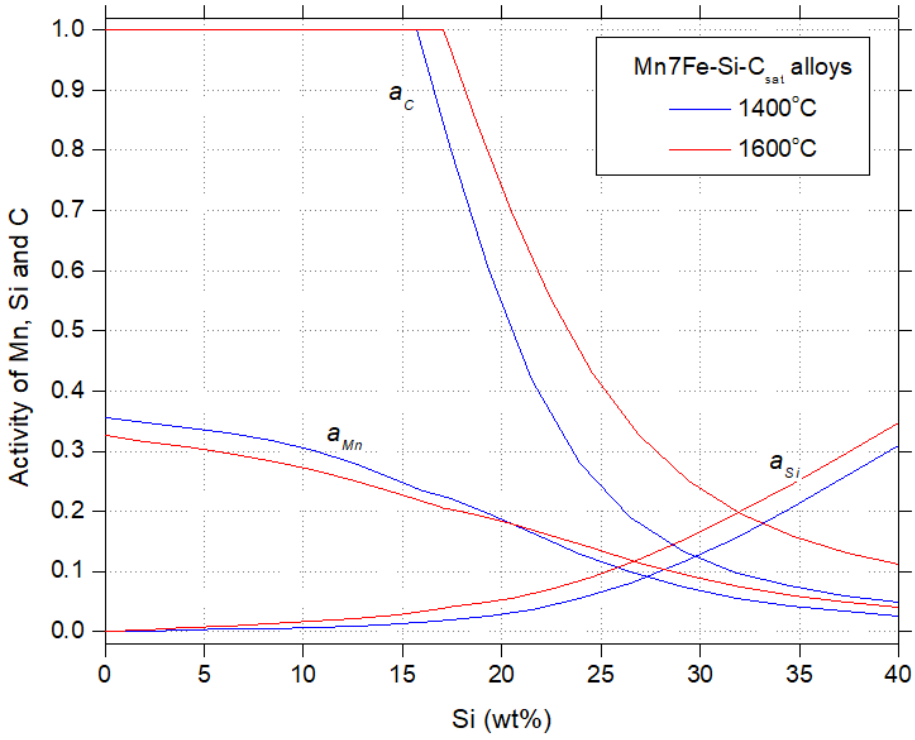

Figure 1.8: Activities of manganese and silicon as function of silicon content [6]

Figure 1.8 shows that the silicon activity increase with increasing silicon content and that the manganese activity decreases with increasing silicon content. The activity of carbon decreases when the silicon content increase above 18% at 1600°C.

In production of silicomanganese, the slag that is formed consists of manganese oxide, silicon oxide, calcia, alumina and magnesia. This is the Mn-Si-Ca-Al-Mg-O system. The system consists of a high number of components, and phase diagrams of some of the subsystems will be shown here. Figure 1.9 shows the MnO-SiO2 system, figure (a) shows calculated phase diagram and figure (b) shows the calculated activities of MnO and SiO_2 at 1400°C, 1500°C and 1600°C.

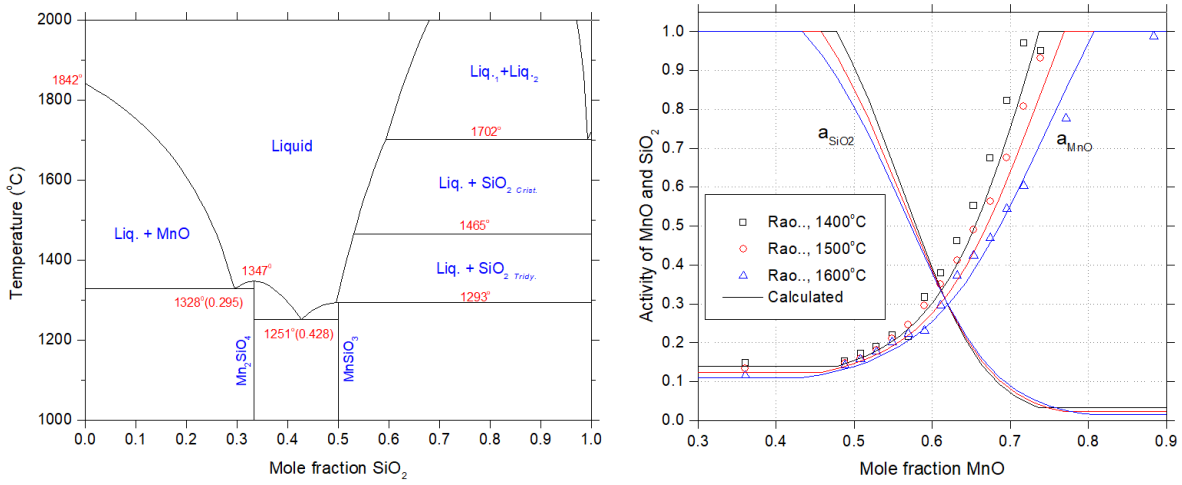

Figure 1.9: (a) Calculated phase diagram and (b) calculated activitites of MnO and SiO2 at 1400, 1500 and 1600°C. Measured activities of MnO by Rao & Gaskell (1981) [6]

Figure 1.9 (b) shows that the activity of manganese oxide increase as the mole fraction of manganese oxide increases, while the activity of silicon oxide decreases as the mole fraction of manganese oxide increase. The activity of manganese oxide increases with increasing temperature.

All oxides of aluminium, calcium and magnesium ends in the slag. The ores contain Al_2O_3, SiO_2, CaO and sometimes MgO. Ash from the coke contain SiO_2, Al_2O_3 and smaller amounts of CaO and MgO. In addition, fluxes containing MgO and CaO are usually added to the raw material mix. Since SiO_2 is more stable than MnO, less SiO_2 than MnO is reduced from slag to metal phase. CaO, MgO and Al_2O_3 are more stable and are not reduced at the temperatures achieved in the ferromanganese process. Reactions that are of main interest for the manganese process are reactions shown in equations 1.25 - 1-29:

$$(SiO_2) + 2C = \underline{Si} + 2CO(g) \quad 1.25$$
$$(MnO) + C = \underline{Mn} + CO(g) \quad 1.26$$
$$(SiO_2) + 2\underline{Mn} = \underline{Si} + 2(MnO) \quad 1.27$$
$$(SiO_2) + \underline{Si} = 2SiO(g) \quad 1.28$$
$$\underline{Mn} = Mn(g) \quad 1.29$$

where parenthesis denotes slag phase and underline denotes metal phase. Graphite is the stable carbon phase coexisting with alloy until silicon content reaches about 18% for manganese-silicon melt. When silicon content increases further, silicon carbide is the stable carbon containing phase [6]. As silicon carbide is stable, the activity of carbon is no longer equal to unity. Corresponding activities of silicon and carbon have to be determined by reaction shown in equation 1.30.

$$\underline{Si} + \underline{C} = SiC(s) \quad 1.30$$

When the partial pressures of silicon oxide and manganese oxide gas (p_{SiO2} and p_{MnO}) are quite low at e.g temperatures below 1600°C, graphite is stable and the most important reactions that occur are 1.25, 1.26 and 1.27, where 1.27 occurs as a combination of 1.25 and 1.26.

1.2 Carbon material

Carbon materials are important in production of manganese ferroalloys. There are several carbon materials that can be used as reducing agents in metal production, like coke, coal, charcoal, anthracite, petroleum coke and wood. Selection of reducing agent depends on a number of considerations, like requirements from the process and product, availability and cost, and environmental aspects. The chemical characteristics of the reducing agent affects the reactivity of the reductant and influences the product quality, amount of reduction material used and the specific energy consumption. Physical properties of the reducing agent affect efficiency and productivity of the smelting and reduction process.

The interaction between the carbon material used as reducing agent and silicomanganese slag is the focus of this project. Reduction of manganese oxide and silicon oxide from slag to metal are the main reactions, and the interaction between the reducing agent and the slag is therefore important to the production. The carbon materials used in this study is coke, which is used in all Norwegian manganese furnaces today, and charcoal which is considered a CO_2 neutral carbon source when used for metal production. This section contains a brief description of these two carbon materials, as well as a comparison of their characteristics.

1.2.1 Coke

Coke is made by coking of coal or coal blends. Coal is not used in production of manganese ferroalloys in closed furnaces, partly due to safety and partly due to environmental considerations. Coking is heating of coal in absence of air, so that the volatile matters in the coal are expelled. The coal used as raw material for coking is crushed to less than 3 mm particle size and can either be from a single coal or from a blend of coals. Different blends give different coke based on the properties of the coal, and the desired properties can therefore be obtained by using a desired blend of coal.

Coking can be divided into low temperature and high temperature coking. In low temperature coking, the coal is heated to 500°C or more, and results in low temperature coke that is often called ‘char’ [6]. Char still contains considerable amount of hydrogen and is of limited metallurgical interest, but can be used for ferrosilicon and silicon production. High temperature coking is when the coal is heated to over 1000°C, and the result is high temperature metallurgical coke [6]. In production of manganese ferroalloys, only this type of coke is used. However, coke used in submerged arc furnaces can be somewhat weaker than coke used in blast furnaces, where the demands of mechanical strength is higher.

During heating in the coking process, the coal mass melts and fuses together before it re-solidifies and condenses into particles large enough for metallurgical use. Almost all volatiles, hydrogen, oxygen, sulphur, nitrogen and others, are expelled as volatile byproducts. The resulting coke contains of 90-95% carbon and 5-10% ash [9], and as low as 1-2 % volatile matters [6]. All ash in the coal is retained in the coke which includes phosphorus, while typically two thirds of the sulphur content in the coal is retained in the coke. Since the weight of coke is typically two thirds of the weight of the coal used as raw

material, the sulphur percentage in the coke is the same as the percentage of sulphur in the coal used as raw material.

Properties of the coke controls different aspects of the production. Chemical properties of the coke controls reactivity of the reductant, influences the amount of reduction material used and affect product quality and energy consumption of the smelting process. Physical properties of the coke affect efficiency and productivity of furnace to a certain extent, and the production and stability of ferromanganese furnaces vary according to type of coke used.

Important properties of coke as a reductant in submerged arc furnace operation is content of moisture, ash, volatile matters and fixed carbon, elemental composition and especially the phosphorus content for manganese ferroalloys, electric resistivity of the material, reactivity towards reaction with CO_2-gas in Boudouard reaction, reactivity of the solid carbon with liquid slag component, and coke strength after Boudouard reaction. The Boudouard reaction is largely decisive for the total consumption of carbon material and electric energy in the furnace. Coke has low reactivity towards the Boudouard reaction along with petroleum coke and anthracite, as opposed to char and charcoal that are expected to have high reactivity towards Boudouard reaction. The electrical resistivity is especially important in electric arc furnaces. High burden resistivity is advantageous as it leads to good overall heat distribution in the furnace. This depends especially on intrinsic resistivity, volume fraction and particle size of the reducing agent used.

1.2.2 Charcoal

Charcoal is made from biomass, usually wood. It is used as reducing agent in production of manganese ferroalloys in open furnaces, especially in Brazil. The charcoal used for this production has usually been made from eucalyptus wood that has a relatively high carbon content compared to other trees, about 53% [10]. The properties of the wood used to produce charcoal affects the properties of the charcoal. Higher carbon content in the wood gives higher carbon content in the charcoal, and higher density of the wood gives higher strength of the charcoal [10].

Charcoal is produced by pyrolysis in large kilns or resorts, not unlike coking. Larger particles of biomass and slow heating favors charcoal for metallurgical use. Byproducts of the production are pyroligneous liquid and volatile matters, and the pyroligneous liquid is usually burnt with gases to provide heating for the production. The yield depends on production conditions. There are several methods and concepts for producing charcoal, but three types are commonly used. The most common method is internal heating where part of the raw material is burnt with a controlled air flow that is added to the process to provide the heat needed to produce charcoal. In another method, external heating, the heating is provided from the outside of the reactor, no air flow is needed, and pyroligneous liquid can be used as fuel for the external heating. In a third method, heating with recirculated gas, part of the pyroligneous vapors are burnt in an external combustion chamber and directed into the reactor where it is in direct contact with the raw material charge [6].

Charcoal has low volume weight, and has a lower fixed carbon content, higher content of volatile matter and rather low content of ash compared to coke, in addition to being porous. The ability charcoal has of making its way down to the cokebed in the furnace may not be as good as the ability coke has, as charcoal has substantial lower mechanical strength than coke. Charcoal has higher resistivity than coke, which has been reported to result in more efficient operation with respect to energy and electrode consumption [11]. Since charcoal has lower volume weight than coke, the freight costs are higher. The manganese industry has not found it feasible to use charcoal as a reduction agent, except plants that are close to charcoal producers, but charcoal is used for iron and steel and ferroalloy industry in addition to household consumption [6].

Since charcoal is made from biomass, it is a CO_2 neutral carbon material and does not emit any excess CO_2 when used for metal production, as long as the amount of trees used for charcoal production is in balance with the amount of trees planted [10]. Coke has some favorable properties over charcoal, but considering the environmental aspect it would be favourable to substitute coke with charcoal in production of manganese ferroalloys. There are large potentials for reducing CO_2-emissions from the manganese ferroalloy industry by using charcoal instead of coke.

1.2.2.1 Charcoal in open vs closed furnaces

As previously mentioned, charcoal contains more volatile matters than coke. In open furnaces, off-gases and dusts from the production are burned at the top of the furnace, and the difference between using coke and charcoal as reduction agent are not large. However, all Norwegian furnaces are closed, which means that the off-gases and dusts from the production needs to be collected and cleaned before being disposed of or utilised elsewhere, e.g. the CO-gas from the production can be sold or used for heating purposes. Norwegian producers use coke as a reducing agent, and if they were to substitute this for charcoal, the collection and treatment systems would need to be altered because of the high amounts of volatile matters in charcoal compared to coke. In the furnace the volatiles in the charcoal will evaporate and condense again at the top of the furnace, which clogs the exhaust and gas cleaning systems. Hence, substituting coke with charcoal is a challenge for a closed furnace, while it is not the same challenge substituting reducing agent in an open furnace.

2. Literature

Some relevant literature and studies will be reviewed. A study on the different properties of charcoal and coke, some studies on the reactivity of manganese slags towards carbon materials performed in different furnaces, studies on the effect of sulphur in the slag and studies comparing argon and CO gas as furnace atmosphere are presented.

2.1 Charcoal and coke

Monsen et al. [12] tested some properties of charcoal and coke that are important to the production of manganese ferroalloys. The report lists some typical properties of charcoal and coke in a table, see table 2.1, these are results of typical chemical analyses and selected properties for reducing agents used in SiMn/FeMn production. Other possible reductants are included in the table for comparison.

Table 2.1: Typical properties for charcoal compared to metallurgical coke (special qualities in brackets) [12]

	Industrial charcoal	Metallurgical Coke	Charcoal from preserved pine	Petrol coke
Fixed carbon (%)	65 – 85 (94)	86-88	93.8	84-90
Volatile matter (%)	15-35 (4)	=1	3.8	9-16
Ashes (%)	0.4-4	10-12	2.4	<1
Ash composition (% of ash):				
SiO_2	5-25	25-55	23	
Fe_2O_3	1-13	5-45	5	
Al_2O_3	2-12	13-30	5	
P_2O_5	4-12	0.4-0.8	-	
CaO	20-60	3-6	11	
MgO	5-12	1-5	-	
K_2O	7-35	1-4	-	
Volume weight on dry basis (kg/m^3)	180 -350	500-550		450-800
CO_2-reactivity at 1060°C (%C/s)	$(2.1 – 2.3)\cdot10^{-2}$	$(0.2 - 0.50)\cdot10^{-2}$	$(2.8 - 3.2)\cdot10^{-2}$	-
Thermal cohesion strength: C.I (%)	74 - 84	93 – 97	93 - 95	-
Thermal abrasion strength: T.I.3 (%)	78 – 82	82 - 89	84	-
Electrical resistance (Ù·m)	5-35 mm	10-20 mm	-	10-20 mm
at 1000°C	0.014 - 0.023	0.003 – 0.008	-	0.012 - 0.035
at 1400°C	0.009 – 0.018	0.003 – 0.009	-	0.007 - 0.021

In the analysis of CO_2 reactivity, Monsen et al used a special CO_2-reactivity test that was developed by NTNU/SINTEF in cooperation with Eramet and Tinfors. A highly reactive

material will have a high reactivity number, reflecting a high rate of the Boudouard reaction. It is undesired to have a high rate of this endothermic reaction in manganese alloy production, due to consumption of energy and reducing agent in the upper part of the furnace. The test was performed using an atmosphere of 50% CO gas and 50% CO_2 gas, a temperature of 1100°C, with a sample amount of 60-100 g. The crucible used was made from stainless steel. The test was stopped after a certain amount of carbon had reacted, by purging with inert gas and removing the sample crucible from the furnace. The results showed that the industrial charcoal made from Brazilian eucalyptus (BE-1, BE-2, BE-3) had a CO_2 reactivity that was 4-12 times higher than for the different cokes and that the cokes had a span in reactivity. The charcoal made from preserved wood (CCa-1, CCA-2) had a somewhat higher CO2 reactivity than the industrial charcoal. These results are shown in figure 2.1.

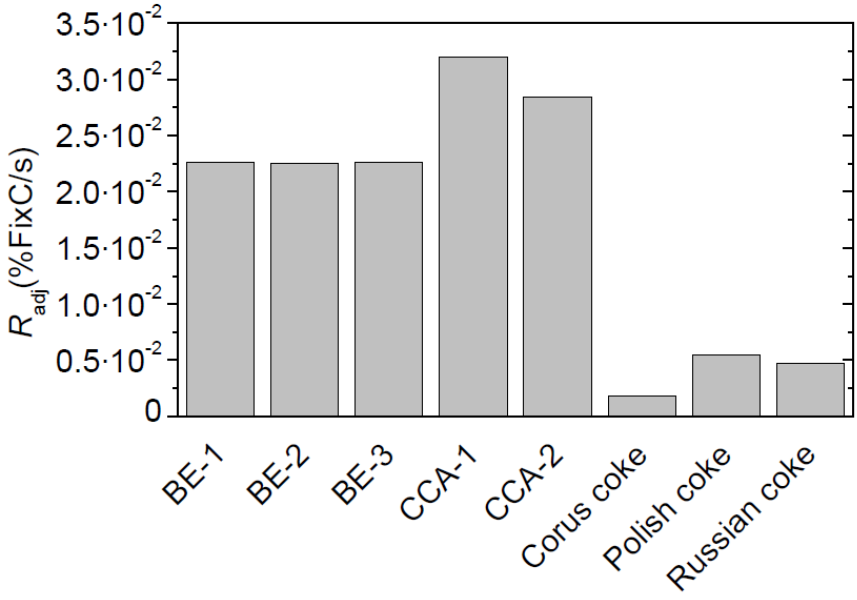

Figure 2.1: CO_2 reactivity at 1060°C of industrial charcoals, charcoal from preserved wood and metallurgical cokes [12]

The thermal abrasion strength and the cohesion strength was tested after the CO_2 reactivity test for the different materials. The cohesion index (C.I.) indicates the ability the material has to maintain its strength (cohesion) after reaction with furnace gas and its ability to withstand generation of fines. The thermal stability index (T.I.3) is measured after tumbling and indicates the materials ability to resist abrasion toward other particles under charge pressure. A high number is preferred for both indices. The results are shown in figure 2.2, and it can be seen that the industrial charcoal has cohesion index in the range of 74-84%, while the metallurgical cokes has higher cohesion indexes of 93-97%. The charcoal made from preserved wood has as high cohesion strength as the cokes. There are only minor differences between the thermal abrasion strength of charcoal and coke based on the thermal stability index.

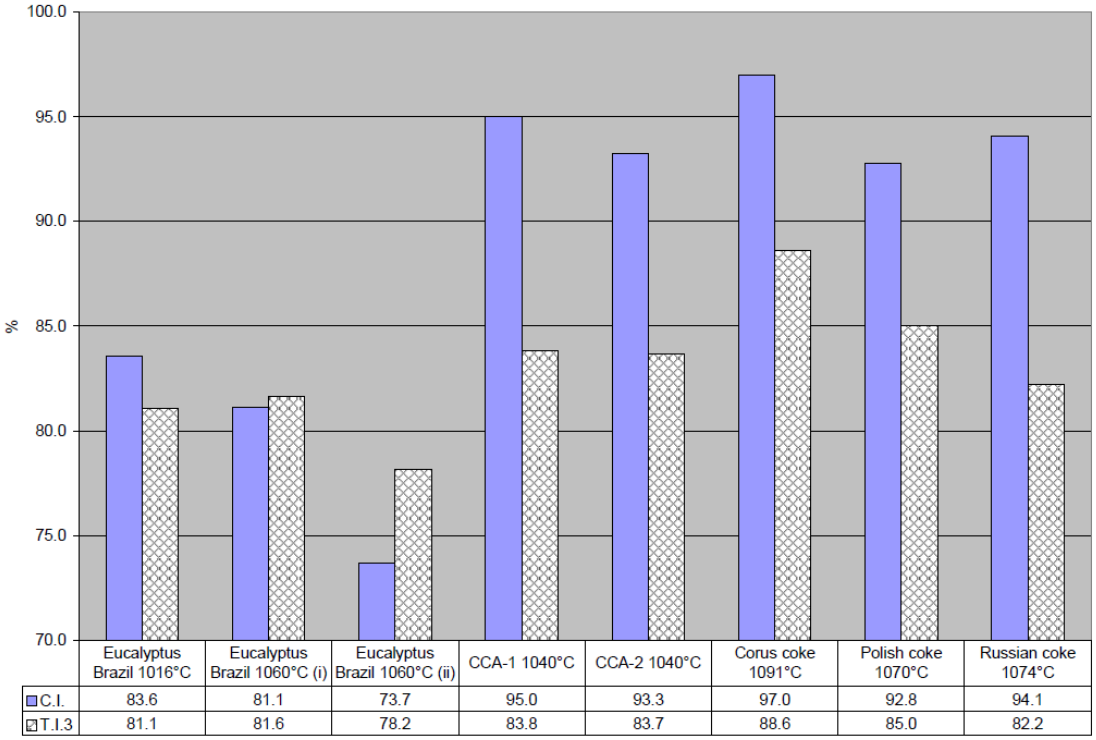

	Eucalyptus Brazil 1016°C	Eucalyptus Brazil 1060°C (i)	Eucalyptus Brazil 1060°C (ii)	CCA-1 1040°C	CCA-2 1040°C	Corus coke 1091°C	Polish coke 1070°C	Russian coke 1074°C
C.I.	83.6	81.1	73.7	95.0	93.3	97.0	92.8	94.1
T.I.3	81.1	81.6	78.2	83.8	83.7	88.6	85.0	82.2

Figure 2.2: Abrasion strength for Brazilian charcoal and charcoal made from preserved wood compared to different metallurgical cokes. [12]

The electrical resistivity of the cokebed is important for the operation of the furnace. The electrical resistivity of dry cokebeds was tested using a method suitable for measuring industrial sized reductants at temperatures up to 1600°C. The carbon material was placed in a high-alumina refractory cylinder built around a graphite electrode, with a layer of insulating material. Weights were added to the top to ensure optimal contact, and the temperature was measured by thermocouples. The current density was kept in the range 7.4-14.1 kA/m^2. Particle sizes were kept below 10% of the diameter of the alumina tube to reduce wall effects. The cokebed was heated to 1600°C. Molybdenum wires were used to measure the voltage. The resistivity was calculated from equation 2.1, where ρ = resistivity, U is cell voltage, I is current, A cross section area, and h is the height between measuring points.

$$\rho = \frac{U \times A}{I \times h} \qquad 2.1$$

The charcoal was heat treated prior to the measurements at 850°C for one hour in a tight container without oxygen access. Figure 2.3 shows the results of the measurement, and a comparison of the different carbon materials. The figure shows that petrol coke has the highest electrical heat resistivity at all temperatures, but had also been heat treated before measurement. The metallurgical cokes had the lowest electrical resistivity, while the resistivity of charcoals is 2-8 times higher than the metallurgical coke in the temperature range 1000-1300°C. At higher temperatures the electrical resistivities of charcoal can be similar to or up to 2-3 times as high than metallurgical coke.

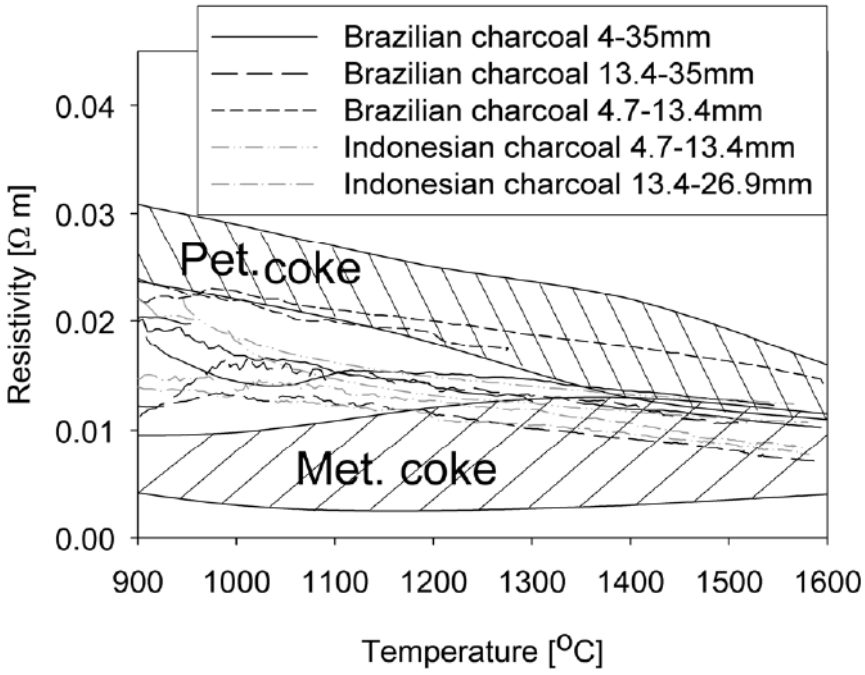

Figure 2.3: Comparison of electrical resistivity of different carbon materials at varying temperature [12]

2.2 Reactivity of slag towards different carbon materials

Some studies on the reactivity of manganese slags towards coke, charcoal and graphite are presented. Studies performed in large furnaces are described first, these include pilot scale experiments, excavations, and experiments in induction furnaces. Studies performed in sessile drop furnaces are then described.

2.2.1 Studies with large furnaces

Monsen, Tangstad and Midtgaard [11] produced silicomanganese in five pilot scale experiments during 2001-2003. They used three different reductants, industrial coke, reactive coke and charcoal. The aim was to produce silicomanganese metal with a silicon content of 18 percent, and to study if there was any difference in the cokebeds when different reductants were used. The charges were made of manganese ores, HC FeMn slag and quartz, and the charge composition for the five different experiments are given in table 2.2. Raw materials were added 11 times during the experiments, and quartz was added from the second charge adding, to avoid build-up of a quartz-bed. The experiments started with 3 or 5 kg cokebed as listed in table 2.2. The electrode tip position was lower in experiment 4 and 5, and the amount of fixed carbon was therefore also somewhat reduced to reduce the volume of the cokebed. Experiment 5 had 50% coke and 50% charcoal on a fixed carbon basis.

Table 2.2: Charge composition used in the five pilot scale experiments of Monsen, Tangstad and Midtgaard. The charge composition is based on 35 kg ore and 15 kg HC slag in each charge [11]

Run no	Starting cokebed (kg)	Charged materials	Moisture (%)	Charge 1 (kg)	Charge 2 (kg)	Charge 3 (kg)	Charge 4-11 (kg)	
1	5	Industrial coke Quartz	13	11.5 0	12 6.5	13 11	13.5 13	
2	3	Reactive coke Quartz	2	10 0	10.5 6.5	11.5 11	12 13	
3	5	Charcoal E_1 Quartz	5	11.5 0	12 6.5	13 11	13.5 13	
4	5	Charcoal E_2 Quartz	7	11.5 0	11.5 6.5	12.5 11	13.0 13.3	12.5 12.5
5	3	Charcoal E_2 Industrial coke Quartz	7 0	5.5 4.8 0	6 5.2 6.5	6.3 5.5 11	6.6 5.7 13.3	

As seen from table 2.2, some quartz and charcoal was withdrawn from charge 7-11 due to a viscous slag and difficult furnace operation. The charge contents were based on assumed slag and metal composition.

The furnace used in these experiments was a 150 kW single electrode furnace located at SINTEF/NTNU. The furnace had alumina monolithic lining and silica sand as lining, this with respect to the excavation, as the outer lining could be easily removed. After the experiments, the furnace was filled with epoxy, and the electrode was cut after hardening. The furnace was taken away in one piece, and a cross section plate sawed out for further studies.

Samples from the excavation plate were investigated by microprobe. Figure 2.4 shows a drawing of the experimental setup.

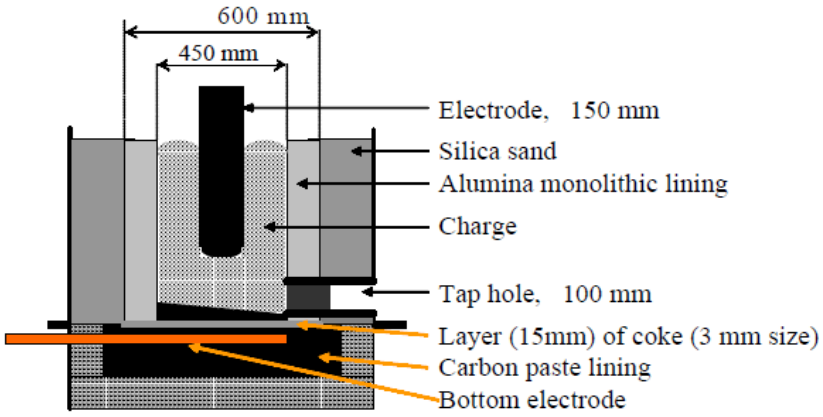

Figure 2.4: Sketch of pilot scale furnace used in the experiments [11]

The furnace was first preheated. As the charging started, a load of 150 kW was aimed for, and tapping was carried out every 80 kWh, which gave 8 taps. The furnace was shut down 50 kWh after the last tap. The electrode position was fixed, and the electrode tip was set to 20 cm above the bottom in run 1-3, and 15 cm for run 4 and 5.

The resistance of the cokebed increased when charcoal was used as a reductant instead of coke. The last run with 50% coke and 50% charcoal also had a high resistance, as shown in table 2.3, along with the rest of the experimental conditions. There was a higher amount of slag in the furnace during run 3-5, which also increases the furnace resistance.

Table 2.3 Furnace operation during stable production [11]

Run no.	Electrode tip position	Current (kA)	Voltage (V)	Load (kW)	Resistance (m·ohm)	Power consumption (kWh/kg metal)	%Si in metal (see ch. 3.3)
1	20 cm	3.9	39	152	10	5.0	18.8
2	20 cm	3.0	50	146	17	4.2	17.3
3	20 cm	2.1	67	138	36	3.5	11.4
4	15 cm	2.1	72	151	36	3.8	13.5
5	15 cm	2.1	71	148	35	3.6	12.9

The chemical analysis showed that the silicon content was lower in the metal produced with charcoal or a mixture of coke and charcoal, but that the manganese reduction was higher, and that the metal production was higher in these runs. The results further indicated that the lowered electrode tip position increased the temperature in the cokebed, which also increased the silicon content in the produced metal some, from 11,4% in run 3 to 13,5% in run 4 as an average for tap 4-8.

The excavation of the furnace after tests found that the cokebeds in test 1-3 were wider, as more coke was charged in these tests, while the cokebed increased further up on the electrode in tests 4-5 where the electrode position was 5 cm lower. Some of the furnace lining was consumed in test 4-5 where the temperature was higher.

The study concluded that charcoal gave higher metal production than coke, but also lowest silicon content in the metal. Reactive coke was in-between charcoal and industrial coke both in metal production and silicon content in the metal, while the industrial coke had the lowest metal production but highest silicon content in the metal. However, the difference between reactive and industrial coke was low, while charcoal had a significant difference. The charcoal also increased the total resistance in the cokebed and gave highest slag production. There was also expected slag intrusion into charcoal pores, which was rarely seen, in contrast to coke where slag frequently penetrated into the pores.

Olsen and Tangstad [7] excavated a 16 MW silicomanganese furnace. The furnace was switched off two thirds of the way into a new tapping cycle during regular operation, and no external cooling was performed. The furnace was well operated before the shut down, and the main raw materials were Groote Eylandt lump manganese ore, FeMn slag, quartz, coke and some dolomitic limestone. The tapped slag temperature was about 1600°C, operating time was above 95% and the metal contained above 18% silicon and the slag about 40% silicon oxide. The electrode tip positions for electrode A, B and C were respectively 60, 110 and 50 cm above the metal bath. The suitable electrode tip position was assumed to be around 60 cm for this furnace. Figure 2.5 shows a sketch based on the excavation, and it can be seen that the cokebed around electrode B was large, which was assumed to have resulted in the unwanted high electrode position. As shown on figure 2.5, there was a area of slag which contained little coke under each electrode.

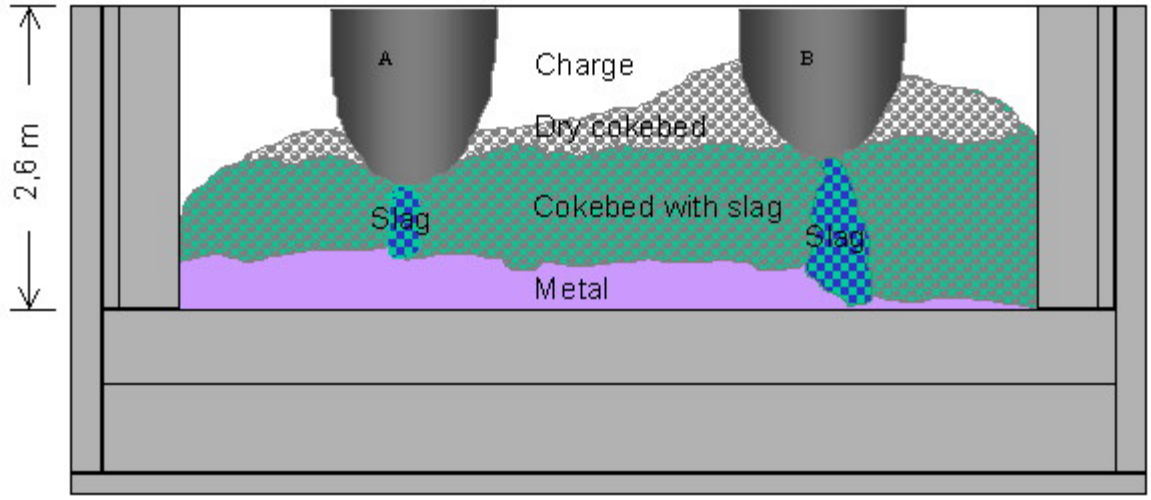

Figure 2.5: Sketch of the excavated 15 MW furnace producing silicomanganese [7]

Samples were collected from the charge, both manually and by drilling. These samples were investigated by visual judgement, XRD, microprobe and chemical analyses.

The study concluded that an electrode tip position of about 60 cm above the metal bath had been suitable for good operation. The sample analyses showed that the MnO_2 in the ore decomposed early to M_2O_3, but that further reduction to Mn_3O_4 was modest. Pre-reduction to MnO of any significance was only observed in the charge fines, in the prereduction zone. Nearly all reduction of MnO was finished at the top of the cokebed, and dissolution and reduction of quartz had taken place in the cokebed zone after main reduction of manganese

oxide was finished. Further, the study concluded that increasing the share of FeMn slag at the expense of Mn-ore leads to a larger slag/metal ratio in the SiMn process, which in turn leads to higher energy consumption per ton alloy.

Gaal et al. [13] tested two graphites, industrial coke, anthracite and eucalyptus charcoal with MnO and SiO_2 containing slags. The carbon materials were characterized and the amount of fixed carbon, the porosity, the ash content and sulphur content were analyzed by XRD analysis. In addition, the CO_2 reactivity was measured at 1000°C in a 100% CO_2 atmosphere. The results of these tests are listed in table 2.4.

Table 2.4: Summary of physical and chemical properties of carbonaceous materials used in the study [13]

Property (unit)	G1	G2	Anthracite	Industrial Coke	Eucalyptus Charcoal
Fix C (%)	99.87	99.62	94.3	89.36	81.3
Ash (wt%)	0.13	0.38	2.8	10.64	0.43
VM (wt%)	-	-	3.0	-	18.3
Porosity (%)	23.5	25.5	4.9	27.5	27.3
Average pore diameter (μm)	0.05	0.03	0.02	0.57	0.46
Median pore dia. (area)* (μm)	0.012	0.009	0.009	0.008	0.019
Median pore dia. (vol)**(μm)	1.8	0.6	0.03	26.8	12.4
Total pore area (m^2/g)	11.70	18.80	6.34	1.86	3.86
Skeletal density (g/ml)	2.20	2.17	1.62	1.45	0.90
d (Å)	3.4	3.4	3.5	3.5	3.8
Lc (Å)	260.5	215.3	14.2	23.4	11.5
Approx. fraction amorphous C	***	***	0.42	0.18	0.69
S content (ppm)	42	35	2600	5600	20
CO_2 react. (s^{-1})	$1.3x10^{-4}$	$5.4x10^{-5}$	$3.17x10^{-5}$	$2.78x10^{-5}$	$7.23x10^{-4}$

*pore diameter of pores contributing 50% of the pore area
**pore diameter of pores contributing 50% of the pore volume
***negligible

As seen from table 2.4, the porosity of the reductants does not vary significantly, with exception of anthracite. The pore sizes varies, with larger pores for coke and charcoal than for graphite and anthracite. The sulphur content of the charcoal is low compared to the anthracite and coke.

The graphite materials G1 and G2 were tested in a small resistance furnace with a vertical tube heating element. For the other three carbon materials, experiments were performed in an induction furnace to investigate the reduction behaviour. 500 g industrial slag was first heated to 1600°C in a graphite crucible and held for 20 minutes before 100 g of coke, anthracite or charcoal was added. The contents of the crucible was stirred every 5 minutes with a graphite rod. In the first experiment the extent of reduction by the graphite was determined, and no reductant was added. After the tests, the crucible contents was quenched in a graphite mould, and the reductants were separated, weighed and analysed.

The results of the tests in the induction furnace showed that the coke was least reactive, while charcoal and anthracite were similar, depending on the criteria used to compare them. Charcoal had good reduction kinetics, as it reduced more of the slag than both coke and anthracite, while producing more metal per unit carbon, with larger concentration of Si in the metal. The reductant used had a significant influence on the SiO_2 reduction, but did not have a large effect on the MnO reduction.

The study concludes that the reactivity of the three carbon materials from highest to lowest was eucalyptus charcoal, anthracite and industrial coke.

Monsen et al. [12] ran a pilot test with metallurgical coke, reactive coke and charcoal as reducing agent in an induction furnace with increasing CO_2 reactivity. The pilot test was a continuation of the pilot scale experiments by Monsen, Tangstad and Midtgaard in 2004, where the aim was to produce silicomanganese with 18% silicon, and to see if there was found any significant differences in the cokebed when using different reductants. The aim of this experiment was to see if a colder charge top would improve the previous results of run 5. The ore and coke were moistened to 10% and 8%, respectively. The amount of HC FeMn slag, quartz and ore on a dry basis was the same, and the raw materials used are listed in table 2.5. The starting cokebed was 5 kg in run 6.

Table 2.5: Charge composition (kg, wet), based on 35 kg dry ore and 15 kg HC slag in each charge [12]

Run no	*Starting coke-bed (kg)*	*Charged materials*	*Moisture (%)*	*Charge 1 (kg)*	*Charge 2 (kg)*	*Charge 3 (kg)*	*Charge 4-11 (kg)*
5	3	Charcoal	7	5.5	6	6.3	6.6
		Industrial coke	0	4.8	5.2	5.5	5.7
		Quartz	0	0	6.5	11	13.3
		Ore	0	35	35	35	35
6	5	Charcoal	7	5.5	6	6.3	6.7
		Industrial coke	8	5.1	5.6	6.0	6.3
		Quartz	0	0	6.5	11	13.3
		Ore	10	38.8	38.8	38.8	38.8

The 150kW single electrode furnace at SINTEF/NTNU was used, and a sketch of the furnace was shown in figure 2.4. The furnace was excavated in the same way after test 6 as after the 5 first tests.

The furnace was preheated before the test, as charging started a load of 150kW was aimed for, and tapping was carried out every 80 kWh which gave 8 taps. The electrode tip position was fixed 15 cm above the bottom lining, and the power consumption was the same in test 5 and 6; 3,6 kHh/kg metal produced. Table 2.6 shows some experimental information from test 5 and 6.

Table 2.6: Furnace operation during stable production (average numbers for tap 4-8). Mean slag and metal analyses for the taps 4.8 are shown [12]

Run no.	*Current (kA)*	*Voltage (V)*	*Load (kW)*	*Resistance (mohm)*	*Produced metal (kg)*	*Produced slag (kg)*	*% MnO in slag*	*% SiO_2 in slag*	*%Si in metal*
5	2.1	71	148	35	180	223	19.0	39.2	12.9
6	3.4	48	155	15	151	182	29.1	37.5	16.6

The metal analysis showed that run 6 had a higher silicon content in the metal, and that there was a lower metal production in this run. A more resistant lining was used in run 6, as a lot of the lining dissolved into the slag in run 5, affecting the R-ratio of the slag. The excavation of the furnace after run 5 and 6 were similar, but showed some different current paths between the two runs. The shape of the cokebeds were almost equal, but the size of the cokebed in run 6 was somewhat bigger/wider. Measurements found that 2.0 and 2.7 cm of electrode was consumed in run 5 and 6, respectively.

The study concluded that silicomanganese with 18% silicon could be produced when charcoal was substituting 50% of the coke on a fixed carbon basis. The main difference from previous similar run being that the ore and coke were moistened to keep the charge top colder, avoid carbon burn-off at the top and improve temperature distribution in the furnace.

Nadir [14] tested graphite and coke with synthetic and industrial slag in an IF-75 induction furnace. Figure 2.6 shows a schematic of the apparatus used during the tests. The experiments were performed at low constant power input of 15 kW. A graphite crucible with inner diameter of 12 cm and height of 40 cm was used to contain the raw materials, and the total amount of raw materials used in each experiment was 2000 g. Four experiments were run.

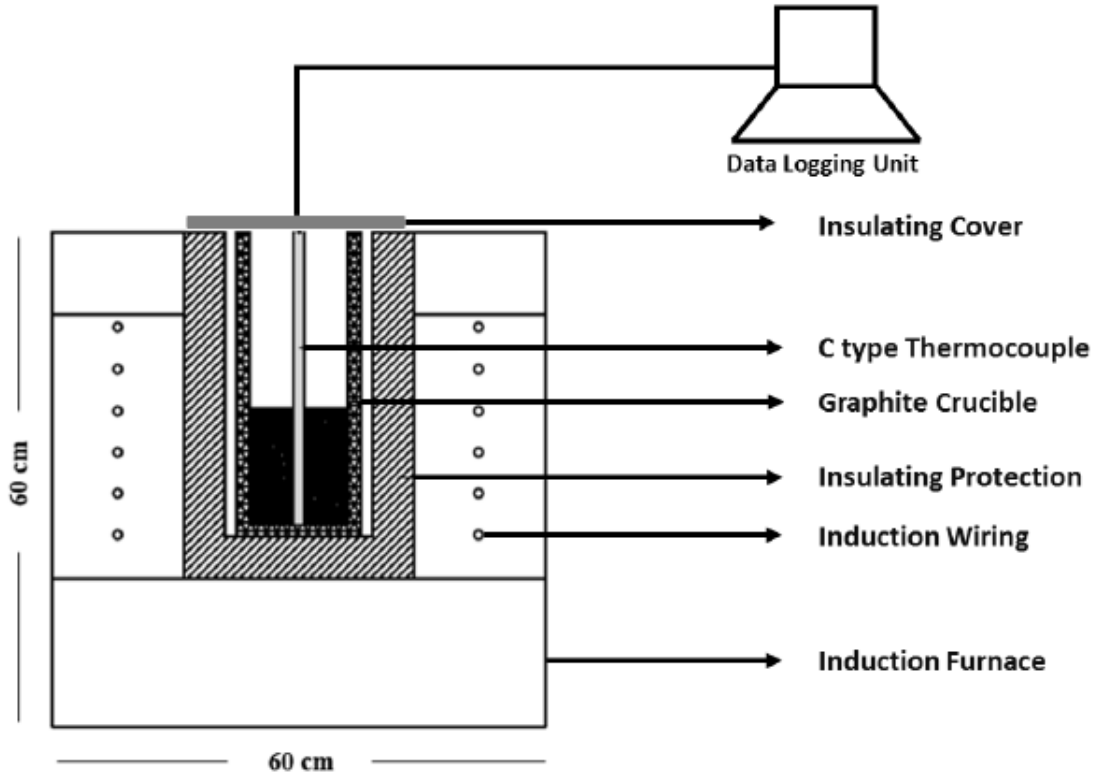

Figure 2.6: Schematic of the induction furnace apparatus used for conducting the kinetic study of MnO reduction for silicomanganese production [14]

The raw materials were added to the crucible and heated to 1650°C, and samples were collected from the slag as the temperature increased from 1200-1650°C, the samples were analysed by EPMA and XRD. Figure 2.7 shows the sum of reducible oxides for the four induction experiments, and how they develop over time.

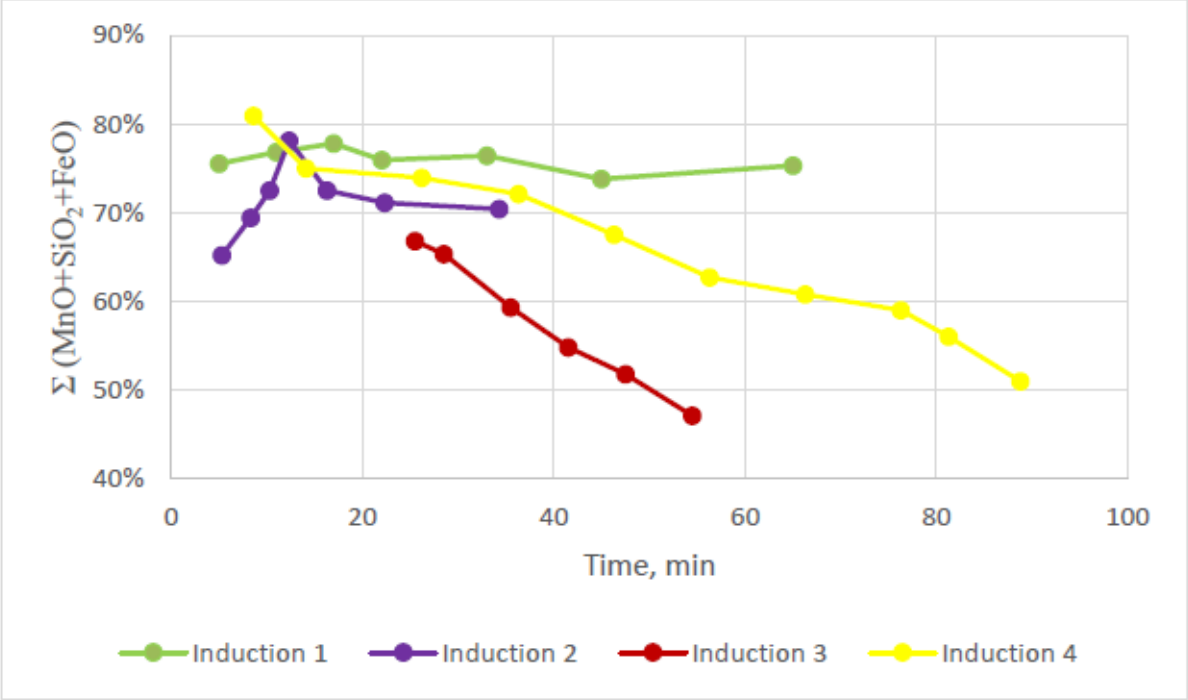

Figure 2.7: Sum of reducible oxides for all the induction furnace experiments as a function of time [14]

Figure 2.7 shows that the amount of reducible oxides does not change much with time for induction 1 and 2. This suggests a lack of reduction and therefore a poor reduction rate for both experiments. Induction 3 and 4 are carried out with synthetic slag with and without sulphur and graphite and coke reduction material and has a promising reduction rate.

The study concludes that the lowest reduction rate was observed in induction 1 and 2 that only used graphite as a reducing agent, and that addition of coke as a reducing agent enhanced the reduction rate as observed for induction 3 and 4.

Jayakumani [15] tested melting and reduction of manganese ores in an induction furnace. The furnace had a maximum power supply of 75 kW, but the maximum power used in the experiments was 10-30 kW. A graphite crucible was used, where 10 cm of coke was added to the bottom, then 7 cm manganese ore and coke was added, and a 10 cm coke layer was added at the top. Figure 2.8 shows the experimental setup used.

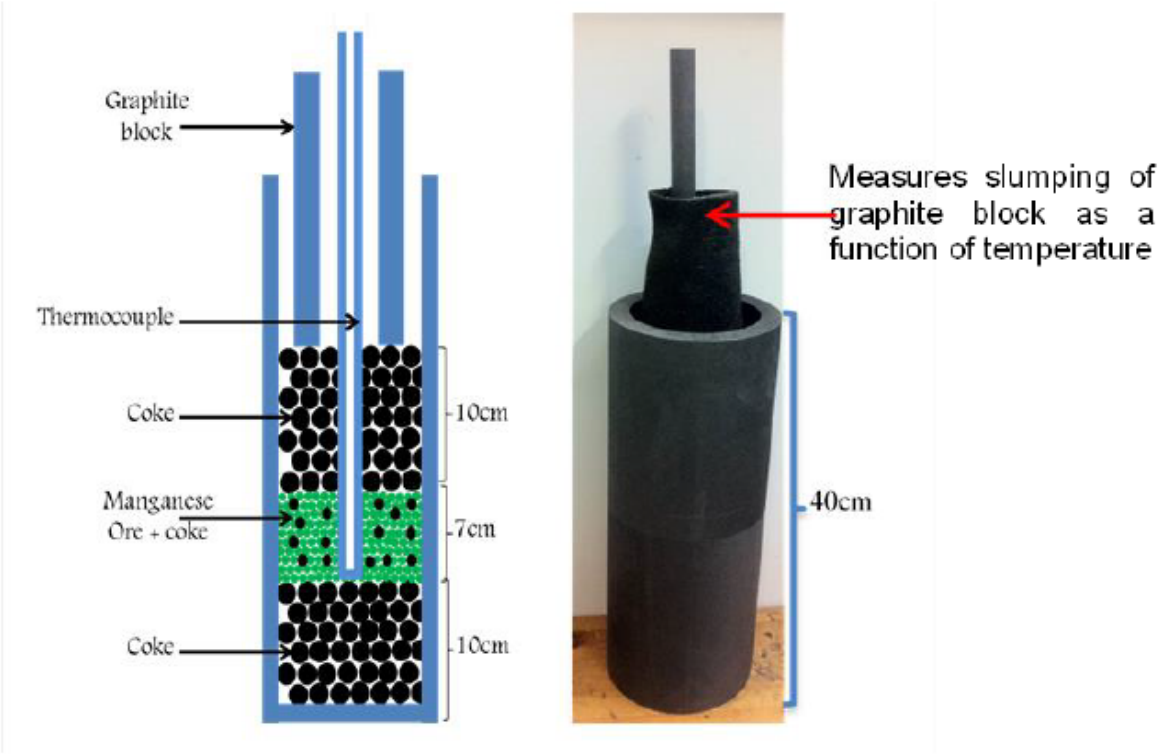

Figure 2.8: Experimental set up in an open induction furnace [15]

The crucible was heated to 1200°C to pre-reduce all the raw materials at a power of about 10-20 kW. The power was then reduced to 5 kW to hold the temperature steady for 10-15 minutes. After prereduction the temperature was increased to 1600°C. After the test, the crucible was filled with epoxy and vertically cut through the middle.

Five different carbonaceous materials of various size were used to investigate how different sizing affects the reduction temperature and reduction behaviour of MnO-containing slags. Coke 1-4 and anthracite are used. The void fraction of the carbon materials were measured as it was expected to affect the flow of slag into the cokebed. Table 2.7 shows the analysis of the different carbon materials used.

Table 2.7: Calculated void fraction of carbon materials used in the study [15]

Carbon Material	Bulk density (kg/dl^3)	Particle density coke (g/cm^3)	Void fraction (α)
Coke2 3-6mm	0,749	1,82	0,59
Coke3 5-10mm	0,623	1,71	0,64
Coke3 +10mm	0,630	1,78	0,65
Coke4 3-6mm	0,642	1,78	0,64
Coke4 5-10mm	0,745	1,78	0,58
Anthracite 5-10mm	0,970	1,68	0,47
Anthracite +10mm	1,007	1,91	0,42

The results show that the smaller coke gives a higher flow into the cokebed or the same flow at lower temperatures, believed to be due to the higher reduction rate of the smaller coke. The reduction rate is lower for larger size coke which can be seen in experiments with larger sized coke (+10mm). Figure 2.9 shows the results for coke 2, coke 3, coke 4 and anthracite. The figure shows that the melting behaviour and reduction rate is dependent on the size of carbon materials, however the difference between the different sizes may sometimes overlap.

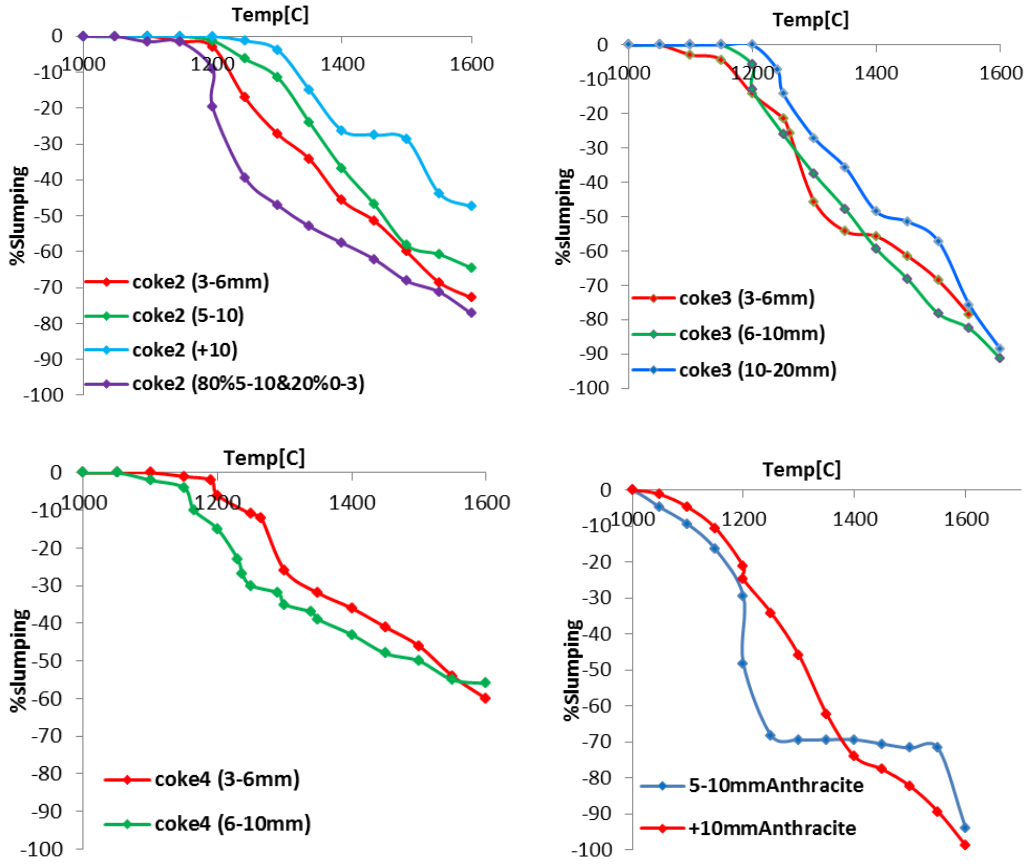

Figure 2.9: Reduction behaviour of manganese raw materials with (a) Coke 2 (b) Coke 3 (c) Coke 4 (d) Anthracite [15]

The study concluded that larger-sized coke had a lower flow of slag, which means lower reduction rate than the tests with small-sized coke, with increasing reduction speed with decreasing coke size. The reduction temperature also decreased some with decreasing carbon material size. In addition, anthracite showed the highest rate followed by coke 3, coke 2 and coke 4. Sessile drop furnace tests showed higher wettability for coke 3 than the other carbon materials.

2.2.2 Studies with sessile drop furnace

Tranell et al. [16] used a sessile drop furnace to test industrial HC FeMn slag with and without metal particles towards industrial coke and eucalyptus charcoal at 1600°C. Reaction time varied between 15 and 30 minutes and both CO gas and argon gas as atmosphere was tested.

The slag used was an industrial HC FeMn slag, which was ground in a carbide disk mill, and then two slags were made by removing the metal (FeMn prills) from one of the slags. Fused slag pieces weighing approximately 0,02 g was used for all tests. The carbon materials were ground to fine powder, sieved, heat treated and added stearic acid before being pressed into substrate disks with diameter 10 mm and thickness 1 mm in a pellet press.

The furnace had argon or CO atmosphere, and the temperature was increased to 950°C in approximately 10 minutes, followed by a rapid heating of 120°C/min to experimental temperature 1600°C. Images were captured every second during the tests. After cooling, the substrates and slag samples were casted in epoxy and investigated by EPMA.

The results indicated that the reduction rate of MnO was higher when initial metal was present in the slag. As for the difference between coke and charcoal as a reducing agent, figure 2.10 shows the development of manganese oxide in the slag as a function of time for tests run on coke and charcoal, using slag with and without metal prills. The figure indicates that the reduction rate is higher when charcoal is used as a reducing agent.

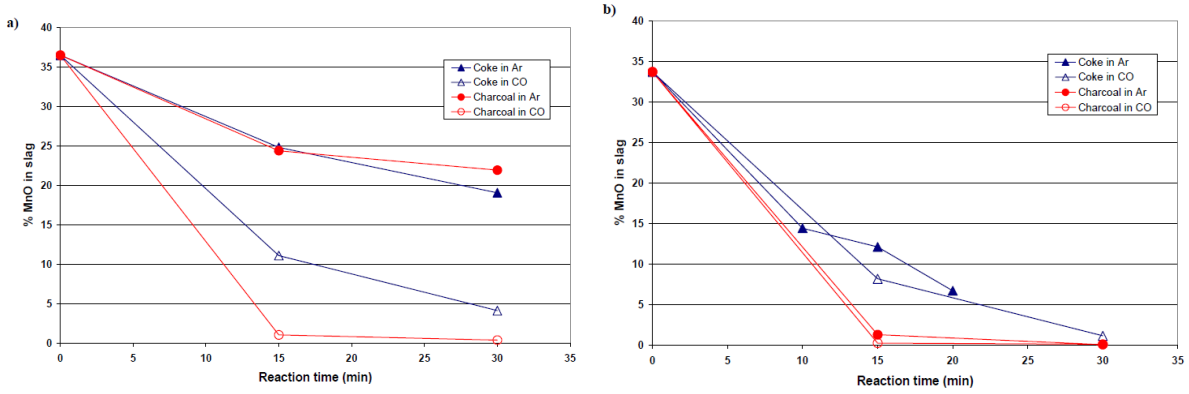

Figure 2.10: Concentration of MnO in reacted slag as a function of time for experiments a) with no metal and b) with metal [16]

The study concluded that initial metal present increased the reduction rate for all materials used compared to no metal present, and that the reduction rate was higher for charcoal than for coke, in general.

Safarian [17] tested synthetic HC FeMn slag with three different MnO contents towards 6 types of graphite, 3 types of coke from single coals, 2 commercial cokes, and charcoal made from eucalyptus in a sessile drop furnace. Both argon and CO atmosphere was tested, at temperatures of 1450°C, 1500°C and 1600°C and hold times of 60, 60 and 30 minutes respectively.

When preparing the slag, fine powders of CaO, MgO, SiO_2 and Al_2O_3 were mixed in a ball mill and melted in a graphite crucible. The slag was then crushed in a carbide disk mill and mixed with MnO, before being melted in a platinum crucible. Slag 1-4 were made by varying the MnO content (45.0, 52.0, 64.5 and 38.7 wt% respectively), and slag 4 also contained FeO (10.4 wt%). The graphites were cut into disks to form a substrate with 10 mm diameter and 3 mm thickness, while coke and charcoal, in addition to some graphite were crushed in a carbide disk mill, sieved to 44-105 µm, added 3 wt% stearic acid as binder and pressed into substrates.

The carbon substrate and a slag particle were placed on the sample holder of the furnace, the furnace chamber was then evacuated and filled with the required atmosphere. The furnace was heated to 950°C in about 10 minutes before it was heated rapidly with a rate of 120°C/min to experimental temperatures of 1450°C, 1500°C and 1600°C where it was held for 60, 60 and 30 minutes, respectively. Pictures were captured every seconds of the tests. The samples from the furnace were analysed using EPMA and SEM.

The results of the tests with graphite showed that the bulk material that was cut into substrates had higher reduction rate than the pressed graphite substrates, as shown in figure 2.11. It was also found that higher temperature gave increased reduction rate of manganese oxide.

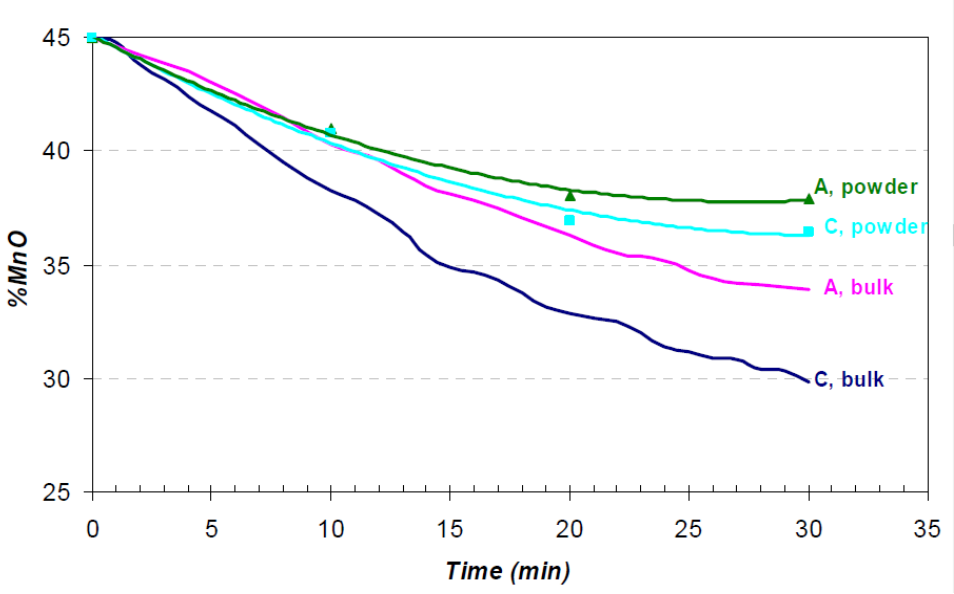

Figure 2.11: The MnO reduction rate by the powder and bulk substrates of graphites A and C at 1600°C in argon atmosphere [17]

Figure 2.12 shows the manganese reduction by different carbon materials. PBC and BBC are industrial cokes while ST, PD and BG are cokes from single coals. The figure shows that charcoal and industrial cokes had faster reduction of manganese oxide than graphite and cokes from single coals.

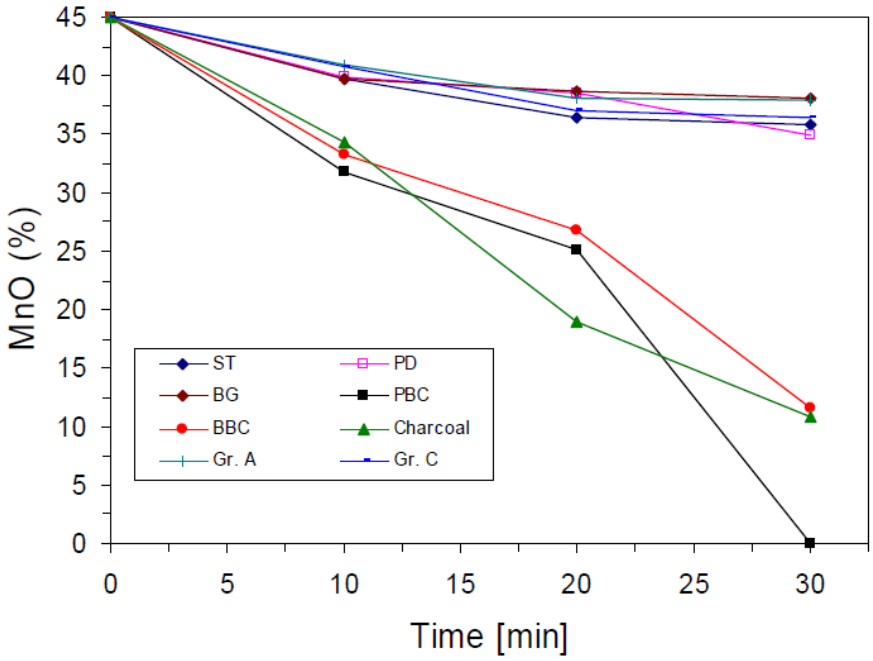

Figure 2.12: The rate of MnO reduction from slag 1 with graphites, cokes and charcoal samples at 1600°C in argon [17]

The study concluded that the carbon materials were not wetted by the slag, as a contact angle between 150° and 160° was observed, and that the MnO reduction rate was affected by the type of graphite substrate used, as higher rate was observed for cut graphite bulk material than for pressed crushed material. Further, the study concludes that the rate of MnO reduction was affected by the type of carbon substrate, it was observed that the charcoal had a higher reduction rate than industrial coke, higher than single coke and higher than graphite. The study also observed evaporation of produced manganese metal.

Safarian et al. [18] tested synthetic and industrial HC FeMn slag with single cokes, industrial cokes and eucalyptus charcoal at 1600°C in CO and argon atmosphere.

The industrial slag was ground in a carbide ring mill, melted in a graphite crucible where the metal and slag phase were separated after quenching. The slag was then ground again, and fused by running an oxygen torch over the powder. The synthetic slag was prepared by mixing all oxides except MnO, melting this, crushing in a disk mill, then mixing this powder with MnO and melting this in a platinum crucible in air. Six carbon materials were used, three synthetic cokes made from single coals, two industrial cokes and an eucalyptus charcoal. All were ground to fine powder, sieved, heat treated in CO at 1600°C, added stearic acid and then pressed into a small graphite crucible.

The furnace was heated slowly to 950°C in approximately 10 minutes before it was heated rapidly at 120°C/min to 1600°C. Images of the slag drop and carbon substrate was captured every second of the test. The test lasted for a predetermined reaction time, after this time the substrates and slag droplets were cast in epoxy and prepared for analysis in EPMA.

The results showed that the reduction rate for manganese oxide was higher for industrial cokes and charcoal than for the single cokes, both for tests run in argon atmosphere and for tests run in CO gas atmosphere, as shown in figure 2.13 (a) and (b). Figure 2.13 (b) also shows that the rate of MnO reduction in CO is initially fast, followed by a slower reduction rate, while figure 2.13 (a) shows that the reduction rates for the single cokes are similar.

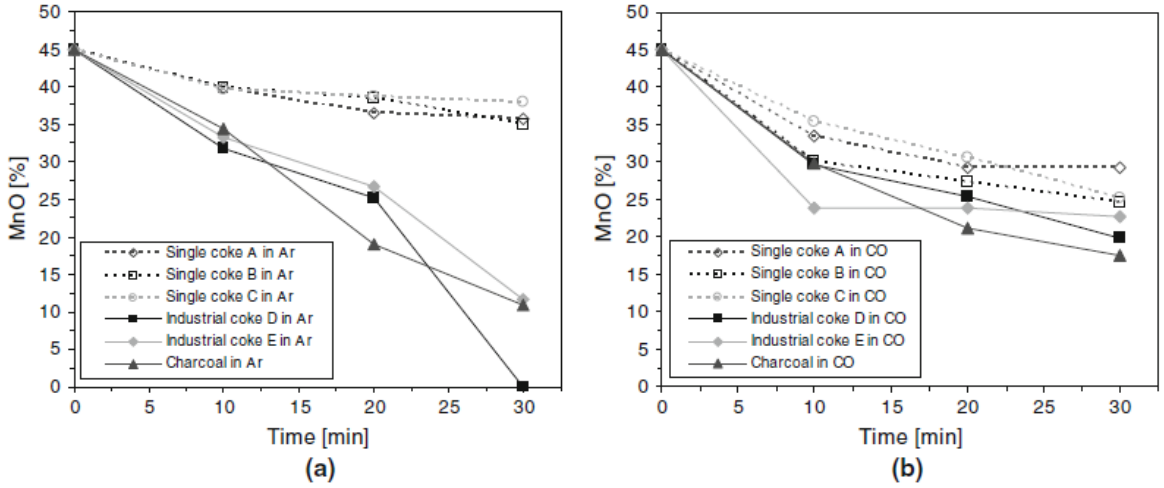

Figure 2.13: Concentration of MnO in reacted synthetic slag with carbonaceous materials as a function of time (a) all substrates in Ar, (b) all substrates in CO [18]

The study concludes that in general, the MnO reduction rate is higher for charcoal than for cokes and that the reduction rate for industrial cokes is higher than it is for the cokes produced from single coals. In addition, that MnO reduction from slags by CO gas is possible.

Safarian and Kolbeinsen [19] tested synthetic ferromanganese slag with six different graphite materials in a sessile drop furnace at 1450°C, 1500°C and 1600°C in argon atmosphere.

The synthetic ferromanganese slag was prepared using powders of oxides, which were mixed in a ball mill before the mixture was melted in a graphite crucible. The slag was then crushed in a carbide disk mill and added MnO before it was melted in a platinum crucible. Six different purified graphites with more than 99,9 wt% fixed carbon content were used. Flat substrates were machined out of graphite blocks, and cut to 3 mm thickness and 10 mm diameter.

A graphite substrate and a 40±1 mg slag particle was placed in the furnace before it was filled with argon gas and heated to 950°C in 10 minutes. The furnace was then heated rapidly with heating rate of 120°C to experimental temperature which was 1450°C, 1500°C or 1600°C. The experimental temperature was held for 60, 60 and 30 minutes respectively. After the tests the samples were weighed, mounted in epoxy and studied by EPMA. Photographs captured during the tests were analysed to obtain slag drop volume and contact angle.

The changes in contact angle were used to evaluate the rate of MnO reduction. The graphites were not wetted by the slag and had a high contact angle, above 150° at the starting point. As the MnO content of the slag did not affect the contact angle much, and there was a lot of fluctuations in the contact angle values, it was difficult to use to find reduction rate of MnO. The volume change of the slag drop was found to be much larger for a certain MnO reduction extent. The slag drop volume was normalized by calculating the slag drop volume over the initial slag drop volume ratio $V_s/V_{s,i}$. Figure 2.14 shows the development of the volume ratio for the different tests.

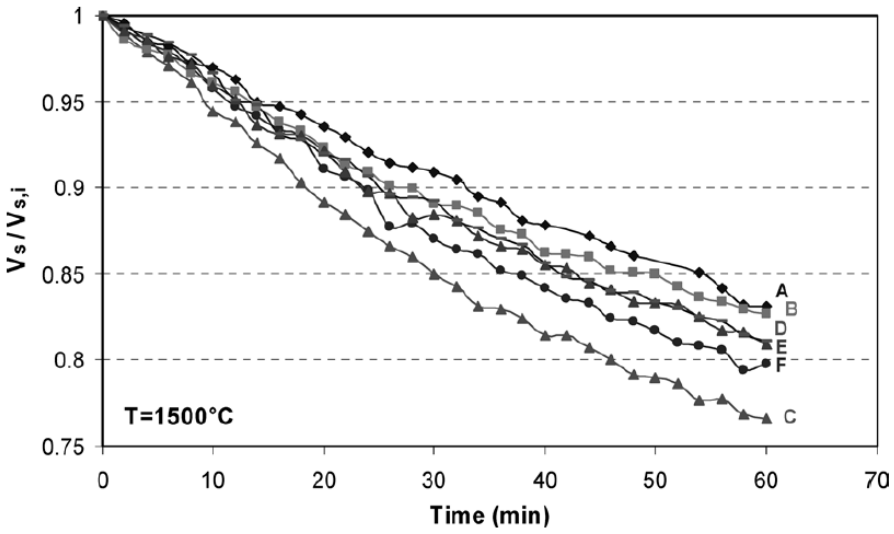

Figure 2.14: The changes in the $V_s/V_{s,i}$ ratio during slag reduction by different graphite substrates at 1500°C [19]

The results of calculating the MnO content development with time showed the same trend for the tests on different graphites at all three temperatures. Only two of the graphites varied some at different temperatures.

The study concluded that the carbon materials were not wetted by high MnO containing slags, and that contact angles above 150° were observed. Further, that the changes in the slag drop volume during reduction were more significant than the changes in the contact angle. The rate of MnO reduction by graphite materials are mainly dependent on temperature and then on carbon properties. The study also observed high evaporation rate of produced manganese through slag reduction in the wettability experiments.

Safarian et al. [20] tested HC FeMn slag with graphite, coke and charcoal in a sessile drop furnace in argon atmosphere at 1600°C. The reduction rates were evaluated by sampling at different reduction times and by chemical analysis of the reduced slag and produced metal.

Synthetic slag was prepared by mixing fine powders of the different oxides, and melting the mix in a graphite crucible. The slag was then crushed in a carbide disk mill before adding MnO and melting in a graphite crucible. The slag was crushed in the carbide disk mill before FeO was added and the slag was melted in a platinum crucible. Pure graphite, a single coke produced from a single coal and eucalyptus charcoal were used as carbon material

substrates. Powders of the materials were prepared in a jaw crusher and then a carbide disk mill, before it was sieved into a size fraction of 44 to 105 µm. The powders were dried at 100°C, added 3 wt% stearic acid then pressed into pellet in small graphite crucibles with a diameter of 10 mm.

The carbon substrate was placed on the sample holder of the furnace, and a 40+-1 mg slag particle was placed on the substrate. The furnace was evacuated and filled with argon gas before the furnace temperature was increased to 950°C in approximately 10 minutes and then heated with heating rate 120°C/min to 1400°C, and kept there for 4 minutes to give FeO time to reduce in a relatively slow reducing stage, before being heated to 1600°C in one minute and kept there for 2, 5 or 8 minutes. The furnace was then cooled fast, and the samples were mounted in epoxy and analysed by EPMA.

The results of the EPMA are shown in figure 2.15. The figure shows the analysis of manganese oxide and iron oxide in the samples run on different carbon material. The figure shows that the reduction of iron oxide was dependent on the carbon material, and that the greatest reduction rate was obtained with coke, and least reduction rate was obtained with graphite. The figure also shows that the content of manganese oxide increases some at first, as the iron oxide content decreases. The manganese oxide reduction is affected by the carbon material used, and the greatest reduction rate is obtained by coke, while the least is obtained by graphite.

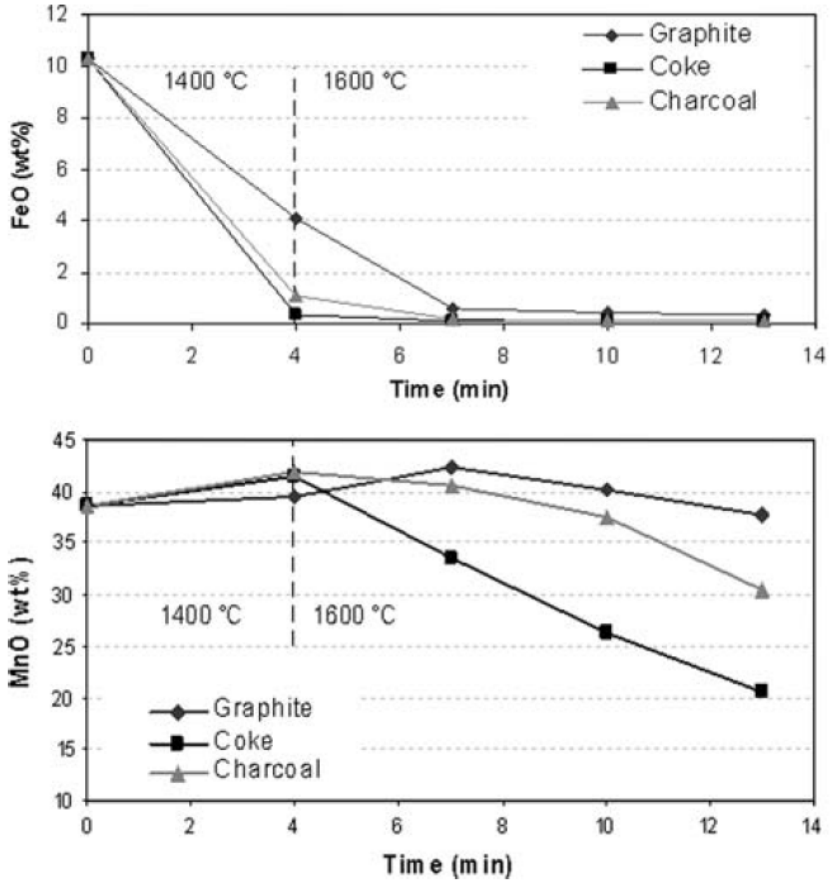

Figure 2.15: The changes in the FeO and MnO concentrations in slag during reaction with carbon materials [20]

The study concluded that the reduction of MnO and FeO takes place simultaneously, with a fast initial rate of FeO reduction and that the MnO reduction is initially slow and that the speed increases significantly after the FeO reduction stage. The reduction of MnO and FeO are affected by the carbon material used. The slag is reduced faster by coke than by charcoal, and much faster than by graphite. The study also observed evaporation of produced manganese.

Sun et al. [21] tested synthetic and industrial FeMn slag with graphite and coke in a sessile drop furnace at 1450-1550°C in argon atmosphere.

The slags used were three industrial MnO-SiO_2-CaO-Al_2O_3-MgO-Na_2O-Fe multicomponent slags and three synthetic MnO-SiO_2-CaO-Al_2O_3 quaternary slags. The synthetic slags were prepared by mixing SiO_2, CaO and Al_2O_3, melting in a muffle furnace, crushing and grounding the slag before mixing with MnO. The mixture was then sintered in an induction furnace, and the sinter was ground and pressed into tablets. Four different carbonaceous materials with two different surface roughnesses were used; three cokes and a graphite. These materials were cut into plates of 10x10x2 mm, followed by surface progressive grinding. Several of the substrates were roughened while other were polished.

A solid slag sample was mounted on the substrate, which was placed on the sample holder. The furnace was filled with argon gas, the temperature was heated rapidly until the slag was melted and was kept there for a decided amount of time, 1-3 hours. The gas from the furnace was analysed for gas composition by an IR gas analyser. The slag samples were analysed by XRF. The carbon substrate and slag sample was mounted in resin and the slag-substrate interface was analysed by SEM.

The results of the XRF analysis for test 1, the development of MnO and SiO_2 content with time are shown in figure 2.16. The figure shows that the manganese oxide content of the slag decreases with time, and that there is an initial increase in silicon oxide content, both are results of manganese oxide reduction from the slag. Silicon oxide is also reduced from the slag. This trend was more obvious for experiments in which coke and/or industrial slag was used.

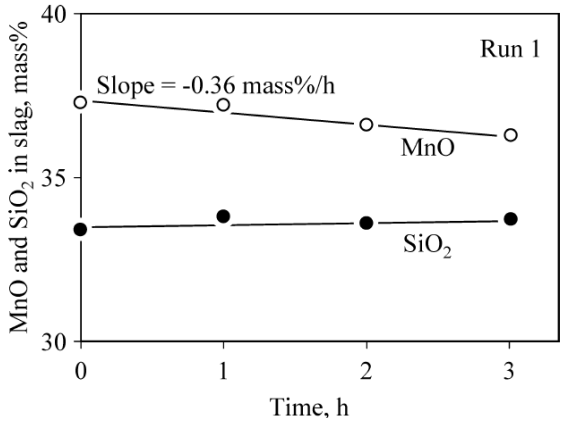

Figure 2.16: Variation of MnO and SiO_2 content in slag with time for run 1 [21]

The reduction rate of MnO was approximated by finding the slope of the MnO concentration line for each experiment, as shown in figure 2.15 for experiment 1. The results showed that the reduction of manganese oxide from the slag at 1450°C was below the detectable level, and that it increased significantly as temperature was increased to 1550°C. The results also showed that the reduction rates in tests with coke substrates or industrial slags were generally higher than in tests with graphite substrates and synthetic slags.

The study concluded that the reduction rate of manganese oxide increased with increasing manganese oxide content in the slag, temperature, and ash content in the coke. Further, that the MnO reduction rate was higher for the industrial slag than for the synthetic slag and that the MnO reduction rate was higher when coke was used than when graphite was used as substrate. Further, a correlation between MnO reduction rate and contact angle was observed, where a tendency for the reduction rate to increase with decreasing contact angle or better wettability was observed.

Safarian and Tangstad [22] tested synthetic FeMn slag with industrial coke and charcoal made from eucalyptus in a sessile drop furnace at 1500°C and hold times of 15, 30 and 60 minutes, in argon atmosphere.

Powders of pure oxides were mixed for the synthetic slag. The mix was then melted in a graphite crucible, and the obtained slag was crushed using a carbide disk mill. The powder was then added MnO, FeO and CaS, and was melted in a platinum crucible. The carbon materials were cut into discs to use as substrates.

Pieces of synthetic slag with 100±1 mg weight was placed on the carbon substrate on the sample holder of the furnace. The furnace was evacuated and filled with argon gas, was then rapidly heated to 1500°C and was held at this temperature for 15, 30 or 60 minutes before being rapidly cooled. A camera captured pictures during the tests, and the samples were analysed by EPMA.

Results of the EPMA showed that the average MnO content of the tests run for 60 minutes were around 10% lower for tests run with coke substrate (33,4% MnO) than for tests run with charcoal substrates (43,9% MnO). This indicates that the coke substrates were more reactive than the charcoal substrate. As the tests run for 15 and 30 minutes had a two-phase slag, with following difficulties of analysing slag composition with EPMA, the normalized slag drop volume, $V_s/V_{s,i}$ was plotted, and is shown in figure 2.17. The slope of the curve can be considered as the slag-carbon reactivity parameter. The figure indicates that coke substrates has a higher slag-carbon reactivity than charcoal substrates, and higher reactivity for coke than for charcoal is observed.

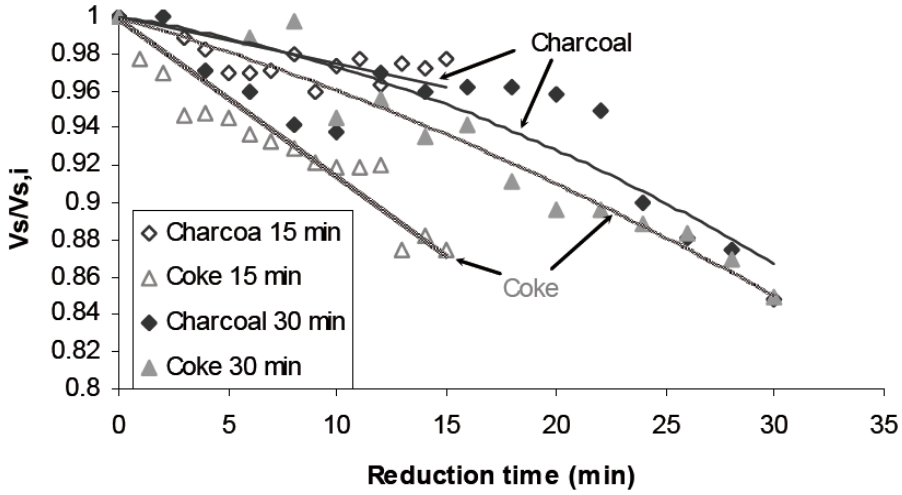

Figure 2.17: The changes of the normalized volume of slag droplet reduced by carbon substrates at 1500°C within 15 and 30 minutes [22]

The study found that the reactivity of synthetic FeMn slag was higher towards coke substrates than towards charcoal substrates.

Nadir [14] tested synthetic and industrial slag with coke, anthracite, graphite and carbon black in a sessile drop furnace, in CO atmosphere at 1600°C. The carbon black was pressed into pellets using a uniaxial press, while the coke, graphite and anthracite were grinded into pellets. A total of seven experiments were performed, four with synthetic slag and three with industrial slag. The development of the sum of reducible oxides, volume fraction and contact angles were recorded for all tests.

Figure 2.18 shows the composition profile curve, while figure 2.19 shows the volume fraction curve of the different tests. The composition profile curve showed similar trends for all the experiments. The first 5 minutes after melting had a higher negative slope which indicates higher reduction rate, for the temperature range 1200-1300°C, which means that this reduction is primarily FeO reducing to Fe. The second part of the curve represents MnO and SiO_2 reduction, shows a limited slope which is primarily a result of the MnO reducing to Mn and secondarily SiO_2 reducing to Si. The curves suggests a very limited extent of reduction for both industrial and synthetic slag. The volume fraction curve shows similar results as the composition profile curve, the first part shows a negative slope as the iron oxide reduces to iron, then the second part show little change as there is very limited reduction of silicon oxide and manganese oxide.

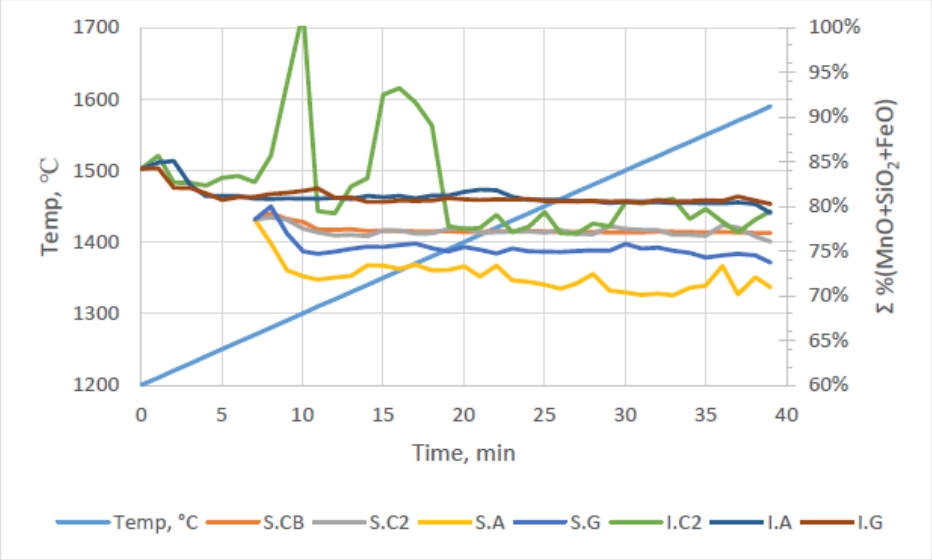

Figure 2.18 Temperature and sum of reducible oxides vs time profiles for all the sessile drop experiments [14]

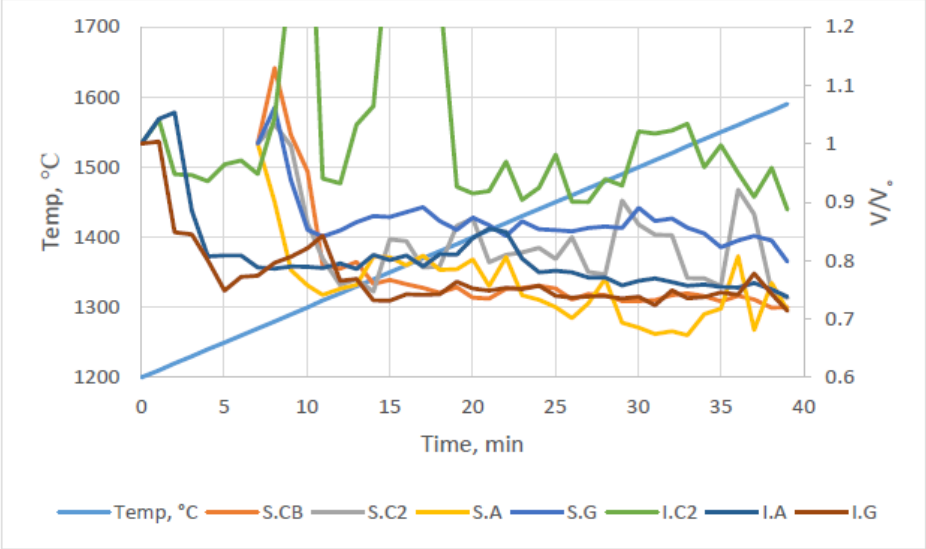

Figure 2.19: Temperature and V/V_s vs time profiles for all the sessile drop experiments [14]

The study observes that the reactivity of all different carbon substrates toward synthetic and industrial charge is very low, and that MnO is the main constituent of reducible oxides to have actually undergone reduction. The study conclude that the difference in reactivities of different carbon substrates are minimal, and that the higher reactivities obtained in induction 3 and 4 performed in the same study, mentioned in chapter 2.21, is not a consequence of the higher reactivity of coke 2 over graphite.

2.3 Effect of sulphur in the slag on reduction rate

Nadir [14] tested synthetic slag with and without sulphur in an induction furnace with coke and graphite. Two tests were run for synthetic slag with sulphur, and two tests were run for slag that did not contain sulphur. Induction test 1 and 3 had slag that contained sulphur, test 2 used industrial slag, while test 4 had synthetic slag that did not contain sulphur. Test 1 and 2 were carried out with graphite, while 3 and 4 were carried out with graphite and coke. Figure 2.7 which was shown in section 2.2.1 shows the amount of reducible oxides for the four tests, and how they develop over time. The figure shows that test 3 has a faster declining trend of the reducible oxides, which indicates that the reduction rate is higher for this test than for test 4 that has the same carbon material and synthetic slag without sulphur.

The study concluded that addition of sulphur in the synthetic slag enhanced the reduction rate as observed from a faster reduction rate in induction test 3 compared to induction test 4.

Kim and Tangstad [23] tested three different charges, where one contained Assmang ore, one contained HC FeMn slag and one contained a mix of ore and HC slag, with coke as a reducing agent. The charges were melted in a graphite crucible in a TGA furnace in CO atmosphere, and 16 experiments were run for each charge type, where the hold temperature varied with 10°C for each run, in the temperature range 1500-1650°C. The furnace temperature was first increased rapidly to 1200°C, held there for 30 minutes to ensure complete pre-reduction, before it was increased to hold temperature. During the experiments, the mass change data were logged every 5 second, and charge samples were mounted in epoxy and analysed by EPMA.

The study found that the initial amount of sulphur in the charges seemed to explain the different reaction rates observed. The assmang charge had 0,16 wt% initial sulphur content, and the lowest reduction rate, while the mixed charge had 0,29 wt% sulphur and the reduction rate was higher than for the assmang charge. The HC FeMn slag charge had 0,39 wt% sulphur initial content, and had a lower reduction rate than the mixed charge, which may imply that there is an optimal amount of sulphur for maximizing its effect on the reduction rate. Figure 2.20 shows rate constants found in the study compared to the initial amount of sulphur in the charge.

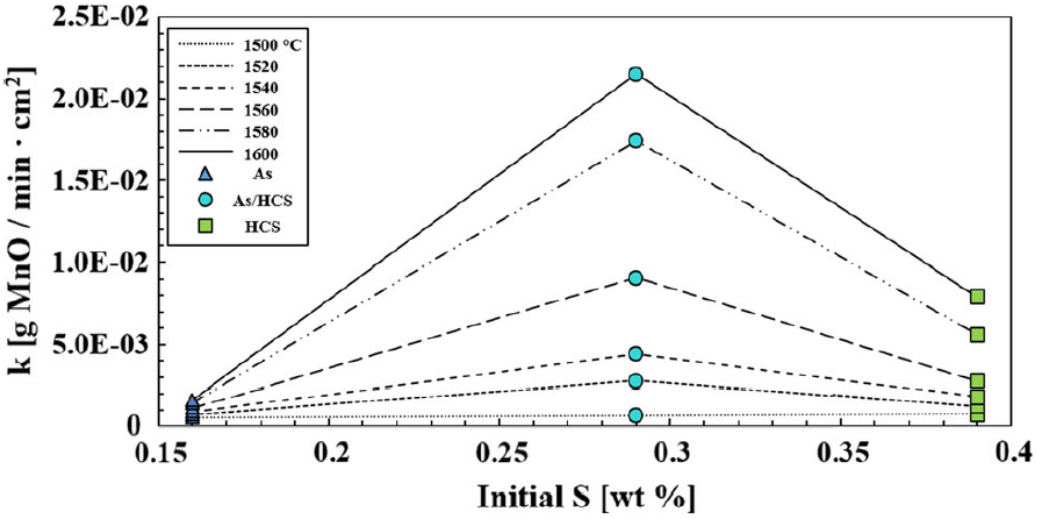

Figure 2.20: Rate constants compared with initial sulfur amount at different temperatures [23]

The study concluded that the reduction rates were more affected by small amounts of sulphur than the slag basicity. Further, that sulphur was observed to increase the reduction rate, but that further experiments were required to isolate the effect of sulphur.

Li and Tangstad [24] tested synthetic slag with four different contents (0, 0.2, 0.44 and 1.0 wt%) of sulphur towards carbon black in a vertical graphite tube furnace and a sessile drop furnace in CO atmosphere.

In the vertical graphite tube furnace the charge was added to a graphite crucible, the furnace was heated to 1250°C and kept there for 30 minutes before it was heated to 1600°C and kept there for 60 minutes. The weight loss of the samples were recorded every 5 seconds. For the tests in the sessile drop furnace, the carbon black was first pressed into substrates, slag and substrate was then placed in the furnace and heated rapidly to 1200°C before being heated more slowly to 1600°C. images were captured from the furnace every 0.5 seconds.

Figure 2.21 shows the recorded weight loss with time for the four slags when run in the vertical tube furnace. The figure shows that the weight loss increases with increasing sulphur content, except for slag with the highest content of sulphur (1wt%), that has less weight loss than the slag with 0,44 wt% sulphur. This indicates that the sulphur increases the reduction rate, and that there is an optimal sulphur content.

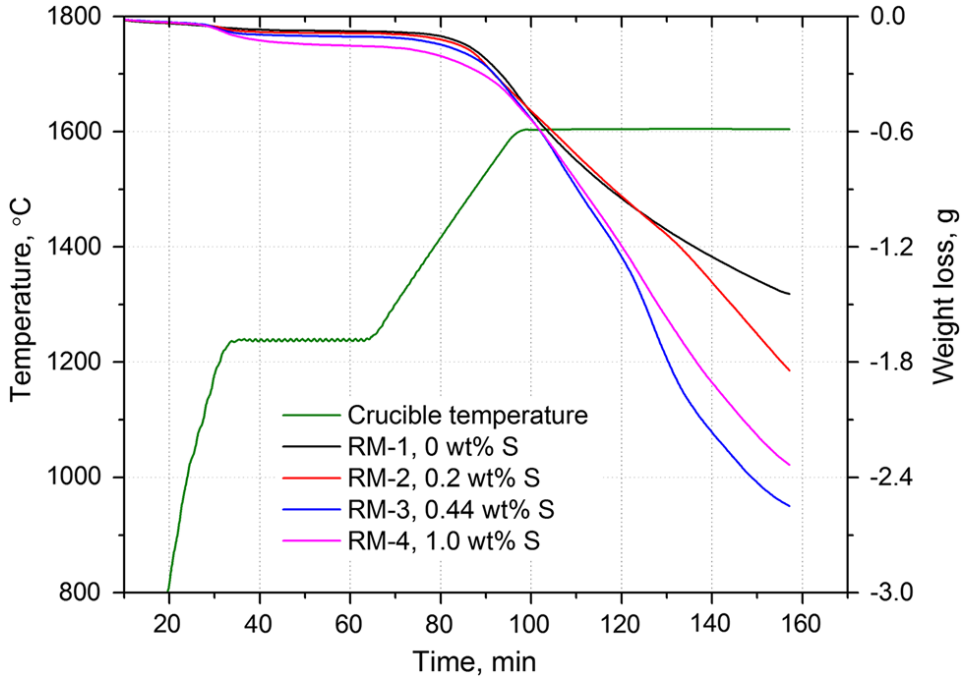

Figure 2.21: Temperature profile and thermogravimetric curves for experiments with different sulfur contents in slag using carbon black as the reductant [24]

The study confirmed that small amounts of sulphur in the slag significantly improved the reduction of MnO and SiO_2. The study also concluded that the sulphur content did not have an obvious effect on contact angle between slag and carbon black. The study also observed that the manganese content in the metal decreased with increasing sulphur content, a result of the silicon and iron content in the metal increasing with increasing sulphur content.

2.4 Argon vs CO as reduction atmosphere

Tranell et al. [16] tested industrial HC slag with industrial coke and eucalyptus charcoal in a sessile drop furnace at 1600°C, and tested argon and CO gas as furnace atmosphere. The samples were then investigated in an EPMA.

Figure 2.22 shows the MnO reduction and how it develops over time for the two carbon materials. As can be seen from the figure, the tests run with both coke and charcoal in argon atmosphere has a less steep slope for manganese oxide content in the slag than the tests run with charcoal and coke in CO gas. This indicates that the reduction rate of manganese oxide in the slag is higher when CO gas is used, both for coke and charcoal as a substrate.

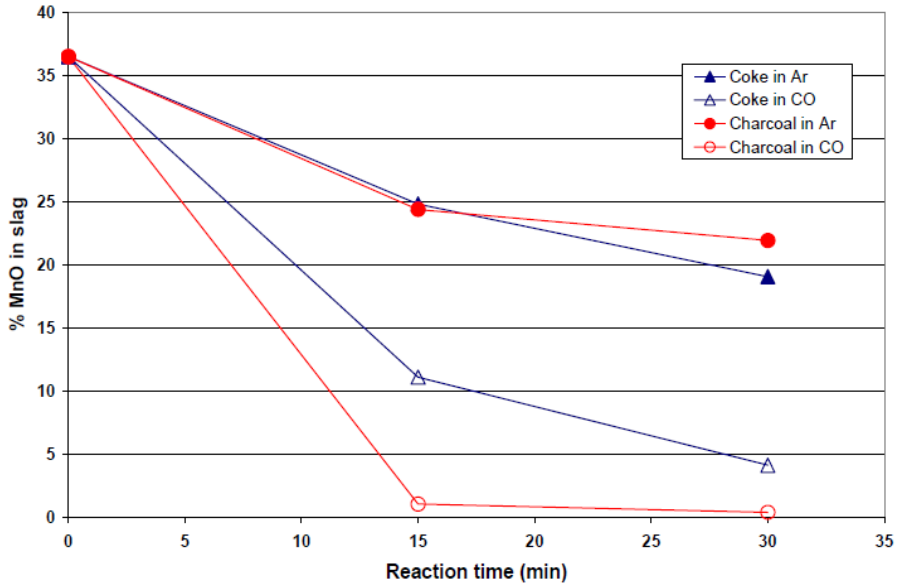

Figure 2.22: The concentration of MnO in reacted slags as a function of time [16]

The study concluded that CO gas as furnace atmosphere gave a higher reduction rate of manganese oxide than argon gas as furnace atmosphere.

Safarian [17] tested synthetic FeMn slag with graphites, cokes from single coals, industrial cokes and charcoal in a sessile drop furnace at 1450, 1500 and 1600°C in CO and argon atmosphere.

Figure 2.23 shows the reduction of manganese oxide in argon and CO atmosphere for single cokes at 1600°C. The figure shows that the tests run in CO gas had higher reduction rate of manganese oxide than the tests run in argon gas when single coke substrates were used.

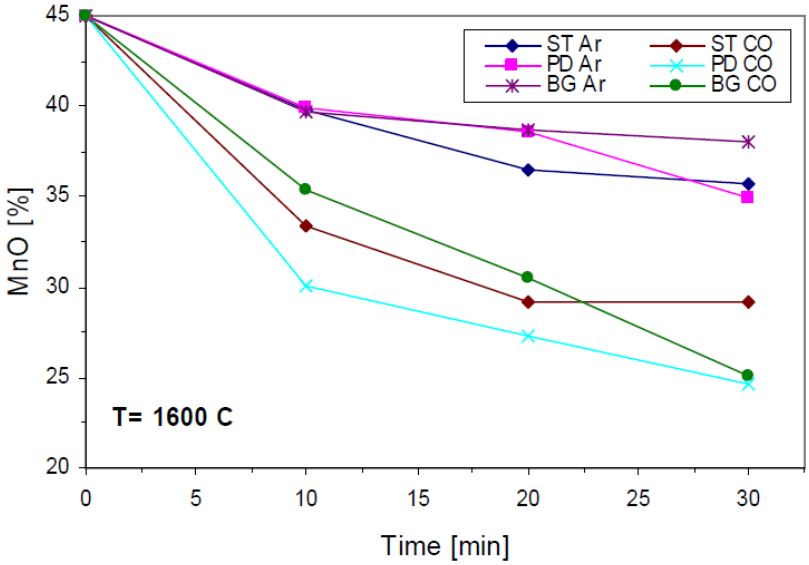

Figure 2.23: The MnO reduction by single cokes in Ar and CO gases at 1600°C [17]

The study concluded that the rate of MnO reduction from high MnO containing slags in argon gas atmosphere were lower than in CO gas atmosphere.

Safarian et al. [18] tested industrial HC FeMn slag and synthetic slag with synthetic coke made from a single coal, industrial coke and eucalyptus charcoal in argon and CO gas atmospheres. The synthetic slag was also tested with glassy carbon substrate in argon and CO gas atmosphere. The samples from the tests were investigated using EPMA.

The results of the tests run with industrial slag towards industrial coke and charcoal indicated a clear trend that the reduction of manganese oxide was higher in CO gas, for both carbon materials. The tests run with synthetic slag towards three different single cokes indicated that the reduction rate of manganese oxide was higher in CO gas than in argon gas. Tests run with synthetic slag towards industrial cokes and charcoal did not show a clear trend.

Figure 2.24 shows the results from the tests run with synthetic slag towards mirror and rough surfaces of glassy carbon. The figure shows a clear trend of a higher reduction rate of manganese oxide from the slag when CO gas is used as reduction atmosphere.

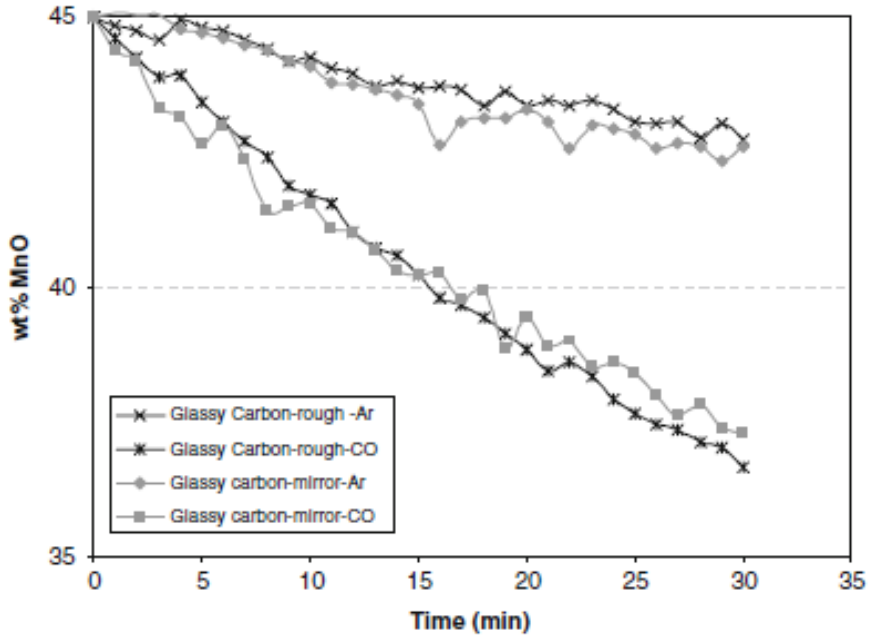

Figure 2.24: Changes in the MnO content of synthetic slag during reduction in Ar and CO atmospheres on mirror and rough surfaces of glassy carbon [18]

The study concluded that a reduction in CO gives a higher initial reduction rate than a reduction in argon does. However, an argon gas atmosphere provided a higher extent of reaction.

3. Experimental

3.1 Method

Two variations of synthetic silicomanganese slag were prepared by mixing appropriate amounts of the different oxides, and then pressed into pellets. Synthetic slag was used instead of industrial slag to ensure homogeneous composition, and the wanted composition of the slag.

Due to varying porosity and hardness of the carbon materials charcoal and coke, they were crushed, sieved and pressed into pellets in the form of discs. The weight and density of the carbon material pellets were recorded. The properties of charcoal and coke are not necessarily homogeneous distributed, which also is a motivation for crushing and pressing the material into discs. [17]

The tests were performed in a sessile drop furnace where a carbon material pellet and a slag pellet was tested. The two carbon materials and the two slags were tested with each other at three different reduction times, 5, 15 and 30 minutes. The development of the slag drop during tests was recorded by a camera, and the slag drop volume and contact angle were measured.

After the tests, the slag samples were casted in epoxy or iodine epoxy and then grinded and polished to get a surface of the slag and metal for analysis. They were then analysed with a scanning electron microscope (SEM), and the results were assessed with regards to silicon oxide and manganese oxide reduction. At the end of the project, the samples were analysed with an electron probe micro analyzer (EPMA) to verify the results from the SEM.

3.2 Slag preparation

The master slag used in this project was the same slag as was used in the specialisation project TKP4580 [25]. The total amount of master slag was 22,6 g, and it was prepared in September 2018 by adding more silicon oxide, manganese oxide and sulphur oxide to an already existing slag. The contents of the slag before and after addition of the oxides are listed in table 3.1, while table 3.2 shows the distribution of oxides in the master slag by weight percentage.

Table 3.1: Contents of slag before and after addition of extra oxides fall 2018

	MnO	**SiO_2**	**Al_2O_3**	**CaO**	**MgO**	**Fe_2O_3**	**FeS**
Before [g]	7,47	6,39	1,66	2,58	0,66	1,22	-
Addition [g]	2,43	0,41	-	-	-	-	0,27
Final content [g]	9,90	6,80	1,66	2,58	0,66	1,22	0,27

Table 3.2: Distribution of oxides in master slag by weight percentage

	MnO	**SiO_2**	**Al_2O_3**	**FeO**	**CaO**	**MgO**	**S**
[wt%]	42,88	29,45	7,19	6,02	11,17	2,86	0,43

This master slag was divided into two parts, where one part made slag 1 and the other part was adjusted by addition of oxides to make slag 2.

3.2.1 Slag 1

The portion of the master slag that was used as slag 1 weighed 6,0 g and the components of the slag are listed in table 3.3, calculated content by weight from the contents of the master slag, and the calculated oxide contents by weight percentage.

Table 3.3: Calculated contents of slag 1 by weight and weight percentage

	Calculated [g]		**Calculated [wt%]**
MnO	2,57	*MnO*	42,88
SiO_2	1,77	*SiO_2*	29,45
Fe_2O_3	0,32	*FeO*	6,02
Al_2O_3	0,43	*Al_2O_3*	7,19
CaO	0,67	*CaO*	11,17
MgO	0,17	*MgO*	2,86
FeS	0,07	*S*	0,43
Total	6,00	*Total*	100,0

The slag was pressed into pellets with a diameter of 5mm using an uniaxial press. The pellets were pressed for approximately 15 seconds under 1kN pressure. The mass was weighed before pressing, and was approximately the same for all pellets, around 0,1 g. Some mass was lost when adding the powder to the press, the weight of the pellets are listed in table 3.4. The pellets are numbered using the number 1 and a letter, which describes that the pellets are made from slag 1.

Table 3.4: Weight of pellets made from slag 1

Pellet number	**Weight of pellet [g]**
1A	0,1002
1B	0,0993
1C	0,1042
1D	0,1033
1E	0,1034
1F	0,1004
1G	0,1002
1H	0,0985
1I	0,1037
1J	0,1012
1K	0,0988
1L	0,0991
1M	0,0998
1N	0,1077
1P	0,1033

3.2.2 Slag 2

The remaining 15,4g of the master slag was basis for slag 2. The slag was added manganese oxide, silicon oxide, iron(III) oxide and iron sulphate according to table 3.5. The total amount of slag 2 after addition was 20,36 g, likely due to some slag loss when transferring it between containers.

Table 3.5: Calculated and weighed additions to master slag to make slag 2

	Calculated amount [g]	**Weighed amount [g]**
Original slag	15,4	15,4
MnO	2,67	2,67
SiO_2	1,47	1,47
Fe_2O_3	0,81	0,81
FeS	0,07	0,07
Total weight	20,42	20,36

Slag 2 was then mixed in a carbide disk mill, to ensure homogenous particle size and distribution. The disk was first cleaned by running quartz in it two times, in addition to washing and drying the mill chamber in between. After the mill was washed, slag 2 was added to the mill chamber, and was run in the mill twice for 45 seconds at 700 rpm. Table 3.6 lists the components of slag 2 by weight and weight percentage

Table 3.6: Calculated contents of slag 2, by weight and weight percentage

	Calculated [g]		**Calculated [wt%]**
MnO	9,27	*MnO*	45,42
SiO_2	6,01	SiO_2	29,41
Fe_2O_3	1,62	*FeO*	8,72
Al_2O_3	1,11	Al_2O_3	5,42
MgO	0,44	*CaO*	8,43
CaO	1,72	*MgO*	2,16
FeS	0,25	*S*	0,4

Slag 2 was then pressed into pellets using an uniaxial press with diameter 5 mm, and approximately 0,1 gram of slag 2 was pressed under approximately 1kN for 15 seconds. The weights of the pellets are listed in table 3.7. The pellets are numbered by letters in addition to the number 2, which indicates that these pellets are made from slag 2.

Table 3.7: Weight of pellets made from slag 2

Pellet number	**Weight of pellet [g]**
2A	0,1076
2B	0,0952
2C	0,0998
2D	0,1002
2E	0,1062
2F	0,1077
2G	0,1048
2H	0,1013
2I	0,1084
2J	0,0995
2K	0,1079
2L	0,1021

3.3 Carbon material preparation

Coke and charcoal were used as substrates for the experiments. The coke that was used in this project was the same as coke A from the specialisation project TKP4580, while the charcoal used in this project was the charcoal made from hardwood used in project TKP4580 [25].

3.3.1 Coke

Some properties of the coke material used are listed in table 3.8. The table includes moisture content, fixed carbon content, volatile matter content, ash content, and the content of phosphorus and sulphur for the coke. Figure 3.1 shows a picture of the coke pieces before crushing to powder.

Table 3.8: Properties of the coke used. Complements of Ferroglobe Mangan Norge

	H_2O %	**Fix C %**	**Vol %**	**Ash %**	**P %**	**S %**
Coke	12,8	89,15	1,17	9,68	0,07	0,49

Figure 3.1: Picture of the coke before crushing

The coke was crushed using a mortar. Due to the hardness of the coke, this was a time-consuming process. The coke was then sieved into the fractions less than 100 µm, 100-250 µm and more than 250µm. The fraction of 100-250µm was added 30 wt% water and 3 wt% binder, as listed in table 3.9.

Table 3.9: Weight distribution of coke, binder and water for pellet mix

Coke, 100-250µm	**Binder, CMC**	**Water**
4,0106 g	0,1784 g	1,7818 g

This mix was pressed in an uniaxial press, at approximately 9 kN for 15 seconds and with a diameter of 10 mm. There was some trouble when pressing the pellets, since the pellet did not easily loosen from the surfaces of the pressing tools. This gave pellet 0-3 uneven surfaces at one side, and pellets 4-15 were therefore pressed into graphite cups so that only one side of the pellet needed to be loosened from the pressing tools, and this resulted in even surfaces of the pellets. After pressing, the pellets were placed in a heating cabinet and dried at 100°C for 24 hours. Table 3.10 lists weight pressed, weight of pellet before drying, weight of pellet after drying and height of pellet measured after drying. As the table shows, some mass was lost during pressing, this was mostly water.

Table 3.10: Weights and height of coke pellets

Number	**Mass pressed [g]**	**Wet pellet weight [g]**	**Dry pellet weight [g]**	**Dry pellet height [mm]**
0	0,2900	0,2140*	0,1878*	2,25*
1	0,5118	0,4160*	0,3544*	4,15*
2	0,4230	0,3303*	0,2785*	3,29*
3	0,4003	0,3210*	0,2385*	3,41*
4	0,2505	0,5473	0,5330	4,63
5	0,2167	0,5182	0,5099	4,32
6	0,2140	0,5215	0,5167	4,41
7	0,2160	0,5252	0,5179	4,46
8	0,2157	0,5235	0,5175	4,45
9	0,2050	0,5104	0,5059	4,33
10	0,2028	0,5138	0,5090	4,41
11	0,2048	0,5151	0,5151	4,46
12	0,2034	0,5138	0,5127	4,54
13	0,2090	0,5167	0,5146	4,55
14	0,2045	0,5197	0,5159	4,58
15	0,2008	0,5104	0,5063	4,54

*Pellets 0-3 were not pressed into graphite cups, affecting weight and height.

3.3.2 Charcoal

Some properties of the charcoal materials are listed in table 3.11. The table includes the moisture content, ash content, volatile matter contents and fixed carbon. The two latter on a dry basis (d.b) and dry ash free basis (daf). This charcoal is made from hardwood and is complementary of RISE PFI. Figure 3.2 shows a picture of the charcoal before crushing.

Table 3.11: Properties of charcoal materials used. Complements of Rise PFI

	H_2O	**Ash (750°C)**	**volatile matters**		**C-fix**	
	wt%	wt%, d.b.	wt%, d.b.	wt%, daf	wt%, d.b.	wt%, daf
Charcoal	7,4	1,9	20,5	20,9	77,6	79,1

Figure 3.2: Picture of charcoal before crushing

The charcoal was crushed in a mortar. The porous nature of the charcoal made the crushing an easy task. The crushed charcoal was then sieved and divided into fine material below 100µm, a fraction of 100-250µm, and larger material with size above 250µm. The fraction of 100-250µm was added 60 weight% water and 3 weight% binder. The water content was increased from 30% used in specialisation project TKP4580 to 60% as 30% was not enough to mix the charcoal into a coherent mass before pressing. Table 3.12 shows the weights of the charcoal, binder and water mixed.

Table 3.12: Weight distribution of charcoal, binder and water for pellet mix

Charcoal, 100-250µm	**Binder, CMC**	**Water**
3,4956 g	0,2858 g	5,6917 g

The mass was then pressed into pellets with diameter 10mm, each pellet being pressed into a graphite cup. This to increase the weight of the pellet to stabilize it in the furnace, as there were experienced problems with the charcoal pellet moving inside the furnace during tests performed in the specialisation project TKP4580. The pellets were pressed for 15 seconds at approximately 9 kN. The pellets were then placed in a heating cabinet and dried at 100°C for 24 hours. Table 3.13 shows an overview of the pellets pressed, with mass pressed, weight of wet and dry pellet with graphite cup, and height of dry pellet with graphite cup.

Table 3.13: Weights and heights of charcoal pellets

Number	**Mass pressed [g]**	**Weight of wet pellet w/ graphite cup [g]**	**Weight of dry pellet w/ graphite cup [g]**	**Height of dry pellet w/ graphite cup [mm]**
1	0,210	0,4339	0,4091	4,16
2	0,2035	0,4345	0,4056	4,13
3	0,2170	0,4497	0,4169	4,24
4	0,2113	0,4433	0,4119	4,21
5	0,1988	0,4434	0,4107	4,15
6	0,2160	0,4538	0,4180	4,27
7	0,2181	0,4491	0,4143	4,19
8	0,1991	0,4399	0,4045	4,07
9	0,2166	0,4563	0,4159	4,23
10	0,2093	0,4545	0,4145	4,27
11	0,2113	0,4500	0,4086	4,17
12	0,2155	0,4477	0,4197	4,34
13	0,2173	0,4536	0,4231	4,46
14	0,2012	0,4511	0,4201	4,31
15	0,2040	0,4558	0,4227	4,42
16	0,2140	0,4680	0,4310	4,49

3.4 Sessile drop furnace tests

The furnace used for the tests was a sessile drop furnace. This furnace was circular with an outer shell with water cooling and a temperature element and inner shell made from graphite. The furnace has a sample holder made from graphite which is inserted to the middle of the furnace during tests. The temperature is controlled by a thermocouple placed under the sample holder and a Keller PZ40 pyrometer measures the temperature of the sample holder. Images can be recorded during tests using a Sony XCD-SX910CR digital video camera with a Navitar 1-50993D telecentric lens. Tests can be performed in vacuum, argon or CO-gas atmosphere. Figure 3.3 shows a picture of the furnace, where the pyrometer and sample holder can be seen on the left side of the furnace and the thermocouple and camera can be seen at the right side of the furnace. Figure 3.4 shows a schematic overview of the experimental setup.

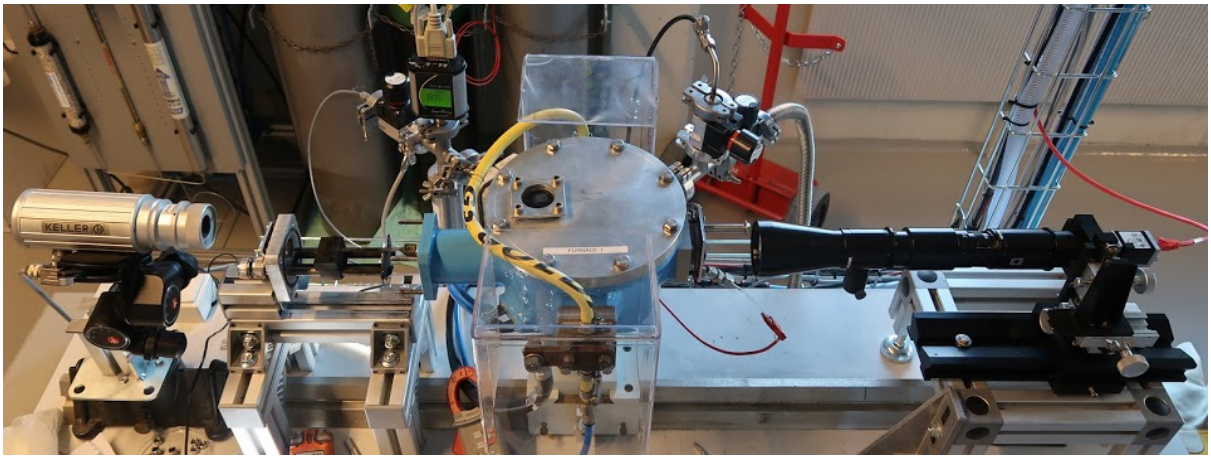

Figure 3.3: Picture of the sessile drop furnace used in the tests

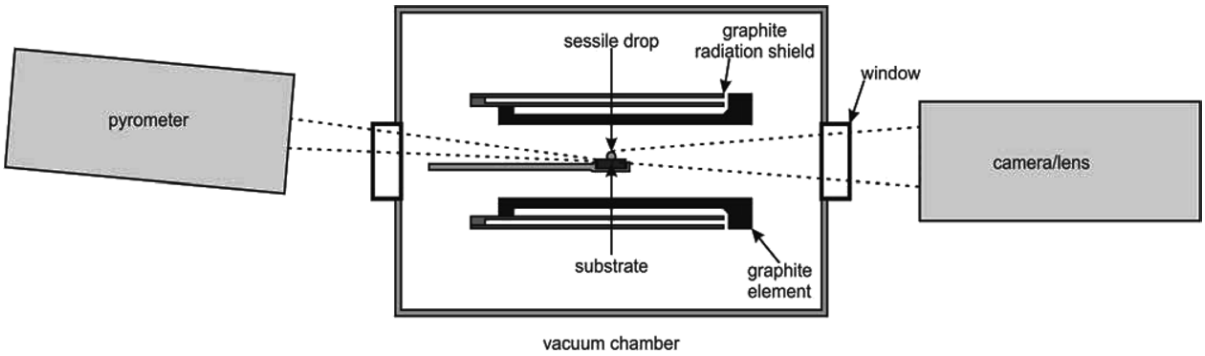

Figure 3.4: Schematic overview of the experimental setup.

During the project, a total of 22 test were performed. The tests were run in a sessile drop furnace, in CO atmosphere, and at 1600°C. The carbon pellet was placed on the sample holder and the slag pellet was placed centered on top of the carbon pellet, before the furnace was closed and the sample holder inserted to the center of the furnace. A vacuum pump was used to evacuate the furnace, before it was filled with CO-gas. The current schedule was then started, and the furnace was heated to 1600°C by the heating curve

shown in figure 3.5. During heating the furnace was kept at 1250°C for one minute to give the iron oxide in the slag time to reduce to metallic iron. As the furnace temperature reached 1600°C, the time was started, and the furnace was kept at this temperature for a certain hold time. In two of the tests the slag drop moved to close to the edge of the carbon pellet, and the test was stopped before the hold time was reached. The flowrate of CO-gas was 0,1 L/min, until the two last minutes of cooling when the furnace was flushed with argon gas at 0,5 L/min. The furnace was then evacuated and filled with argon gas, before it was opened and the sample removed from the furnace.

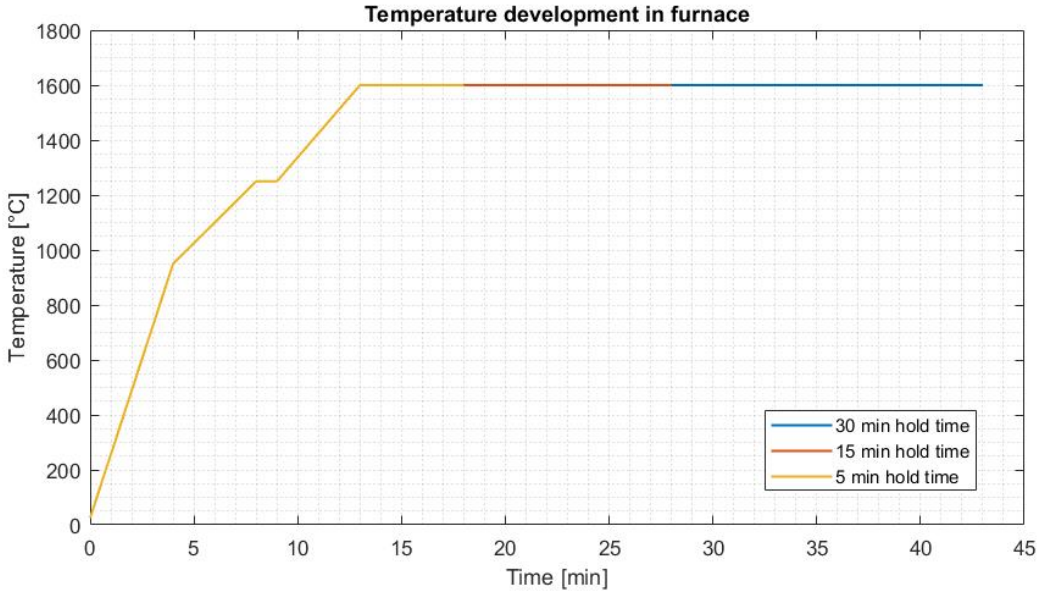

Figure 3.5: Heating curve for tests in sessile drop furnace.

Table 3.14 shows an overview of the experiments that were performed during the project. The pyrometer temperature had a large deviation from the thermocouple temperature. The thermocouple temperature was checked by melting iron in the furnace, and this confirmed that the thermocouple temperature was close to actual temperature in the furnace. The pyrometer was adjusted to point at the sample holder, but as this did not decrease the deviation this temperature was only used to compare the temperature between the different tests. As the table shows, the pyrometer temperature changed some between the tests, as was expected.

Table 3.14: Overview of the tests performed in sessile drop furnace

Nr	C-mat	Slag	TC temp	Pyr temp	Duration
1	charcoal	Slag 1	1604	1490	30 min
2	coke	Slag 1	1600	1489	30 min
3	charcoal	Slag 1	1600	1489	15 min
4	coke	Slag 1	1600	1486	15 min
5	charcoal	Slag 1	1600	1486	5 min
6	coke	Slag 1	1600	1486	5 min
7	coke	Slag 1	1600	1486	5 min
8	charcoal	Slag 1	1600	1485	5 min
9	charcoal	Slag 1	1600	1488	15 min
10	coke	Slag 1	1600	1489	15 min
11	charcoal	Slag 2	1600	1487	30 min
12	coke	Slag 2	1600	1485	5 min
13	coke	Slag 2	1300	-	0 min
14	coke	Slag 2	1600	1487	30 min
15	charcoal	Slag 2	1600	1484	15 min
16	charcoal	Slag 2	1600	1484	15 min
17	coke	Slag 2	1600	1482	4 min
18	charcoal	Slag 2	1600	1481	5 min
19	coke	Slag 2	1600	1481	15 min
20	charcoal	Slag 2	1600	1479	15 min
21	charcoal	Slag 2	1600	1479	5 min
22	coke	Slag 2	1600	1478	2,5 min

As table 3.14 shows, slag 2 was tested towards charcoal for 15 minutes three times, while slag 2 was tested towards coke for 15 minutes once. This was due to a mislabelling, where the charcoal pellet used in test 16 was marked as a coke pellet, a mistake that was not discovered until after the tests in the sessile drop furnace were finished.

3.5 Contact angle and volume measurements

Measuring the contact angle is a common way of measuring the wettability of a surface or material. How the contact angle of a liquid drop is measured on a solid surface is illustrated in figure 3.6. The contact angle is determined by properties of both the solid material and the liquid drop and the interaction between them. A wetting liquid has a contact angle between 0 and 90° while a non-wetting liquid has a contact angle between 90 and 180°. [26] [27]

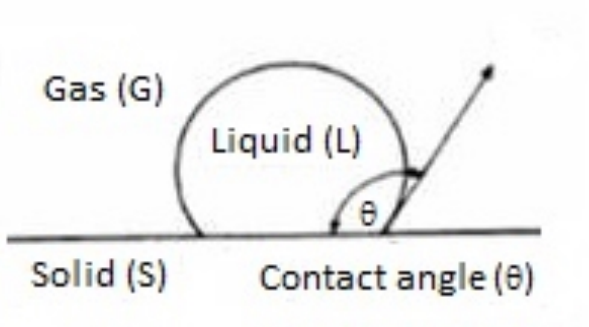

Figure 3.6: Illustration of contact angle of a liquid droplet on a solid surface

During the tests in the sessile drop furnace, images were captured at different intensity. Contact angle and volume of the slag drop can be measured automatically by the software used to control the tests (Wetting Low Vacuum Furnace), and this can also be done by a software for treatment of the data after the tests (Wetting Furnace Post Process). These softwares are designed by Sintef for this purpose and are not commercially available. However, none of the softwares were able to measure contact angle, and only the after treatment software was able to measure volume of the slag drop automatically. The slag drop volume was difficult to interpret, as shown in figure 3.7 for test 2 and in figure 3.8 for test 14, both due to odd readings in the start, and due to frequent and large changes in slag drop volume towards the end of the test. These measurements does not reflect the volume expansion of the slag drop, and are not considered to be real measurements. What can be interpreted from the section in the middle is that the slag drop volume decreases some at first, then increase some before the high frequent changes starts. The figures also shows that the contact angle is not measured, and is zero for the whole test.

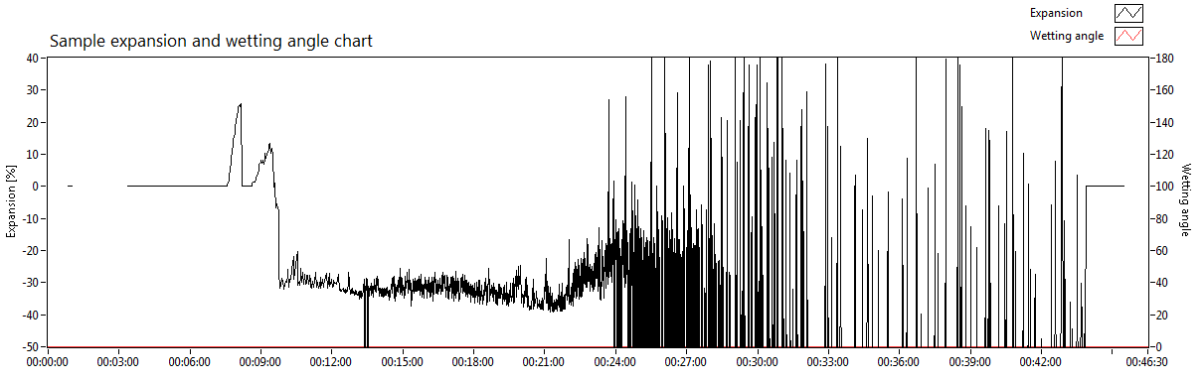

Figure 3.7: Contact angle and volume recorded by Wetting Post Process for test 2

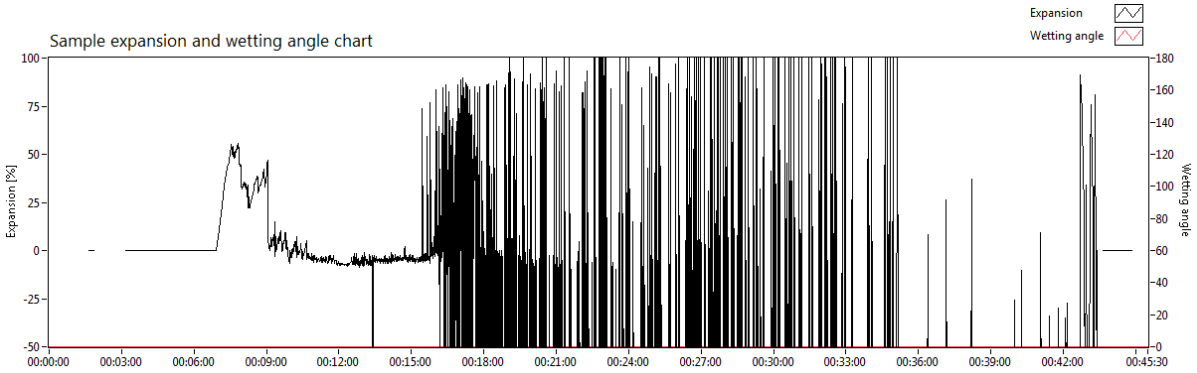

Figure 3.8: Contact angle and volume recorded by Wetting Post Process for test 14

To get useful data, the contact angle and volume of the slag drop was measured manually using the surface tension software Fta32 Video on a selected amount of images for each test. The first image was as the slag drop melted, which is used as reference point for the slag drop volume. It needs to be noted that at this point the slag drop often had not obtained a complete circular shape, which made the readings difficult and less accurate as the program is intended for circular droplets. However, the volume of the slag drop started to increase immediately after melting, which made it disadvantageous to select an image where the slag drop had obtained a more circular shape. The difference between the slag drop at melting and five seconds after melting is shown in figure 3.9 for test 4, the slag drop volume measured in these two images are 5,9 and 6,3 µl respectively.

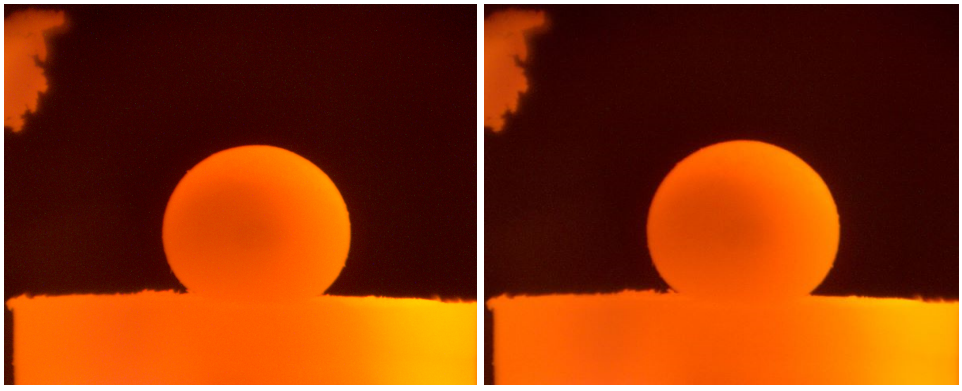

Figure 3.9: Image of slag drop as it has melted and 5 seconds after melting for test 4

As the lowest volumes of the slag drop when there is no gas in the droplet is the most interesting. Images were selected based on the same times for each sample (at melting and after 0, 1, 2, 3, 5 , 7.5, 10, 12, 15, 22, 30 minutes after the furnace reached 1600°C), and the images captured at these times were assessed visually to find the image with the lowest volume. The image with the lowest slag droplet volume was typically an image taken after gas escaped the slag droplet, where the slag droplets volume decreased substantially from one image to the next, before increasing again to the next image due to new gas. There is a possibility that the slag droplet still contained some gas on the images that were selected for measurement, which gives an uncertainty to the measurements taken. However, the measurements can still be used to show the trend of development for the slag drop volume and contact angle.

As a comparison to figures 3.7 and 3.8, figures 3.10 and 3.11 shows the manually measured volume for test 2 and test 14, respectively. The volume is given in µl, which is the unit the Fta 32 Video software used for measurement. However, the software was not calibrated between the tests regarding camera adjustments and distance from the camera to the slag drop. These measurements can therefore not be used to compare volume between tests, as the measurements may be wrong. The measurements can still be used to show trends, as is the purpose in these two figures. Figures 3.10 and 3.11 show a clearer trend than figures 3.7 and 3.8, but as mentioned as a possibility with these measurements, the volume increase around 15 minutes due to gas trapped in the slag droplet.

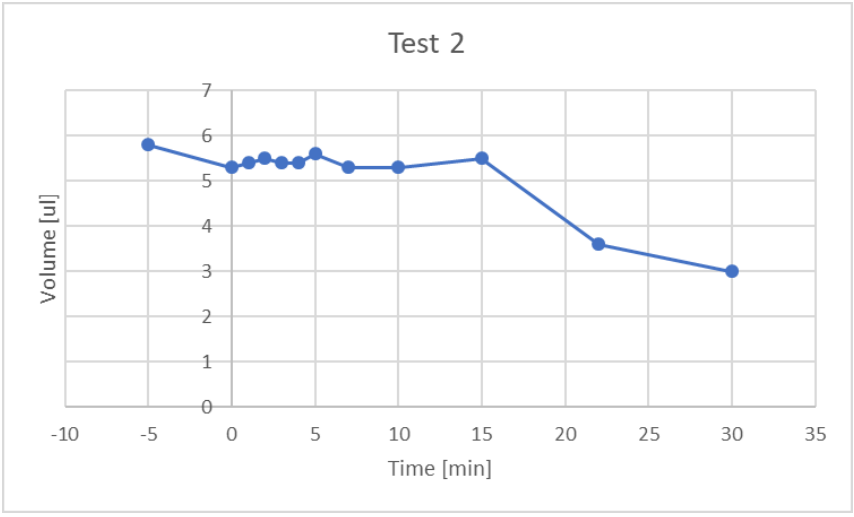

Figure 3.10: Volume of slag drop measured manually for test 2

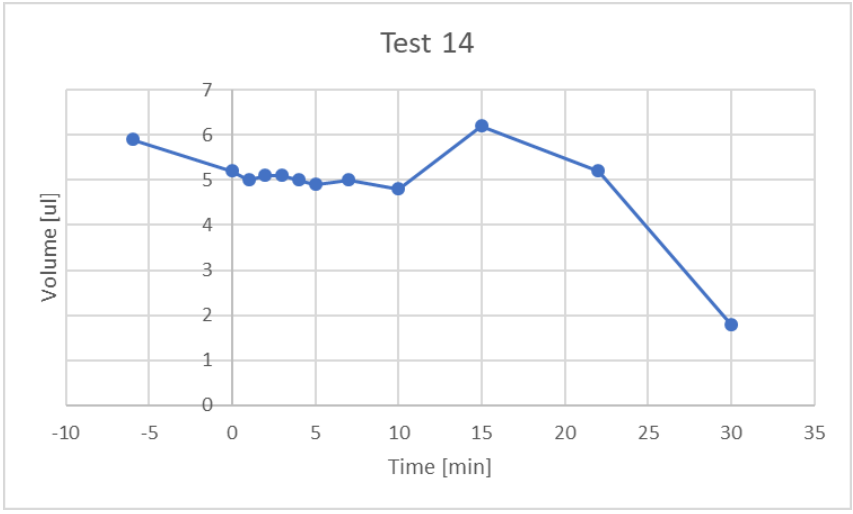

Figure 3.11: Volume of slag drop measured manually for test 14

Charts showing the development of slag drop relative volume and temperature, and contact angle and temperature are presented for each test in chapter 4. All results of volume and contact angle are based on manual measurements using the software Fta 32 Video, and the volume results are presented as relative volume where the volume as the slag drop melts is the reference for the volume. The time is always defined to be zero as the furnace temperature reaches 1600°C.

3.6 Sample preparation

After the tests in the sessile drop furnace, all samples were weighed before they were cast into epoxy. To be able to study the carbon materials in the SEM, the tests where the slag drop was attached to the carbon substrate were casted into iodine epoxy. Unfortunately, for nine of the samples, the slag drop was no longer attached to the carbon substrate after the tests, either because it came loose as the test was stopped, during handling of the samples after test (wrapping/unwrapping, weighing) or because the substrate fell apart after the test. The slag droplets of these samples were therefore cast into ordinary epoxy, as there was no carbon substrate to study.

The nine samples cast into ordinary epoxy were cast at once, while the thirteen samples cast into iodine epoxy were cast in three rounds as an ice bath was required to keep the iodine epoxy cool the first hours after casting. The ice was changed when needed, and the samples were kept in the ice bath for approximately 2,5 hours after casting. The samples cast into ordinary epoxy were placed in a vacuum chamber for 5 minutes before hardening, to remove air bubbles in the epoxy. Due to the exothermic nature of the iodine epoxy mixture, these samples were kept in the vacuum chamber for only two minutes while changing the ice before they were placed into the ice bath again. Figure 3.12 and 3.13 shows pictures taken during casting. Figure 3.12 shows five samples and the surplus of epoxy in ice bath during iodine epoxy casing, and figure 3.13 shows nine samples cast in epoxy and five samples cast in iodine epoxy after hardening.

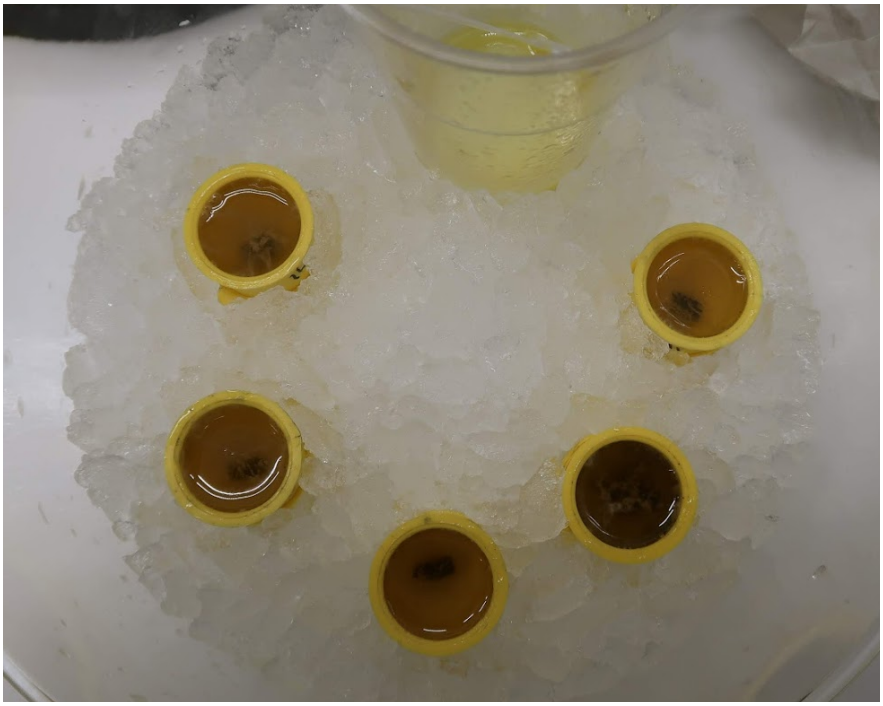

Figure 3.12: Samples in ice bath during iodine epoxy casting

Figure 3.13: Hardened samples, nine in epoxy and five in iodine epoxy.

After casting the samples were polished using SiC paper and water on a manual grinding plate. Each sample was grinded at paper with P value 320 until an appropriate surface of the sample was reached, before papers with P value 500, 800, 1200, 2400 and 4000 were used.

The samples were polished in a Struers TegraPol-31 using polishing plates and diamond suspensions. Both the single samples setting and a sample holder was used to polish the samples, as the top of the epoxy was uneven for some samples, making them unfavorable for the single samples setting. The samples were first polished using 9µm diamond suspension and an Akasel Aka-Largan polishing plate, then by using 3µm diamond suspension and a Struers MD Mol polishing plate, before using a 1µm diamond suspension and a Struers MD Nap polishing plate. At one point the lab ran out of 1µm diamond suspension, and a few samples were therefore not polished with the MD Nap polishing plate before being analysed.

The samples were coated with carbon using a Cressington 208 carbon coater, and then wrapped in aluminum foil which was secured to the sample surface with carbon tape. The samples were then placed in a heating cabinet overnight before being analysed in the SEM. The samples were analysed by EPMA at the end of the project.

3.7 Chemical analysis and imaging in SEM and EPMA

It was planned to analyse the samples with electron probe micro analyser, EPMA, as was done in the specialisation project TKP4580 [25]. However, as the demand for EPMA was high the latency was higher than expected, and the samples could not be analysed before the end of the project. The samples were therefore first analysed in a scanning electron microscope (SEM), and then in the EPMA the end of the project. The results from the EPMA analyses were used to verify the results from the SEM analyses.

A scanning electron microscope (SEM)is a microscope that uses a beam of accelerated electrons to study a sample. The electron beam is passed through lenses and apertures so that a focused beam hits the sample, but is not destructive. The sample to be investigated is mounted in a chamber that is pumped down to vacuum. The electron beam generates high-energy backscatter electrons, low-energy secondary electrons and x-rays from the sample, which are captured by detectors and used to display the sample. X-ray analysis can give quantitative analysis of the elements that are present in the sample. SEM uses EDS, electron dispersive spectrometer, which identifies the elements in the sample by the energy of the x-ray emitted. [28] [29] [30]

An electron probe micro analyzer (EPMA) is a microbeam instrument used primarily for chemical analysis of solid samples. The sample is hit with an electron beam that has high enough energy to generate x-rays from the sample, but is not destructive. Both the electrons that scatter off the sample and the x-rays generated from the sample can be analysed. The electron beam is also used to view an image of the sample, where areas with higher densities appear brighter than areas with lower densities. Back-scatter electrons can give information about the average composition of the material, by measuring the amount and energy of electrons that bounce off the sample surface. X-ray analysis can give precise quantitative elemental analysis of small areas at the sample surface. EPMA uses WDS, wavelength dispersive spectrometer, where the wavelength and intensity of the x-rays that are generated are used to determine which elements are present. [31] [32]

The samples were placed in the SEM and images were captured at 5000, 2000 or 1000, 500 and 100 times magnification for both metal and slag, in addition to an image of the whole sample. Images for each test are presented in chapter 4. For samples where only the slag was cast in epoxy, the carbon substrate was placed in the SEM to study the surface of the substrate where the slag droplet had been. Images were captured and are presented in chapter 4.

Chemical analysis by EDAX EDS was then performed, which identified the different elements that were present in the samples, and the distribution of the different elements in the samples. The voltage and aperture used were the same for all samples, 10kV and 60µm. The analysis duration was 30 seconds for each measuring point, and the slag and metal was analysed at minimum two different spots on the sample. Each area was magnified around 1000x, and the areas were typically analysed with two point analyses and one selected area

analysis, this depended on the area being analysed. Areas with two-phase slag were e.g. analysed with more points to find the composition of the different phases.

At the end of the project the samples were analysed by EPMA. The slag of each sample was analysed with defocused electron beam of 10-20 µm diameter, except for sample 13 where the two phases in the slag were large and had to be analysed separately. Sample 13 was analysed with five point measurements for the light slag phase and five point measurements for the dark slag phase. The other samples were analysed with five defocused measurements, while the samples that contained both glassy and two-phase slag were analysed with five defocused measurements of the glassy slag and five defocused measurements of the two-phase slag. The metal in the samples were analysed with three defocused measurements, and for the samples containing more than one metal droplet, two different metal droplets with largest sizes were analysed with three defocused measurements each.

3.7.1 Difference in results from analysis with EPMA and SEM

As EPMA and wave dispersive spectroscopy is known to be more accurate than SEM and electron dispersive spectroscopy, some samples from the specialisation project TKP4580 [25] were analysed in SEM to compare the results. While EPMA gave the results as oxides for the slag, the SEM gave results as element weight distribution, and the oxide distribution in the slag had to be calculated. This was done by multiplying the weight percentage for the different elements with the factors listed in table 3.15. These factors are molecular weight of the oxides over the molecular weight of the elements, to get the weight distribution of the oxides in the slag.

Table 3.15: Factors used to find oxide weight distribution in the slag

MnO/Mn	**SiO_2/Si**	**FeO/Fe**	**Al_2O_3/2Al**	**CaO/Ca**	**MgO/Mg**	**SO_3/S**
1,29	2,14	1,29	1,89	1,40	1,66	2,50

Four samples from the specialisation project were tested in SEM, samples 3, 4, 5 and 7. The results from the EPMA analysis conducted in fall 2018 and the results from the SEM analysis conducted in spring 2019 are listed for the four tests in table 3.16. The results are weight percentage of the different oxides in the slag of the samples, and the sum is also listed. The ratio between the weight percentage measured in SEM and the weight percentage measured in EPMA is also listed (SEM/EPMA), where a number close to one means little variation between the measurements.

Table 3.16: Results from SEM and EPMA analysis for samples from specialisation project

Test 3	**MnO**	**SiO_2**	**FeO**	**Al_2O_3**	**CaO**	**MgO**	**SO_3**	**Sum**
SEM [wt%]	0,73	47,68	0,00	15,32	19,88	5,39	0,00	89,01
EPMA [wt%]	1,90	46,02	0,03	17,11	25,54	6,10	0,02	96,72
SEM/EPMA	0,38	1,04	0,00	0,90	0,78	0,88	0,00	
difference	−1,17	1,66	−0,03	−1,79	−5,66	−0,71	−0,02	−7,71
Test 4	**MnO**	**SiO_2**	**FeO**	**Al_2O_3**	**CaO**	**MgO**	**SO_3**	**Sum**
SEM [wt%]	25,80	41,14	0,00	10,45	14,52	4,32	0,14	96,36
EPMA [wt%]	25,99	40,99	0,08	9,81	14,60	4,16	1,99	97,62
SEM/EPMA	0,99	1,00	0,00	1,07	0,99	1,04	0,07	
difference	−0,19	0,15	−0,08	0,64	−0,08	0,16	−1,85	−1,25
Test 5	**MnO**	**SiO_2**	**FeO**	**Al_2O_3**	**CaO**	**MgO**	**SO_3**	**Sum**
SEM [wt%]	5,40	43,50	0,00	16,42	23,72	6,09	0,00	95,13
EPMA [wt%]	5,55	43,62	0	15,83	24,14	6,07	0,13	95,34
SEM/EPMA	0,97	1,00	-	1,04	0,98	1,00	0,00	
difference	−0,15	−0,12	0,00	0,59	−0,42	0,02	−0,13	−0,21
Test 7	**MnO**	**SiO_2**	**FeO**	**Al_2O_3**	**CaO**	**MgO**	**SO_3**	**Sum**
SEM [wt%]	9,08	43,50	0,00	14,53	20,72	5,79	0,00	93,62
EPMA [wt%]	9,63	45,86	0,03	13,86	21,83	5,51	0,76	97,48
SEM/EPMA	0,94	0,95	0,00	1,05	0,95	1,05	0,00	
difference	−0,55	−2,36	−0,03	0,67	−1,11	0,28	−0,76	−3,86

The table shows that there is generally small deviation between the measurements conducted by SEM and measurements conducted by EPMA. Considering sample 4, 5 and 7, the largest and lowest values for the SEM/EPMA factor are 1,07 and 0,94. All the differences for these sample, except SO_3 for sample 4 that has 1,85 percentage points difference, are less than one percentage points. The sums of these three samples all have differences lower than 4 percentage points. All these differences and SEM/EPMA factors are within acceptable limits for error.

Sample 3 shows the largest differences, where the largest differences in SEM/EPMA factor is for MnO with 0,38, CaO with 0,78 and MgO with 0,88. The actual differences are less than two percentage points for MnO and MgO, while CaO has a high difference of 5,66 percentage points. The difference between the sums is 7,71 percentage points, which is also high. However, considering the results of the other three samples, this sample can pass as an outcast.

The conclusion from this comparison is that the differences between the results from SEM and EPMA analysis are within tolerable limits. The results from SEM analysis can therefore be used to evaluate the samples from the tests run in this project.

3.7.2 Analysis of two-phase slag

Several of the samples had two-phase slag. The pattern and size of the two phases in the slag varied, and some samples had both glassy and two-phase slag. This made the analysis of the slag complicated, considering the distribution between the two phases in the slag. As the samples were analysed, the two phases were analysed by point analysis in addition to selected area analysis. Table 3.17 lists the results of the analyses for sample 8 and sample 12, which both had two phase slag and glassy slag. The table lists the results of the point analyses of the light and dark phase of the two-phase slag, the results of the selected area analyses of the two-phase slag and the results of the selected area and point analysis of the glassy slag.

Table 3.17: Analysis of samples 8 and 12, which contained both glassy and two-phase slag

Sample 8	**O**	**Mn**	**Si**	**Fe**	**Al**	**Ca**	**Mg**	**S**
Light phase	40,54	34,86	11,73	0	0,96	4,22	3,34	0
Dark phase	47,11	13,98	15,21	0	8,58	10,84	0	0
Area	43,04	24,87	12,97	0	4,45	7,20	2,04	0
Glassy	43,52	25,99	12,87	0	3,84	6,94	1,76	0
Glassy	43,34	26,41	13,06	0	3,98	7,04	1,87	0
Glassy	43,04	26,55	13,11	0	4,04	7,14	1,91	0
Sample 12	**O**	**Mn**	**Si**	**Fe**	**Al**	**Ca**	**Mg**	**S**
Light phase	38,80	38,73	11,73	0	0,72	2,94	2,21	0
Dark phase	44,97	17,38	15,90	0	7,31	9,21	0	0,71
Area	41,52	29,89	13,21	0	3,23	5,13	1,11	0
Area	41,12	30,46	13,12	0	3,15	5,07	1,20	0
Area	40,56	30,28	13,12	0	3,14	5,26	1,41	0
Area	41,08	30,73	13,03	0	3,14	5,34	1,18	0
Glassy	41,72	30,12	13,07	0	3,02	4,96	1,27	0
Glassy	41,28	30,91	13,02	0	2,94	5,04	1,20	0
Glassy	40,87	30,52	12,95	0	3,15	5,18	1,45	0

The table shows that the composition of the light and the dark phase of the two-phase slag are different. The light phase contains more manganese and magnesium while the dark phase contains more silicon, aluminum, calcium and sulphur. Manganese is the heaviest element in the slag when the iron is reduced to metal, which is the reason that the phase containing manganese appears lighter than the phase not containing manganese. As can be seen from table 3.17, the difference between the selected area analyses of the two-phase slag and the analyses (both selected area and point analyses) of the glassy slag is relatively small for all elements, in both samples.

The conclusion from this comparison is that the selected area analyses of two-phase slag is a good approximation of the slag composition. The results from selected area analyses are therefore used to find slag composition for the samples that have two-phase slag.

3.7.3 Trace elements in analysis

During chemical analysis, several of the samples showed trace of elements that were not expected to be present in the slag. Most of these elements were small amounts of 0,5 wt% or less, but especially bromine had several high readings of up to 7 wt%. However, half of the 22 samples had no other elements present than O, Mn, Si, Fe, Al, Ca, Mg, S and C, which were the elements expected to be in the slag. This, in addition to no pattern between which samples had trace elements and if the slag used was slag 1 or slag 2, made contaminations an unlikely explanation of the trace elements.

When processing the analysis results, a pattern between the aluminum and bromine results appeared. Table 3.18 lists the analysis results for aluminum, bromine and the sum of aluminum and bromine for sample 3, 10 and 11 are listed, in addition to if point or selected area analysis was used for the analyses. All three samples had glassy slag.

Table 3.18: Results of chemical analysis of aluminum and bromine for sample 3, 10 and 11

Sample 3	**Al [wt%]**	**Br [wt%]**	**Al + Br [wt%]**
Area	6,37	0	6,37
Area	0,65	7,11	7,76
Area	0,23	7,45	7,68
Point	2,31	4,80	7,11
Sample 10	**Al [wt%]**	**Br [wt%]**	**Al + Br [wt%]**
Area	5,30	0	5,30
Point	1,97	4,16	6,13
Point	2,32	3,82	6,14
Area	5,54	0	5,54

Point	2,55	3,67	6,22
Point	2,93	3,21	6,14
Sample 11	**Al [wt%]**	**Br [wt%]**	**Al + Br [wt%]**
Area	5,21	4,13	9,34
Area	4,89	4,69	9,58
Point	3,45	6,45	9,90
Area	3,51	6,45	9,82
Point	3,27	6,65	9,92

As can be seen from table 3.18, the results of the aluminum analyses varies between different analyses for the same sample. The same can be seen for the bromine analyses, when the results of aluminum are lower, the results of bromine are higher. The variation in the sum of aluminum and bromine has less deviations, which could indicate that some of the aluminum is interpreted as bromine in the analysis. Since this it not for all tests, it may be due to placement of the sample in the SEM, that the surface is uneven or has some tilt. From the results of sample 3 and 10 it appears that the sum of bromine and aluminum is some higher for samples that had bromine than for analyses without bromine results. The same trend was observed for magnesium and dysprosium, and for sulfur and lead.

The conclusion from this comparison is that summarising the bromine and aluminum contents still seems as a fair approximation of the aluminium content of the sample, and for all samples that had bromine present in the SEM analysis the bromine is included in the aluminium content. in the same way, dysprosium is included into the magnesium content and lead is included in the sulfur content.

3.7.4 Metal analyses

The metal analyses conducted in SEM for the samples show that the composition of the metal varies within different metal droplets in the same sample for some samples, while other samples shows little or no variation between different metal droplets in the same sample. Table 3.19 shows the average metal analyses in weight percentage for samples 10, 11, 12, 16, 20 and 22, for different metal droplets in the samples.

Table 3.19: Metal results from SEM for samples 10, 11, 12, 16, 20 and 22.

	Mn [wt%]	Fe [wt%]	Si [wt%]	Sum
Sample 10 - large metal droplet	51,15	32,82	4,46	88,42
Sample 10 - small metal droplet	81,07	1,92	6,96	89,96
Sample 11 - large metal droplet	54,07	22,51	20,26	96,84
Sample 11 - medium metal droplet	67,28	7,92	21,64	96,83
Sample 11 - small metal droplet	78,35	0,44	16,38	95,17
Sample 12 - large metal droplet	27,52	53,69	1,38	82,59
Sample 12 - small metal droplet	25,99	53,14	0,00	79,12
Sample 16 - largest metal droplet	61,85	9,79	9,63	81,28
Sample 16 - second largest metal droplet	63,91	5,87	8,72	78,50
Sample 20 - large metal droplet	70,22	11,87	7,58	89,67
Sample 20 - medium metal droplet	80,05	1,37	8,06	89,49
Sample 22 - large metal droplet	28,56	54,04	0,14	82,74
Sample 22 - small metal droplet	32,26	53,08	0,00	85,34

The sums listed in table 3.19 are low, this is due to varying magnitude of carbon analyses, in addition to results of carbon and other trace elements for some samples. The table shows that for sample 10, 11 and 20, there is a clear trend of the manganese content increasing and iron content decreasing with decreasing size of the metal droplet. The silicon content also varies some. However, sample 22 shows little variation in iron and silicon content and a bit higher variation in manganese content of the metal droplets, sample 16 shows little variation in manganese and silicon and a bit higher variation in iron content of the metal droplets, while sample 12 shows little variation between the metal composition of the large and the small metal droplet.

The conclusion after assessing the metal analyses of these samples is that the metal analyses from SEM is less consistent than the slag analysis from SEM. The composition may be affected by which metal droplet is analysed, and evaporation of produced metal may also affect the composition, previous studies have observed evaporation of produced manganese [17] [19] [20]. The metal composition shown in the results in chapter 4 is therefore calculated from the SEM slag analyses, while the SEM metal analyses are included in the appendix.

3.7.5 Normalisation of slag results

As mentioned, the results from SEM were converted from elements to oxides by multiplying with different factors. After this was done, the sum of oxides was not always close to 100%. The sums varied from 77,2 for test 9 to 101,2 for test 7. This was assumed to be a result of inaccurate measurement of oxygen in the SEM results, which lead to a different amount of oxygen in the calculated oxides sum and the SEM results sum. To verify this assumption the amount of oxygen measured in SEM was compared to the amount of oxygen that was calculated to be in the different oxides. The difference between the calculated and measured oxygen was then subtracted from the sum of the calculated oxides into a new sum. After this, all tests had new sum with value between 94,1 for test 9 and 100,4 for test 2. Table 3.20 shows sum of calculated oxides, amount of oxygen measured in SEM, amount of oxygen in calculated oxides, difference between measured and calculated oxygen, and new sum of some tests to demonstrate the normalisation.

Table 3.20: Normalisation of oxygen content in sum of oxides for tests 1,4 7, 9, 15 and 20

Test	**Sum calculated oxides**	**Oxygen measured in SEM [wt%]**	**Oxygen in calculated oxides [wt%]**	**Difference in oxygen**	**New Sum**
1	99,40	42,77	41,96	-0,81	100,21
4	80,67	46,21	31,64	-14,56	95,24
7	101,26	35,89	39,50	3,62	97,65
9	77,24	49,90	32,18	-17,71	94,96
15	80,40	48,67	33,49	-15,18	95,57
20	97,25	38,10	37,83	-0,28	97,53

The table shows that the measured amount of oxygen usually was higher than the amount calculated in the oxides, which indicates that the measurement in the SEM was higher than the actual oxygen content. SEM is less accurate in measurement of light elements, such as oxygen [30]. When the measurement of oxygen was higher than the actual content of oxygen, the sum of the calculated oxides would be lower than 100%. Since the new sums in table 3.20 were close to 100%, it confirmed that the difference between the sum of calculated oxides and 100% corresponded to the difference between measured oxygen and calculated oxygen in the oxides.

The conclusion from this comparison is that the amounts of oxides in the slag can be normalised so the sum of calculated oxides is 100% and not e.g. 77,24% as for test 8. This is therefore done for all tests before the results from SEM are assessed further.

4. Results

In this chapter, the results from the experimental work performed in the project will be presented. The result of each test includes description of visual observation, selected pictures taken in the furnace during test, contact angle and relative volume development based on selected measurements, pictures of sample after test, pictures taken of the sample in SEM, slag composition measured by SEM and metal composition calculated from slag composition. Reduction degrees are presented as the weight of manganese reduced over the total weight of manganese, and as the weight of silicon reduced over the total weight of manganese in the sample, as shown in equations 4.1 and 4.2.

$$R_{Mn} = wt_{Mn,red} / wt_{Mn,tot} \quad (4.1)$$

$$R_{Si} = wt_{Si,red} / wt_{Mn,tot} \quad (4.2)$$

The highest possible reduction degrees are calculated for slag 1 and slag 2, and gives an idea of which magnitude these numbers are in. The calculations uses the slag composition listed in table 3.3 and table 3.6 for slag 1 and slag 2, and the assumption that maximum reduction results in a slag that contains 5 wt% MnO and 40 wt% SiO_2. FeO is assumed to be totally reduced to iron, and the other oxides; Al_2O_3, MgO, CaO and SO_3 are assumed to be irreducible. These assumptions gave the following maximum reduction degrees for slag 1 and slag 2:

Slag 1: $R_{Mn,max} = 0,954$ and $R_{Si,max} = 0,186$
Slag 2: $R_{Mn,max} = 0,964$ and $R_{Si,max} = 0,224$

The results presented in this chapter are sorted into groups based on carbon material and slag used in the tests. Results for tests run with charcoal and slag 1 are presented first, then results for tests run with charcoal and slag 2, before tests run with coke and slag 1, and last tests run with coke and slag 2 are presented. Within the different groups the tests are ordered by descending hold time.

4.0 Results of carbon material pellets

All carbon material pellets that were used in tests were pressed into a graphite cup. Measurements were performed on 5 graphite cups to get average values for weight, height, diameter, inner diameter and inner height. These measurements and the calculated average are listed in table 4.1. This info was used to get the pellet weight without graphite cup, and to calculate the pellet density without the graphite cup.

Table 4.1: Measurement and calculated average value for graphite cups

Weight [g]	**Outer diameter [mm]**	**Inner diameter [mm]**	**Outer height [mm]**	**Inner height [mm]**
0.3281	10,07	8,03	3,09	1,01
0.3300	10,06	8,05	3,10	0,95
0.3298	10,08	8,03	3,07	1,04
0.3328	10,05	8,01	3,11	0,96
0.3311	10,05	8,06	3,11	0,98
0,3304	*10,06*	*8,04*	*3,10*	*0,99*

Table 4.2 and 4.3 shows details of the carbon material pellets that were used in the sessile drop furnace tests. This includes weight of pellet before and after drying and the calculated moisture loss, the height and density of pellet with graphite cup, and calculated density without the graphite cup.

Table 4.2 shows that the moisture loss of the pellets varies between 23,96 and 34,61 percent. The density of the charcoal pellets varies between 599,3 and 635,3 kg/m^2. Table 4.3 shows that the moisture loss varies between 0 and 6,59 percent, and that the density varies between 1140,2 and 1261,7 kg/m^2. The tables also show that there is significant difference between charcoal and coke for both moisture loss and density.

Table 4.2: Details of charcoal pellets used in furnace tests

Nr	Wet weight [g]	Dry weight [g]	Moisture loss [%]	Diameter [mm]	Height [mm]	Density [kg/m^3]
1	0,4339	0,4091	23,96	10	4,16	606,8
5	0,4434	0,4107	28,93	10	4,15	622,9
6	0,4538	0,4180	29,01	10	4,27	633,2
7	0,4491	0,4143	29,31	10	4,19	635,3
8	0,4399	0,4045	32,32	10	4,07	604,3
9	0,4563	0,4159	32,08	10	4,23	632,4
10	0,4545	0,4145	32,23	10	4,27	607,9
11	0,4500	0,4086	34,61	10	4,17	599,3
12	0,4477	0,4197	23,87	10	4,34	620,8
14	0,4511	0,4201	25,68	10	4,31	634,0
15	0,4558	0,4227	26,39	10	4,42	614,8

Table 4.3: Details of coke pellets used in furnace tests

Nr	Wet weight [g]	Dry weight [g]	Moisture loss [%]	Diameter [mm]	Height [mm]	Density [kg/m^3]
4	0,5473	0,5330	6,59	10	4,63	1216,0
5	0,5182	0,5099	4,41	10	4,32	1261,7
6	0,5215	0,5167	2,51	10	4,41	1247,5
7	0,5252	0,5179	3,74	10	4,46	1223,4
8	0,5235	0,5175	3,10	10	4,45	1227,1
9	0,5104	0,5059	2,50	10	4,33	1226,8
10	0,5138	0,5090	2,61	10	4,41	1196,0
11	0,5151	0,5151	0,00	10	4,46	1205,1
12	0,5138	0,5127	0,59	10	4,54	1142,6
13	0,5167	0,5146	1,12	10	4,55	1148,9
14	0,5197	0,5159	2,00	10	4,58	1140,2

4.1 Results from tests with charcoal and slag 1

Test 1, 3, 9, 5, and 8 were run with slag 1 towards charcoal. Table 4.1.1 shows the weight measurements of the slag pellet and charcoal pellet before the test, and the weight measurement of the slag and charcoal after the test, in addition to the weight loss.

Table 4.1.1: Weight measurement of tests run with charcoal and slag 1

	Time	**Charcoal weight [g]**	**Slag weight [g]**	**Total weight before [g]**	**Weight after [g]**	**Weight loss [g]**	**Weight loss [%]**
1	30	0,0787	0,1002	0,1789	0,1087	0,0702	39,24
3	15	0,0803	0,1034	0,1837	0,1013	0,0824	44,86
9	15	0,0741	0,0988	0,1729	0,1156	0,0358	12,47
5	5	0,0876	0,1002	0,1878	0,1469	0,0409	21,78
8	5	0,0839	0,1012	0,1851	0,1441	0,0410	22,15

The table shows that the two tests run for 15 minutes had both the highest and the lowest weight loss in percentage. The test run for 30 minutes had high weight loss, while the tests run for 5 minutes had roughly the same weight loss.

4.1.1 Test 1

The first test was run with charcoal pellet 1 and slag sample 1A at 1600°C for 30 minutes. The slag pellet moved some while the furnace was evacuated with the vacuum pump. The slag pellet melted at approximately 1200°C, and there was some activity through bubbling as the furnace was kept at 1250°C. The activity continued and increased some as the temperature was heated to hold temperature 1600°C. At hold temperature the activity kept the same intensity for 10-15 minutes. During this time, the bubbling was not so frequent, but the bubbles were very large. The activity decreased after 20 minutes and the activity kept a lower level for the remaining time of the test.

Figure 4.1.1.1 shows pictures taken of the slag drop in the furnace. The pictures are taken before start at 25°C, after melting at 1200°C, as the furnace temperature reached 1600°C, and after 5, 15 and 30 minutes at 1600°C. The figure shows that the charcoal pellet shrunk some and the slag drop moved some during heating, and that the slag drop changed shape and contact angle during the test.

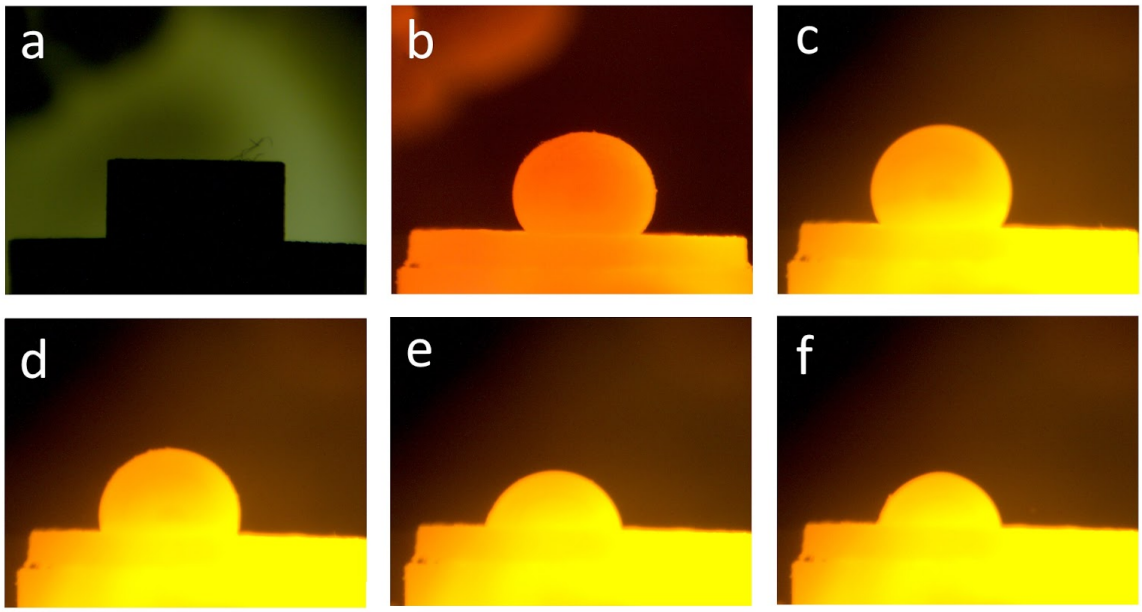

Figure 4.1.1.1: Pictures of test 1; a - at start of the test; b - as the slag melted; c - as the temperature reached 1600°C; d - after 5 minutes at 1600°C; e - after 15 minutes; f - after 30 minutes

Figure 4.1.1.2 shows photographs of the slag drop and charcoal pellet after it was removed from the furnace. The slag drop has a pale orange/transparent color and some metal droplets could be made out in the bottom of the slag drop, while the charcoal pellet is porous and fragile.

Figure 4.1.1.2: Pictures of slag and charcoal removed from the furnace after test 1

Figure 4.1.1.3 shows the development of the contact angle and temperature, while figure 4.1.1.4 shows the development of the relative volume and temperature for test 1. The figures show that the contact angle starts at about 120 degrees as the slag drop melts, and decreases steadily until 15 minutes before it remains around 80 degrees for the rest of the test. The relative volume decreases from one minute after melting to five minutes after melting, then keeps steady until ten minutes before it decreases steeply until 15 minutes. The volume then only decreases some for the rest of the test. The main trend of both contact angle and volume is that they decreases as the reduction time increases, but that the contact angle flattens after 15 minutes.

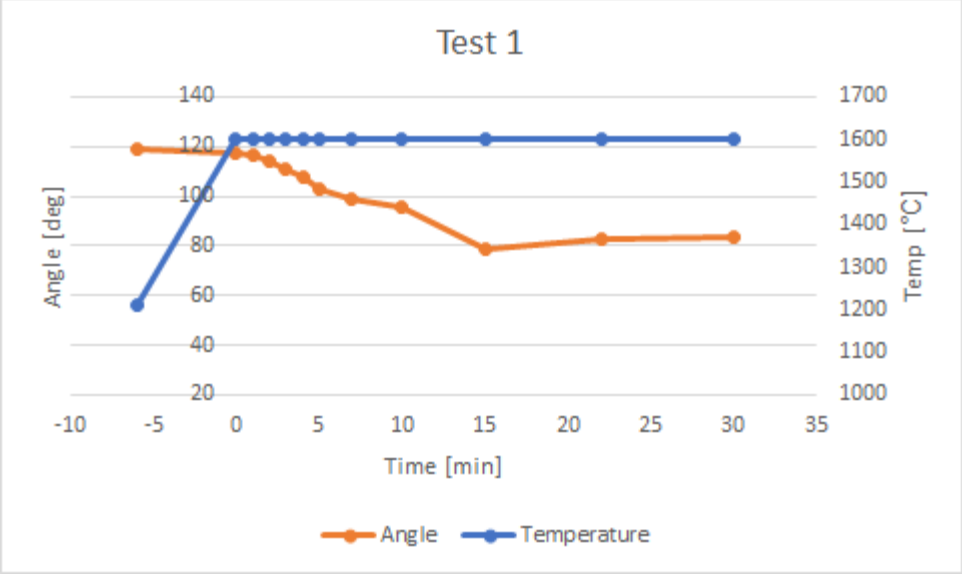

Figure 4.1.1.3: Contact angle and temperature development of test 1

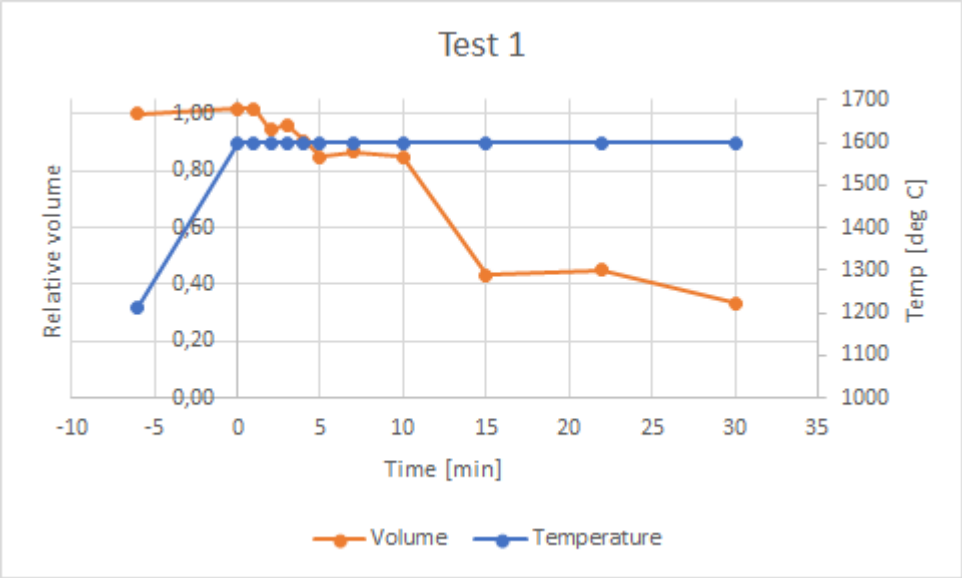

Figure 4.1.1.4: Relative volume and temperature development for test 1

Figure 4.1.1.5 shows a picture of the sample taken in the SEM. The figure shows that the sample has two metal droplets of considerable size at the surface, and that the charcoal pellet was at the right side of the slag drop in the figure. Figure 4.1.1.6 shows the slag phase of the sample magnified, and it shows that the slag is glassy, as is expected with this reduction time. Figure 4.1.1.7 shows details of the largest metal droplet magnified 1000 times, and it shows that the metal has some cracks, but no structure on the surface.

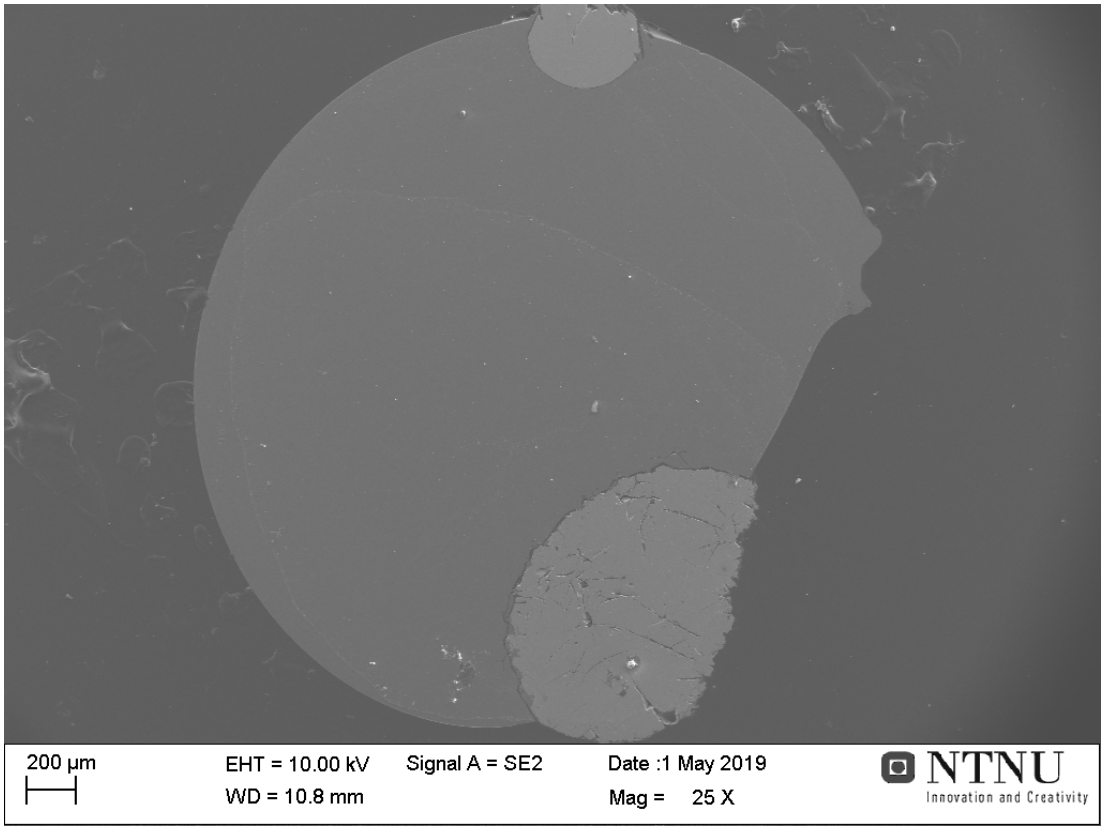

Figure 4.1.1.5: Picture of sample 1 taken in SEM

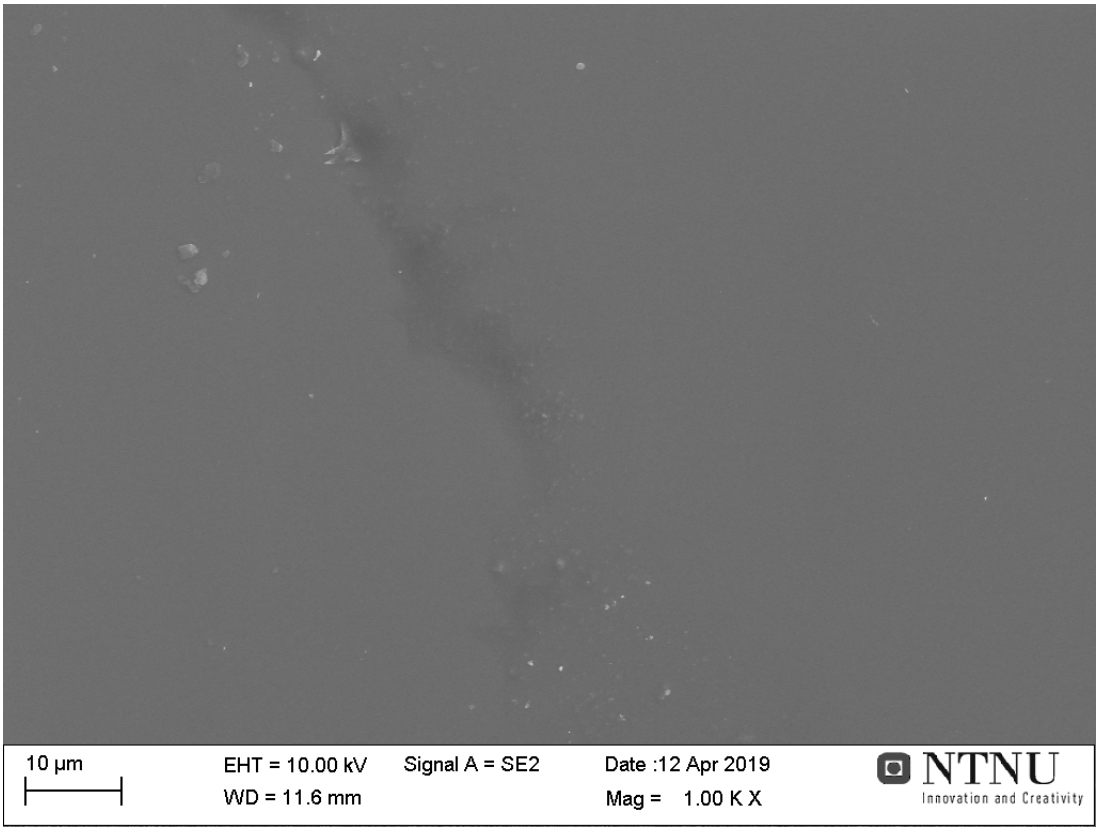

Figure 4.1.1.6: Slag phase of sample 1 magnified 1000 times

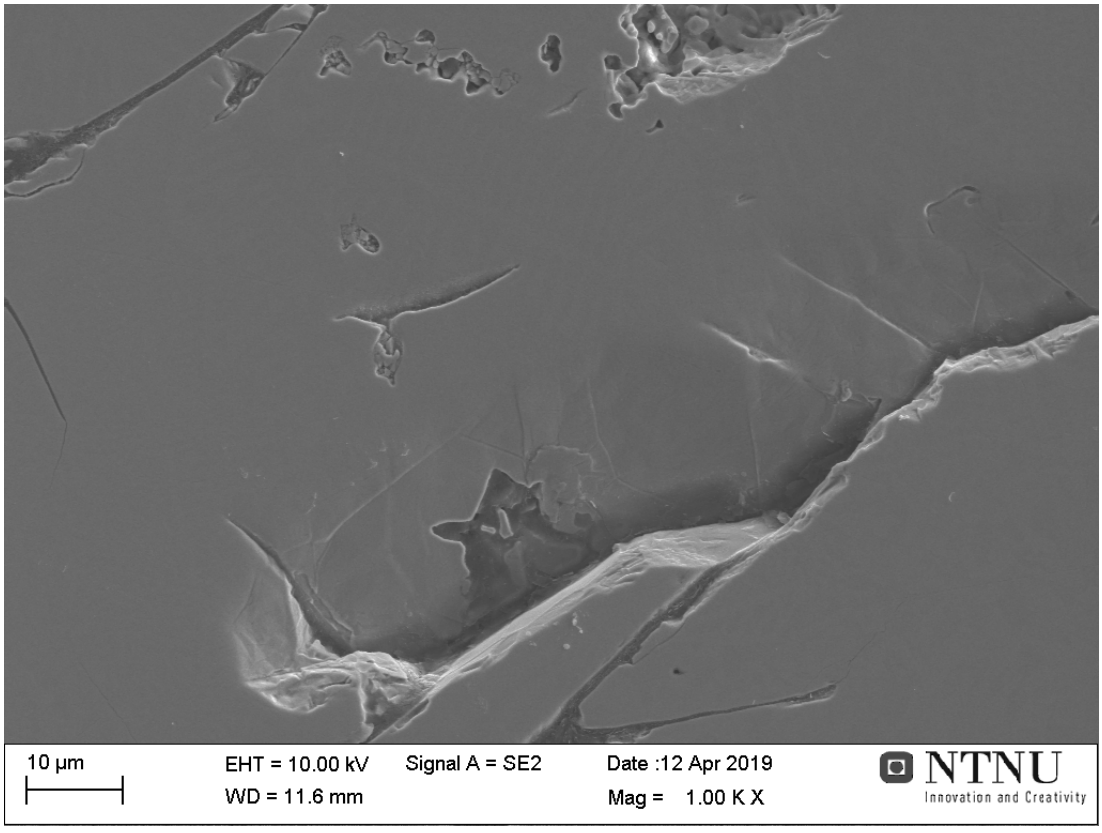

Figure 4.1.1.7: Metal phase of sample 1 magnified 1000 times

Figure 4.1.1.8 shows an image taken in SEM taken of the charcoal pellet after test. The figure shows a crater where the slag drop was, as the slag drop worked its way down into the charcoal pellet during reduction. There is a piece of the edge lying in the crater that has broken off. The rest of the pellet seems rather unaffected from the reduction.

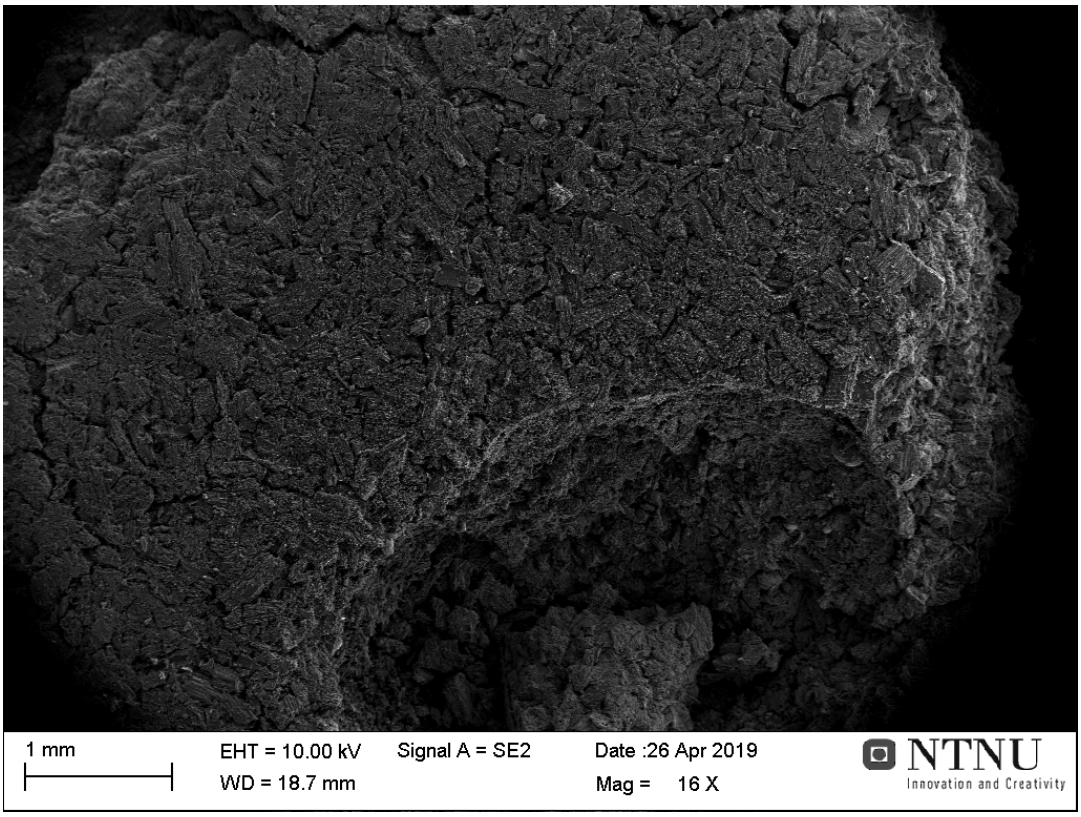

Figure 4.1.1.8: Image of charcoal pellet from test 1 taken in SEM

Table 4.1.1.1 lists the composition of the slag measured by SEM and EPMA, and the composition of the metal calculated from the slag composition measured by SEM. The slag has a bit higher than the desired MnO content of 5%, while the metal has a low content of silicon compared to the desired 18%. The results from SEM and EPMA analyses are similar, which is expected.

Table 4.1.1.1: Slag composition measured by SEM and EPMA for sample 1, and metal composition calculated from SEM results

Slag (measured)	**MnO**	**SiO_2**	**FeO**	**Al_2O_3**	**CaO**	**MgO**	**SO_3**
SEM [wt%]	12,38	43,58	0,06	16,89	20,35	5,35	1,21
EPMA [wt%]	12,71	46,60	0,02	14,02	20,90	5,52	1,06
Metal (calculated)	**Total**	**Mn**		**Si**		**Fe**	
[wt%]	100	77,39		9,95		12,66	
[g]	0,0368	0,0285		0,0037		0,0047	

Reduction degrees for test 1 are R_{Mn} = 0,857 and R_{Si} = 0,110

4.1.2 Test 3

The third test was run with charcoal pellet nr 5 and slag sample 1E, at 1600°C for 15 minutes. The slag sample melted and formed a slag drop at 1209°C, and some activity was observed in the slag drop as the temperature was kept at 1250°C. As the temperature was increased to hold temperature, the activity increased some. During the reduction, the activity observed was many bubbles with small volume expansion. The volume expansion of the slag drop increased after 10 minutes at 1600°C, and for the rest of the test the slag drop expansion was large.

Figure 4.1.2.1 shows pictures taken during test 3, these pictures are taken before start, after the slag drop melted at 1209°C, as the furnace temperature reached 1600°C, after 5 and 15 minutes at 1600°C. The figure shows that the charcoal pellet shrunk some during heating, and that the slag drop changed shape and contact angle during the test.

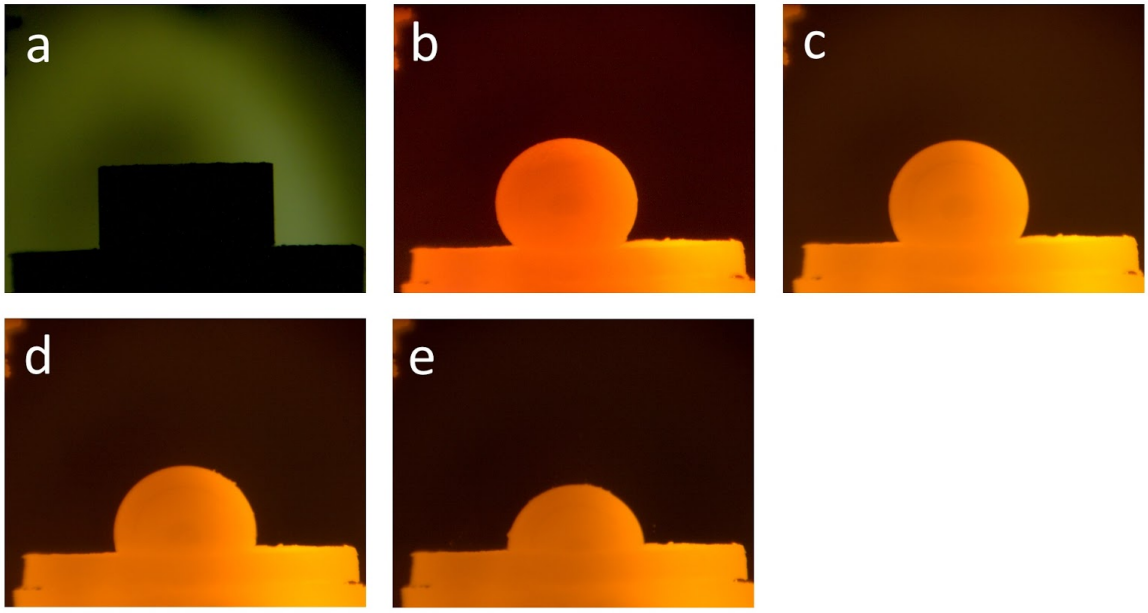

Figure 4.1.2.1: Pictures from test 3; a - before start at 25°C; b - after melting at 1209°C; c - at 1600°C; d - after 5 minutes at 1600°C; e - after 15 minutes

Figure 4.1.2.2 shows photographs of the slag drop and charcoal pellet after they were removed from the furnace. The figure shows that the slag drop had a pale orange transparent color, where some metal was visible in the front end of the slag drop, and that the slag drop moved some towards the edge of the charcoal pellet during the test.

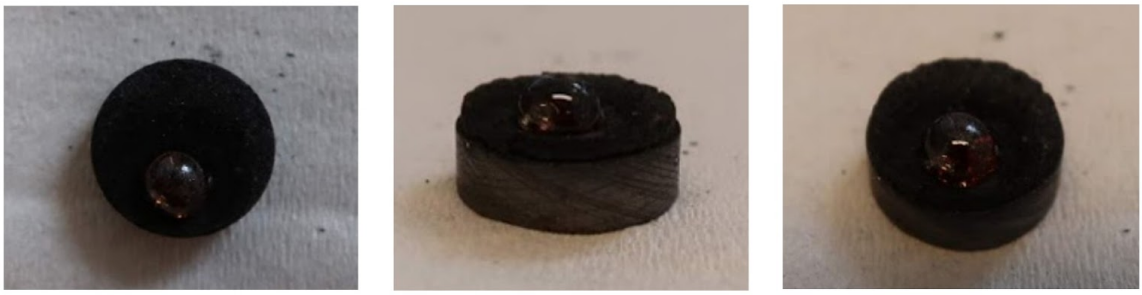

Figure 4.1.2.2: Pictures of slag drop and charcoal pellet after test 3

Figure 4.1.2.3 shows the development of the contact angle and temperature, while figure 4.1.2.4 shows the development of the relative volume and temperature of test 3. The figures shows that the contact angle and the volume decreases as long as the test lasts. The contact angle decreases evenly while the volume shows some fluctuations, likely caused by gas being trapped in the slag drop.

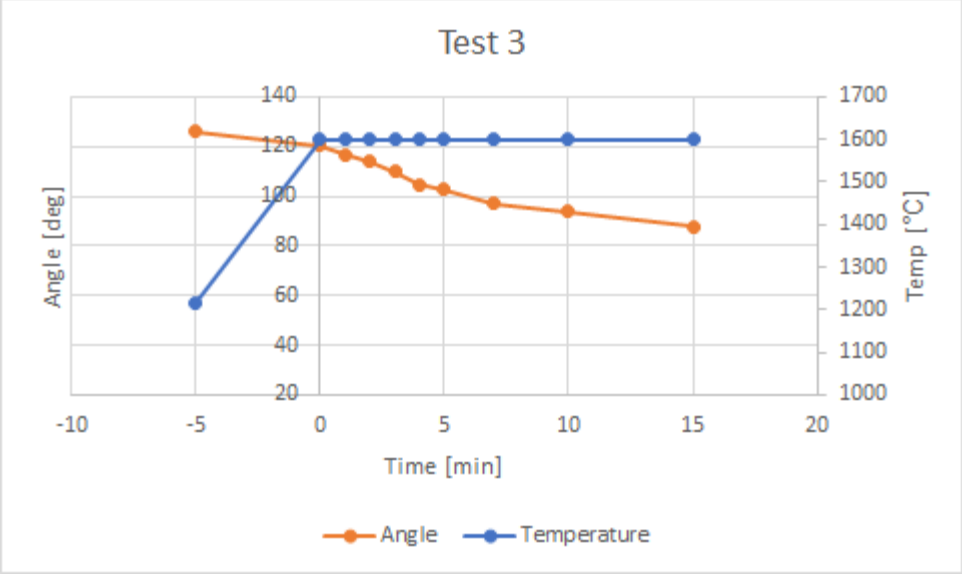

Figure 4.1.2.3: Contact angle and temperature development for test 3

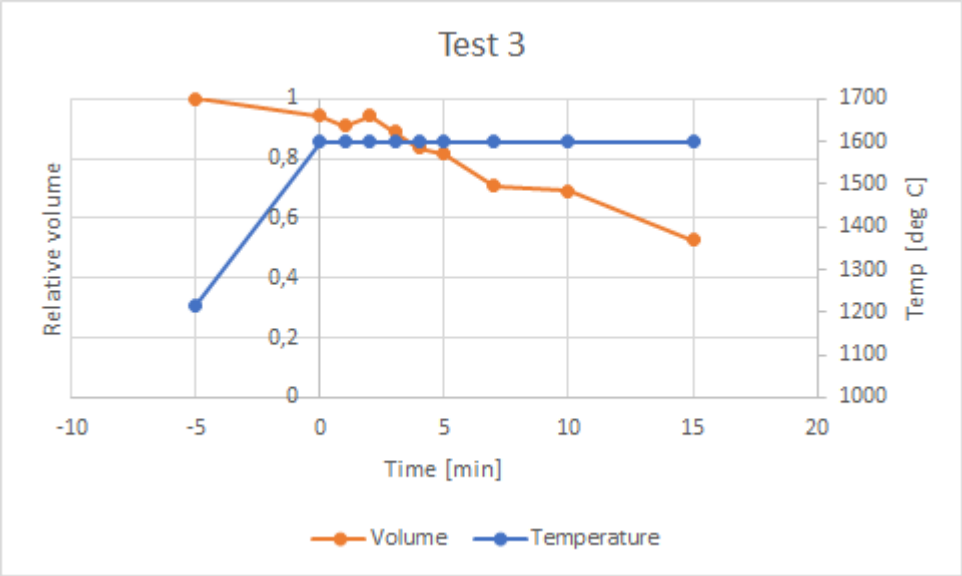

Figure 4.1.2.4: Relative volume and temperature development of test 3

Figure 4.1.2.5 shows a picture of the sample taken in SEM. The figure shows that there are two metal droplets present on the surface of the sample, and that the charcoal pellet can be made out at the bottom of the figure. Figure 4.1.2.6 shows the slag phase of sample 3 magnified 1000 times, while sample 4.1.2.7 shows the metal phase magnified 1000 times. The figures show that the metal and slag phase are both uniform/glassy.

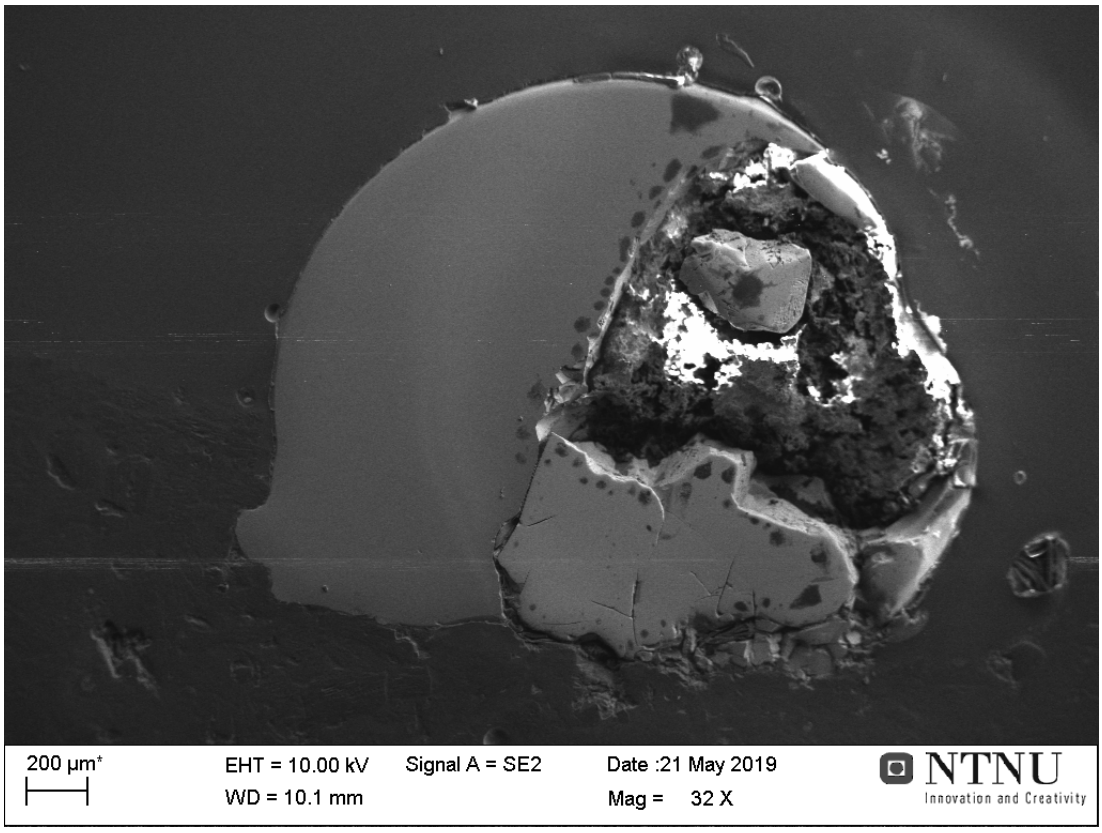

Figure 4.1.2.5: Picture of sample 3 taken in SEM

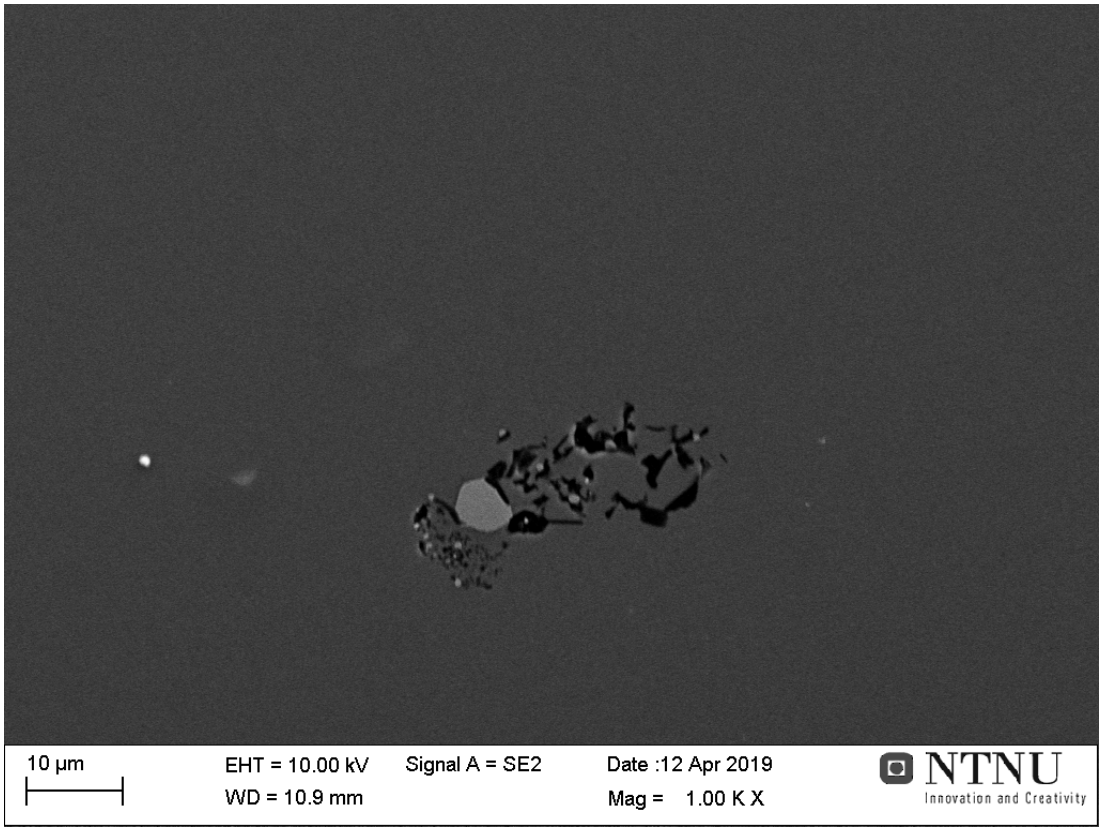

Figure 4.1.2.6: Slag phase of sample 3 magnified 1000 times

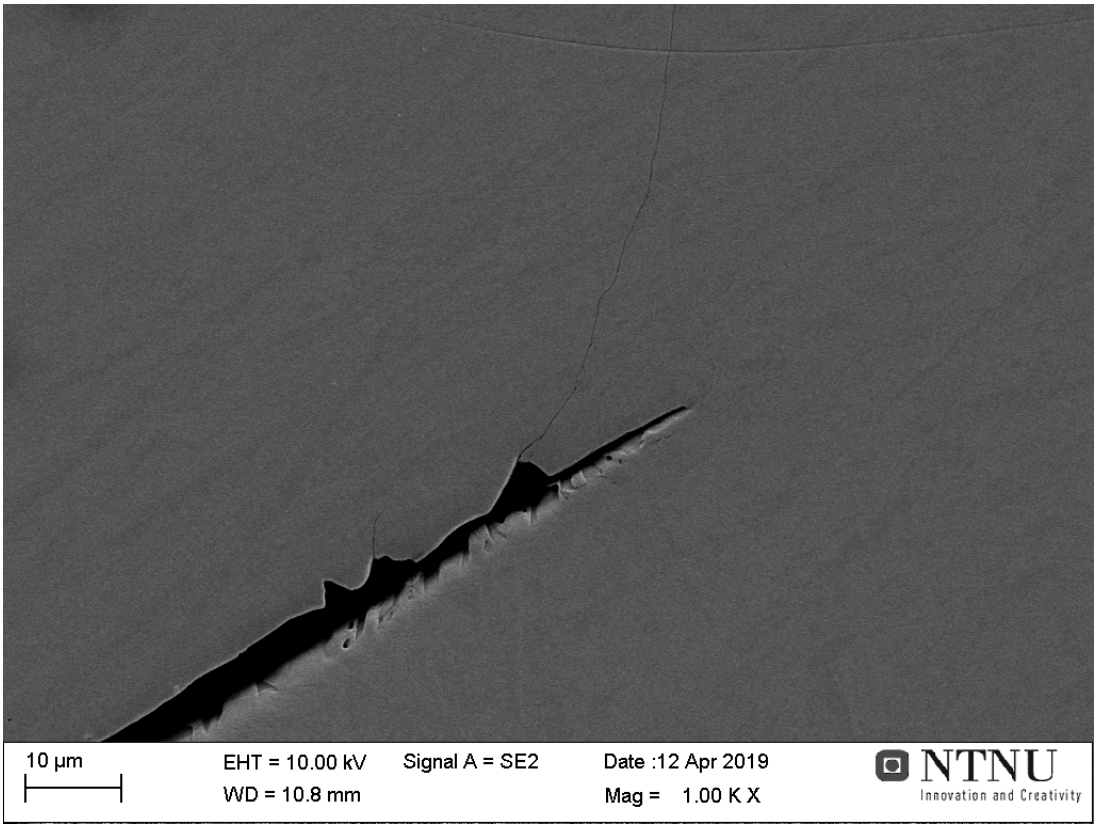

Figure 4.1.2.7: Metal phase of sample 3 magnified 1000 times

Table 4.1.2.1 lists the composition of the slag measured by SEM and EPMA, and the composition of the metal calculated from the slag composition measured by SEM. The slag has a high content of MnO compared to the desired 5%, while the metal has a low content of silicon compared to the desired 18%. The slag contents measured by SEM and EPMA are similar, but the difference for SiO_2 and Al_2O_3 is higher than for the other oxides.

Table 4.1.2.1: Slag composition measured by SEM and EPMA for sample 3, and metal composition calculated from SEM results

Slag (measured)	**MnO**	**SiO_2**	**FeO**	**Al_2O_3**	**CaO**	**MgO**	**SO_3**
SEM [wt%]	26,18	38,03	0,06	13,15	16,39	4,74	1,45
EPMA [wt%]	26,81	41,53	0,07	10,84	16,36	4,48	1,36
Metal (calculated)	**Total**	**Mn**		**Si**		**Fe**	
[wt%]	100	73,60		9,83		16,57	
[g]	0,0290	0,0214		0,0029		0,0048	

Reduction degrees for test 3 are R_{Mn} = 0,662 and R_{Si} = 0,083

4.1.3 Test 9

The ninth test was run with charcoal pellet 8 and slag pellet 1K, at 1600°C for 15 minutes. The slag sample melted at 1193°C, and showed some activity as the temperature was held at 1250°C, however there were few bubbles and low volume expansion.As the temperature was increased to 1300°C the volume expansion of the slag drop increased, while the amount of bubbles increased as temperature reached around 1380°C. As temperature reached 1440°C the slag drop had one expansion where the volume increased significantly, and this was the highest volume expansion observed in the test. After this there were more bubbles and lower volume expansion. The activity increased some after the furnace reached 1600°C, and the activity increased further for the first minutes after. There were more bubbles, but low volume expansion. There was also observed some particles flying at the sides of the slag drop, which may indicate activity where the gas did not enter the drop. After 12 minutes, the volume expansion of the bubbles increased some, before the activity decreased for the last one and a half minutes of the test.

Figure 4.1.3.1 shows some pictures of the slag drop in the furnace during test 9. The pictures show the slag sample before heating at 25°C, after melting at 1193°C, as furnace temperature reached 1600°C, and after 5 and 15 minutes at 1600°C. The figure shows that the charcoal pellet shrunk and almost came loose from the craphite cup during heating, and that the slag drop changed shape and contact angle during the test.

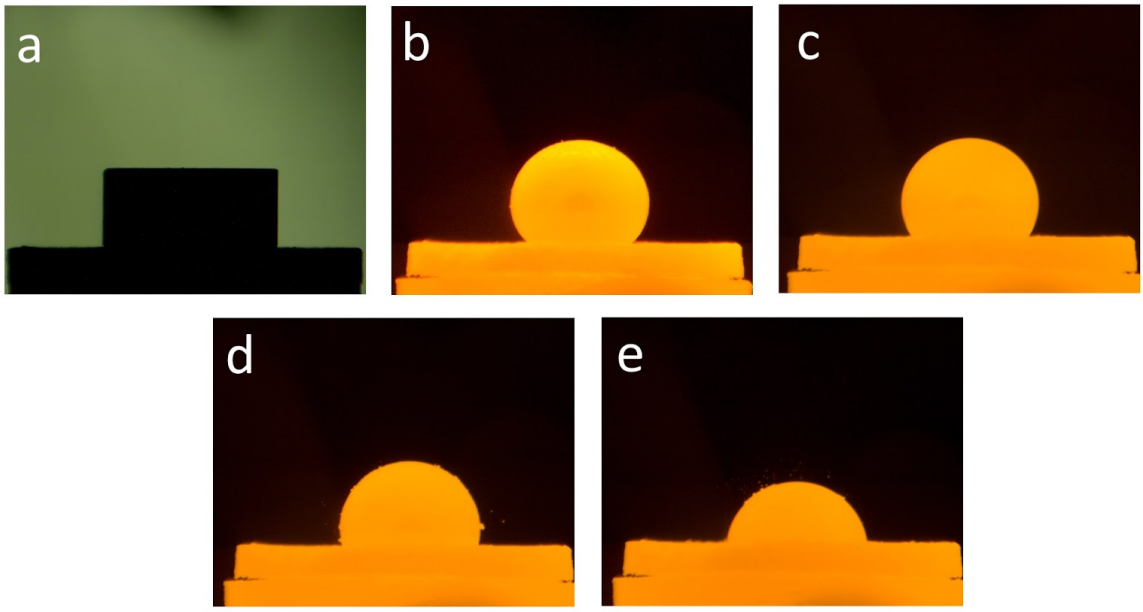

Figure 4.1.3.1: Pictures taken of test 9 in the furnace; a - before heating at 25°C; b - after melting at 1193°C; c - as furnace reaches 1600°C; d - after 5 minutes at 1600°C; e - after 15 minutes at 1600°C.

Figure 4.1.3.2 shows pictures of the slag drop and charcoal pellet after test 9. The figure shows that the slag drop had an orange transparent color, and that there was a metal droplet on the side of the slag drop close to the charcoal pellet. In addition, more metal droplets can be made out between the slag drop and the charcoal pellet.

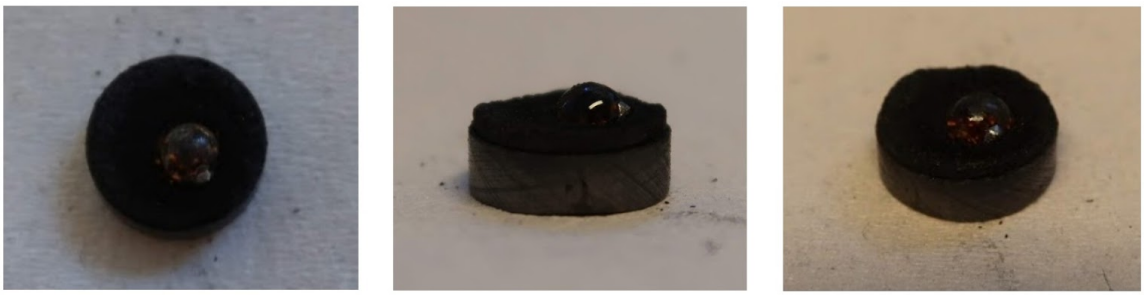

Figure 4.1.3.2: Pictures taken of slag drop and charcoal pellet after test 9

Figure 4.1.3.3 shows the development of the contact angle and temperature of test 9 while figure 4.1.3.3 shows the development of the relative volume and temperature of test 9. The figures show that the contact angle decreases steadily with time for the whole test, while the volume has a decreasing trend with some fluctuations. The fluctuations are likely due to some gas trapped in the slag drop.

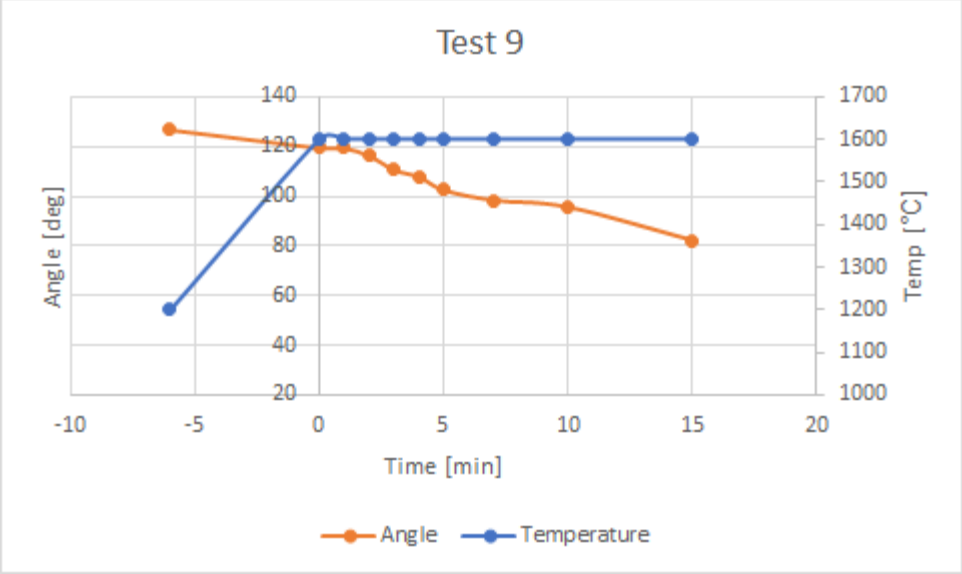

Figure 4.1.3.3: Contact angle and temperature development for test 9

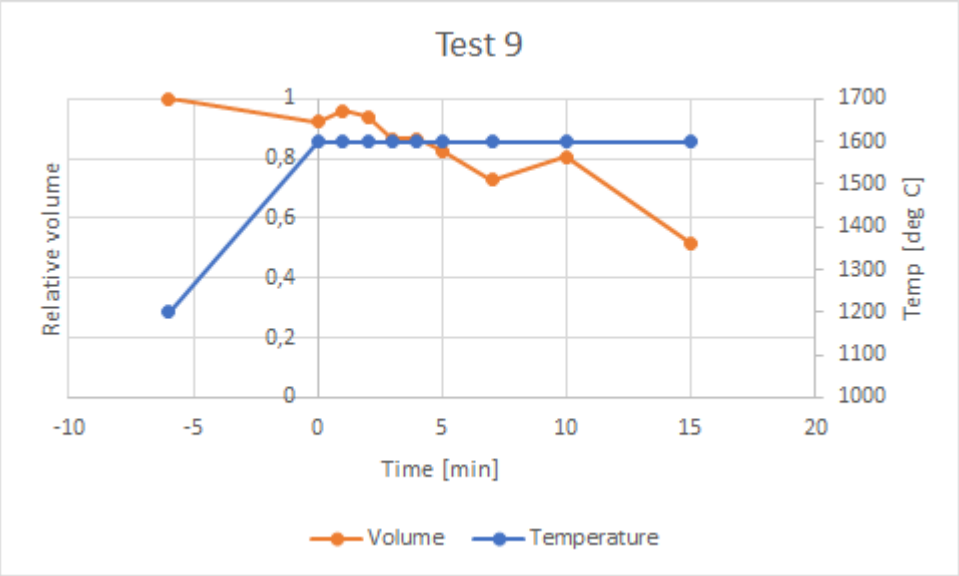

Figure 4.1.3.4: Relative volume and temperature development for test 9

Figure 4.1.3.5 shows an image taken of sample 9 in the SEM. The figure shows that there are three metal droplets inside the slag of considerable size, and the charcoal pellet can be seen at the bottom of the figure. Figure 4.1.3.6 shows the slag phase of the sample magnified 1000 times, and shows that the slag is glassy. Figure 4.1.3.7 shows the metal droplet magnified 1000 times, and shows that there is little or no structure at the surface of the metal.

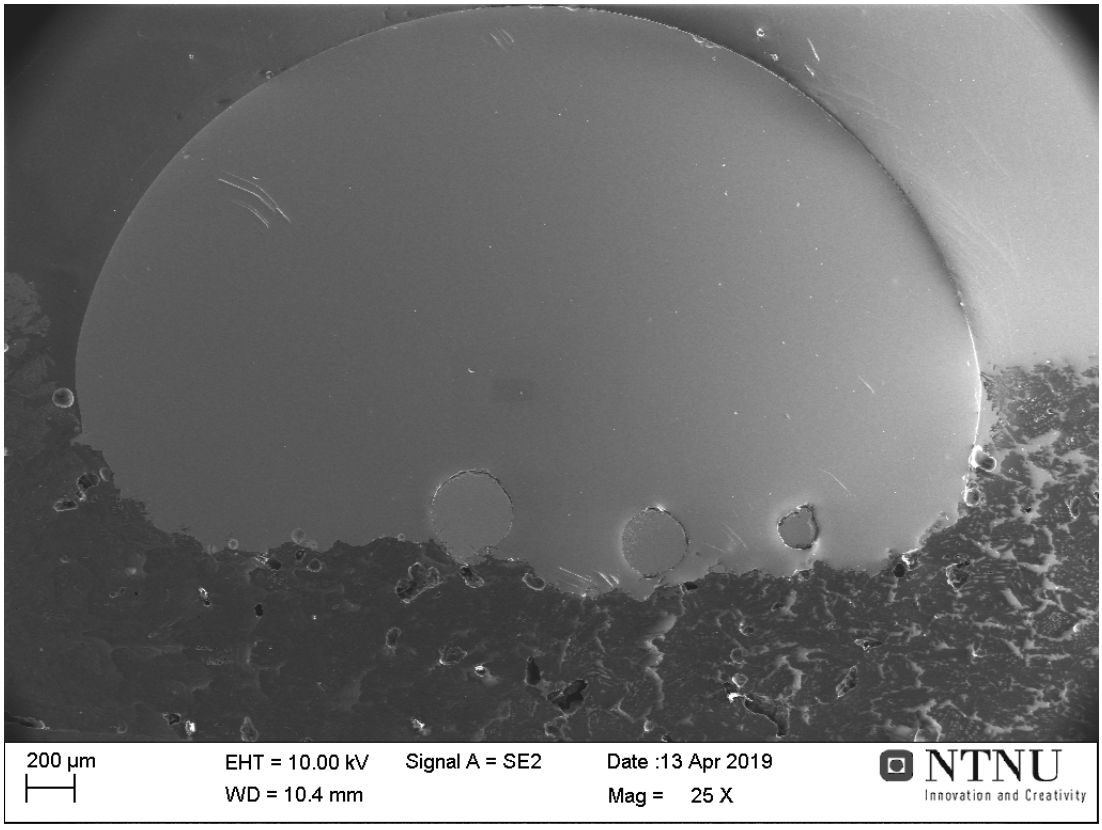

Figure 4.1.3.5: Image of sample 9 taken in SEM

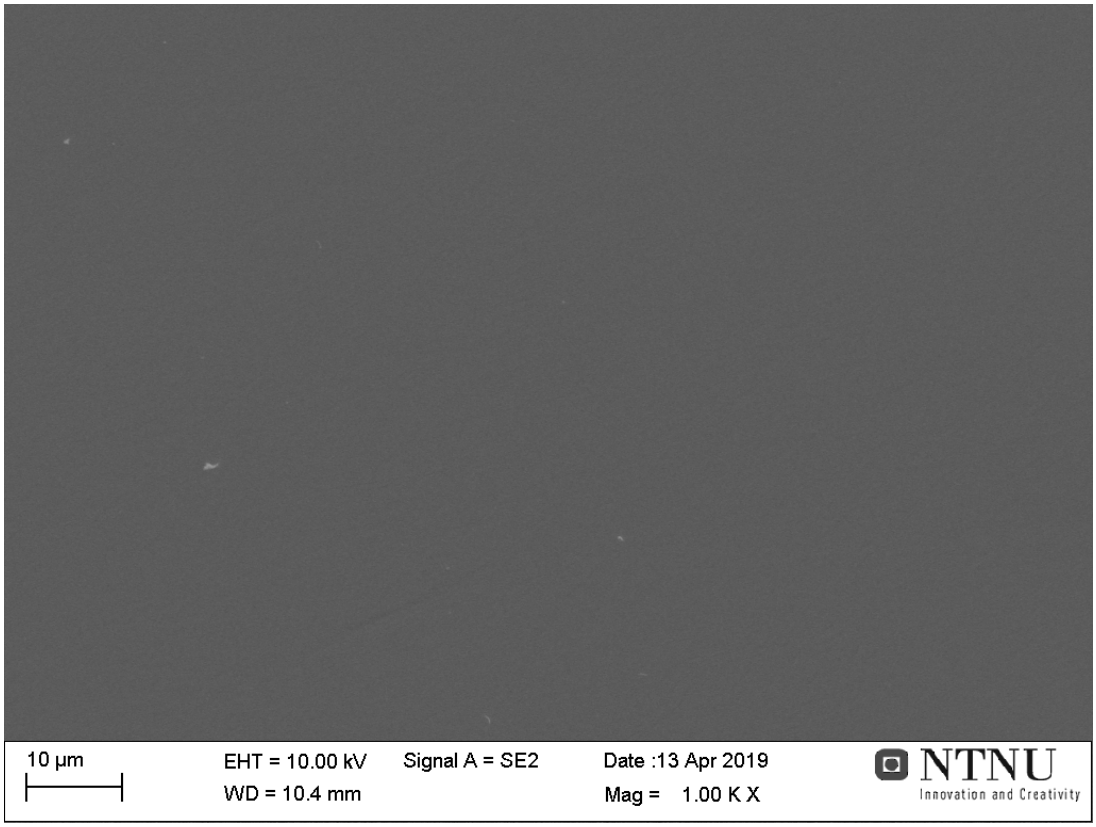

Figure 4.1.3.6: Details of the slag phase of sample 9 magnified 1000 times

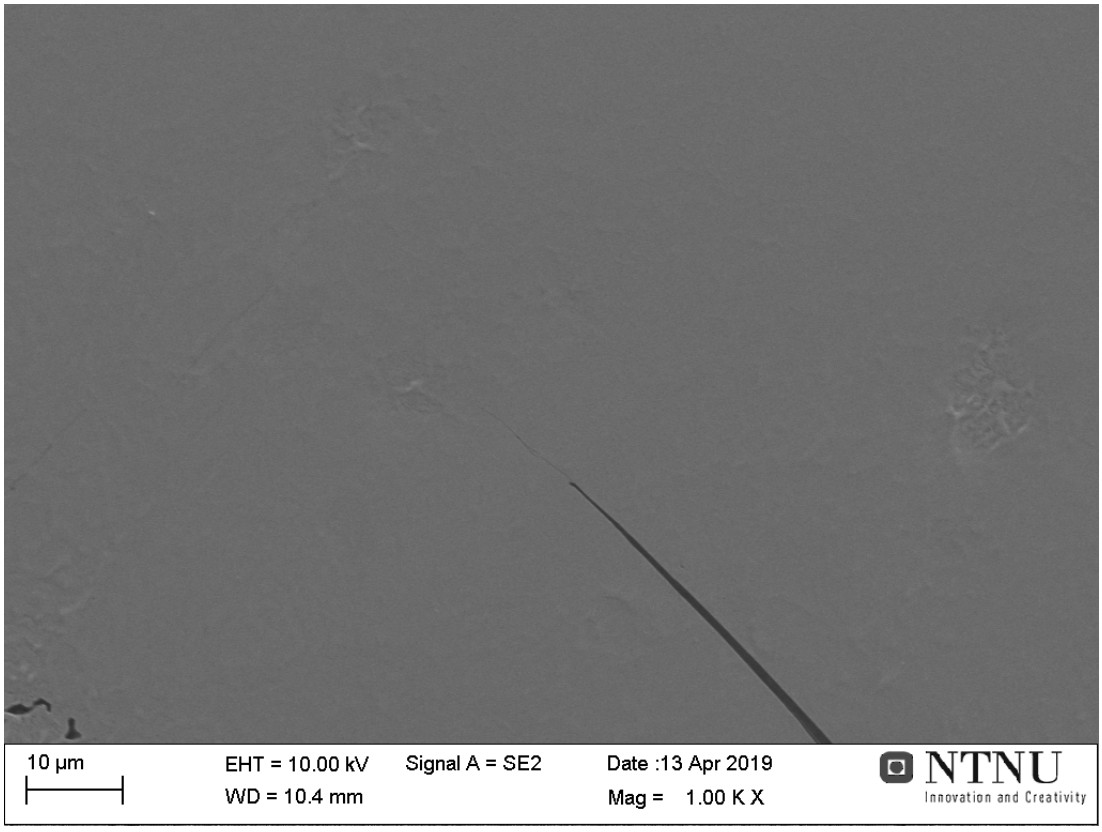

Figure 4.1.3.7: Details of the metal droplet in sample 9 magnified 1000 times.

Table 4.1.3.1 lists the composition of the slag measured by SEM and EPMA, and the composition of the metal calculated from the slag composition measured by SEM. The slag has high content of MnO compared to the desired 5%, while the metal has very low content of silicon compared to the desired 18%. The results from the SEM and EPMA analysis are similar, as is expected.

Table 4.1.3.1: Slag composition measured by SEM and EPMA for sample 9, and metal composition calculated from SEM results

Slag (measured)	**MnO**	**SiO_2**	**FeO**	**Al_2O_3**	**CaO**	**MgO**	**SO_3**
SEM [wt%]	19,41	45,19	0	13,52	16,43	5,44	0
EPMA [wt%]	21,98	43,85	0,05	11,82	17,98	4,81	1,35
Metal (calculated)	**Total**	**Mn**		**Si**		**Fe**	
[wt%]	100	80,72		3,67		15,61	
[g]	0,0296	0,0239		0,0011		0,0046	

Reduction degrees for test 9 are R_{Mn} = 0,729 and R_{Si} = 0,033

4.1.4 Test 5

The fifth test was run with charcoal pellet 6 and slag sample 1G, at 1600°C for 5 minutes. The slag sample melted and formed a slag drop at 1207°C. There were some activity as the furnace was kept at 1250°C for one minute, observed as bubbling with low volume expansion. The activity increased some between 1350°C and 1600°C, with a bit higher volume expansion and fewer bubbles. As the furnace reached 1600°C and for the rest of the test, the volume expansion of the slag drop decreased and the amount of bubbles increased.

Figure 4.1.4.1 shows pictures taken of the slag drop during the test. The pictures show the slag sample before heating at 25°C, after melting at 1207°C, as the furnace is heated to 1600°C, and after 5 minutes at 1600°C. The figure shows that the charcoal pellet shrunk some during heating, and that the slag drop moved some during the test, in addition to changing contact angle and shape.

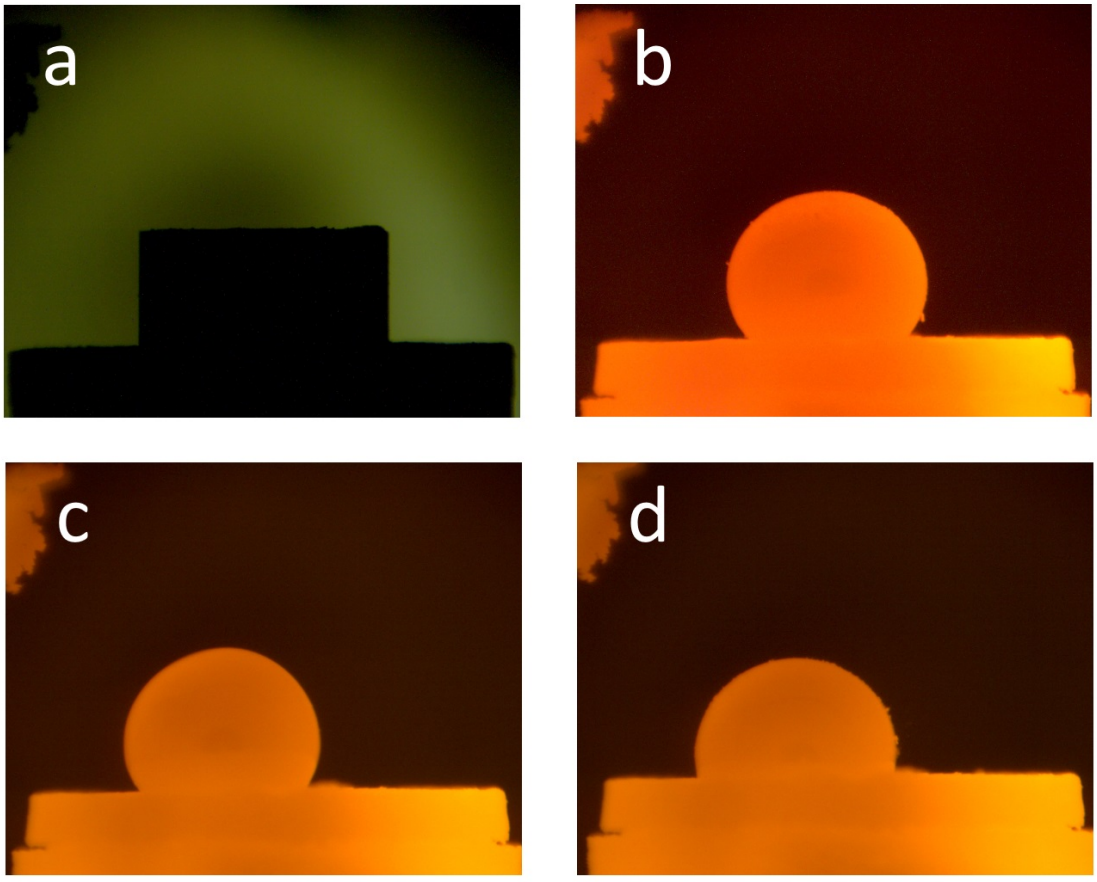

Figure 4.1.4.1: Pictures taken of test 5 in the furnace; a - before heating at 25°C; b - after melting at 1207°C; c - as furnace reaches 1600°C; d - after 5 minutes at 1600°C

Figure 4.1.4.2 shows pictures of the slag drop and charcoal pellet after test 5. The figure shows that the slag drop mainly had a pale green non-transparent color on the surface, where but that there were some “cracks” with orange transparent color. The slag drop also had some charcoal particles at the surface.

Figure 4.1.4.2: Pictures of slag drop and charcoal pellet after test 5

Figure 4.1.4.3 shows development of the contact angle and temperature of test 5 while figure 4.1.4.4 shows development of relative volume and temperature of test 5. The figures show that the contact angle decreased with reduction time, and that the relative volume had a decreasing trend but some fluctuations, likely caused by gas trapped in the slag drop on some of the images analysed.

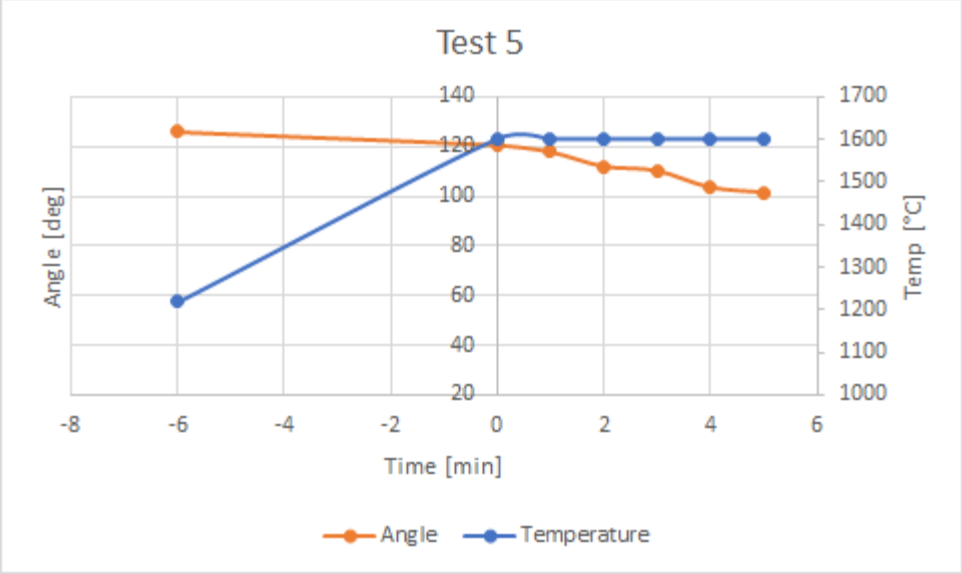

Figure 4.1.4.3: Contact angle and temperature development for test 5

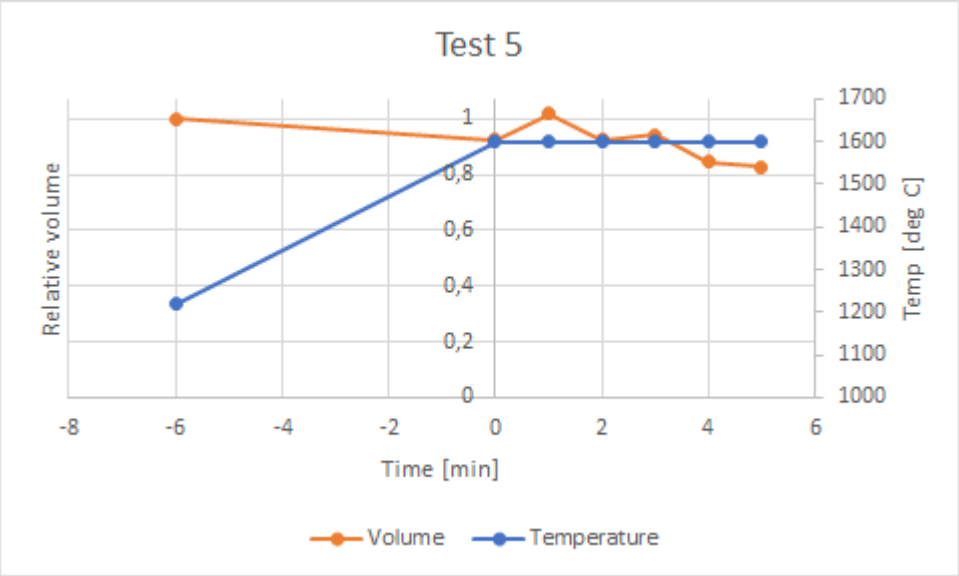

Figure 4.1.4.4: Relative volume and temperature development for test 5

Figure 4.1.4.5 shows a picture of sample 5 taken in SEM. The figure shows that the sample has two metal droplets of considerable size in the slag. It can be seen from the figure that the slag drop has reduced its way down into the charcoal pellet, even though the charcoal pellet is not visible in the figure. Figures 4.1.4.6 and 4.1.4.7 shows details of the slag in sample 5, both with 1000 times magnification. The figures show that the pattern and size of the two-phase slag varies across the sample. Figure 4.1.4.8 shows the metal phase at 1000 times magnification, and that the metal has clear structure at the surface.

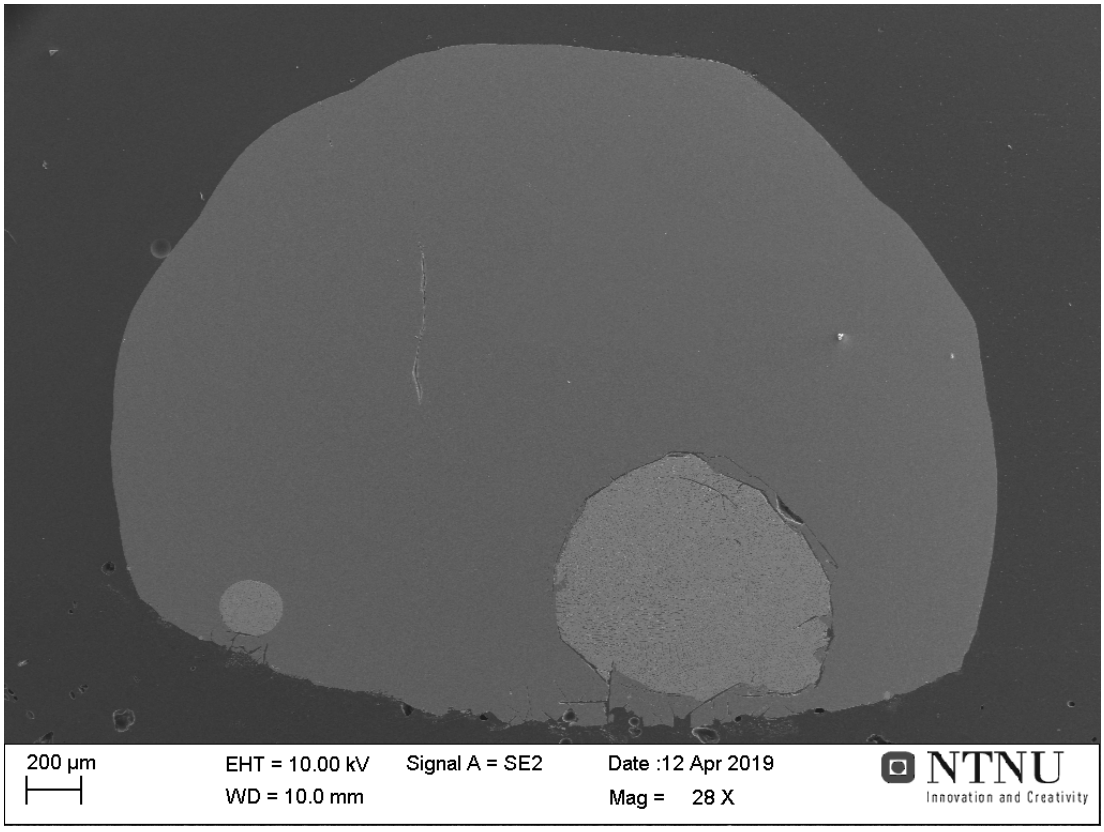

Figure 4.1.4.5: Picture of sample 5 taken in SEM

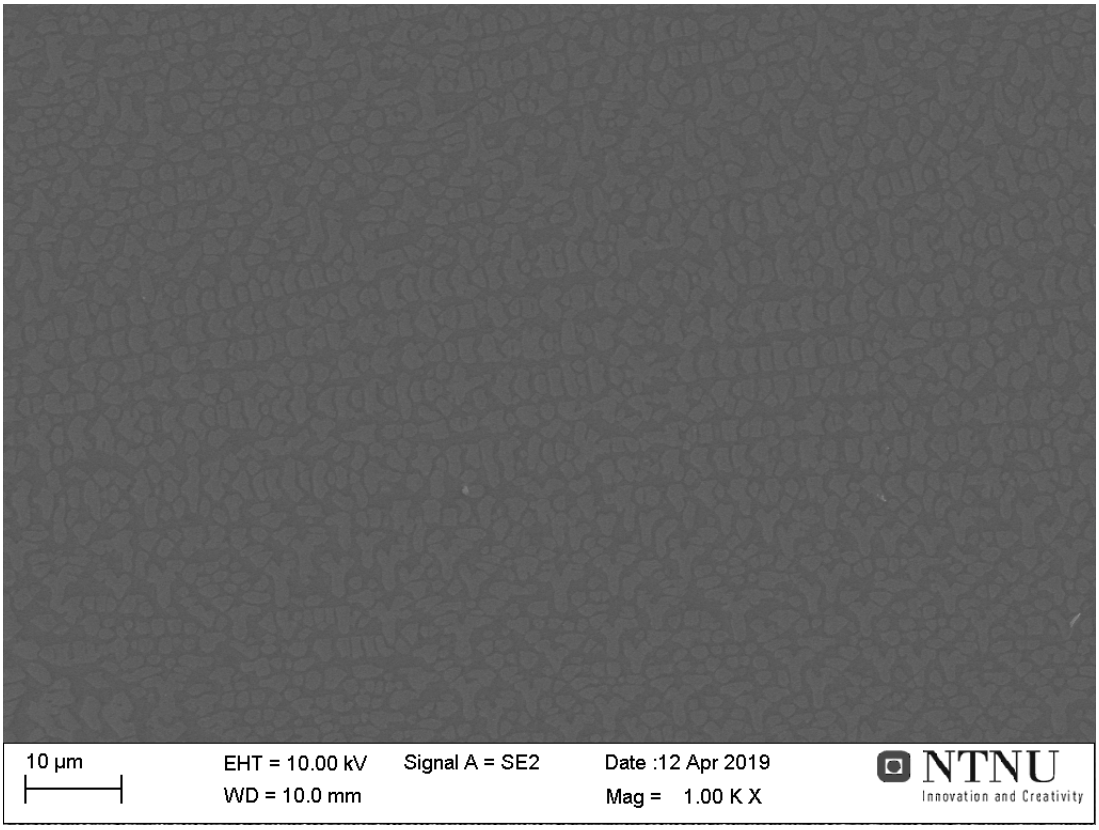

Figure 4.1.4.6: Fine two-phase slag of sample 5 magnified 1000 times

Figure 4.1.4.7: Larger two-phase slag of sample 5 magnified 1000 times

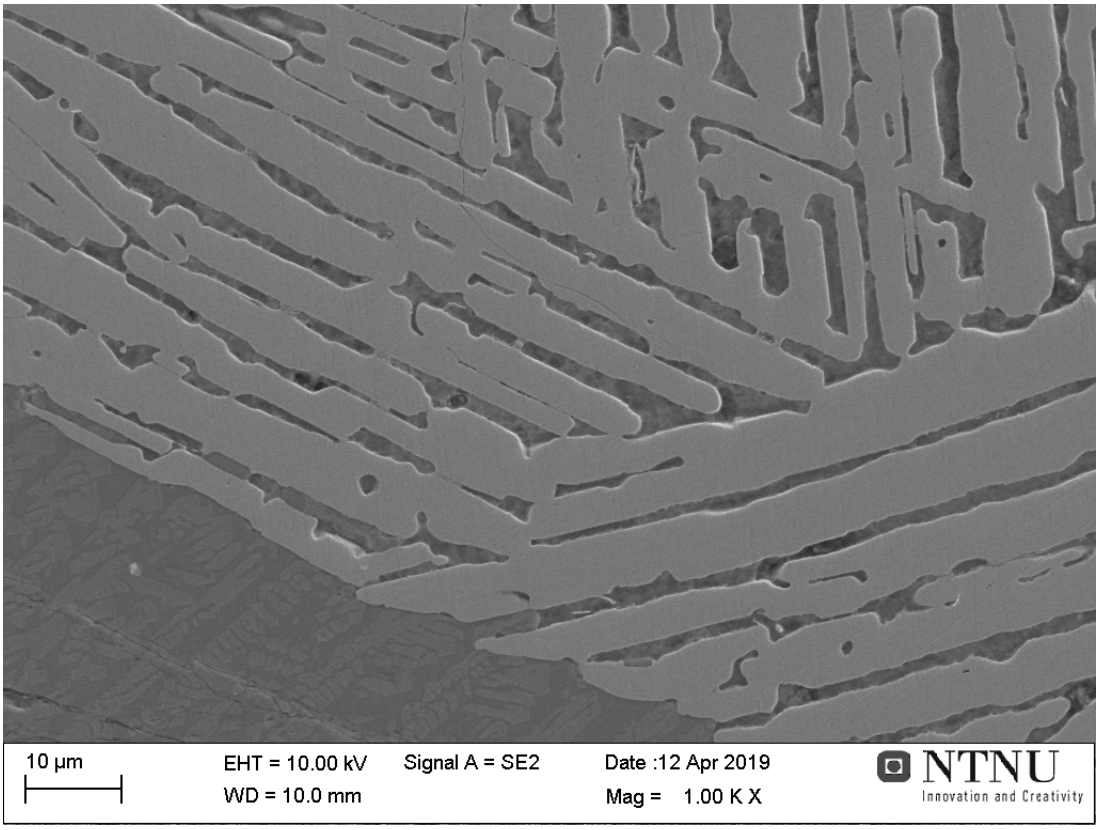

Figure 4.1.4.8: Metal phase of sample 5 magnified 1000 times

Table 4.1.4.1 lists the composition of the slag phase measured by SEM and EPMA, and the composition of the metal calculated from the slag composition measured by SEM. The slag has a high content of MnO, while the metal has a silicon content that is a bit lower than the desired 18%. The slag composition measured by SEM and EPMA is similar, as is expected.

Table 4.1.4.1: Slag composition measured by SEM and EPMA for sample 5, and metal composition calculated from SEM results

Slag (measured)	**MnO**	**SiO_2**	**FeO**	**Al_2O_3**	**CaO**	**MgO**	**SO_3**
SEM [wt%]	37,57	32,65	0,22	11,66	13,16	3,70	1,04
EPMA [wt%]	38,19	34,27	0,10	9,29	13,23	3,63	1,10
Metal (calculated)	**Total**	**Mn**		**Si**		**Fe**	
[wt%]	100	62,41		13,02		24,57	
[g]	0,0186	0,0116		0,0024		0,0045	

Reduction degrees for test 1 are R_{Mn} = 0,348 and R_{Si} = 0,073

4.1.5 Test 8

The eight test was run with charcoal pellet 7 and slag pellet 1J, at 1600°C for 5 minutes. The slag drop melted at 1190°C. There was little activity after melting, but it increased some as the temperature was held at 1250°C. Few bubbles with relatively high volume expansion was observed. As the temperature reached about 1460°C, the volume expansion of the slag drop was significant, and this was the highest volume observed during the test. As the temperature was increased further and came close to 1600°C, the activity increased with more bubbles and low volume expansion. The activity increased some again after 3 minutes at 1600°C, and was at the same level for the rest of the test.

Figure 4.1.5.1 shows some pictures taken from the furnace during test 8. The pictures show the slag sample before heating, after melting, as the furnace temperature reaches 1600°C and after 5 minutes at 1600°C. The figure shows that the charcoal pellet shrunk some during heating, and that the slag drop moved some in addition to the contact angle changing during the test.

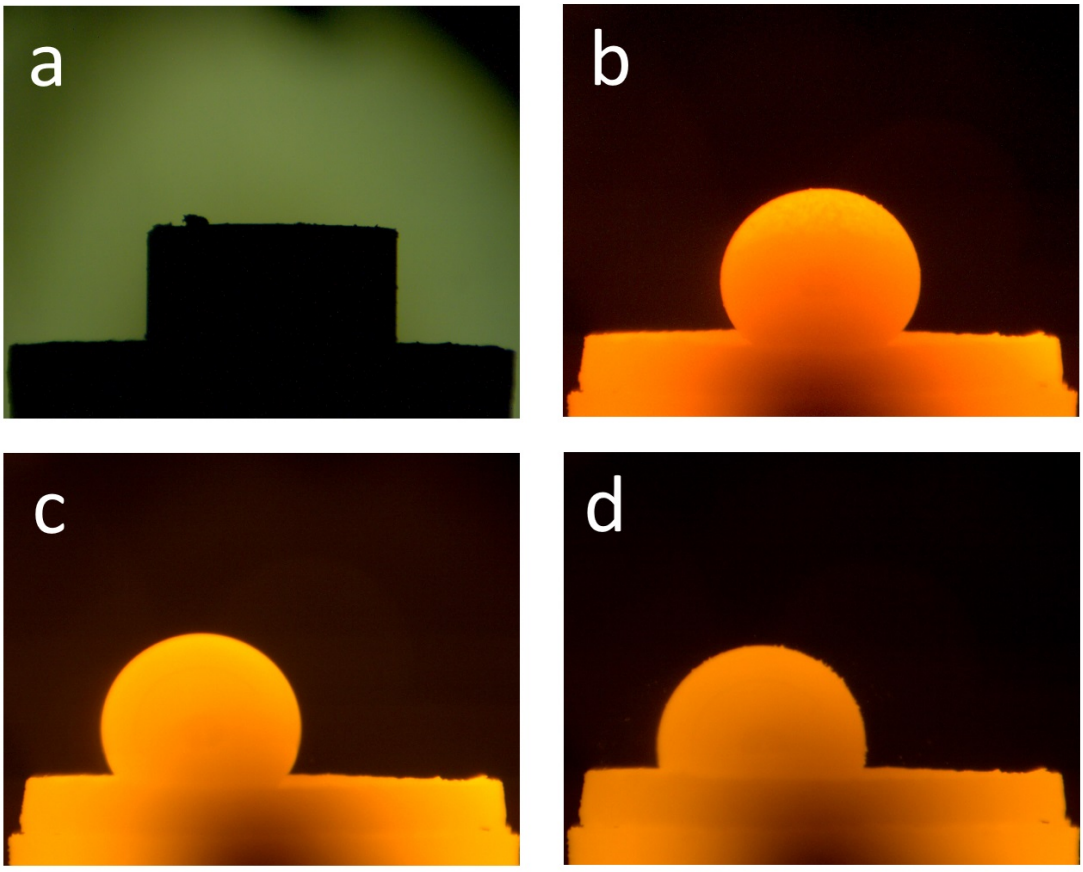

Figure 4.1.5.1: Pictures taken during test 8; a - before heating at 25°C; b - after melting at 1190°C; c - as furnace temperature reaches 1600°C; d - after 5 minutes at 1600°C

Figure 4.1.5.2 shows pictures taken of the slag drop and charcoal pellet after test 8. The figure shows that the slag drop had a mixed surface, where the surface mainly was pale non-transparent green, with some areas of orange transparent color, in addition to a metal droplet being visible in the front of the slag drop.

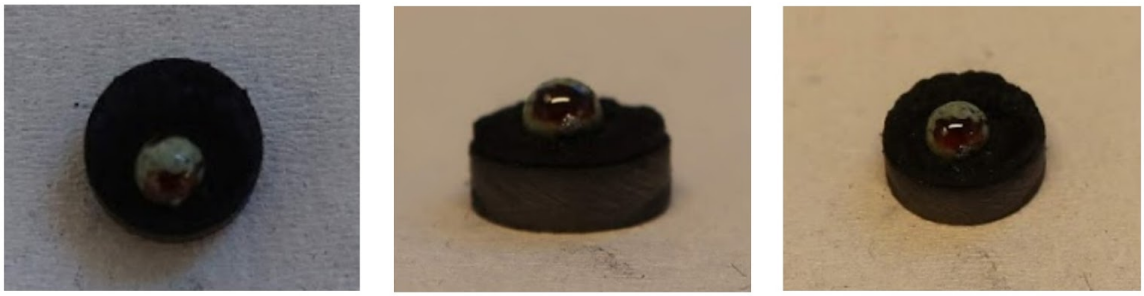

Figure 4.1.5.2: Pictures of the slag drop and charcoal pellet in test 8

Figure 4.1.5.3 shows the development of contact angle and temperature during test 8, while figure 4.1.5.4 shows the development of relative volume and temperature of test 8. The figures show that the contact angle decreases during the hold time of the test, and that the relative volume also decreases with increasing hold time.

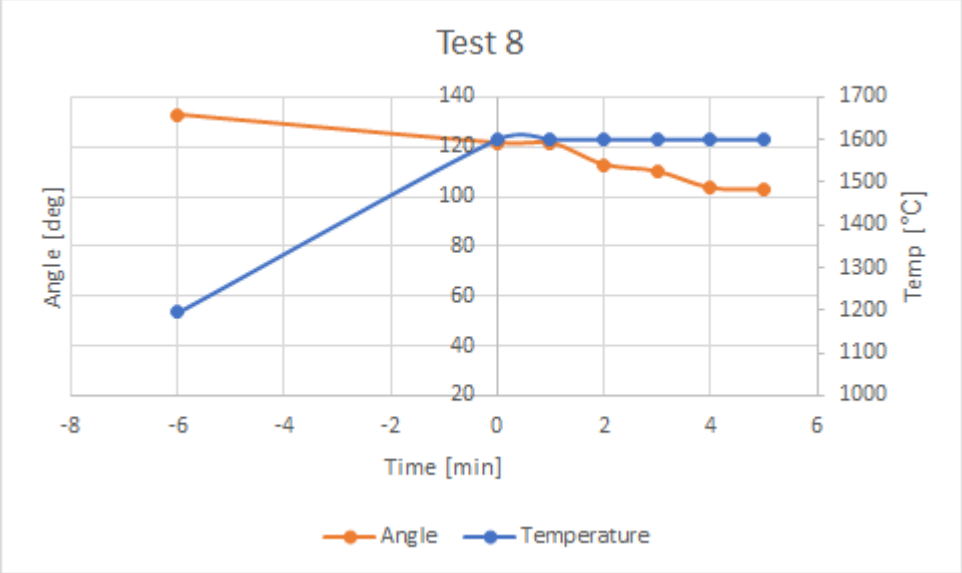

Figure 4.1.5.3: Contact angle and temperature development of test 8

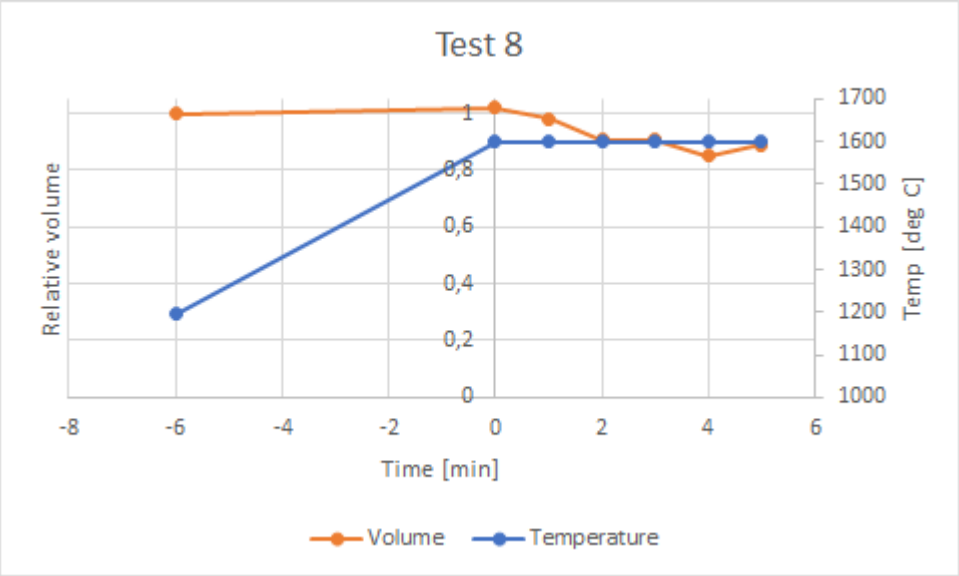

Figure 4.1.5.4: Relative volume and temperature development of test 8

Figure 4.1.5.5 shows an image of sample 8 taken in SEM. The figure shows that the sample has one metal droplet of significant size at the sample surface, and the charcoal pellet can be made out at the bottom of the figure. Figure 4.1.5.6 shows details of the two-phase slag magnified 1000 times, and show that the two-phase slag has varying size and shape. Figure 4.1.5.7 shows details of the glassy slag of sample 8. Figure 4.1.5.8 shows details of the metal droplet magnified 1000 times, and shows that the metal has some structure at the surface.

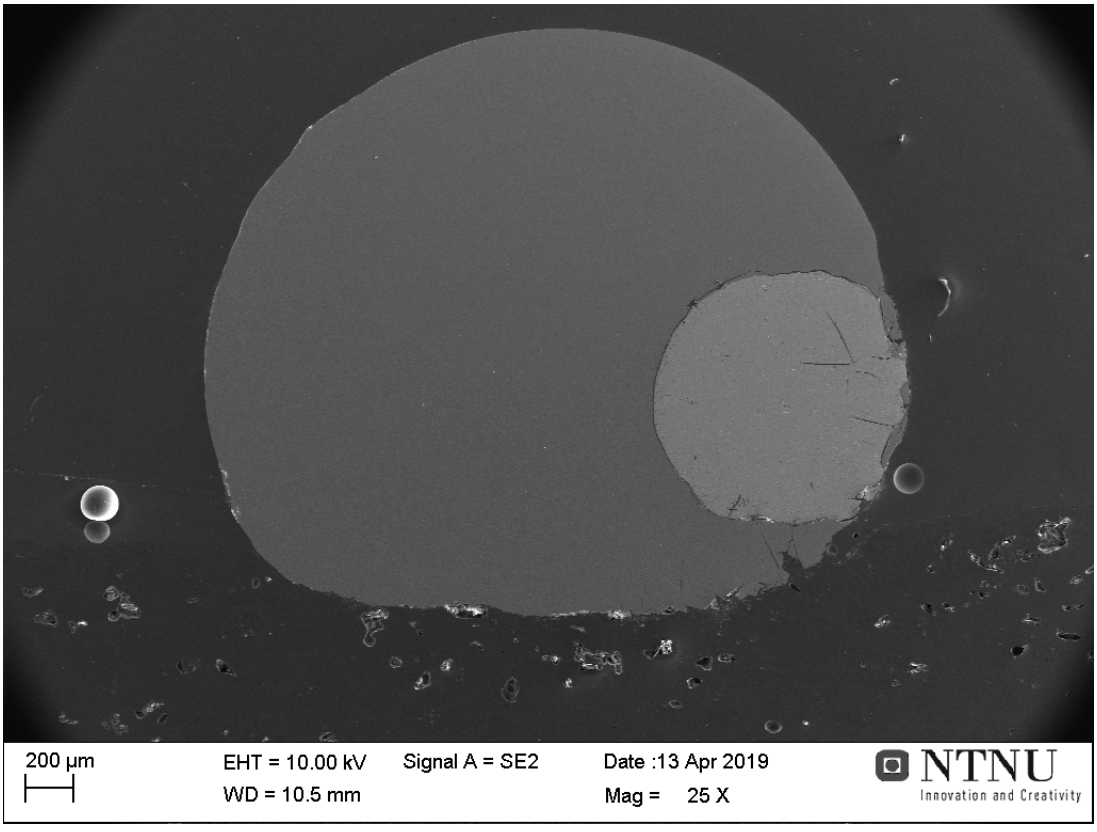

Figure 4.1.5.5: Image of sample 8 taken in SEM

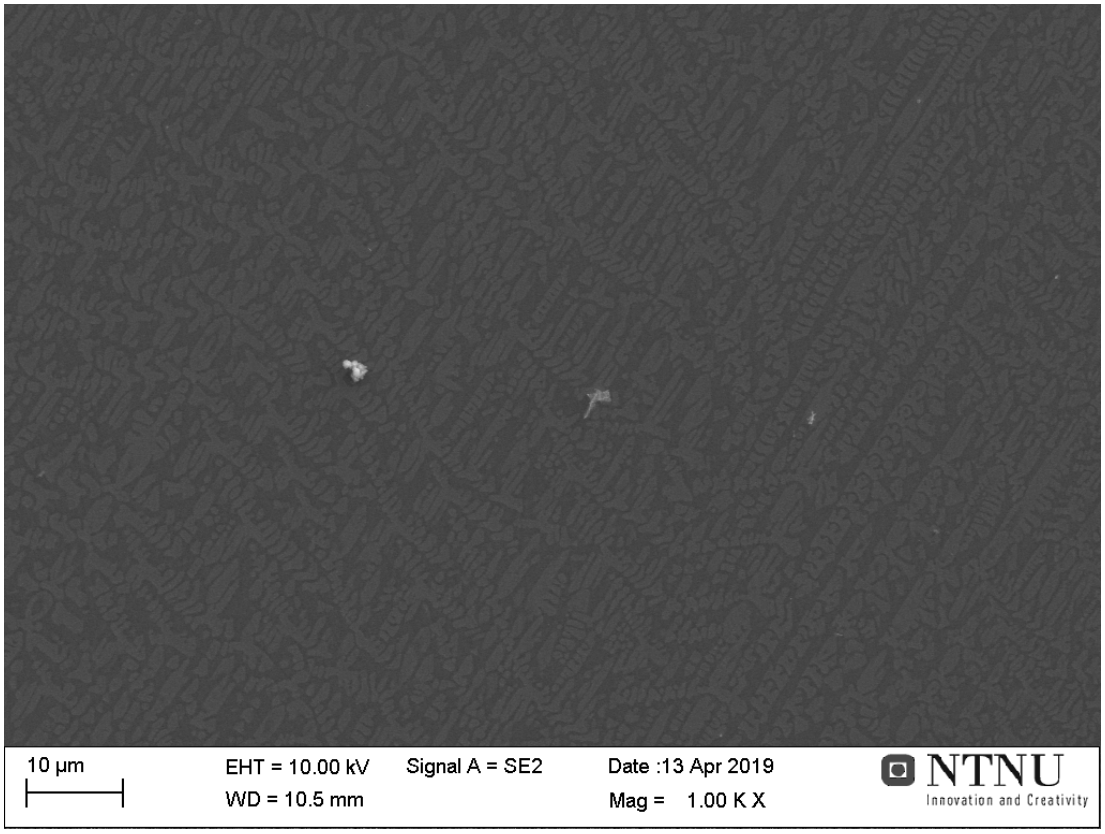

Figure 4.1.5.6: Details of two-phased slag in sample 8 magnified 1000 times

Figure 4.1.5.7: Details of glassy slag in sample 8 magnified 1000 times

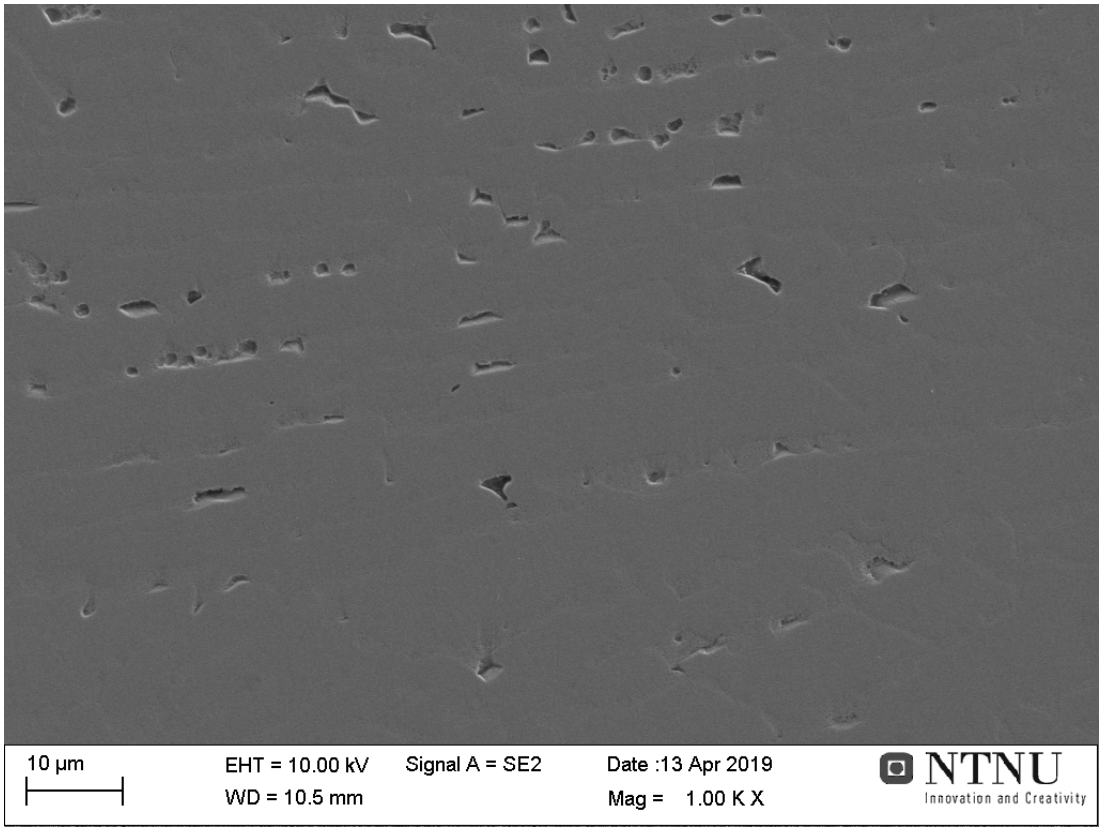

Figure 4.1.5.8: Details of metal in sample 8 magnified 1000 times

Table 4.1.5.1 lists the composition of the slag measured by SEM and EPMA, and the composition of the metal calculated from the slag composition measured by SEM. The slag has high MnO content, while the metal has very low content of silicon compared to the desired 18%. The results of SEM and EPMA analysis are similar, as is expected.

Table 4.1.5.1: Slag composition measured by SEM and EPMA for sample 8, and metal composition calculated from SEM results

Slag (measured)	**MnO**	**SiO_2**	**FeO**	**Al_2O_3**	**CaO**	**MgO**	**SO_3**
SEM [wt%]	40,83	33,89	0	9,39	12,07	3,83	0
EPMA [wt%]	38,08	35,34	0,09	8,95	13,32	3,50	1,15
Metal (calculated)	**Total**	**Mn**		**Si**		**Fe**	
[wt%]	100	56,43		3,97		39,60	
[g]	0,0119	0,0068		0,0005		0,0047	

Reduction degrees for test 1 are R_{Mn} = 0,201 and R_{Si} = 0,014

4.2 Tests run with charcoal and slag 2

Test 11, 15, 20, 18, and 21 were run with slag 2 towards charcoal. Table 4.2.1 shows the weight measurements of the slag pellet and charcoal pellet before the test, and the weight measurement of the slag and charcoal after the test, in addition to the weight loss.

Table 4.2.1: Weight measurement of tests run with charcoal and slag 2

	Time	**Charcoal weight [g]**	**Slag weight [g]**	**Total weight before [g]**	**Weight after [g]**	**Weight loss [g]**	**Weight loss [%]**
11	30	0,0855	0,1076	0,1931	0,1038	0,0893	46,25
15	15	0,0841	0,1062	0,1903	0,1167	0,0736	38,68
16	15	0,0782	0,1077	0,1859	0,1221	0,0638	34,32
20	15	0,0897	0,0995	0,1892	0,1313	0,0579	30,60
18	5	0,0893	0,1013	0,1906	0,1514	0,0392	20,57
21	5	0,0923	0,1079	0,2002	0,1581	0,0421	21,03

The table shows that the test run for 30 minutes has the highest weight loss in percentage, and that the weight loss decreases with decreasing reaction time, as is expected. The tests run for 15 minutes has a high difference in weight loss percentage, while the two tests run for 5 minutes has no significant difference in weight loss.

4.2.1 Test 11

The eleventh test was run with charcoal pellet 9 and slag pellet 2A at 1600°C for 30 minutes. The slag drop melted at 1195°C, and there was little activity after melting. Around 1300°C the activity had increased, there were few bubbles with large volume expansion, which continued to about 1490°C. As the temperature was increased to 1600°C there was moderate activity, with more bubbles and lower volume expansion. After 5 minutes at 1600°C the activity increased and this kept on for some minutes. After 10 minutes at 1600°C the activity increased further, there were many bubbles but relatively low volume expansion. The activity decreased after about 15 minutes, and decreased further after 18 minutes. At the end the slag drop was almost totally “buried” in the charcoal.

Figure 4.2.1.1 shows photographs captured from the furnace during test 11. The pictures show the slag and charcoal before heating, after slag drop melting, as furnace temperature reaches 1600°C, and after 5, 15 and 30 minutes at 1600°C. The figure shows that the charcoal pellet shrunk some during heating, and that the slag drop changed shape during the test and gradually dug its way into the charcoal pellet.

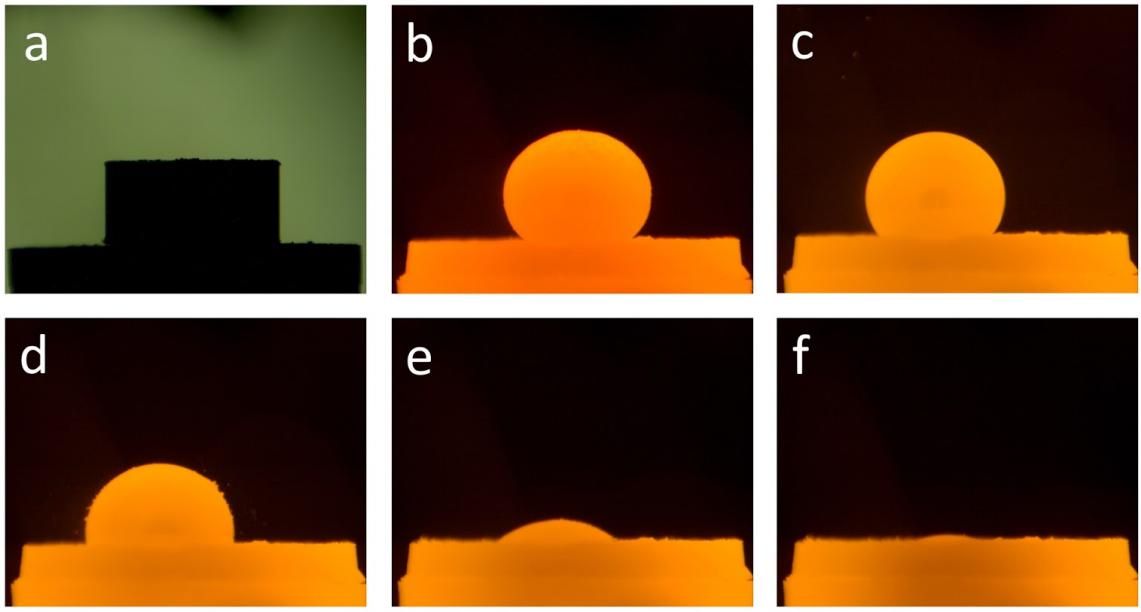

Figure 4.2.1.1: Pictures taken of test 11: a - before heating at 25°C; b - after melting at 1195°C; c - as furnace temperature reaches 1600°C; d - after 5 minutes at 1600°C; e - after 15 minutes; f - after 30 minutes

Figure 4.2.1.2 shows pictures taken of the slag drop and charcoal pellet after test 11. The figure shows that the slag drop was almost completely dug down into the charcoal pellet after the test, and that the slag drop had a pale orange transparent color, a glassy slag. The figure also show that there was visible metal drops between the slag and the charcoal at two sides of the slag.

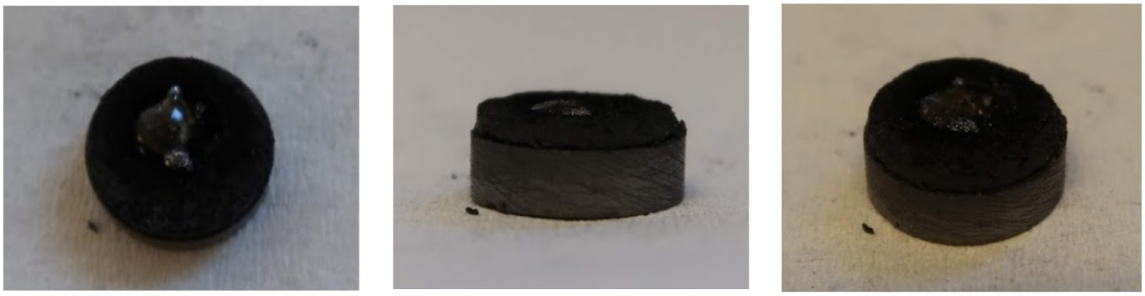

Figure 4.2.1.2: Pictures of slag drop and charcoal pellet after test 11

Figure 4.2.1.3 shows the development of the contact angle and temperature of test 11, while figure 4.2.1.4 shows the development of the relative volume and temperature of test 11. The figures show that the contact angle decreases rapidly with time for the test, except for the measurement at 10 minutes, the relative volume shows the same trend of rapid decreasing with reduction time except for the measurement at 10 minutes. The measurement at 10 minutes is likely caused by gas being trapped in the slag drop.

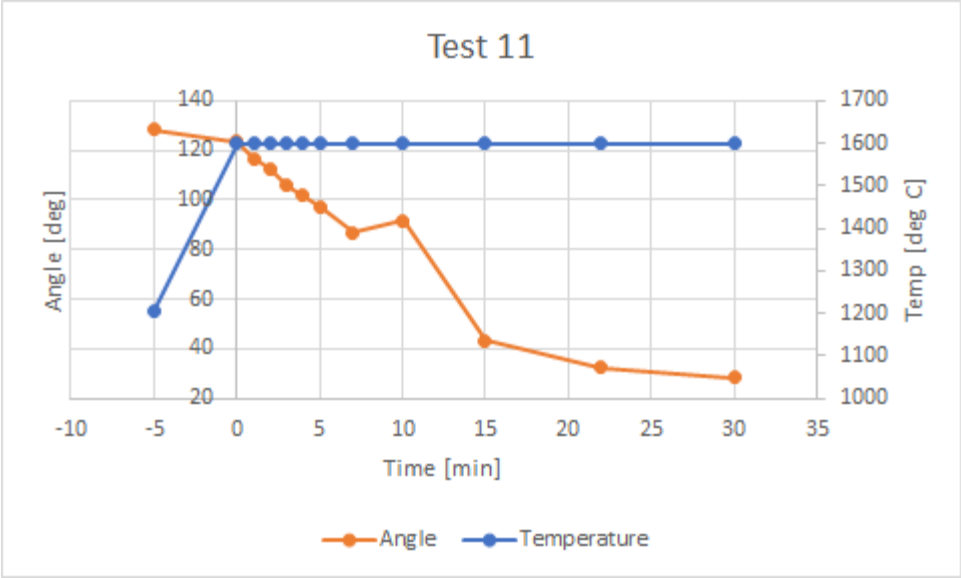

Figure 4.2.1.3: Contact angle and temperature development for test 11

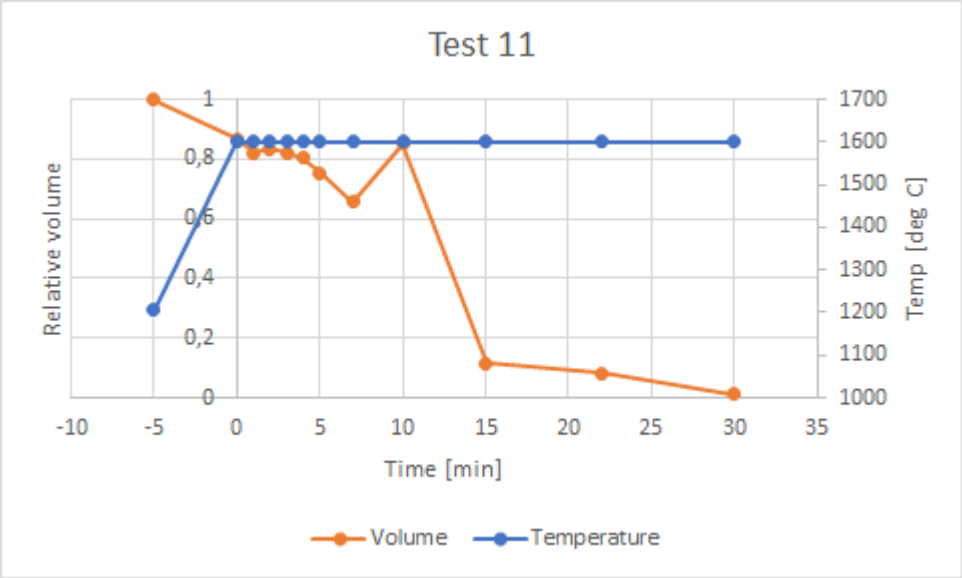

Figure 4.2.1.4: Relative volume and temperature development for test 11

Figure 4.2.1.5 shows an image of sample 11 taken in SEM. The figure shows that there are two large metal droplets, one on each side, and a slag droplet in the middle that is not connected to the two metal droplets at this cross-section. There are also some smaller metal droplets, where one of them is located inside the slag. Figure 4.2.1.6 shows the slag of sample 11 magnified 1000 times, and shows that the slag is glassy. Figure 4.2.1.7 shows details of the metal phase of sample 11. In addition to some cracks in the metal, it can be made out tendencies of structure in the metal in this figure.

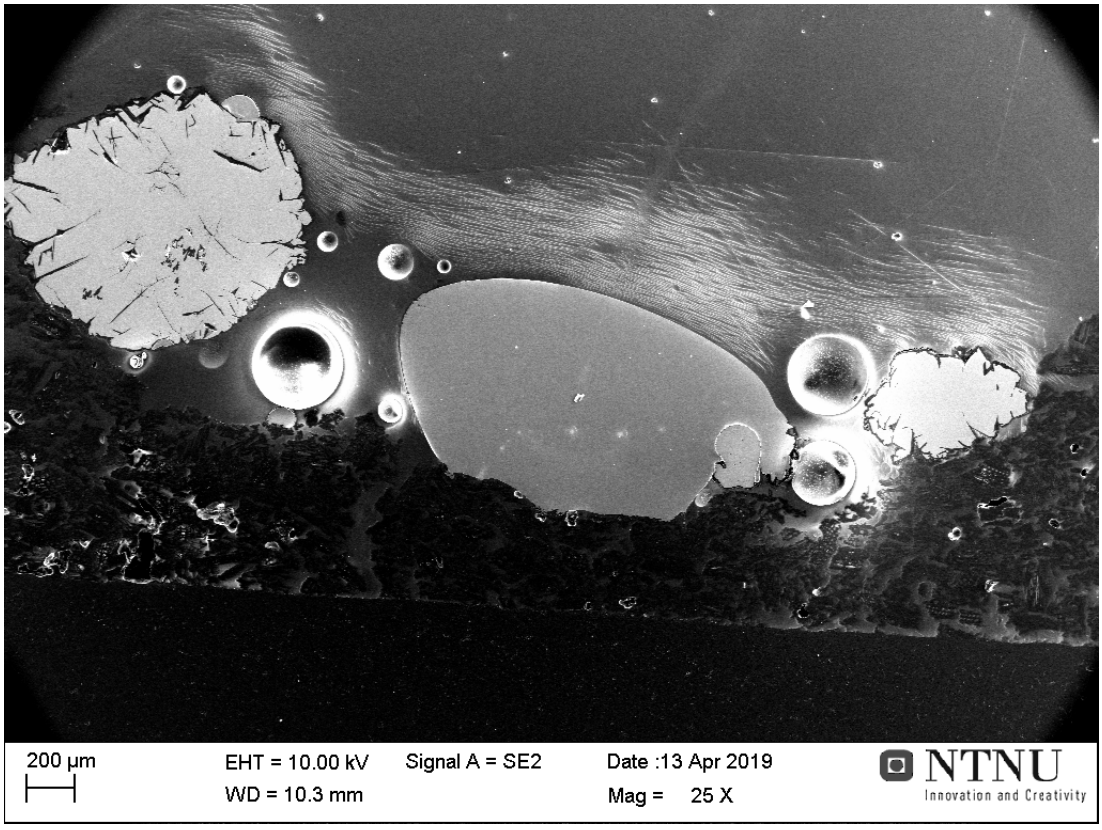

Figure 4.1.2.5: Image of sample 11 taken in SEM, Slag in the middle, and a large metal droplet at each side

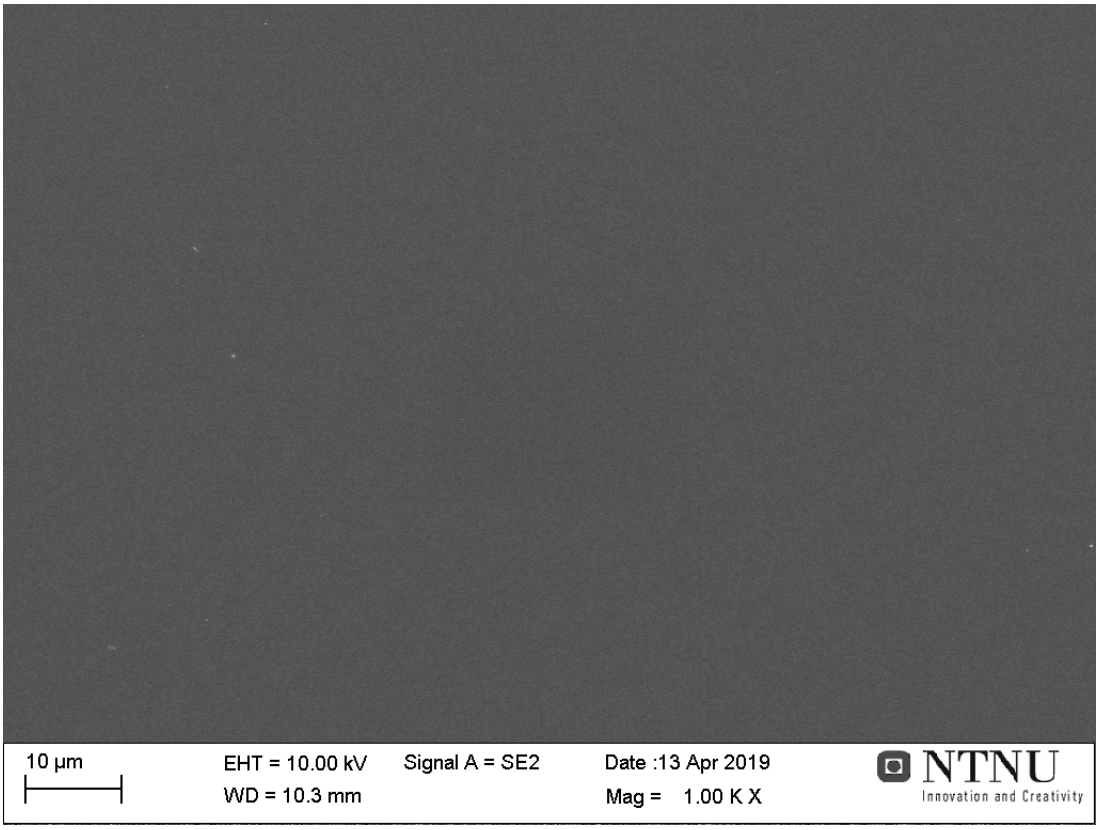

Figure 4.1.2.6: Slag of sample 11 magnified 1000 times

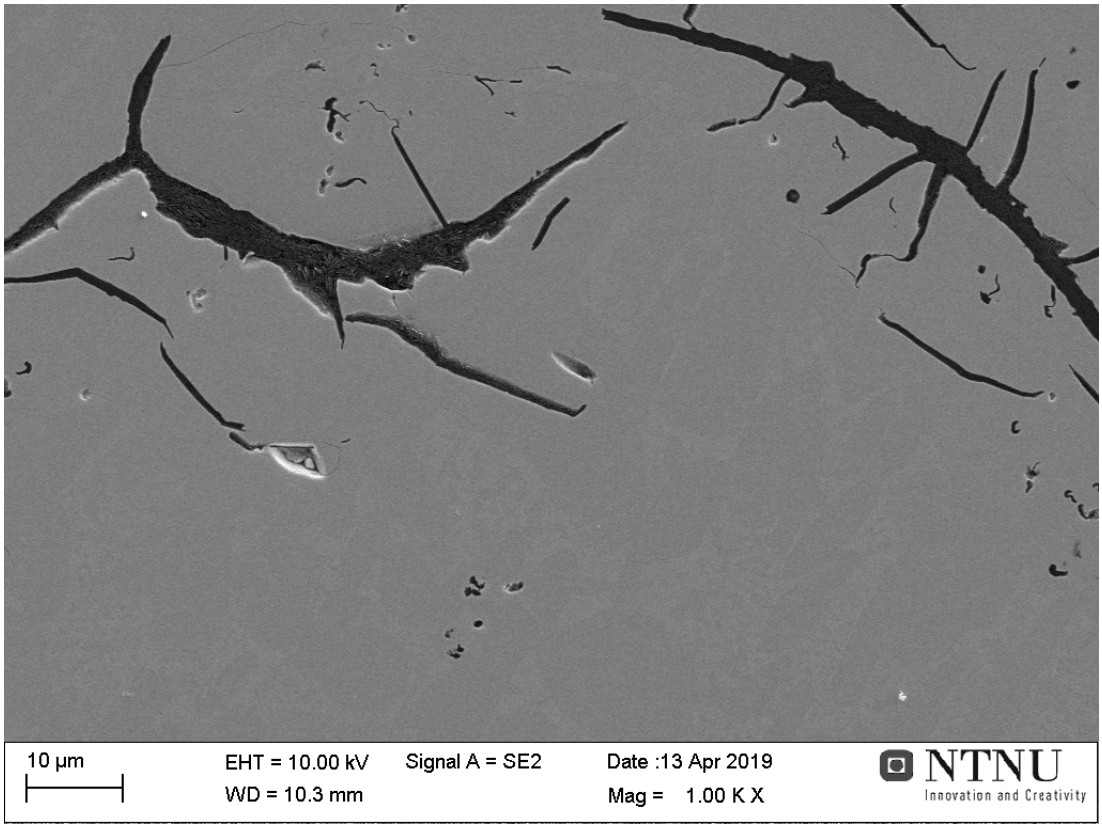

Figure 4.2.1.7: Details of metal phase of sample 11 magnified 1000 times

Table 4.2.1.1 lists the composition of the slag measured by SEM and EPMA and the composition of the metal calculated from the slag composition measured by SEM. The slag has a MnO content that is close to the desired 5%, while the slag has a silicon content that is a bit lower than the desired 18%. The results of the analysis of the slag from SEM and EPMA are similar, as is expected.

Table 4.2.1.1: Slag composition measured by SEM and EPMA for sample 11, and metal composition calculated from SEM results

Slag (measured)	**MnO**	**SiO_2**	**FeO**	**Al_2O_3**	**CaO**	**MgO**	**SO_3**
SEM [wt%]	8,08	45,37	0	18,63	22,21	5,70	0
EPMA [wt%]	8,19	47,50	0,02	15,55	22,73	5,63	0,60
Metal (calculated)	**Total**	**Mn**		**Si**		**Fe**	
[wt%]	100	71,39		13,96		14,65	
[g]	0,0498	0,0355		0,0069		0,0073	

Reduction degrees for test 11 are R_{Mn} = 0,939 and R_{Si} = 0,184

4.2.2 Test 15

The fifteenth test was run with charcoal pellet 10 and slag sample 2E at 1600°C for 15 minutes. The slag drop melted at 1201°C, and there was some activity through bubbling and low volume expansion. At around 1350°C the activity increased some with higher volume expansion of the slag drop. Around 1440°C there was one bubble with high volume expansion, and this was the largest volume expansion observed in the whole test. Around 1500°C the activity increased with low volume expansion and many bubbles. The activity increased further as hold temperature was reached. After 5 minutes at hold temperature there was observed activity both as bubbling and as gas exiting the slag drop close to the charcoal pellet, which was observed by particles scattering from the side of the slag drop. The volume expansion of the slag drop increased after 8 minutes and again after 12 minutes at hold temperature, but the amount of bubbles did not increase a lot.

Figure 4.2.2.1 shows some pictures captured of the slag drop and charcoal pellet during the test. The pictures are taken before heating, after the slag drop melted, as the furnace temperature reached 1600°C, after 5 and 15 minutes at 1600°C. The figure shows that the charcoal pellet shrunk some during heating, that the slag drop shape and contact angle changed during the test, and that the change from 5 to 15 minutes is large.

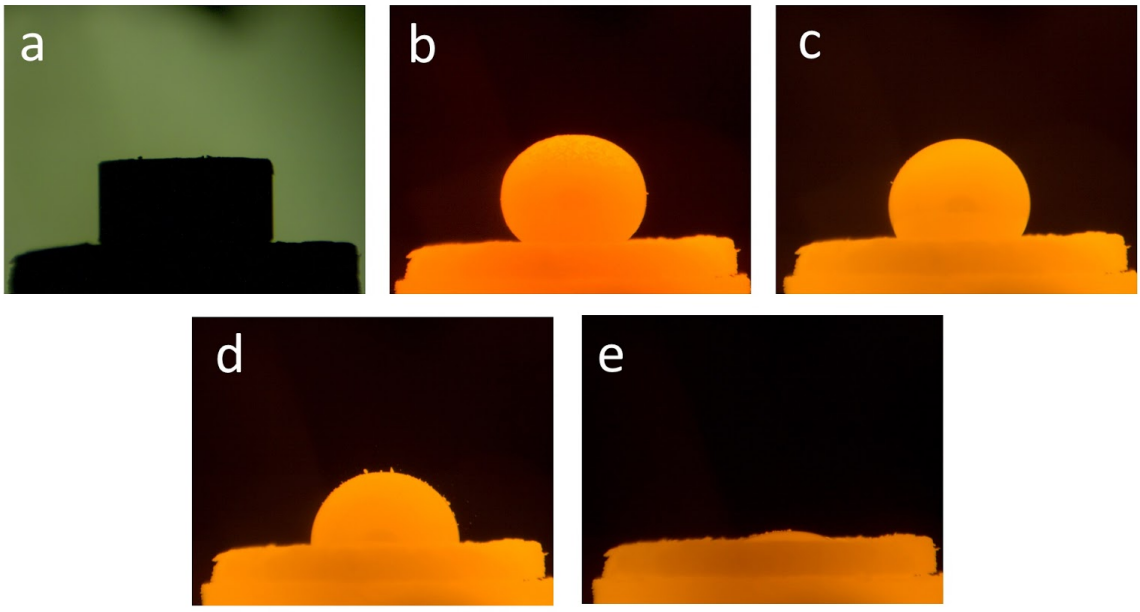

Figure 4.2.2.1: Pictures taken during test 15; a - before heating at 25°C; b - after melting at 1201°C; c - as the furnace reaches 1600°C; d - after 5 minutes at 1600°C; e - after 15 minutes

Figure 4.2.2.2 shows pictures taken of the slag drop and charcoal pellet after test 15. As the figure shows, the slag drop had a pale green non-transparent color after the test, and there are some visible metal drops between the slag and the charcoal. Further, that the slag drop has reduced its way down into the charcoal pellet, as could also be seen on figure 4.2.2.1 e.

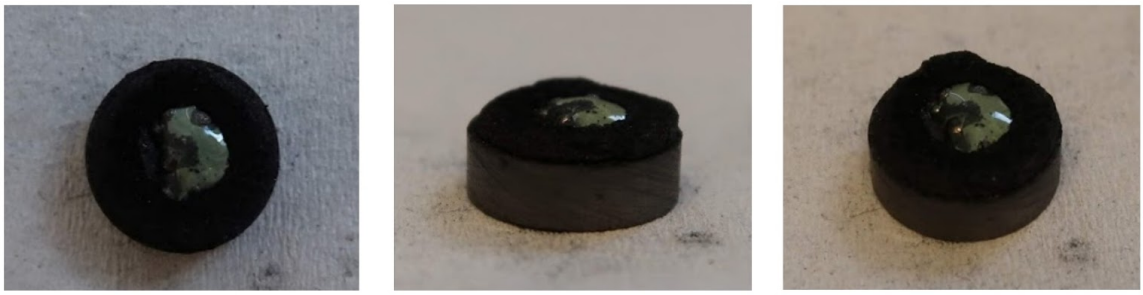

Figure 4.2.2.2: Pictures of slag drop and charcoal pellet after test 15

Figure 4.2.2.3 shows the development of the contact angle and temperature for test 15 while figure 4.2.2.4 shows the development of the relative volume and temperature of test 15. The figures show that the contact angle decreases steeply with time, while the relative volume decreases steeply with an increase at 7 minutes, likely caused by gas trapped in the slag drop.

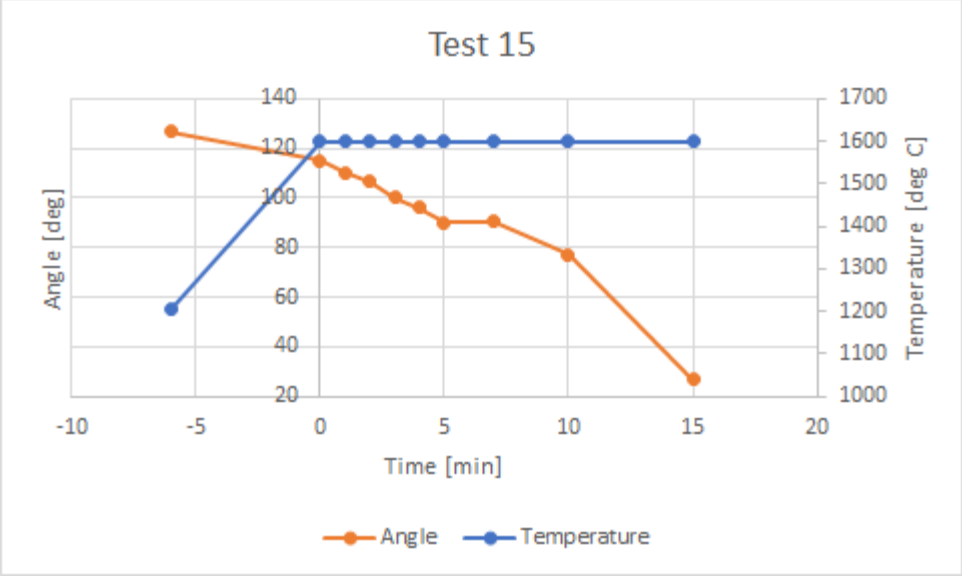

Figure 4.2.2.3: Contact angle and temperature development for test 15

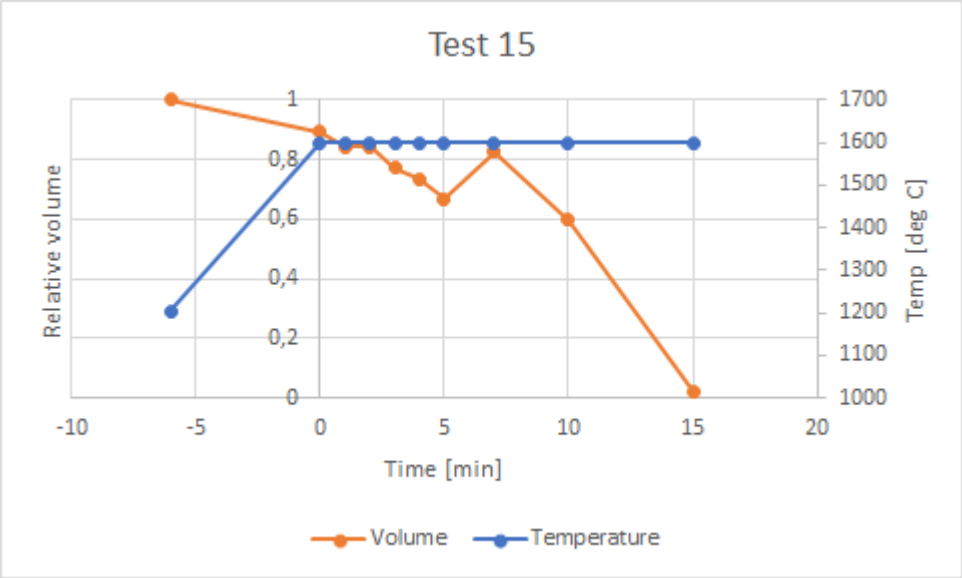

Figure 4.2.2.4: Relative volume and temperature development for test 15

Figure 4.2.2.5 shows an image of sample 15 taken in the SEM. On the figure the charcoal can be maked out on the bottom and the sides of the slag drop. The slag drop has several metal droplets of considerable size. Figure 4.2.2.6 shows details of the slag phase magnified 1000 times, and the figure shows that the slag is glassy. Figure 4.2.2.7 shows details of the metal phase magnified 1000 times, and shows that the metal phase does not have much surface structure.

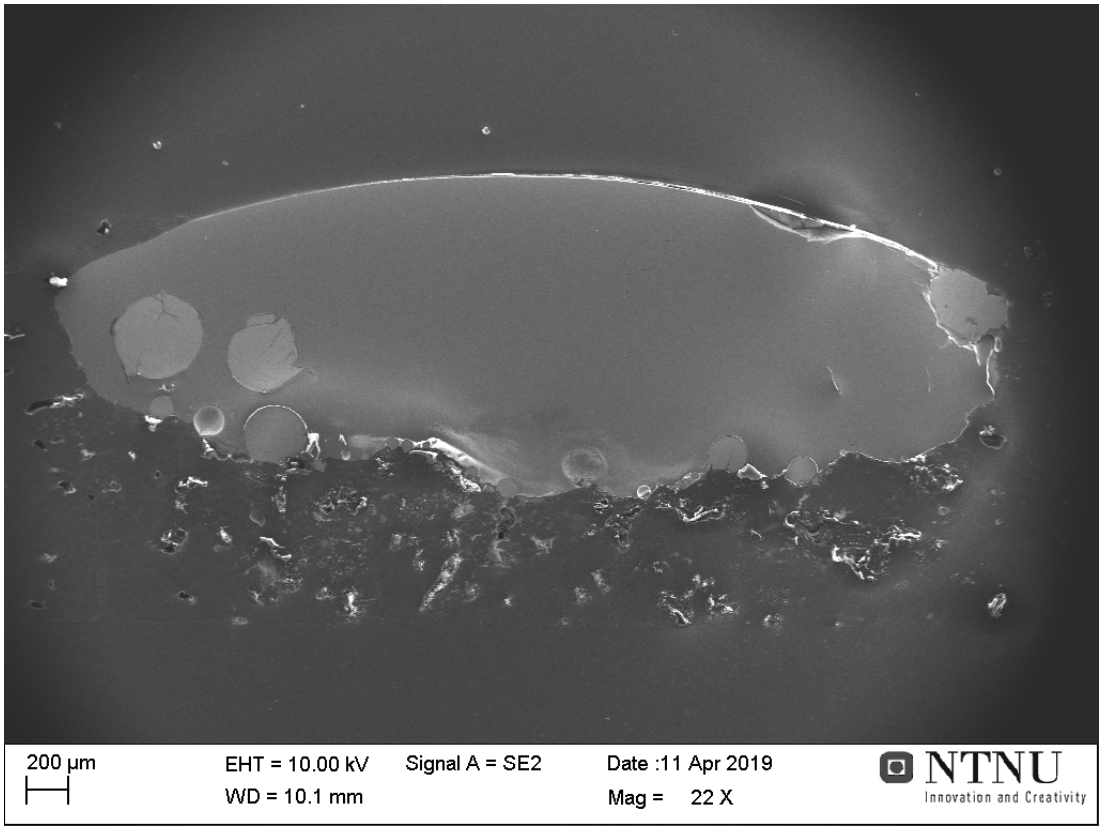

Figure 4.2.2.5: Image of sample 15 taken in SEM

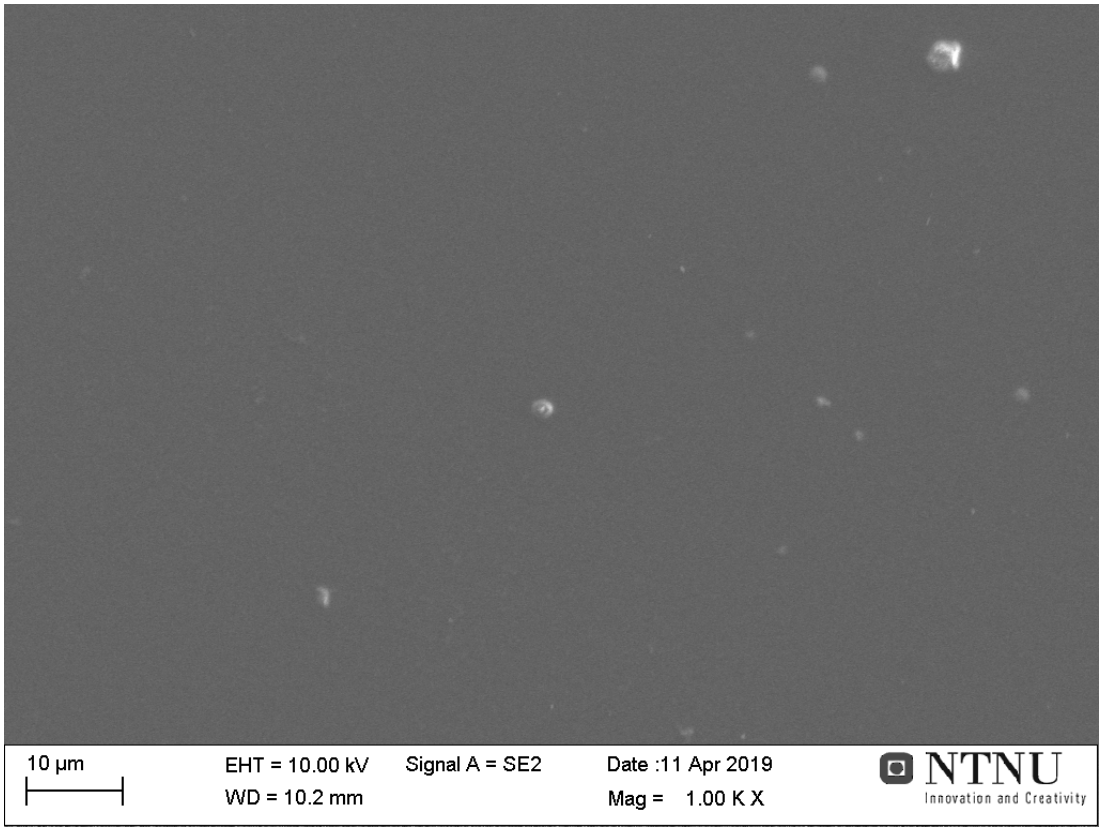

Figure 4.2.2.6: Slag of sample 15 magnified 1000 times

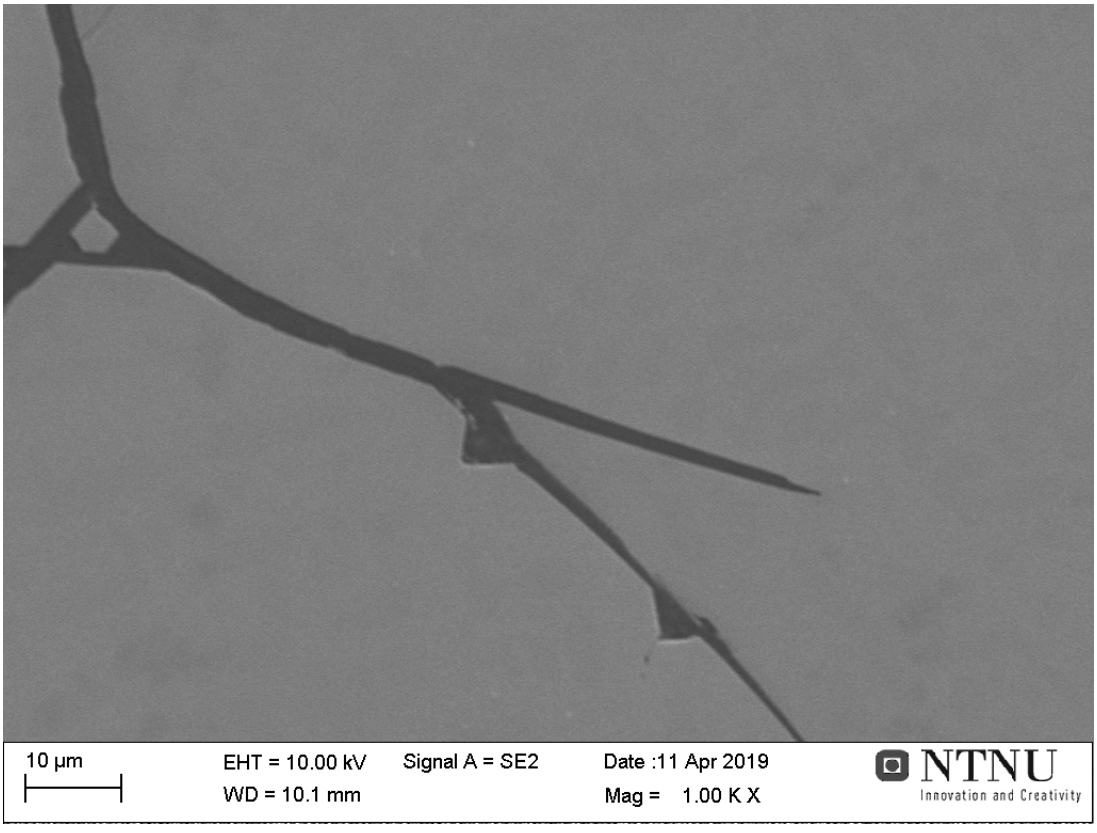

Figure 4.2.2.7: Metal of sample 15 magnified 1000 times

Table 4.2.2.1 lists the composition of the slag measured by SEM and EPMA, and the composition of the metal calculated from the slag composition measured by SEM. The slag has a content of MnO that is higher than the desired 5%, while the metal has a content of silicon that is lower than the desired 18%. The results of SEM and EPMA analysis of the slag are similar, as is expected.

Table 4.2.2.1: Slag composition measured by SEM and EPMA for sample 15, and metal composition calculated from SEM results

Slag (measured)	**MnO**	**SiO_2**	**FeO**	**Al_2O_3**	**CaO**	**MgO**	**SO_3**
SEM [wt%]	18,50	45,09	0	13,57	17,05	5,41	0,39
EPMA [wt%]	17,66	46,28	0,04	12,44	18,32	4,88	1,85
Metal (calculated)	**Total**	**Mn**		**Si**		**Fe**	
[wt%]	100	72,08		10,96		16,96	
[g]	0,0425	0,0306		0,0047		0,0072	

Reduction degrees for test 15 are R_{Mn} = 0,819 and R_{Si} = 0,125

4.2.3 Test 16

The sixteenth test was run with charcoal sample 11 and slag sample 2F at 1600°C for 15 minutes. The slag melted 1201°C, and there was some activity after melting through bubbling and low volume expansion. At around 1400°C, there was high volume expansion of the slag drop, and at 1450°C one large bubble burst, this was the highest volume expansion observed during the test. Around 1550°C the volume expansion was lower and there was more bubbles. As hold temperature was reached the activity increased some, and after 3 minutes at hold temperature there was high activity through bubbling and particles scattering close to the charcoal pellet. After 12 minutes the volume expansion increased while the amount of bubbles decreased.

Figure 4.2.3.1 shows pictures taken from the furnace during test 16. The pictures show the slag drop and charcoal pellet before heating, after melting, as the furnace temperature reaches 1600°C, after 5 minutes and 15 minutes at 1600°C. As the figure shows, the charcoal pellet had some damages before the test, which decreased the width of the pellet. The slag drop moved some on the pellet, and the shape and contact angle changed during the test.

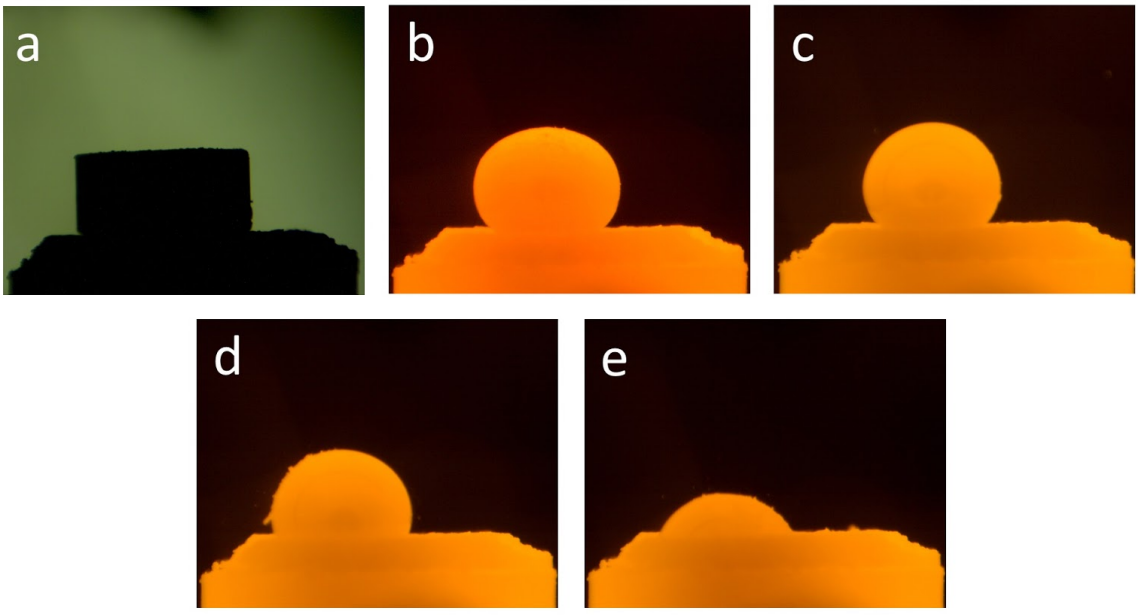

Figure 4.2.3.1: Pictures from test 16; a - before heating at 25°C; b - after melting at 1201°C; c - as furnace temperature reaches 1600°C; d - after 5 minutes at 1600°C; e - after 15 minutes

Figure 4.2.3.2 shows pictures taken of the slag drop and coke pellet after test 16. The figure shows that the slag drop had an orange transparent color after the test, where some metal droplets were visible at the interface between the slag and the charcoal pellet. The area close to the slag drop has a darker color on the charcoal pellet.

Figure 4.2.3.2: Pictures of slag drop and coke pellet after test 16

Figure 4.2.3.3 shows the development of contact angle and temperature of test 16, while figure 4.2.3.4 shows the development of relative volume and temperature of test 16. The figures show that the contact angle decreases with increasing time, and that the relative volume has a decreasing trend with increasing time. Both contact angle and relative volume has a measurement that stands out at 10 minutes, this is likely caused by gas being trapped in the slag drop.

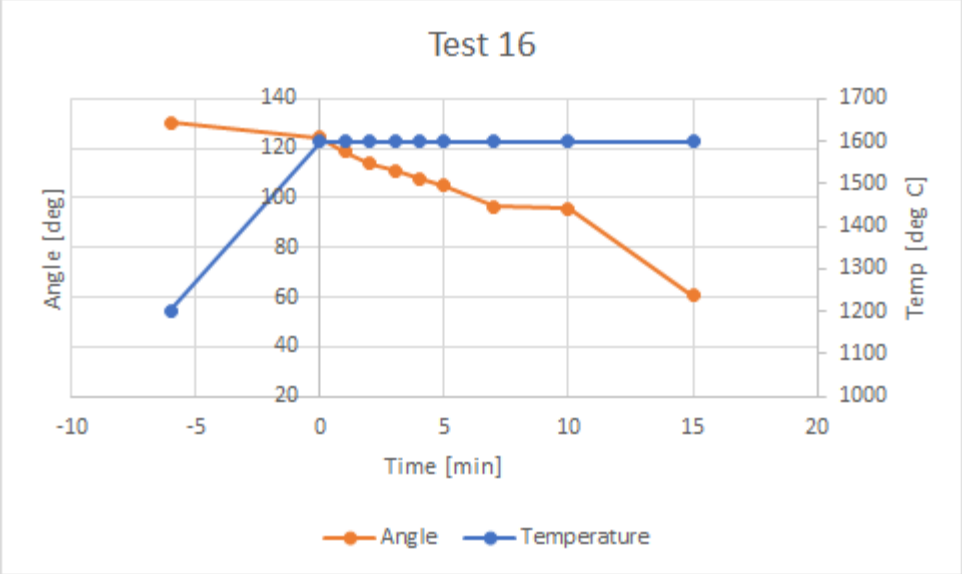

Figure 4.2.3.3: Contact angle and temperature development for test 16

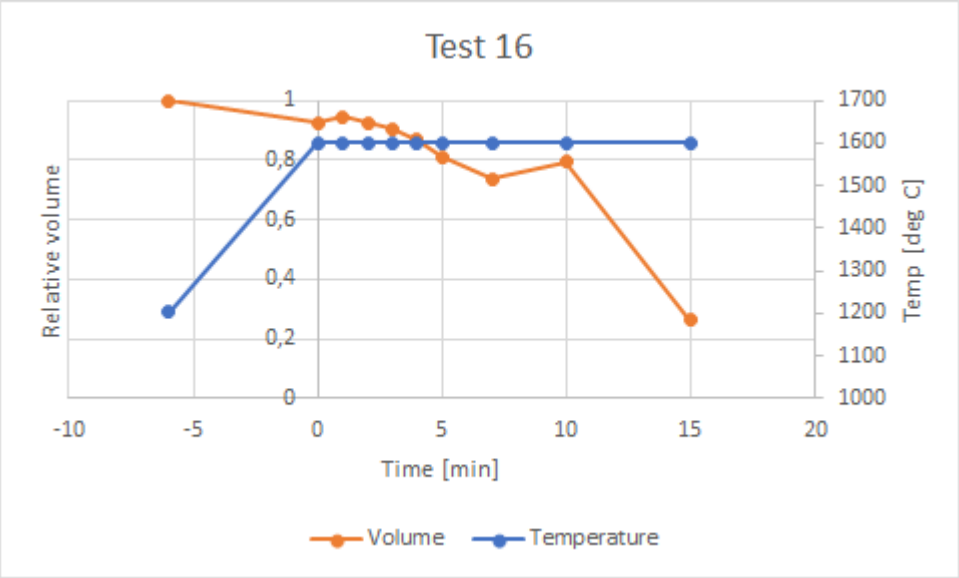

Figure 4.2.3.4: Relative volume and temperature development for test 16

Figure 4.2.3.5 shows an image of sample 16 taken in SEM. The figure shows that the sample has 5 metal droplets of considerable size, and the charcoal pellet can be made out at the left side of the figure. Figure 4.2.3.6 shows details of the slag phase of sample 16, which shows that the slag is glassy. Figure 4.2.3.7 shows details of the largest metal droplet in sample 16 magnified 1000 times, while figure 4.2.3.8 shows details of the next largest metal droplet in sample 16 magnified 1000 times. The figures show that the largest metal droplet is uniform, while there is some structure in the next largest metal droplet.

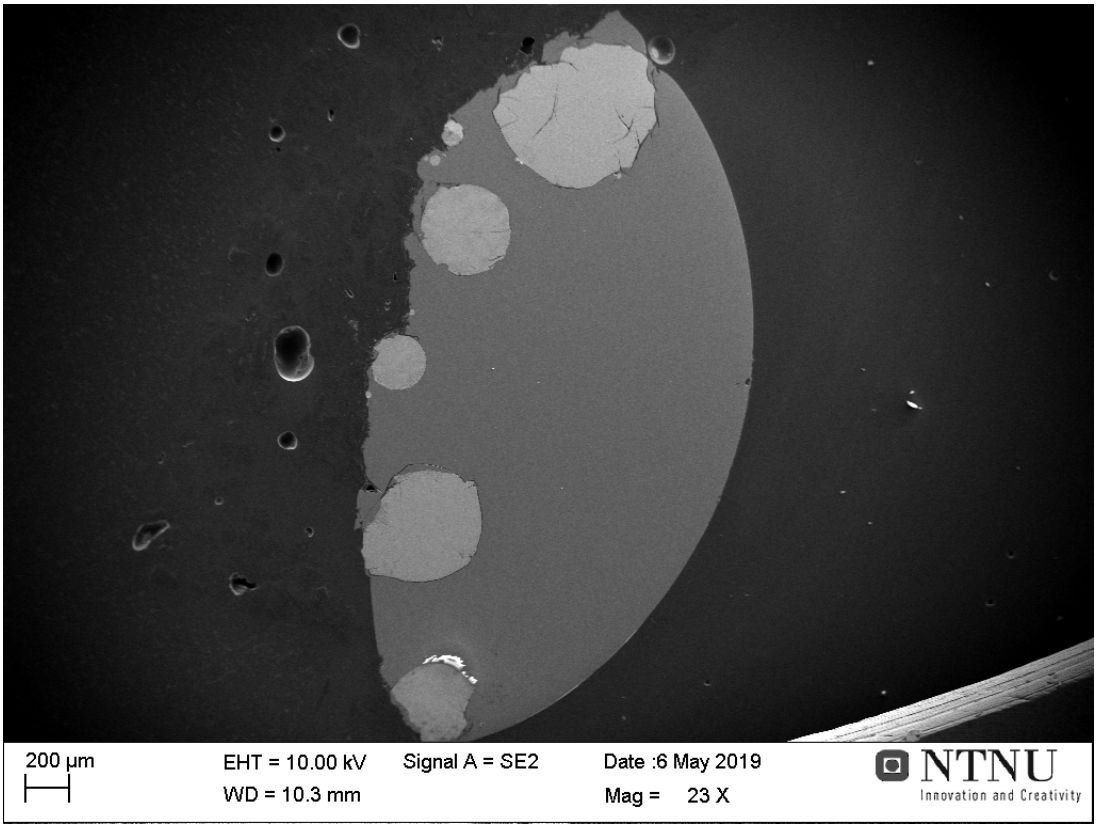

Figure 4.2.3.5: Image of sample 16 taken in SEM

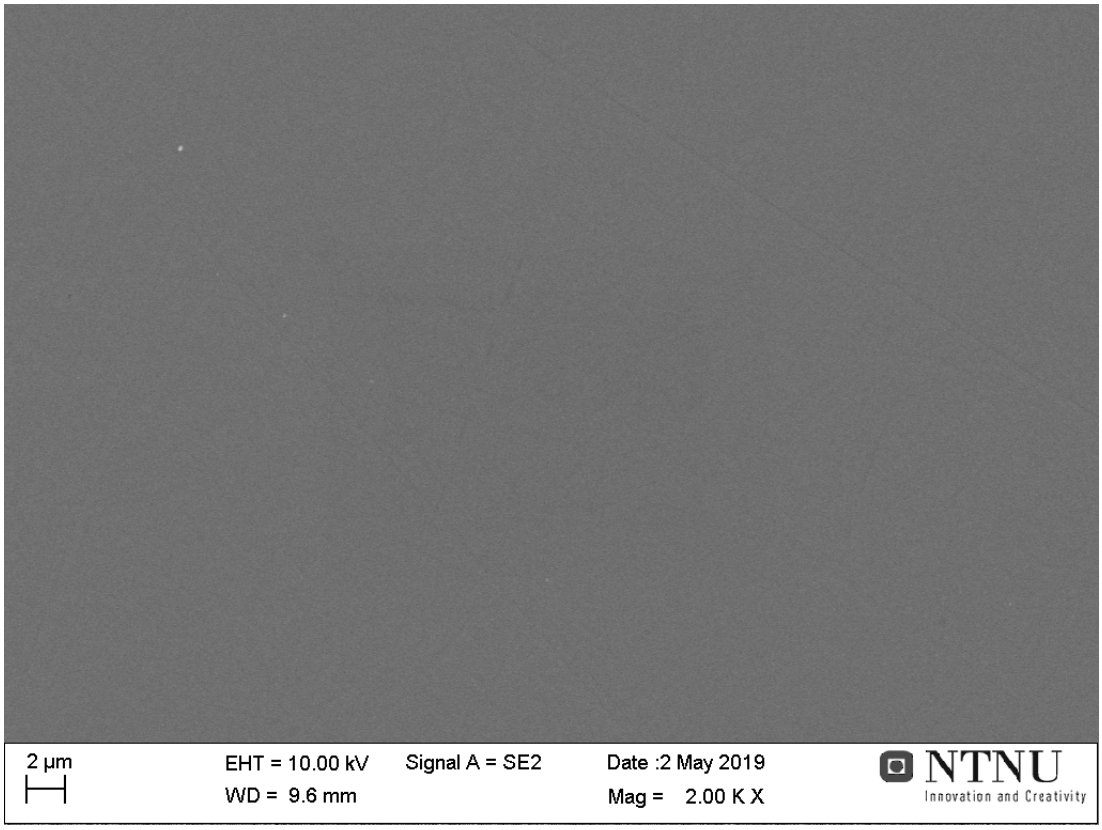

Figure 4.2.3.6: Slag phase of sample 16 magnified 1000 times

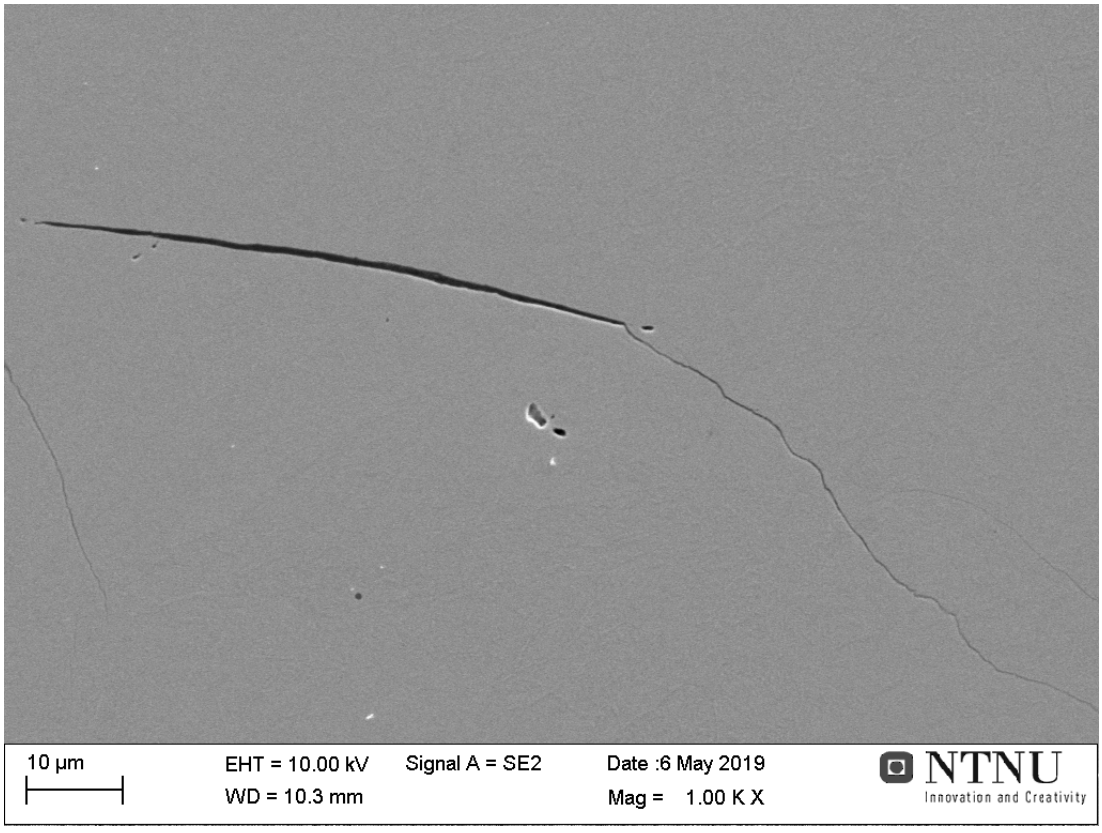

Figure 4.2.3.7: Largest metal droplet of sample 16 magnified 1000 times

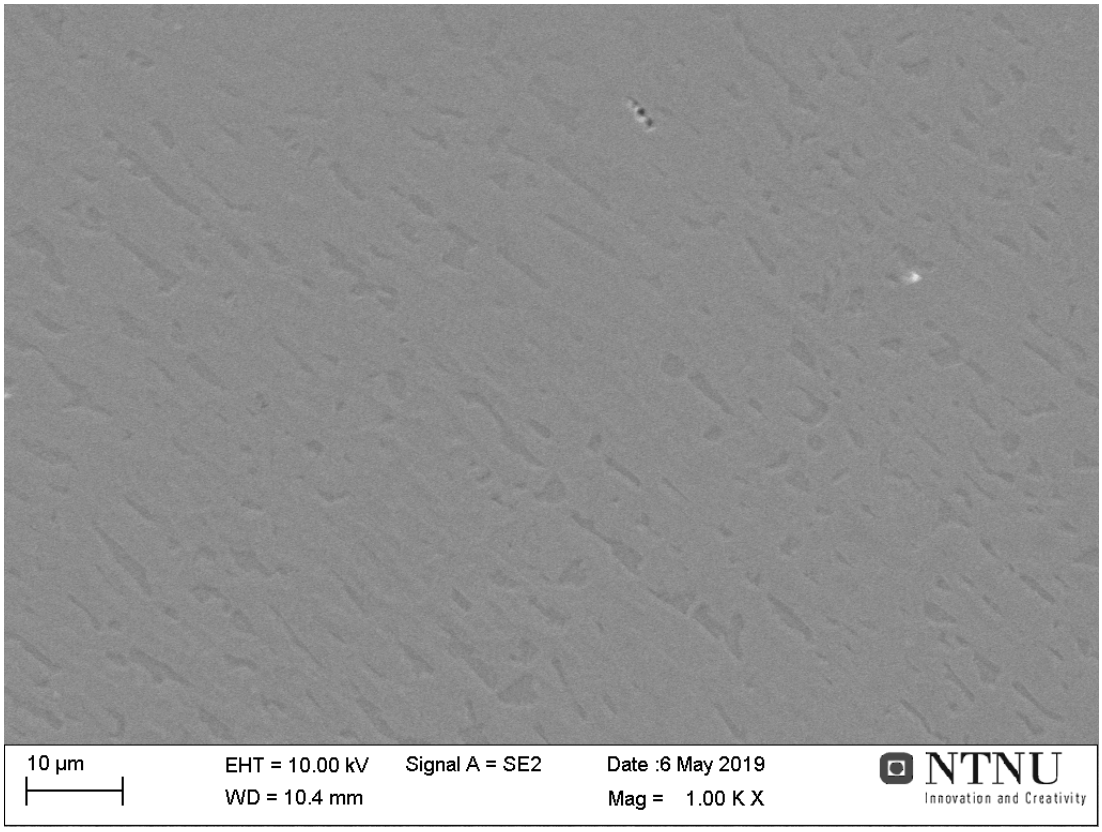

Figure 4.2.3.8: Next largest metal droplet of sample 16 magnified 1000 times

Table 4.2.3.1 lists the composition of the slag measured by SEM and EPMA, and the composition of the metal calculated from the slag composition measured by SEM. The slag has a high content of MnO, while the metal has a low content of silicon. The results of the SEM and EPMA analysis of the slag are similar, as is expected.

Table 4.2.3.1: Slag composition measured by SEM and EPMA for sample 16, and metal composition calculated from SEM results

Slag (measured)	**MnO**	**SiO_2**	**FeO**	**Al_2O_3**	**CaO**	**MgO**	**SO_3**
SEM [wt%]	25,79	43,54	0	11,46	14,04	4,28	0,88
EPMA [wt%]	25,18	44,68	0,08	10,45	15,03	4,12	1,79
Metal (calculated)	**Total**	**Mn**		**Si**		**Fe**	
[wt%]	100	71,83		8,25		19,92	
[g]	0,0366	0,0263		0,0030		0,0073	

Reduction degrees for test 16 are R_{Mn} = 0,695 and R_{Si} = 0,080

4.2.4 Test 20

The twentieth test was run with charcoal pellet 14 and slag sample 2J at 1600°C for 15 minutes. The slag melted at 1202°C, and there was little activity at first, before the activity increased as the temperature was increased to 1300°C. From 1350°C to 1420°C there were few bubbles with high volume expansion, and the volume expansion of the slag drop increased as the temperature was increased to 1500°C. The amount of bubbles increased around 1520°C while the volume expansion of the slag drop decreased. As the furnace temperature reached 1600°C the activity increased and there was activity through both bubbling and gas exiting the slag drop close to the pellet and particles scattering. The amount of particles that were scattered close to the charcoal pellet increased in the first five minutes at 1600°C, while the volume expansion increased after 12 minutes.

Figure 4.2.4.1 shows pictures captured from the furnace during test 20. The pictures show the slag sample and charcoal pellet before heating, after slag drop has melted, as the furnace temperature reaches 1600°C, and after 5 and 15 minutes at 1600°C. The figure shows that the charcoal pellet shrunk some during heating, that the contact angle of the slag drop changed during the test, and that there was some charcoal at the slag drop surface during the test.

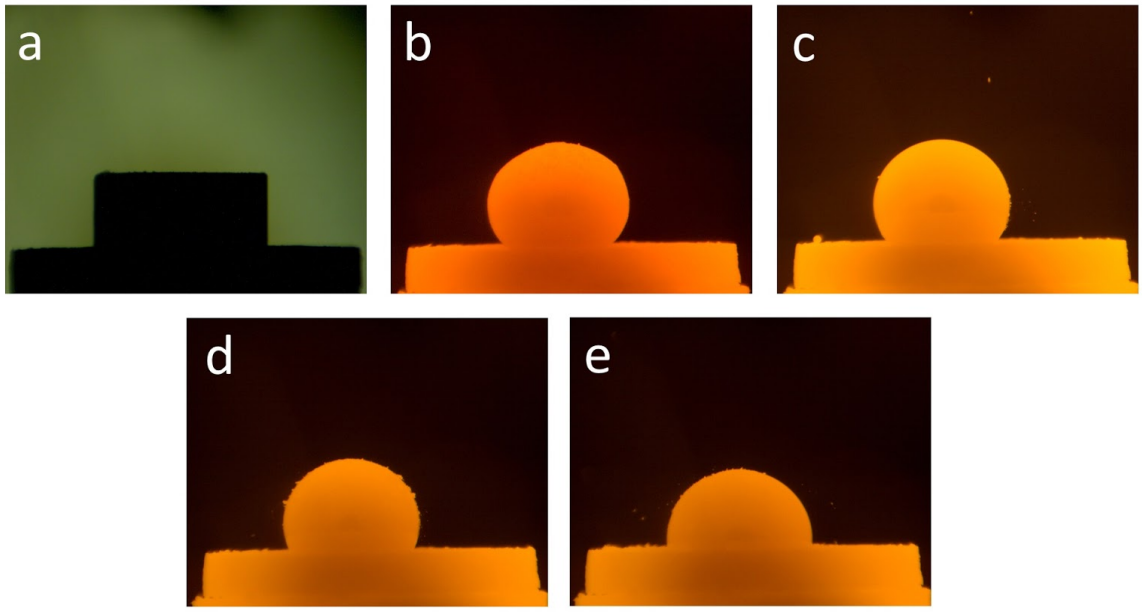

Figure 4.2.4.1: Pictures from test 20; a - before heating at 25°C; b - after melting at 1202°C; c - as furnace reaches 1600°C; d - after 5 minutes at 1600°C; e - after 15 minutes

Figure 4.2.4.2 shows pictures taken of the slag drop and charcoal pellet after test 20. The figure shows that the slag drop has a transparent orange color, and that there are some metal drops at the interface between the slag drop and charcoal.

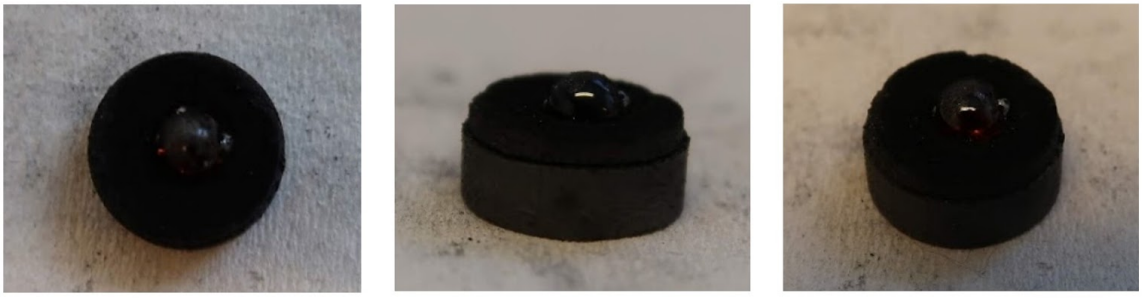

Figure 4.2.4.2: Pictures taken of the slag drop and charcoal pellet after test 20

Figure 4.2.4.3 shows the development of contact angle and temperature for test 20 while figure 4.2.4.4 shows the development of the relative volume and temperature for test 20. The figures show that the contact angle decreases with time, while the relative volume decreases with some fluctuations with time. Considering the end values, both contact angle and relative volume changes moderately during the test.

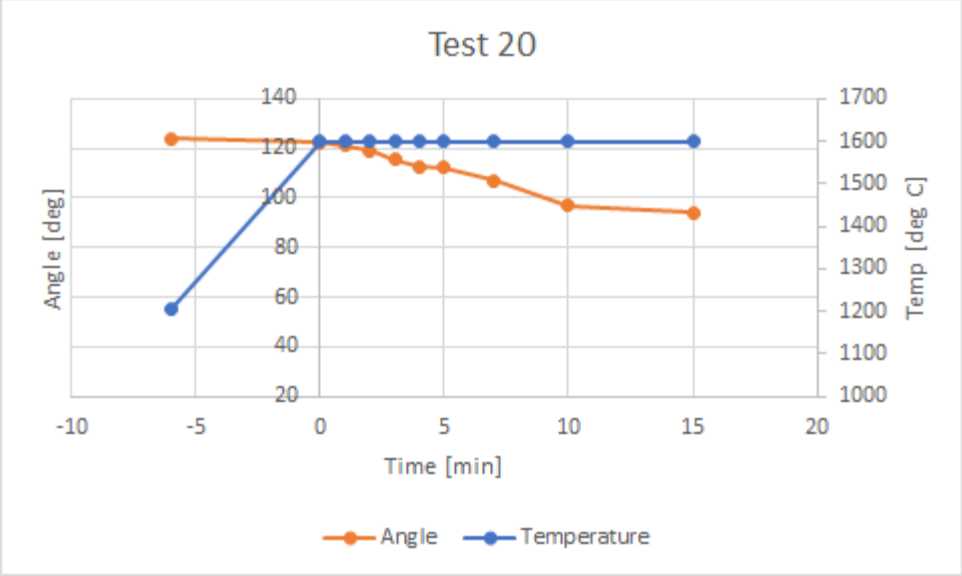

Figure 4.2.4.3: Contact angle and temperature development for test 20

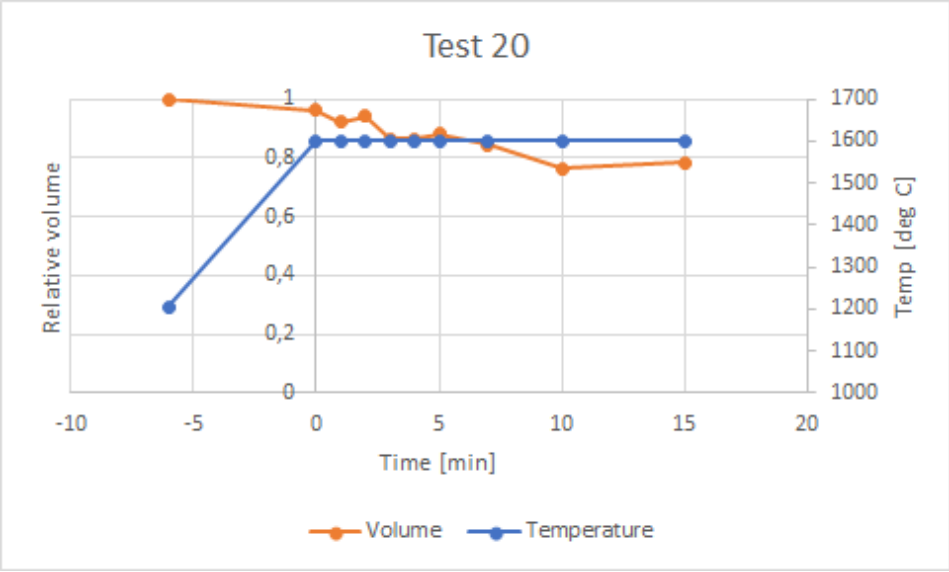

Figure 4.2.4.4: Relative volume and temperature development for test 20

Figure 4.2.4.5 shows an image of sample 20 taken in SEM. The figure shows that the sample has one large and several smaller metal droplets of significant size, close to the charcoal pellet that can be made out at the right side of the figure. Figure 4.2.4.6 shows details of the slag phase magnified 2000 times, and shows that the slag is glassy. Figure 4.2.4.7 shows details of the large metal droplet in sample 20 at magnified 1000 times, and shows that the metal has little or no structure at the surface. However, there was some structure at the surface of the smaller metal droplets in sample 20, which is shown for one of the smaller droplets in figure 4.2.4.8, magnified 2000 times.

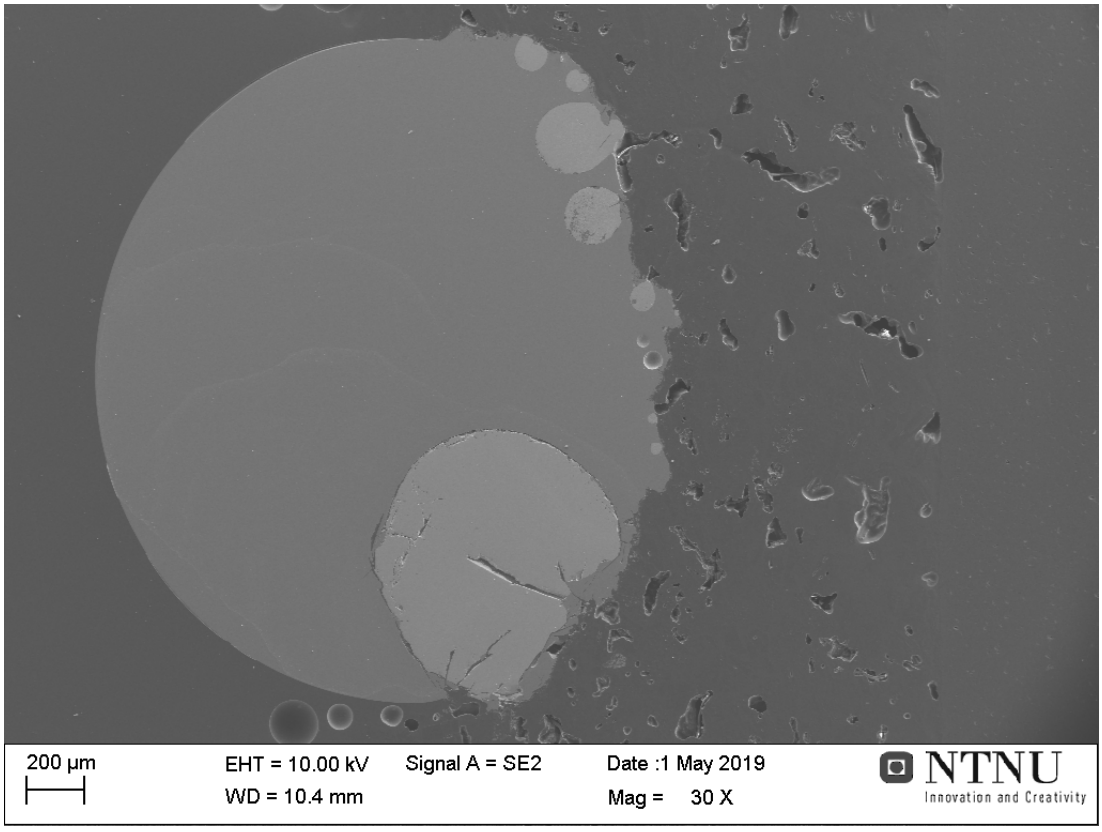

Figure 4.2.4.5: Image of sample 20 taken in SEM

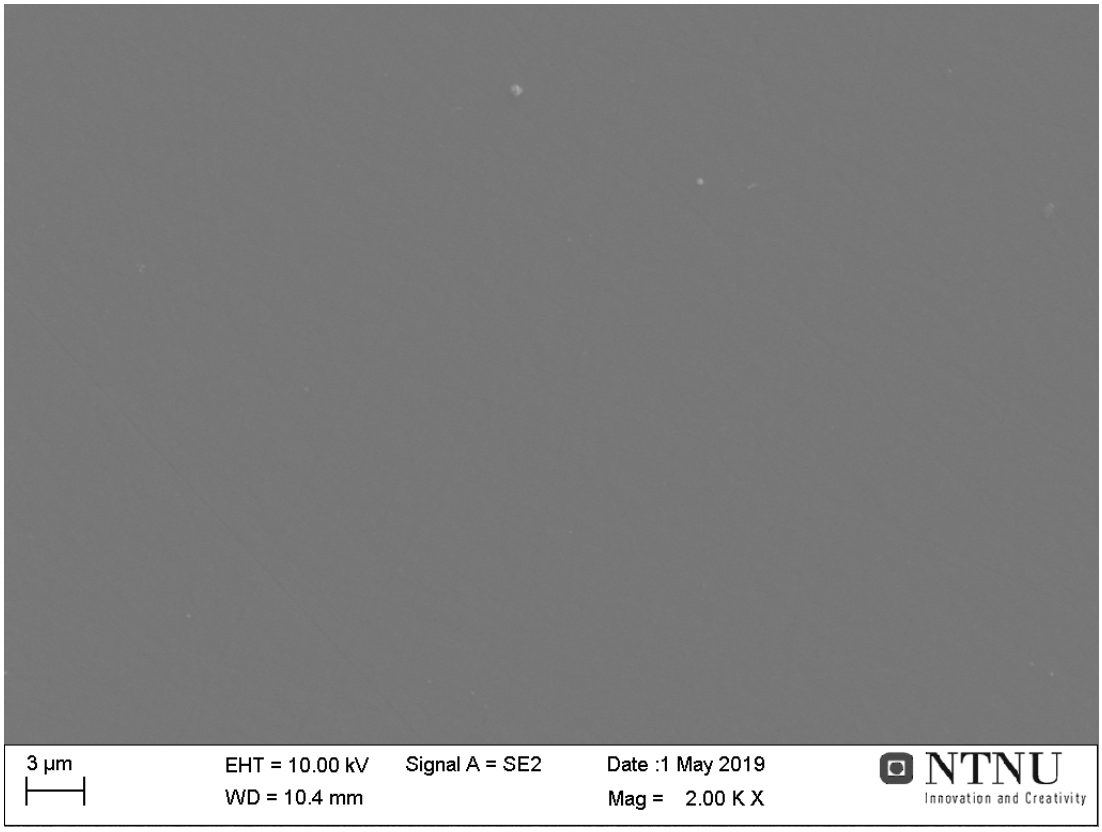

Figure 4.2.4.6: Details of slag in sample 20 at magnification of 2000 times

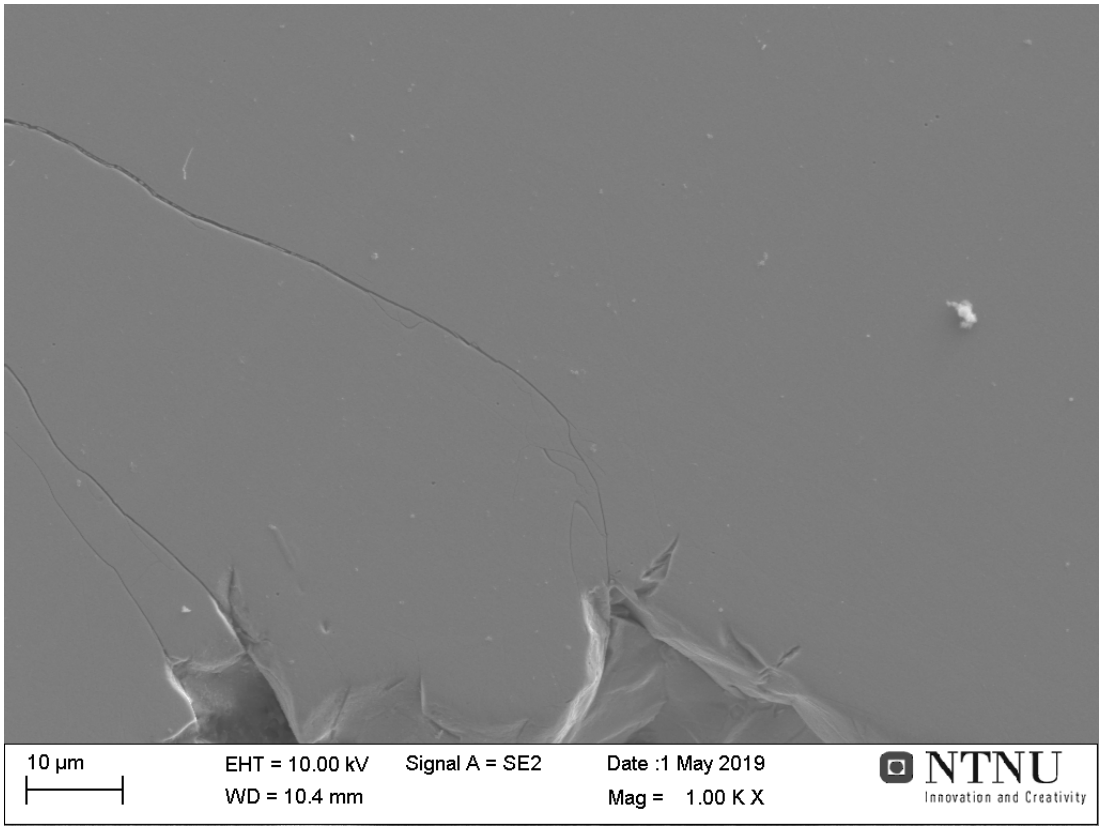

Figure 4.2.4.7: Details of large metal droplet in sample 20 magnified 1000 times

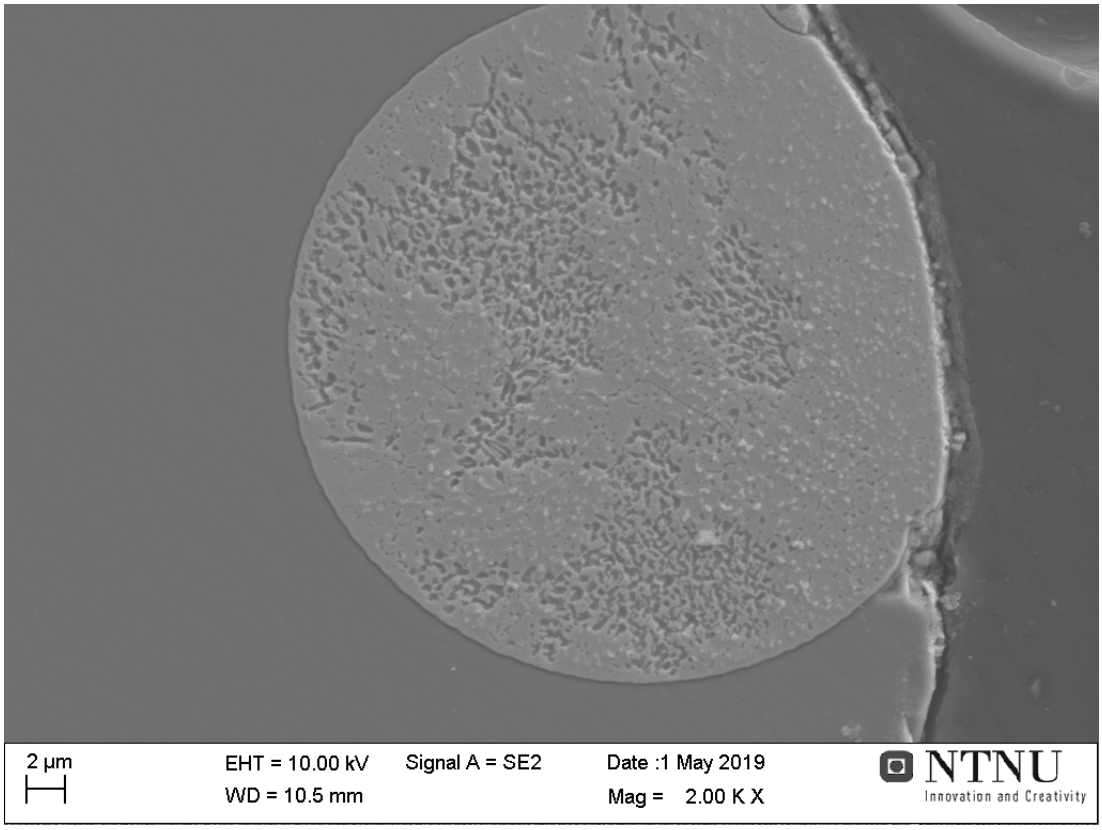

Figure 4.2.4.8: Details of small metal droplet in sample 20 magnified 2000 times

Table 4.2.4.1 lists the composition of the slag measured by SEM and EPMA, and the composition of the metal calculated from the slag composition measured by SEM. The slag has a high content of MnO and the metal has a low content of silicon. The results of the analysis by EPMA and SEM for the slag are similar, as is expected.

Table 4.2.4.1: Slag composition measured by SEM and EPMA for sample 20, and metal composition calculated from SEM results

Slag (measured)	**MnO**	**SiO_2**	**FeO**	**Al_2O_3**	**CaO**	**MgO**	**SO_3**
SEM [wt%]	33,04	41,30	0	9,32	12,79	3,55	0
EPMA [wt%]	32,06	42,31	0,08	8,73	12,86	3,50	1,65
Metal (calculated)	**Total**	**Mn**		**Si**		**Fe**	
[wt%]	100	69,37		6,16		24,46	
[g]	0,0276	0,0191		0,0017		0,0067	

Reduction degrees for test 20 are R_{Mn} = 0,546 and R_{Si} = 0,049

4.2.5 Test 18

The eighteenth test was run with charcoal pellet 12 and slag sample 2H at 1600°C for 5 minutes. The slag melted at 1199°C, and there was little activity right after melting. The activity increased some as the temperature was increased to 1250°C. Around 1445°C the slag drop had one bubble wth significantly high volume expansion, this was the highest volume expansion observed during the test. Around 1490°C there were more bubbles and less volume expansion, and as the hold temperature was reached the activity increased both through bubbling and through particles being scattered close to the charcoal pellet. After four minutes at hold temperature the activity decreased some.

Figure 4.2.5.1 shows photographs captured from the furnace during test 18. The pictures show the slag sample and charcoal pellet before heating, after slag melted, as furnace temperature reached 1600°C, and after 5 minutes at 1600°C. The figure shows that the charcoal pellet shrunk some during heating, that the slag drop contact angle changed some during the test, and that there were some charcoal particles at the slag drop surface towards the end of the test.

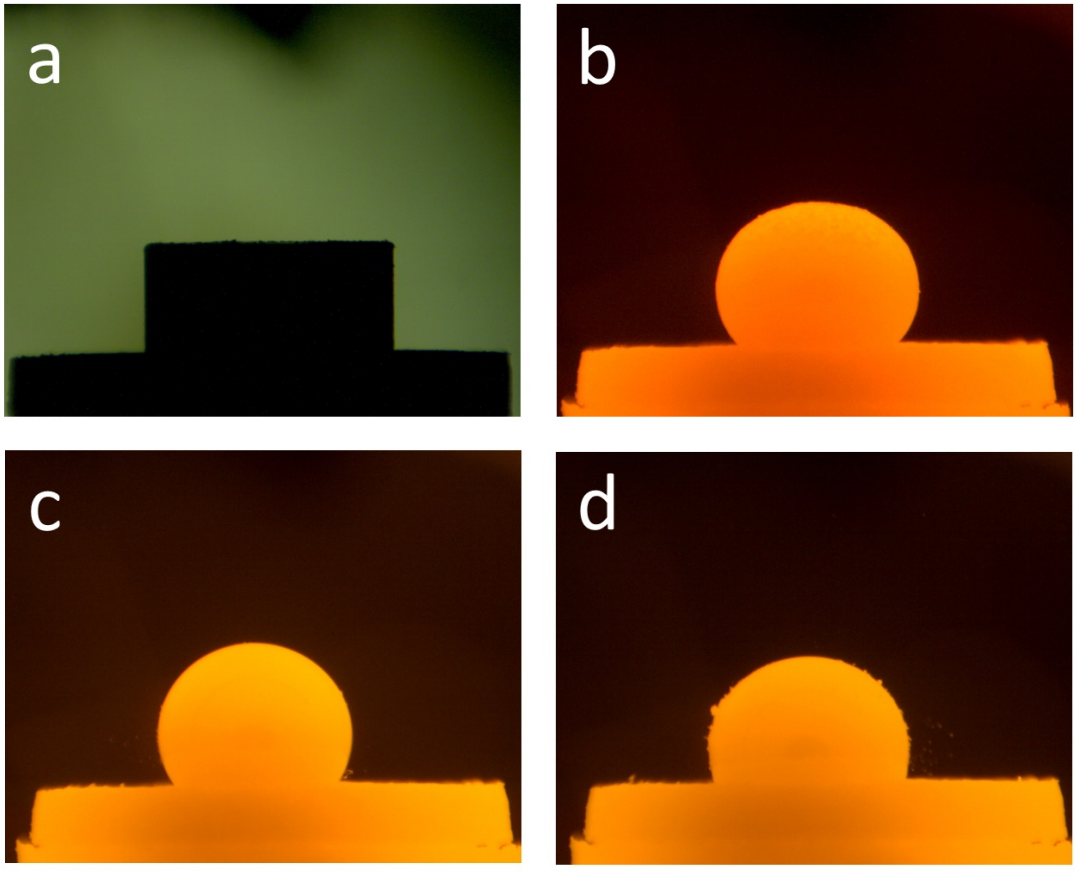

Figure 4.2.5.1: Pictures from test 18; a - before heating at 25°C; b - after melting at 1199°C; c - as furnace reached 1600°C; d - after 5 minutes at 1600°C

Figure 4.2.5.2 shows pictures taken of the slag drop and charcoal pellet after test 18. The figure shows that the slag drop had a pale green non-transparent color, with some charcoal particles at the surface.

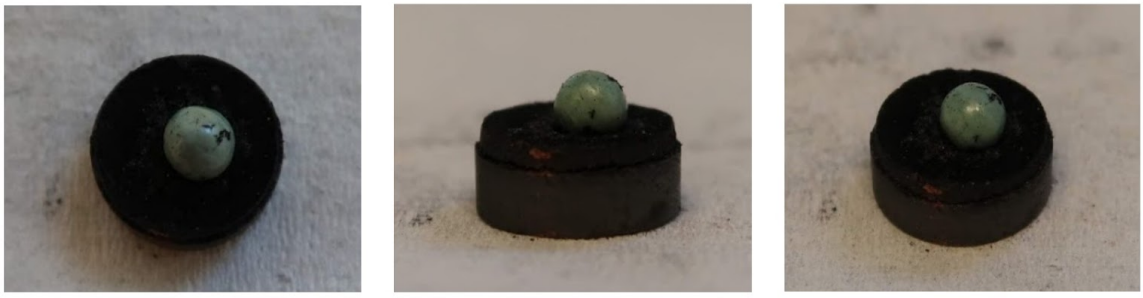

Figure 4.2.5.2: Pictures of slag drop and charcoal pellet after test 18

Figure 4.2.5.3 shows the development of contact angle and temperature for test 18, while figure 4.2.5.4 shows the relative volume and temperature development for test 18. The figures show that the contact angle decreases moderately with time, and that the relative volume decreases with time, except for the measurement at 4 minutes which is higher and likely caused by gas trapped in the slag drop.

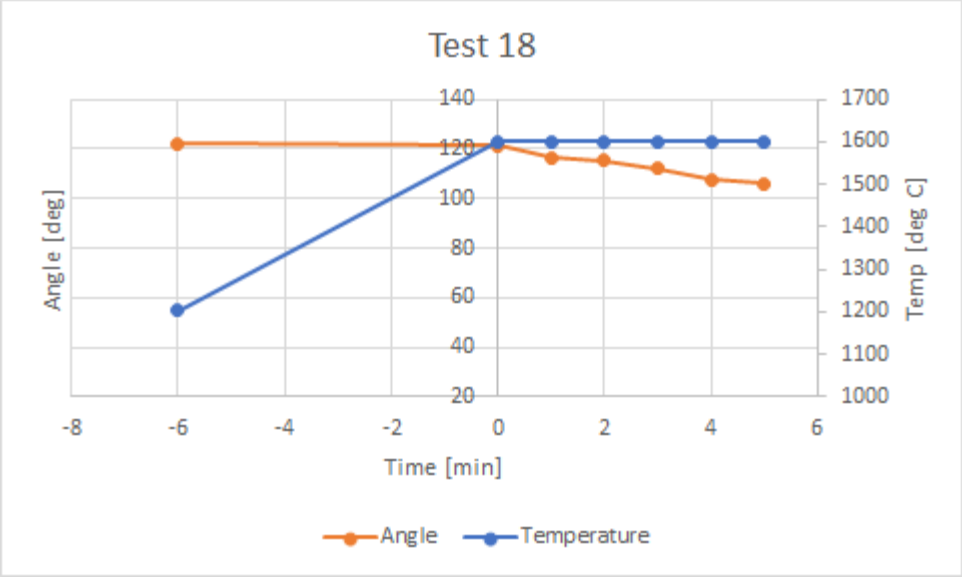

Figure 4.2.5.3: Contact angle and temperature development for test 18

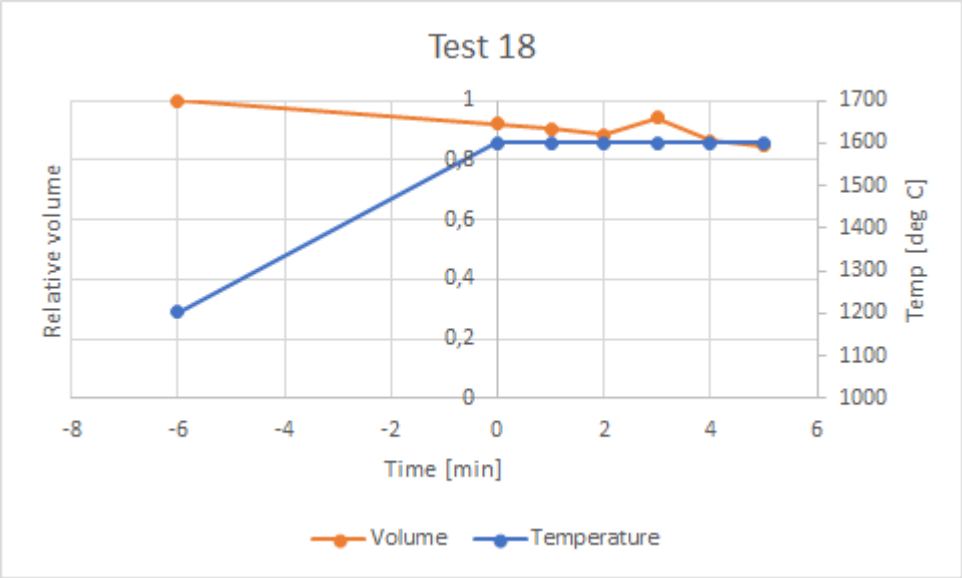

Figure 4.2.5.4: Relative volume and temperature development for test 18

Figure 4.2.5.5 shows an image of sample 18 taken in SEM. The figure shows that the sample has one metal droplet of considerable size. Figure 4.2.5.6 shows details of the slag of sample 18, which consists of two phases, at 2000 times magnification. Figure 4.2.5.7 shows details of the metal droplet of sample 18 magnified 2000 times, the figure shows that there is little or no structure at the metal surface.

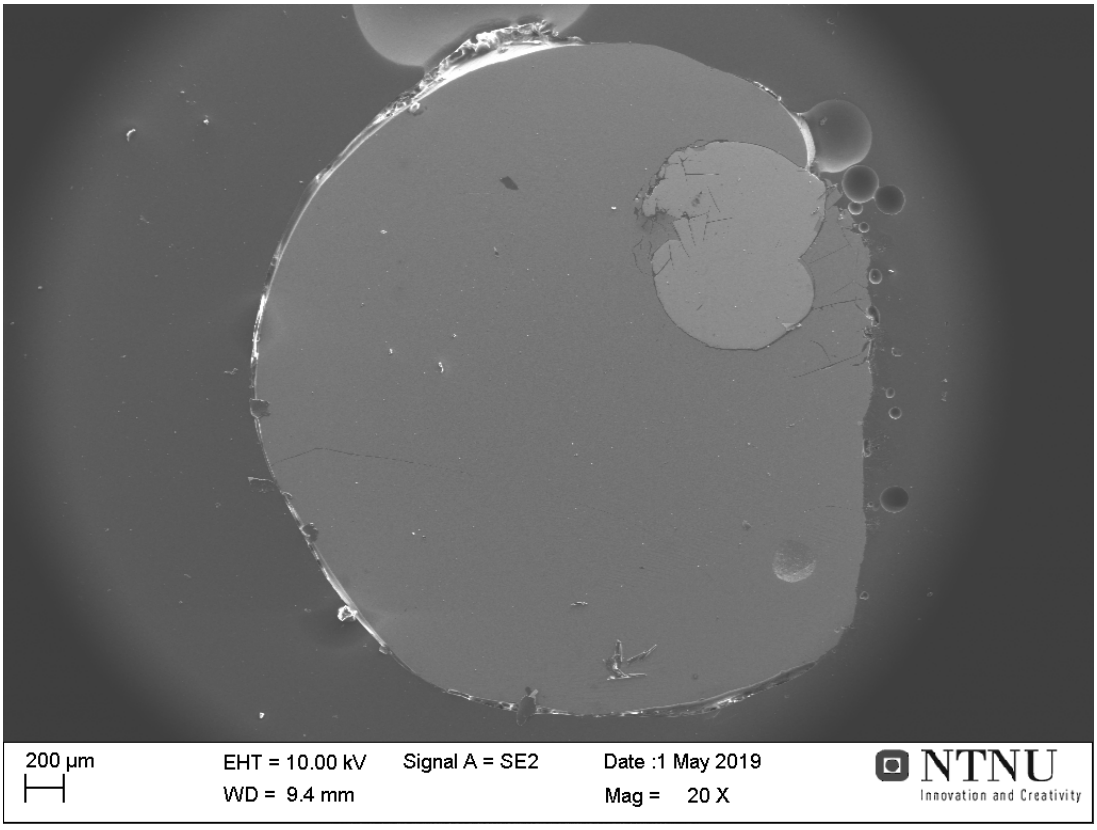

Figure 4.2.5.5: Image of sample 18 taken in SEM

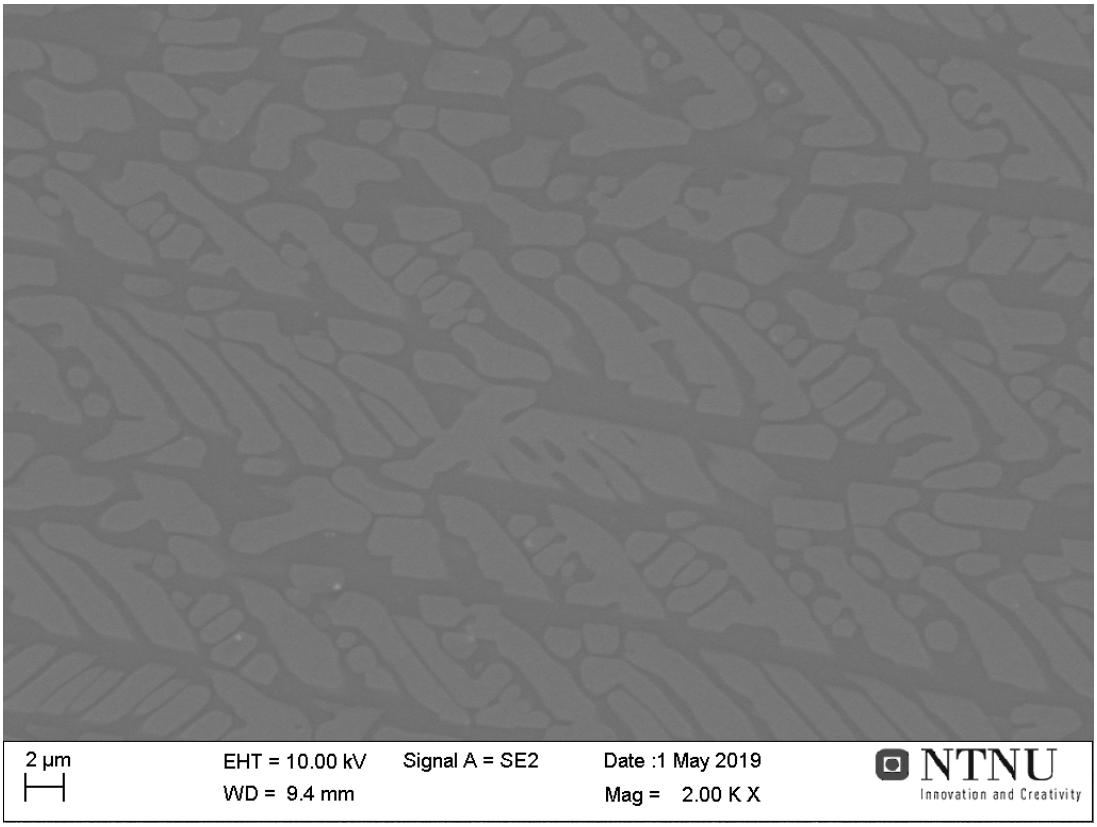

Figure 4.2.5.6: Details of two-phase slag of sample 18 magnified 2000 times

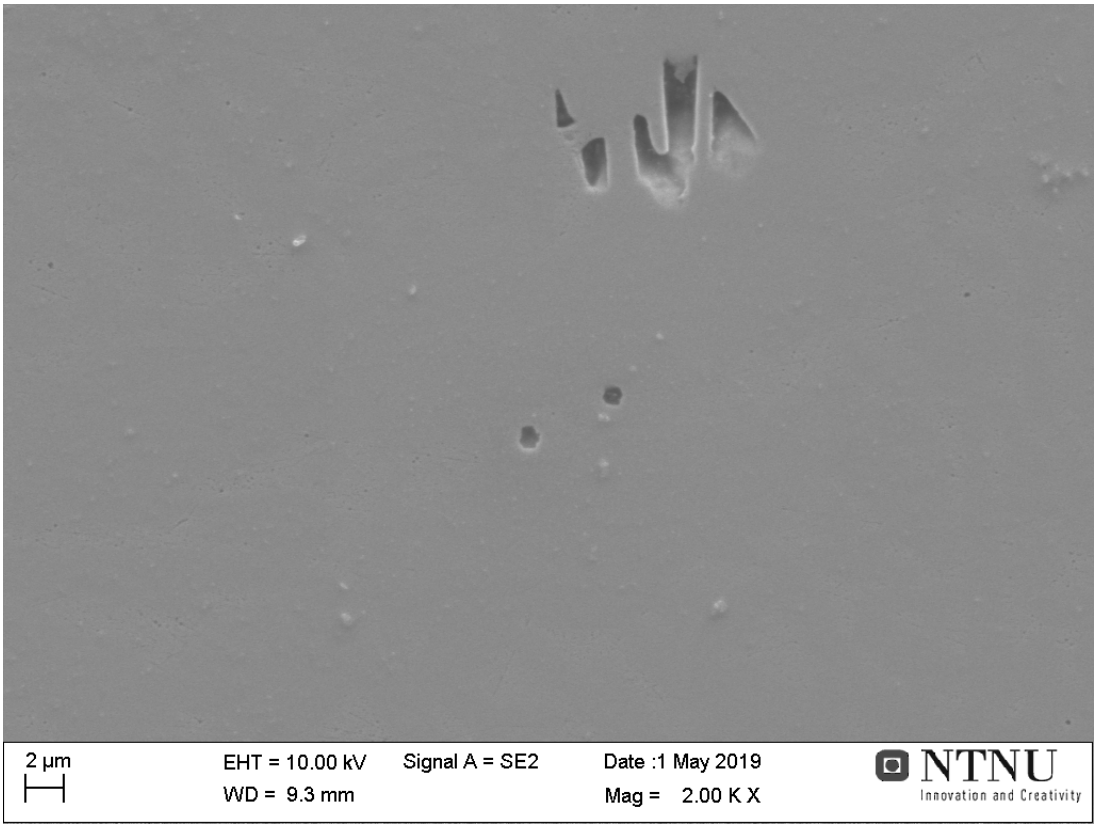

Figure 4.2.5.7: Details of metal in sample 18 magnified 2000 times

Figure 4.2.5.8 shows an image of the charcoal pellet used in test 18 taken in SEM. The figure shows that the charcoal pellet has a large crater where the slag drop was, and that the slag drop worked its way down into the pellet during reduction. The outer parts of the charcoal pellet seems to be unaffected by the reduction.

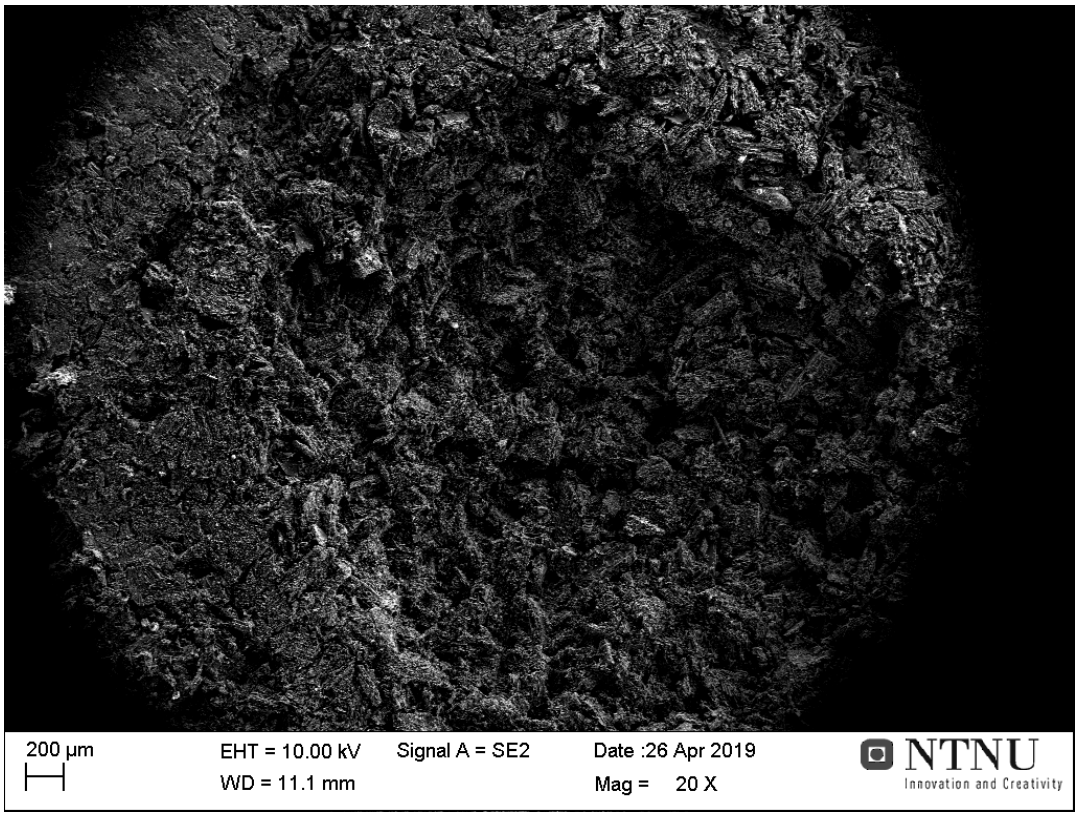

Figure 4.2.5.8: Image of charcoal pellet used in test 18 taken in SEM

Table 4.2.5.1 lists the composition of the slag measured by SEM and EPMA, and the composition of the metal calculated from the slag composition measured by SEM. The slag has a very high content of MnO, while the metal has a low content of silicon compared to the desired 18%, but also a low content of manganese and high content of iron. The results of the analyses from SEM and EPMA for the slag are similar, as is expected.

Table 4.2.5.1: Slag composition measured by SEM and EPMA for sample 18, and metal composition calculated from SEM results

Slag (measured)	**MnO**	**SiO_2**	**FeO**	**Al_2O_3**	**CaO**	**MgO**	**SO_3**
SEM [wt%]	45,88	33,35	0	7,93	10,35	2,50	0
EPMA [wt%]	45,19	34,81	0,15	7,24	9,81	2,55	1,31
Metal (calculated)	**Total**	**Mn**		**Si**		**Fe**	
From SEM [wt%]	100	47,82		10,64		41,54	
From SEM [g]	0,0165	0,0079		0,0018		0,0069	

Reduction degrees for test 18 are R_{Mn} = 0,222 and R_{Si} = 0,049

4.2.6 Test 21

Test 21 was run with charcoal pellet 15 and slag sample 2K at 1600°C for 5 minutes. The slag melted at 1202°C, and around 1250°C there was some activity through bubbling. Around 1300°C there were few bubbles with high volume expansion, and the volume expansion increased around 1420°C. As hold temperature was reached, there were more bubbles with lower volume expansion and activity through particle scattering. The activity maintained the same level for the rest of the test.

Figure 4.2.6.1 shows some pictures captured from the furnace during test 21. The pictures show the slag sample and charcoal pellet before heating, after slag drop has melted, as furnace temperature reached 1600°C, and after 5 minutes at 1600°C. The figure shows that the charcoal pellet shrunk some during heating, that the slag drop moved during the test, and that the contact angle of the slag drop changed some during the test.

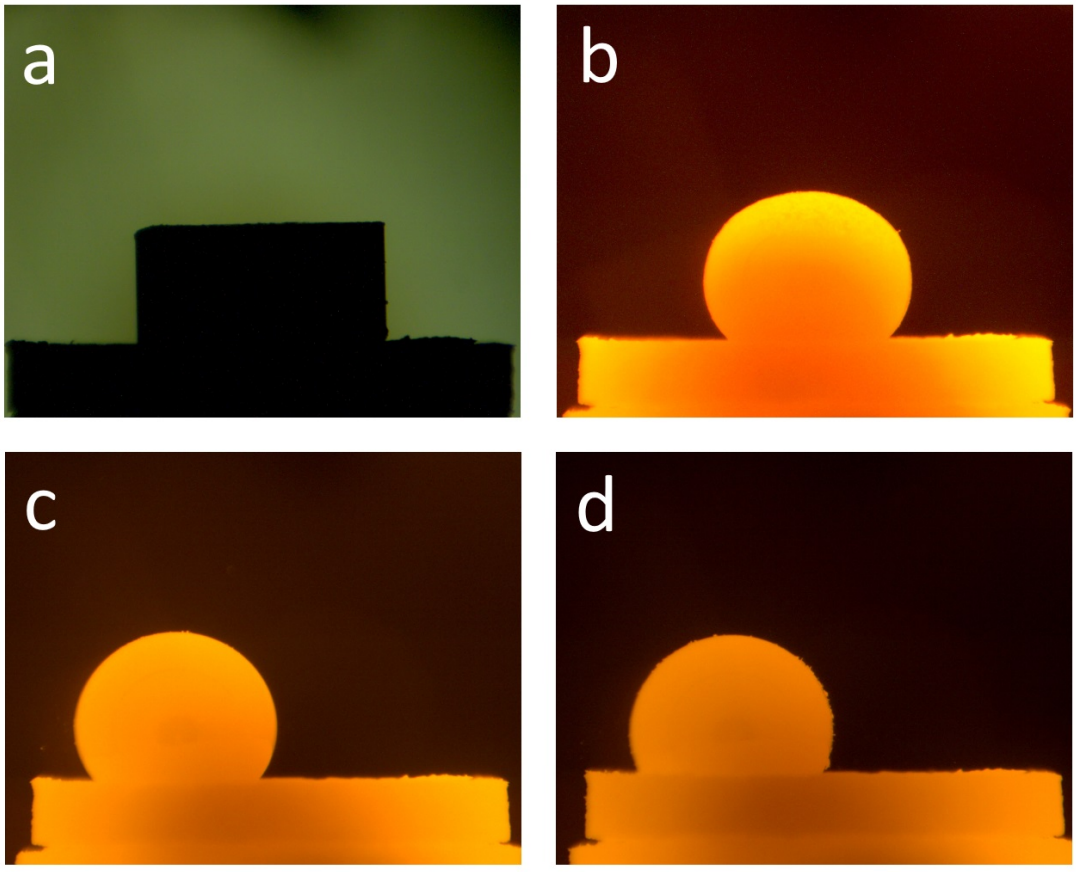

Figure 4.2.6.1: Pictures captured during test 21; a - before heating at 25°C; b - after melting at 1202°C; c - as furnace reaches 1600°C; d - after 5 minutes at 1600°C

Figure 4.2.6.2 shows pictures taken of the slag drop and charcoal pellet after test 21. The figure shows that the slag drop had a pale non-transparent green color, and that the surface of the charcoal pellet had a bit brighter color close to the slag drop.

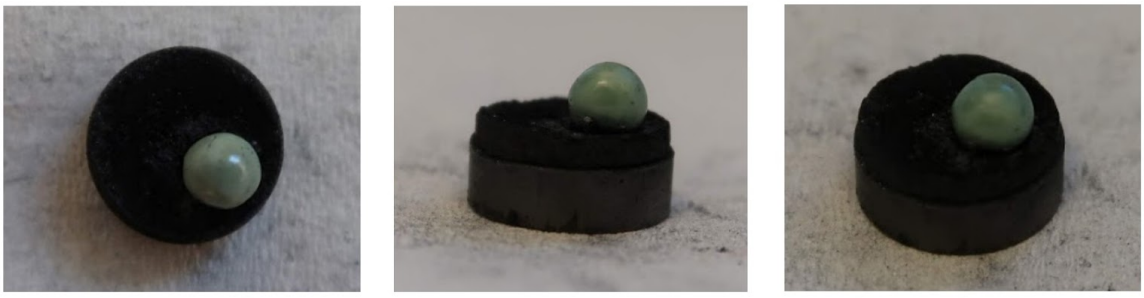

Figure 4.2.6.2: Pictures of slag drop and charcoal pellet after test 21

Figure 4.2.6.3 shows the development of contact angle and temperature for test 21, while figure 4.2.6.4 shows the development of relative volume and temperature for test 21. The figures show that the contact angle decreases mildly with time, and that the relative volume increases some before it decrease. The increase is likely caused by gas trapped in the slag drop.

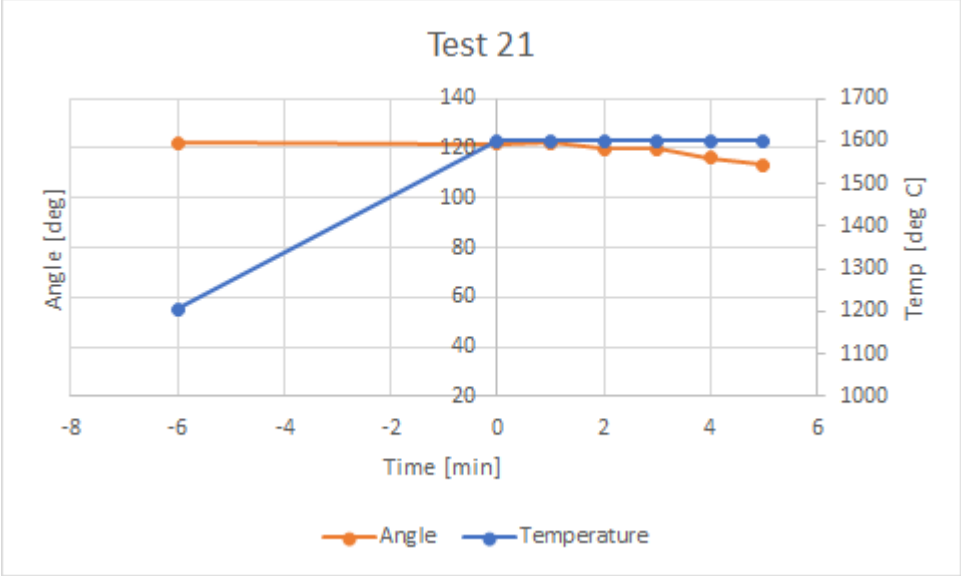

Figure 4.2.6.3: Contact angle and temperature development for test 21

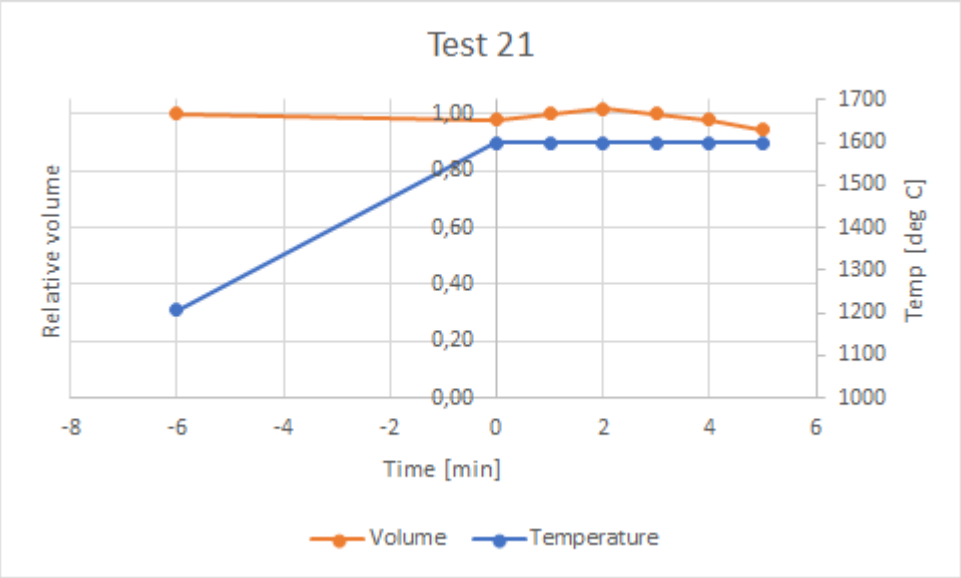

Figure 4.2.6.4: Relative volume and temperature development for test 21

Figure 4.2.6.5 shows an image of sample 21 taken in SEM. The figure shows that there was some particles on the sample surface as it was analysed, and that there is one metal droplet of considerable size in the sample. Figure 4.2.6.6 shows details of the slag magnified 1000 times, which shows that the slag has two phases. Figure 4.2.6.7 shows the slag magnified 47 times, which illustrates that the pattern in the two-phased slag varies in size throughout the sample. Figure 4.2.6.8 shows details of the metal droplet magnified 1000 times, which shows that the metal surface has some structure.

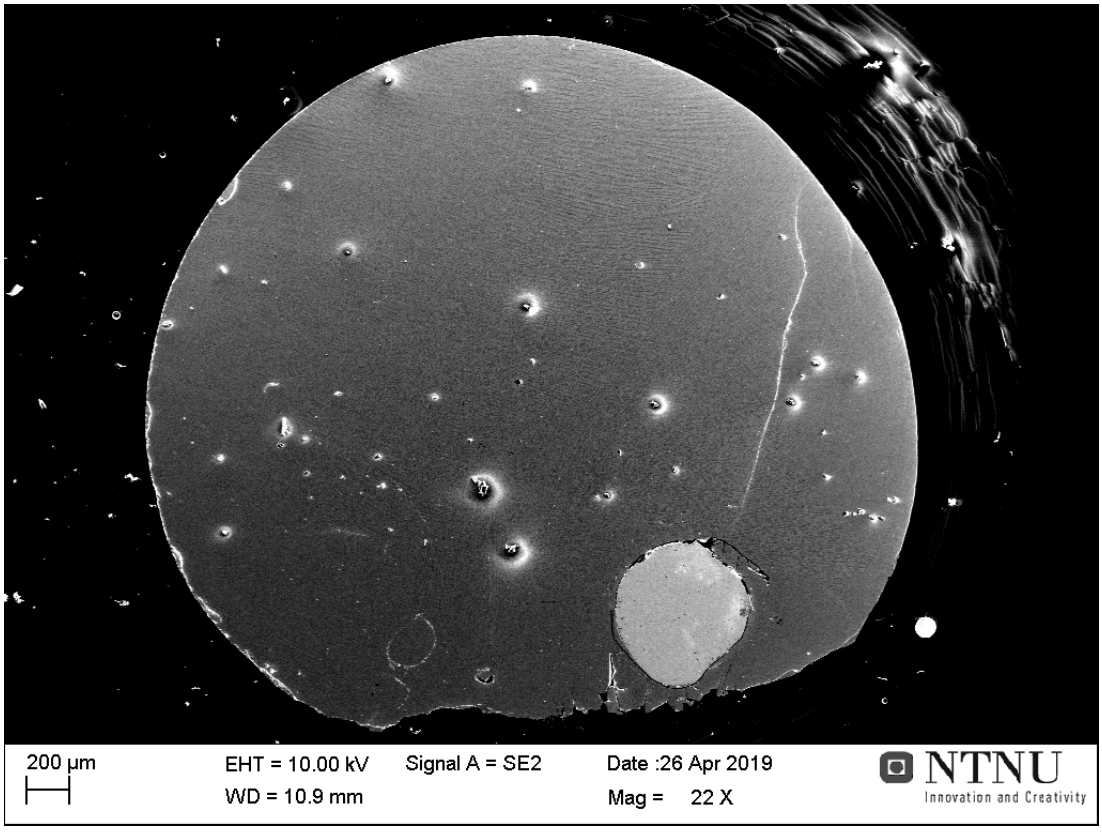

Figure 4.2.6.5: Image of sample 21 taken in SEM

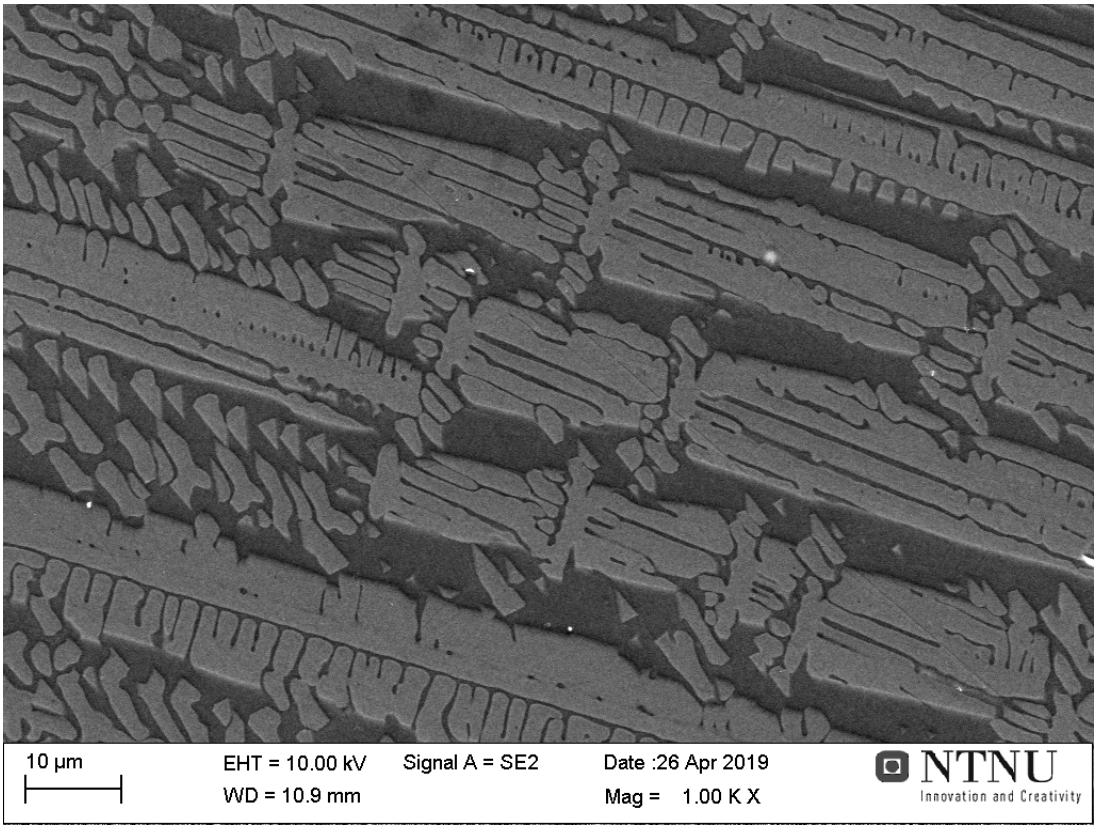

Figure 4.2.6.6: Details of two-phased slag of sample 21 magnified 1000 times

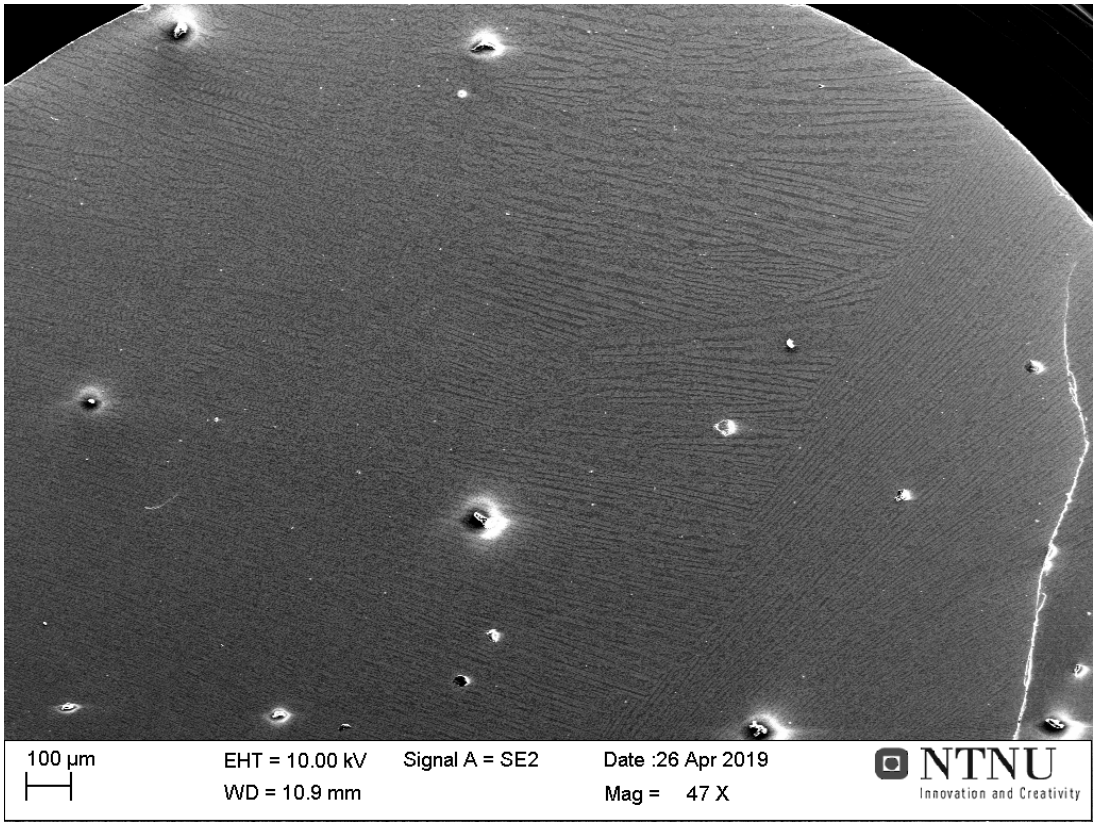

Figure 4.2.6.7: Overview of slag pattern in sample 21 magnified 47 times

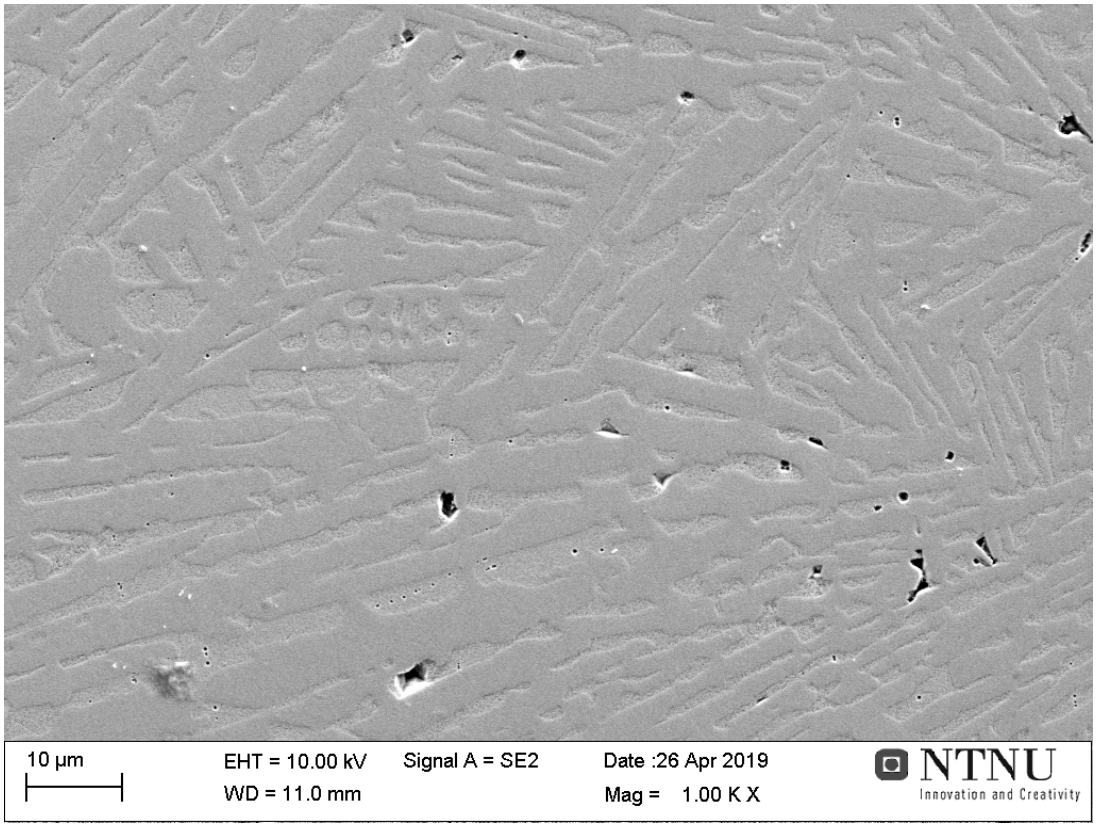

Figure 4.2.6.8: Details of metal droplet of sample 21 magnified 1000 times

Figure 4.2.6.9 shows an image of the charcoal pellet used in test 21 taken in SEM. The figure shows a crater at the right side of the pellet, where the slag drop has worked its way down into the charcoal pellet during reduction. The left side of the charcoal pellet seems unaffected by the reduction, while the part in between seems to be affected. When magnifying this area, there seemed to be micro metal droplets, which could be a result of the activity at the sides of the slag drop close to the pellet during the test.

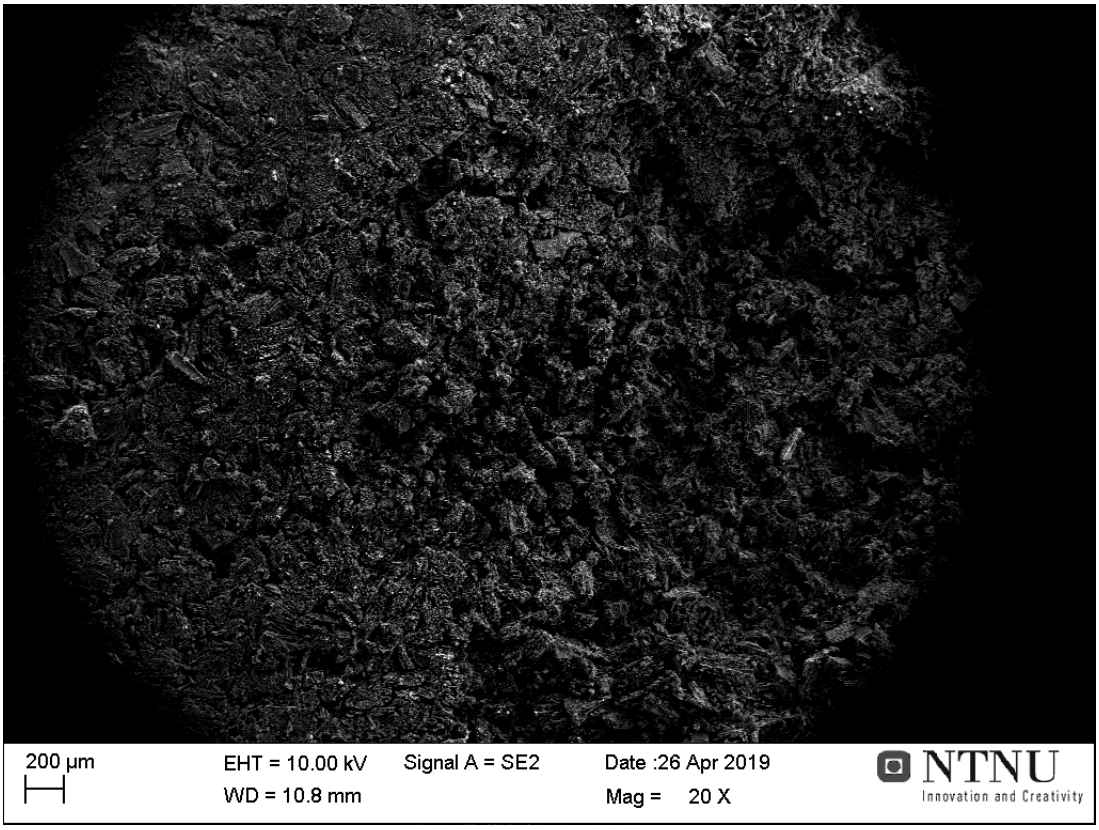

Figure 4.2.6.9: Image of charcoal pellet used in test 21 taken in SEM.

Table 4.2.6.1 lists the composition of the slag measured by SEM and EPMA, and the composition of the metal calculated from the slag composition measured by SEM. The slag has a high content of MnO, while the metal has a lower content of silicon than the desired 18%, high content of iron and low content of manganese. The results of SEM and EPMA analysis are similar for the slag, as is expected.

Table 4.2.6.1: Slag composition measured by SEM and EPMA for sample 21, and metal composition calculated from SEM results

Slag (measured)	**MnO**	**SiO_2**	**FeO**	**Al_2O_3**	**CaO**	**MgO**	**SO_3**
SEM [wt%]	45,94	31,76	0	7,60	9,59	2,95	2,15
EPMA [wt%]	44,91	34,43	0,17	8,00	10,11	2,42	1,31
Metal (calculated)	**Total**	**Mn**		**Si**		**Fe**	
[wt%]	100	44,16		12,47		43,37	
[g]	0,0169	0,0074		0,0021		0,0073	

Reduction degrees for test 21 are R_{Mn} = 0,196 and R_{Si} = 0,055

4.3 Tests run with coke and slag 1

Test were run with slag 1 towards coke. Table 4.3.1 shows the weight measurements of the slag pellet and charcoal pellet before the test, and the weight measurement of the slag and charcoal after the test, in addition to the weight loss.

Table 4.3.1: Weight measurement of tests run with coke and slag 1

	Time [min]	**Coke weight [g]**	**Slag weight [g]**	**Total weight before [g]**	**Weight after [g]**	**Weight loss [g]**	**Weight loss [%]**
2	30	0,2026	0,1033	0,3059	0,2447	0,0612	20,01
4	15	0,1795	0,1004	0,2799	0,2385	0,0414	14,79
10	15	0,1871	0,0991	0,2862	0,2479	0,0383	13,38
6	5	0,1863	0,0985	0,2848	0,2605	0,0243	8,53
7	5	0,1875	0,1037	0,2912	0,2653	0,0259	8,89

The table shows that the percentage weight loss decreases with decreasing reduction time, as is expected. The values of tests run for the same reaction time does not vary significantly, which is also expected.

4.3.1 Test 2

The second test was run with coke pellet 4 and slag sample 1D, at 1600°C for 30 minutes. The slag sample melted at 1207°C. There was some activity through bubbling as the temperature was increased, few bubbles and high volume expansion. Around 1350°C the activity increased with more bubbles and less volume expansion of the slag drop. As hold temperature was reached the activity increased with more bubbles and low volume expansion. After 10 minutes at hold temperature the volume expansion increased and the amount of bubbles were the same. The activity was observed to increase further after 15 minutes before it decreased after 20-25 minutes. For the last minutes of the test, there were few bubbles but high volume expansion of the slag drop.

Figure 4.3.1.1 shows pictures of test 2 in the furnace. There are photos from the start of the test, from the slag drop melted at 1207°C, at 1600°C and after 5, 15 and 30 minutes at 1600°C. The figure shows how the slag drop developed during the test, that the contact angle and shape of the slag drop changed, and that there was some coke particles on the surface of the slag drop towards the end of the test.

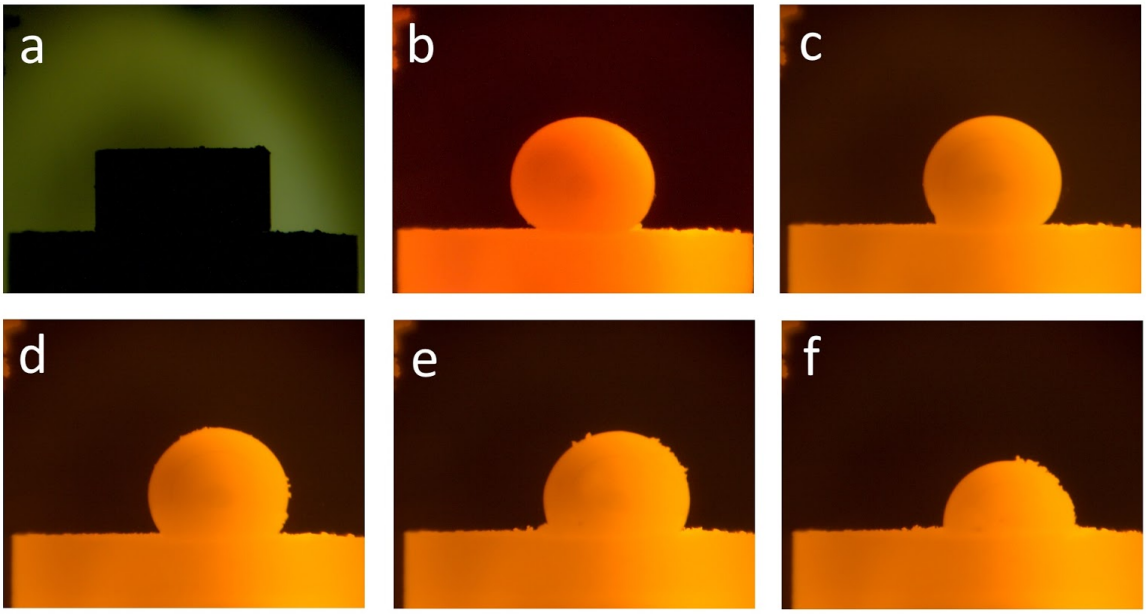

Figure 4.3.1.1: Pictures from test 2; a - before start, at 25°C; b - after melting at 1207°C; c - at 1600°C; d - after 5 minutes at 1600°C; e - after 15 minutes; f - after 30 minutes

Figure 4.3.1.2 shows pictures taken of the slag drop and coke pellet after the test. As can be seen from the figure, the slag drop had a pale green non-transparent color, and some coke at the slag drop surface.

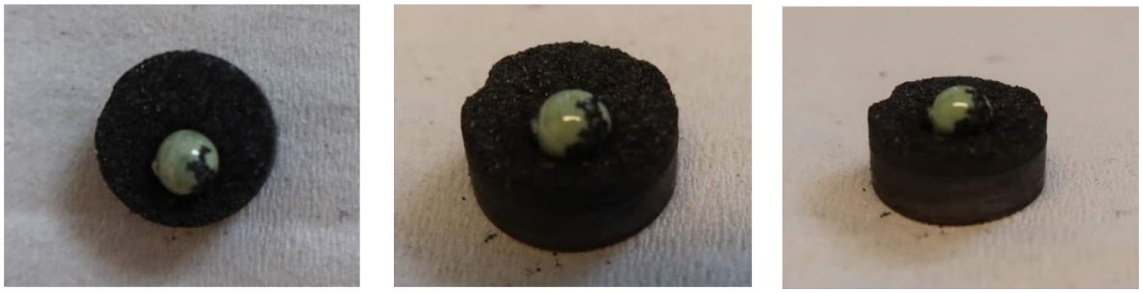

Figure 4.3.1.2: Pictures of slag drop and coke pellet from test 2

Figure 4.3.1.3 shows the development of contact angle and temperature of test 2, while figure 4.3.1.4 shows the development of relative volume and temperature for test 2. The figures show that the contact angle decreases moderately with time, while the trend for the relative volume is that it stays around the same value for the first 15 minutes at hold temperature, then decreases with time for the last 15 minutes. The relative volume has some variations that are likely caused by gas being trapped in the slag drop.

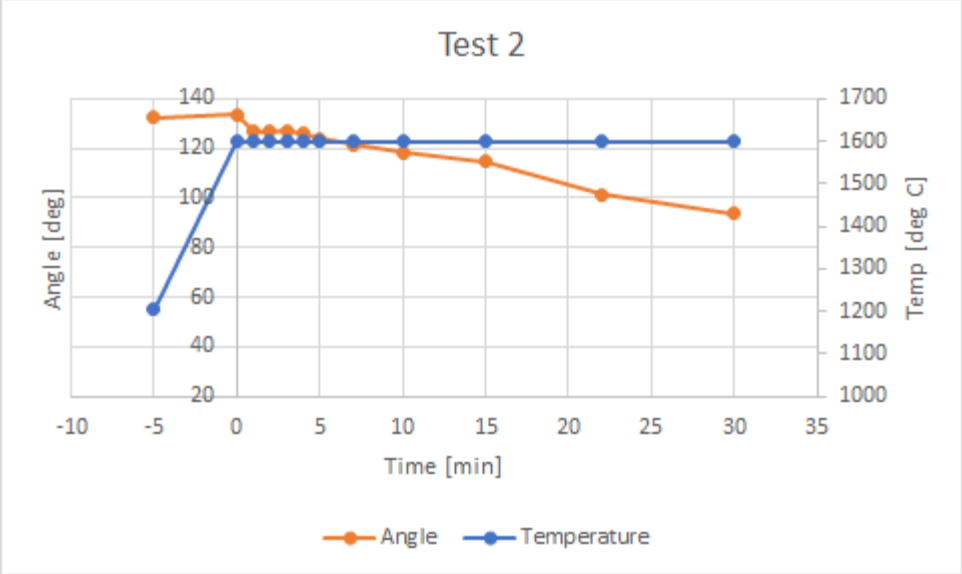

Figure 4.3.1.3: Contact angle and temperature development for test 2

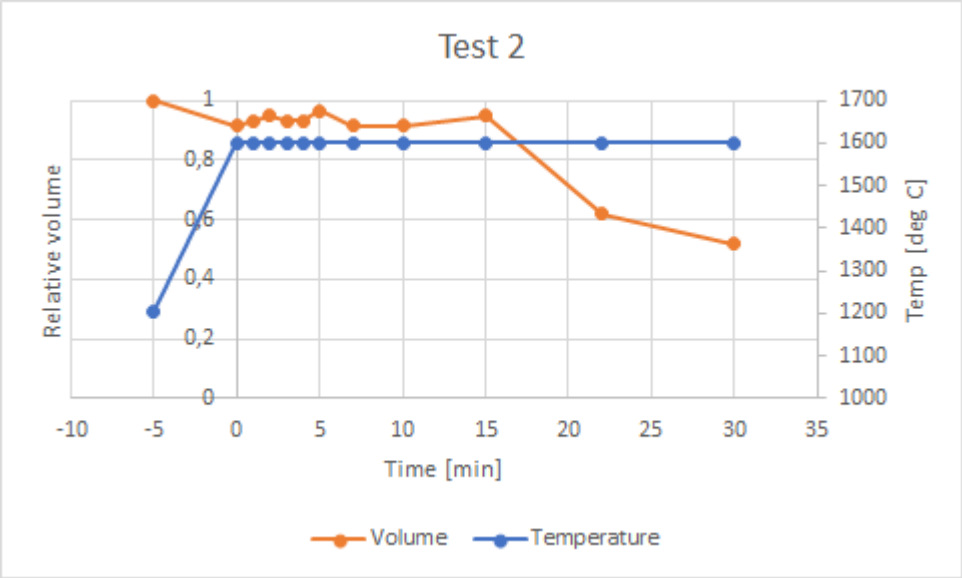

Figure 4.3.1.4: Relative volume and temperature development for test 2

Figure 4.3.1.5 shows an image of sample 2 taken in SEM. The figure shows that there is one metal droplet of significant size, that there was a gas bubble in the slag drop when it solidified, and the coke pellet can be made out at the bottom of the image.. Figure 4.3.1.6 shows the slag phase magnified 1000 times, and shows that the slag phase is glassy, as is expected with this hold time. Figure 4.3.1.7 shows the metal phase of sample 2 magnified 1000 times, and shows that the metal phase is uniform.

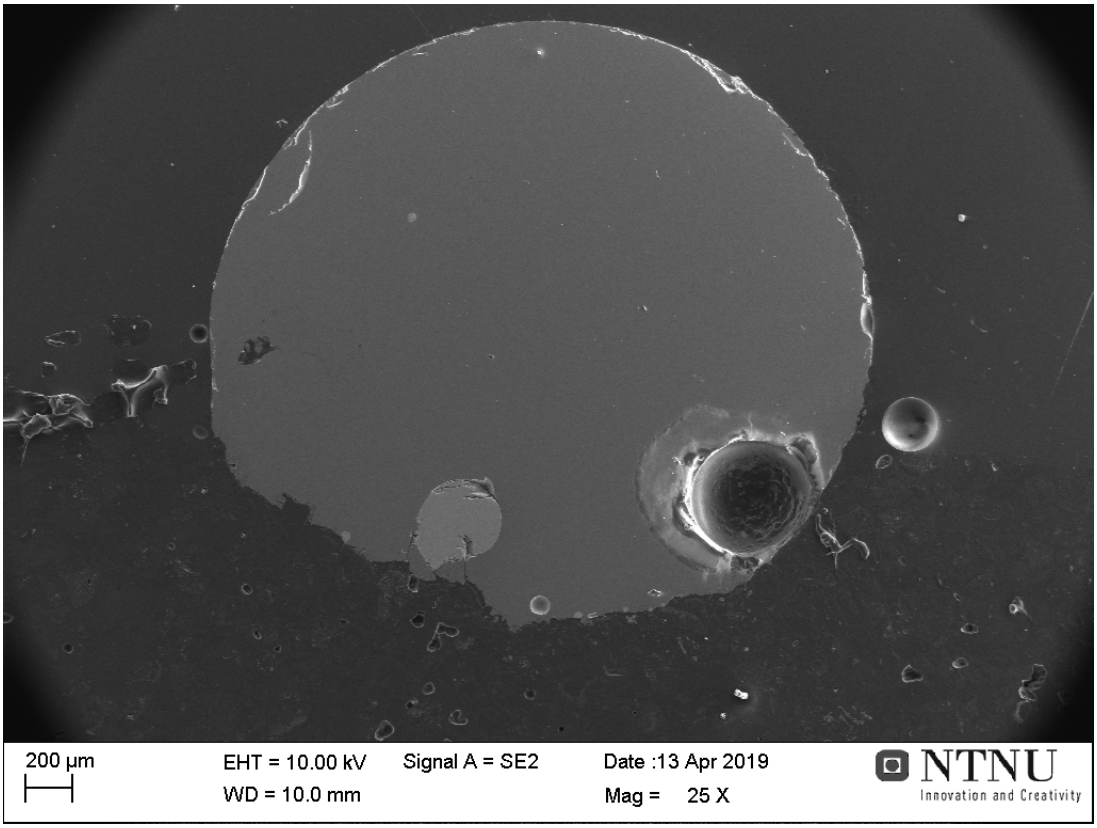

Figure 4.3.1.5: Image of sample 2 taken in SEM

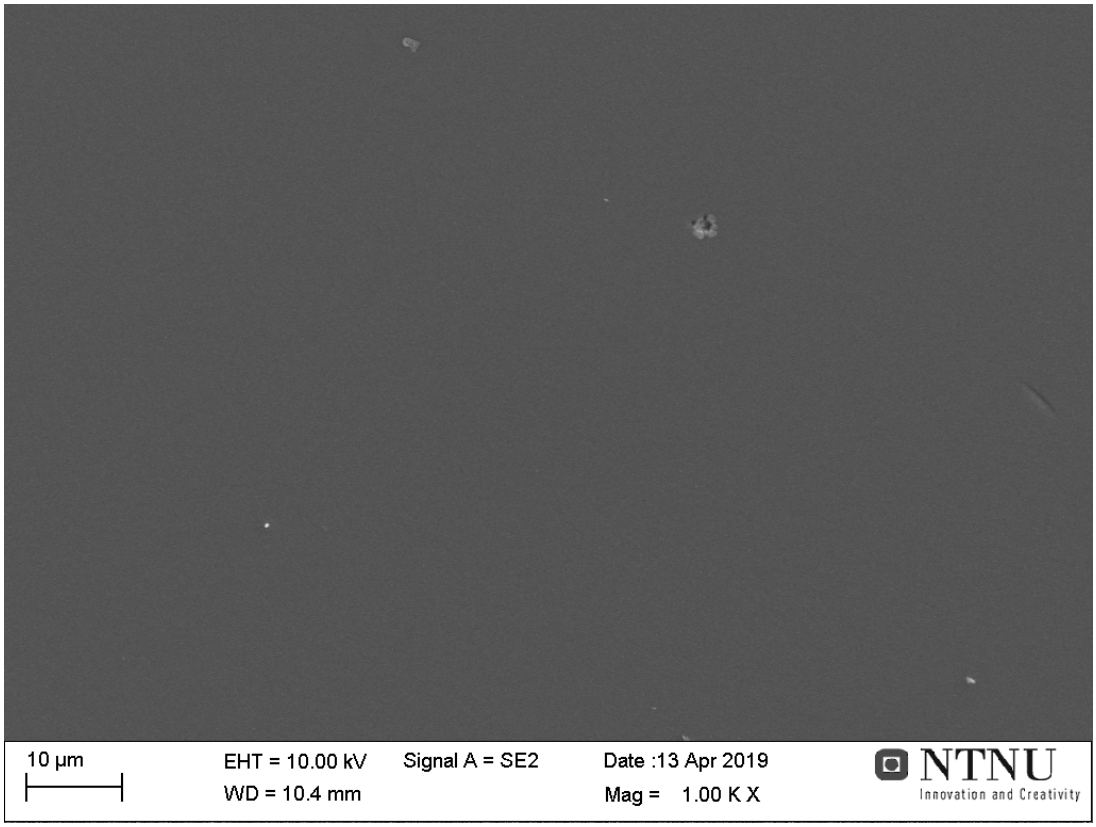

Figure 4.3.1.6: Slag of sample 2, magnified 1000 times

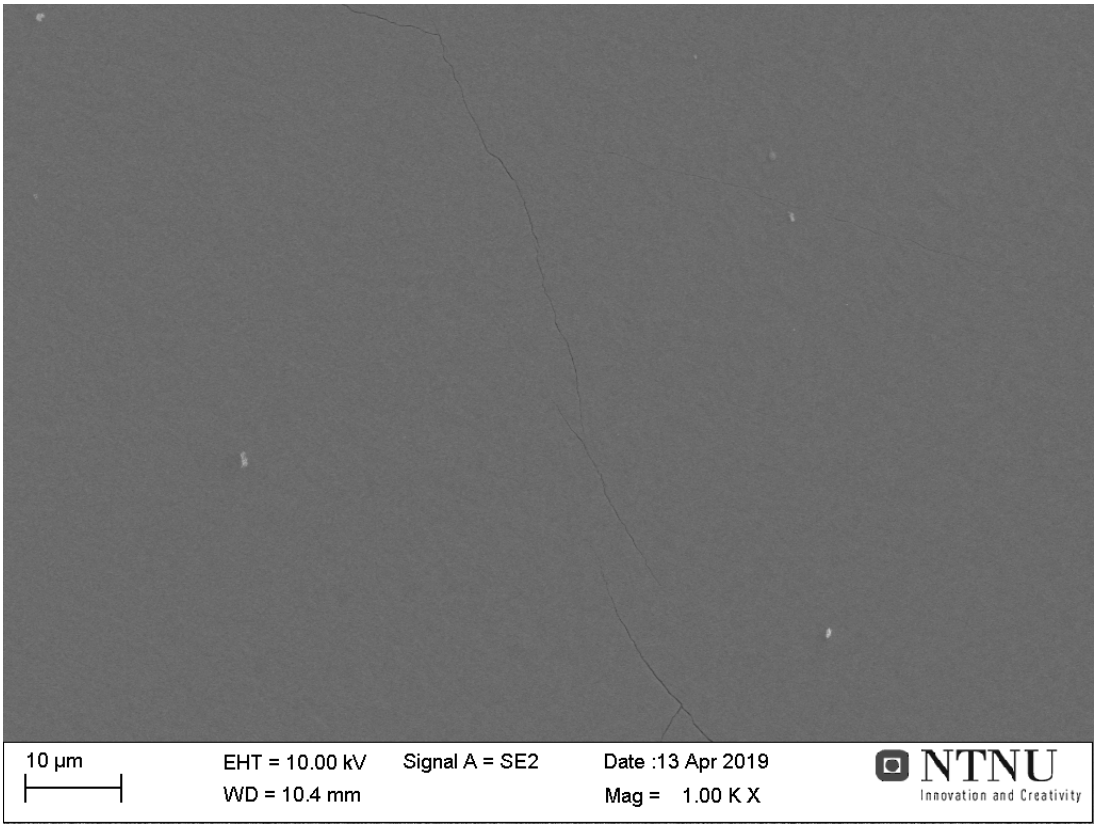

Figure 4.3.1.7: Metal of sample 2, magnified 1000 times

Table 4.3.1.1 lists the composition of the slag measured by SEM and EPMA, and the composition of the metal calculated from the slag composition measured by SEM. The slag has a bit higher content of MnO than the desired 5%, and the metal has a low content of silicon compared to the desired 18%. The results of the SEM and EPMA measurements for the slag are similar, as is expected.

Table 4.3.1.1: Slag composition measured by SEM and EPMA for sample 2, and metal composition calculated from SEM results

Slag (measured)	**MnO**	**SiO_2**	**FeO**	**Al_2O_3**	**CaO**	**MgO**	**SO_3**
SEM [wt%]	13,49	44,10	0,03	15,61	18,56	6,12	2,08
EPMA [wt%]	14,60	46,65	0,03	13,15	18,90	5,30	1,78
Metal (calculated)	**Total**	**Mn**		**Si**		**Fe**	
[wt%]	100	78,53		8,24		13,23	
[g]	0,0364	0,0286		0,0030		0,0048	

Reduction degrees for test 2 are R_{Mn} = 0,834 and R_{Si} = 0,088

4.3.2 Test 4

The fourth test was run with coke pellet 5 and slag sample 1F, at 1600°C for 15 minutes. The slag sample melted into a slag drop at 1208°C. At 1250°C there was some activity through bubbling with small volume expansion. Around 1350°C the activity increased some, and as hold temperature was reached the activity increased some more. There were many bubbles and low volume expansion. The activity increased further after 7 minutes at hold temperature with more bubbles, and after 12 minutes with higher volume expansion. For the last minutes of the test, the volume expansion of the slag drop is high.

Figure 4.3.2.1 shows pictures taken from the furnace during test 4. The pictures are taken at the start of the test, at 25°C, after melting at 1208°C, after the furnace temperature reached 1600°C, after 5 and 15 minutes at 1600°C. The figure shows that the slag drop moved some towards the edge of the pellet during the test, that the slag drop changed contact angle during the test, and that there was some carbon material at the slag drop surface towards the end of the test.

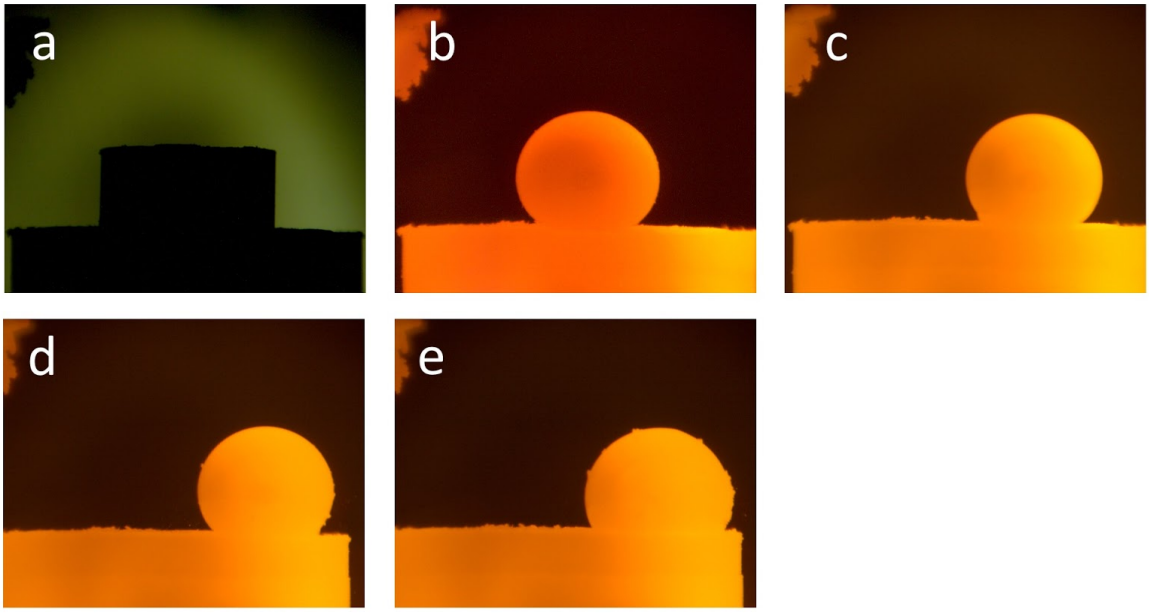

Figure 4.3.2.1: Pictures from test 4; a - before test at 25°C; b - after melting at 1208°C; c - as the temperature reached 1600°C; d - after 5 minutes at 1600°C; e - after 15 minutes

Figure 4.3.2.2 shows pictures of the slag drop and coke pellet taken after the test. The figure shows that the slag drop had a transparent orange color after the test, and a visible metal droplet at the side of the slag drop.

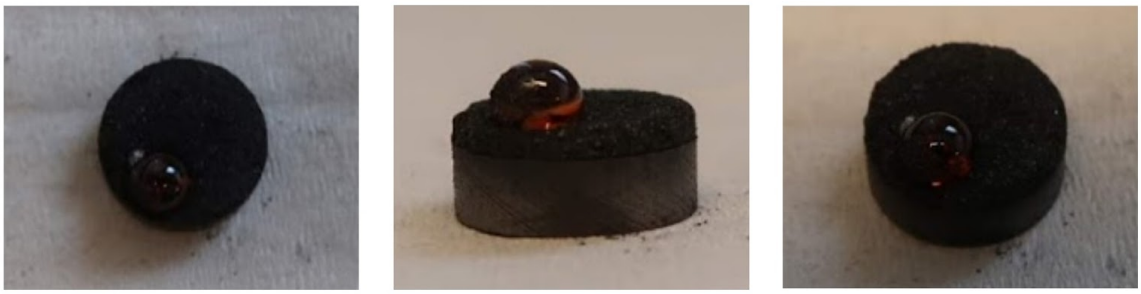

Figure 4.3.2.2: Pictures of slag drop and coke pellet after test 4

Figure 4.3.2.3 shows the development of contact angle and temperature for test 4, while figure 4.3.2.4 shows the development of relative volume and temperature for test 4. The figures show that the contact angle decreases moderately with time except for an increase after two minutes, and that the relative volume first decrease, then increase after two minutes, then decrease until seven minutes before it increases for the rest of the test. The increases are likely caused by gas being trapped in the slag drop.

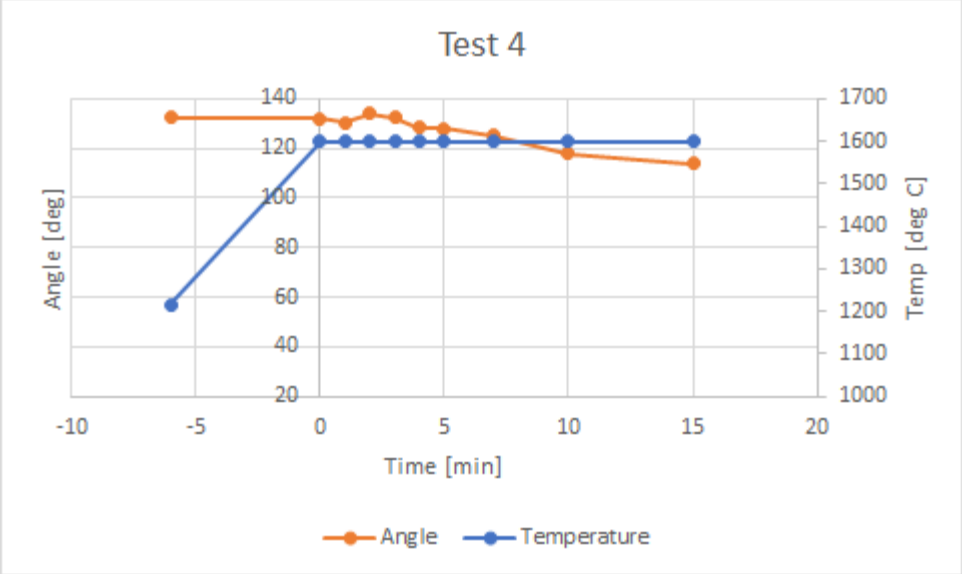

Figure 4.3.2.3: Contact angle and temperature development for test 4

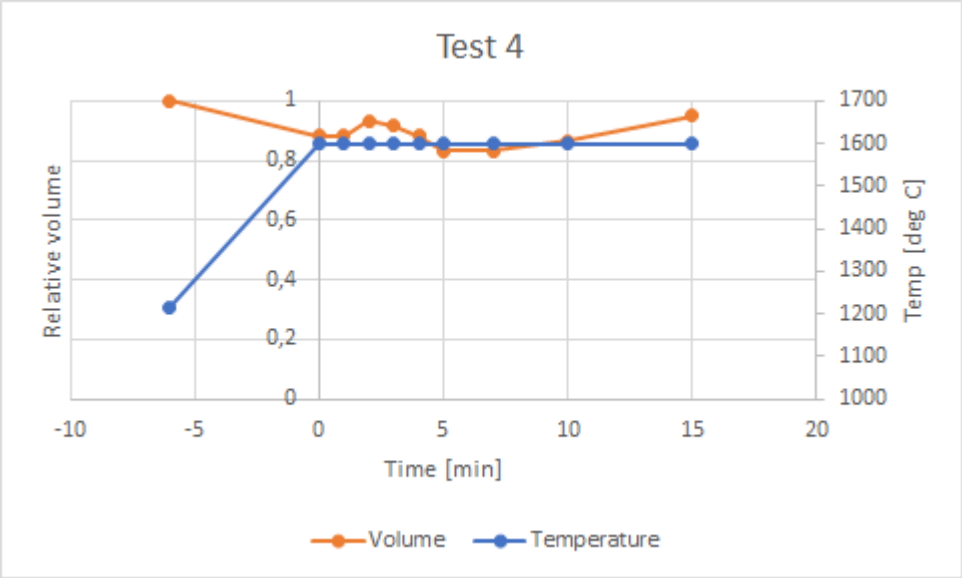

Figure 4.3.2.4: Relative volume and temperature development for test 4

Figure 4.3.2.5 shows a picture of sample 4 taken in SEM. The figure shows that the sample has four metal droplets of considerable size at the surface, and some smaller metal droplets. The coke pellet and graphite cup can be made out at the bottom of the figure. Figure 4.3.2.6 shows details of the slag phase magnified 1000 times, which shows that the slag is glassy. Figure 4.3.2.7 shows details of the largest metal drop magnified 1000 times, and shows that the metal has some structure at the surface.

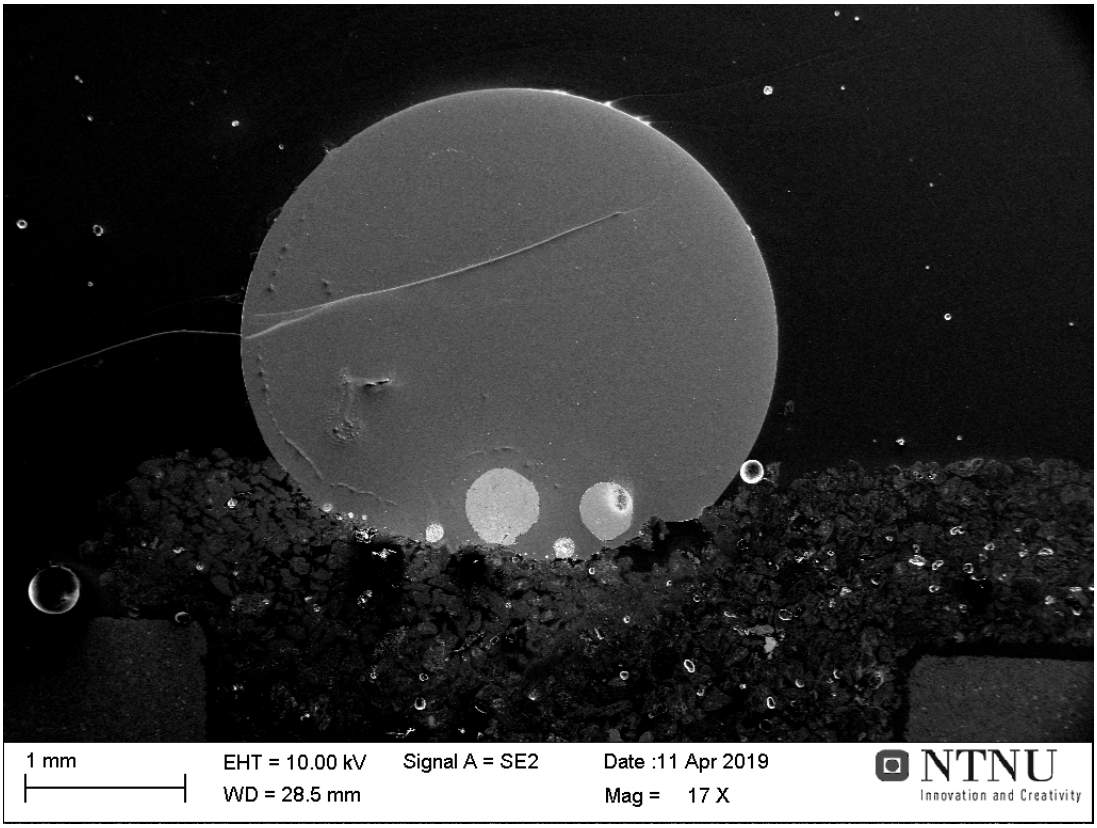

Figure 4.3.2.5: Picture of sample 4 taken in SEM

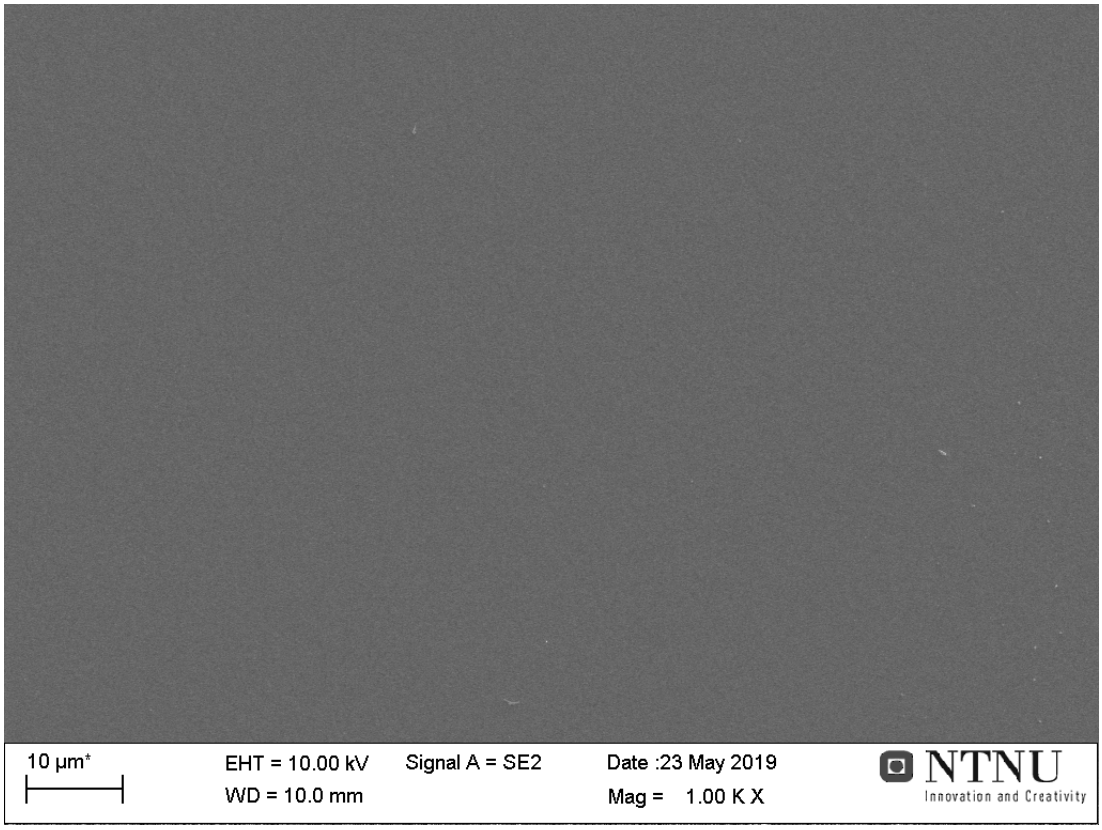

Figure 4.3.2.6: Details of the slag phase of sample 4 magnified 1000 times

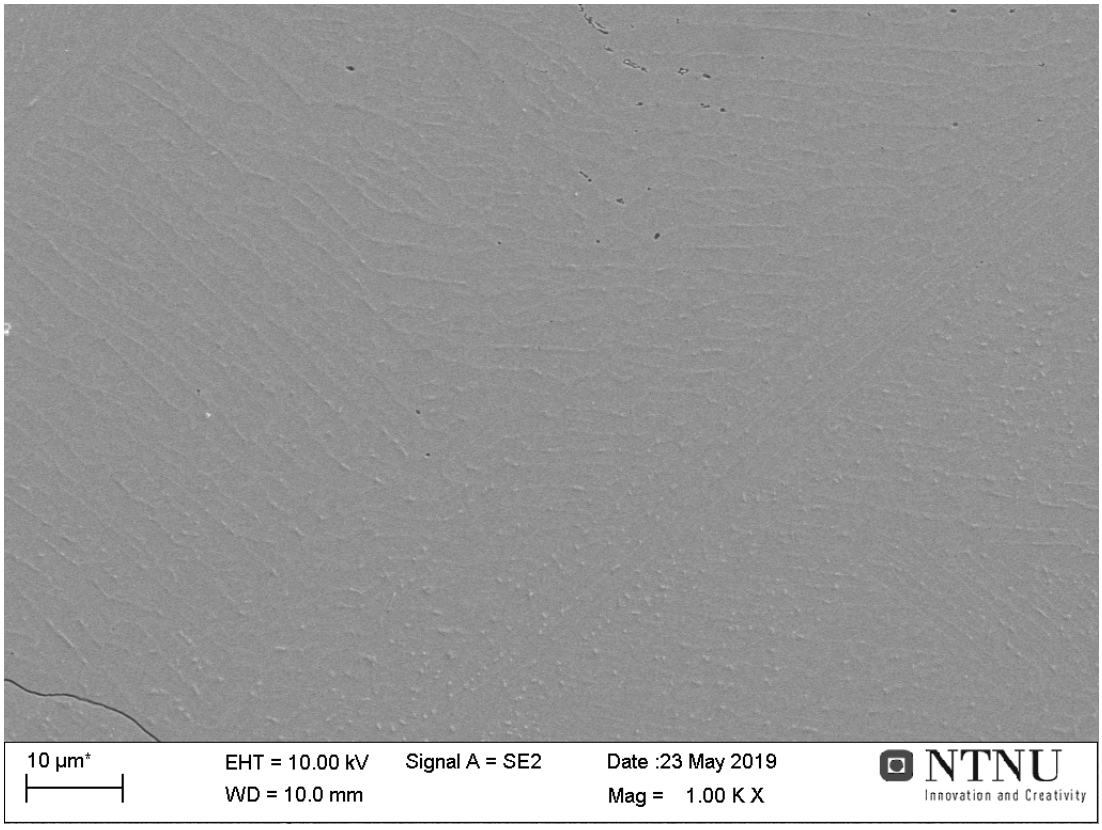

Figure 4.3.2.7: Details of the metal phase of sample 4 magnified 1000 times

Table 4.3.2.1 lists the composition of the slag measured by SEM and EPMA, and the composition of the metal calculated from the slag composition measured by SEM. The slag has a high content of MnO, and the calculated metal composition gives negative silicon content, which is not possible. This is a result of the metal composition being calculated from the measured slag composition. The results of the SEM and EPMA analyses for the slag are similar, as is expected.

Table 4.3.2.1: Slag composition measured by SEM and EPMA for sample 4, and metal composition calculated from SEM results

Slag (measured)	**MnO**	**SiO_2**	**FeO**	**Al_2O_3**	**CaO**	**MgO**	**SO_3**
SEM [wt%]	30,54	40,49	0	10,84	13,72	4,42	0
EPMA [wt%]	28,53	41,77	0,08	10,14	14,98	4,17	1,88
Metal (calculated)	**Total**	**Mn**		**Si**		**Fe**	
[wt%]	100	77,59		-0,45		22,86	
[g]	0,0206	0,0159		-0,00009		0,0047	

Reduction degrees for test 4 are R_{Mn} = 0,478 and R_{Si} = -0,003. The negative silicon content causes a negative reduction degree for silicon.

4.3.3 Test 10

The tenth test was run with coke pellet 8 and slag sample 1L, at 1600°C for 15 minutes. The slag melted at 1192°C. There was some activity at 1250°C, and the activity increased around 1330°C. The slag drop moved some as the temperature reached 1380°C, and some coke particles could be observed at the slag drop surface. The activity through bubbling was relatively low, but there was some activity through particles scattering close to the coke pelle. After 5 minutes at hold temperature the activity increase, with more bubbles and the same volume expansion. The bubbling increased after 10 minutes and after 12 minutes, with more bubbles and the same volume expansion.

Figure 4.3.3.1 shows pictures taken from the furnace during test 10. The pictures show the slag sample before heating, after melting, as the furnace temperature reaches 1600°C, after 5 and 15 minutes at 1600°C. The figure shows that the slag drop moved during the test, that the slag shape and contact angle changed during the test, and that there was some coke particles at the surface of the slag drop towards the end of the test.

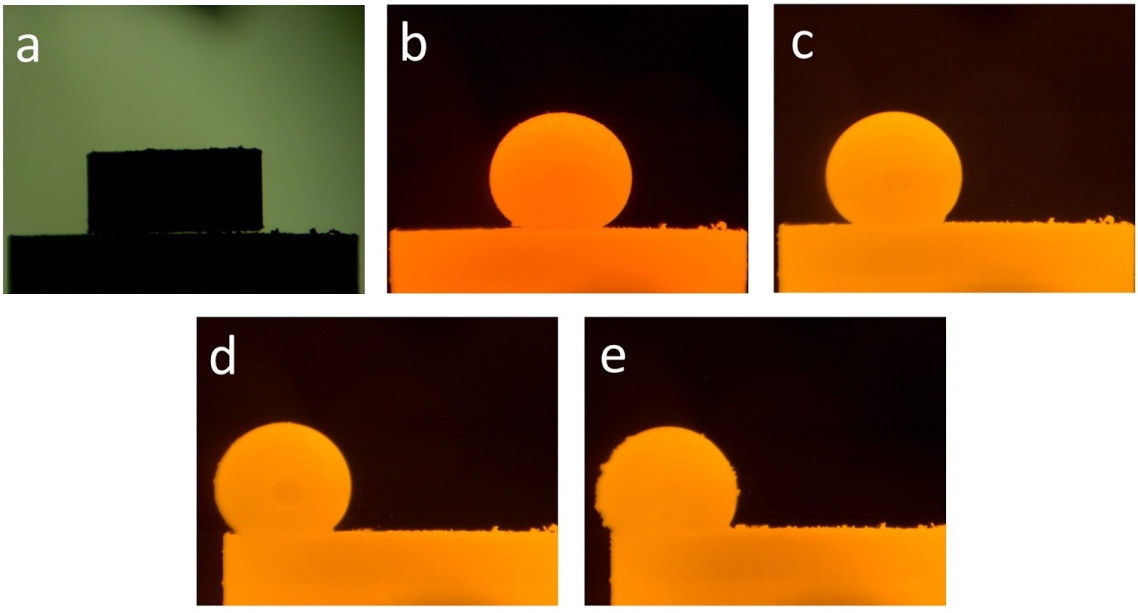

Figure 4.3.3.1: Pictures from test 10; a - before heating at 25°C; b - after melting at 1192°C; c - as furnace reaches 1600°C; d - after 5 minutes at 1600°C; e - after 15 minutes at 1600°C

Figure 4.3.3.2 shows pictures taken of the slag drop and coke pellet after test 10. The figure shows that the slag drop was close to the edge after the test and that the slag drop had a transparent orange color. The figure also shows that there was a metal droplet visible at the side of the slag drop.

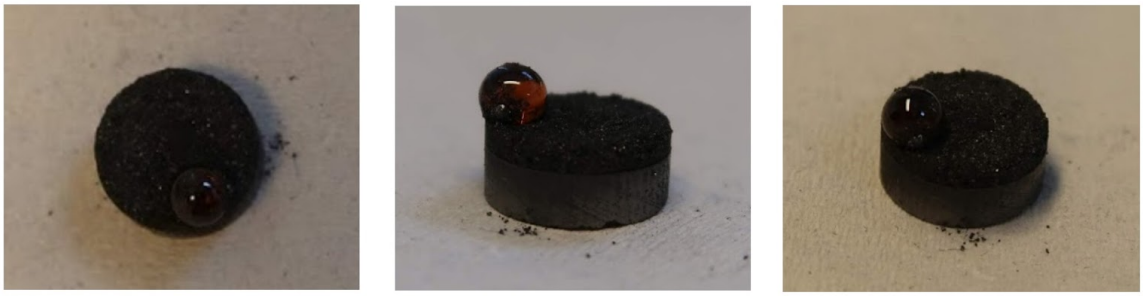

Figure 4.3.3.2: Pictures of slag drop and coke pellet after test 10

Figure 4.3.3.3 shows the development of contact angle and temperature of test 10, while figure 4.3.3.4 shows the development of relative volume and temperature of test 10. The figures show that the contact angle had approximately the same value for the first five minutes of the test, before it decreases moderately for the last 10 minutes of the test. The relative volume decreases moderately during heating and the first minute, before it keeps approximately the same value for the rest of the test.

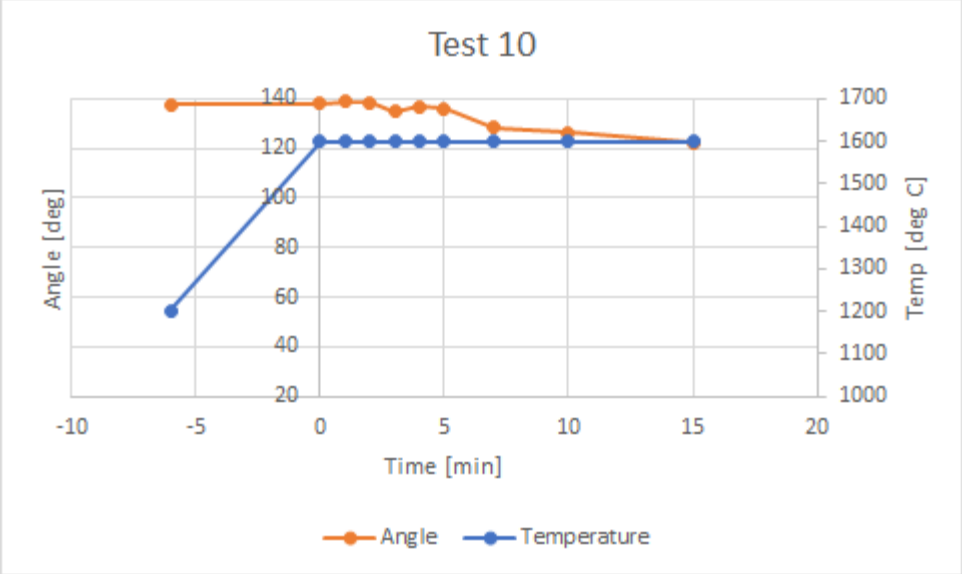

Figure 4.3.3.3: Contact angle and temperature development for test 10

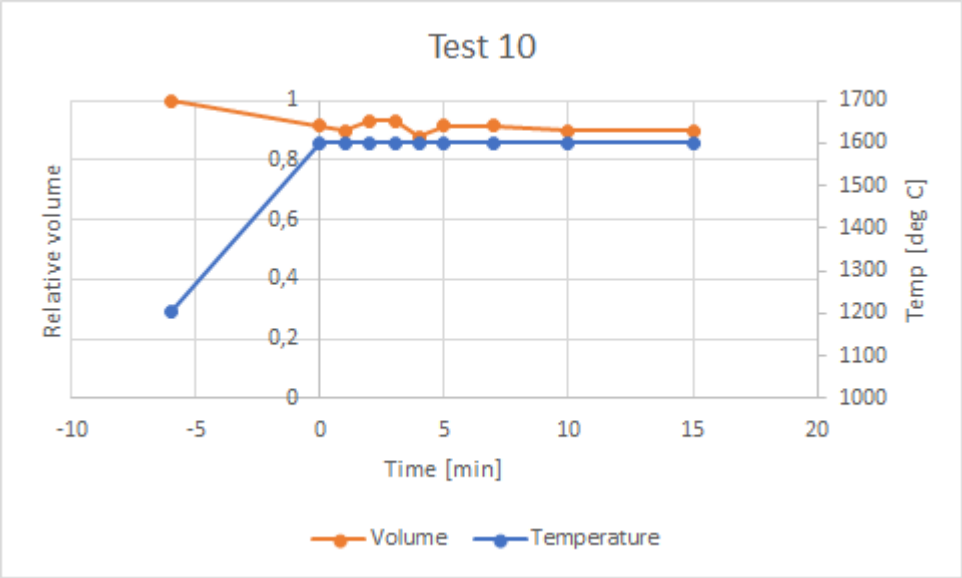

Figure 4.3.3.4: Relative volume and temperature development for test 10

Figure 4.3.3.5 shows an image of sample 10 taken in SEM. The figure shows that there is two metal droplets of considerable size and some small droplets, and the coke pellet is visible at the left side of the slag drop. Figure 4.3.3.6 shows details of the slag magnified 1000 times. The figure shows that the slag phase is glassy and uniform. Figure 4.3.3.7 shows details of the small metal droplet at the upper left side of figure 4.3.3.5 magnified 1000 times, and shows that the metal has some structure.

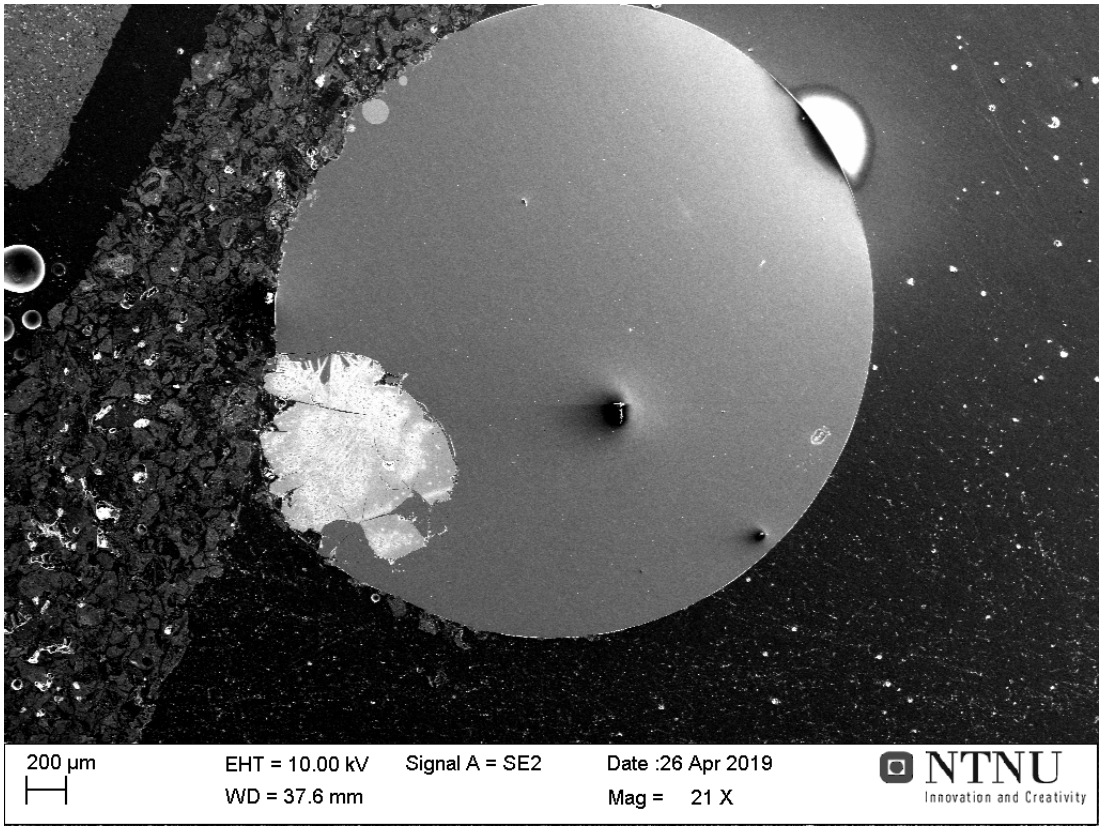

Figure 4.3.3.5: Image of sample 10 taken in SEM

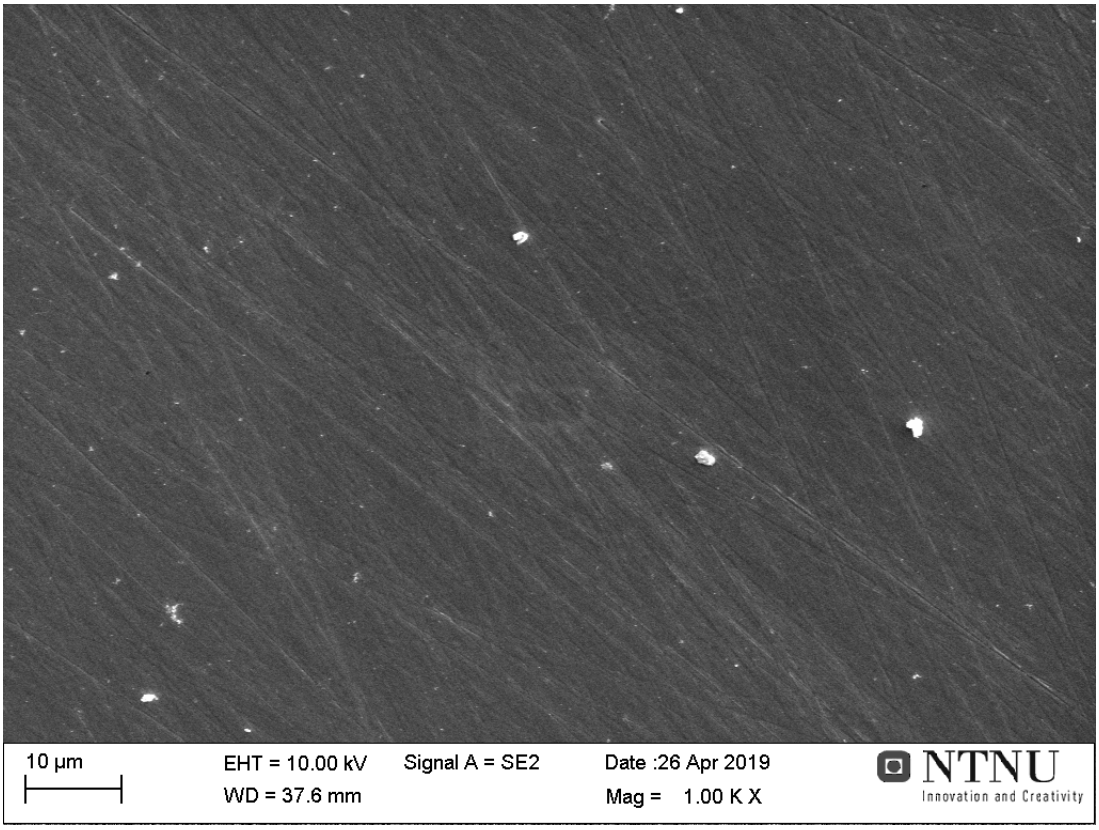

Figure 4.3.3.6: Slag phase of sample 10, magnified 1000 times

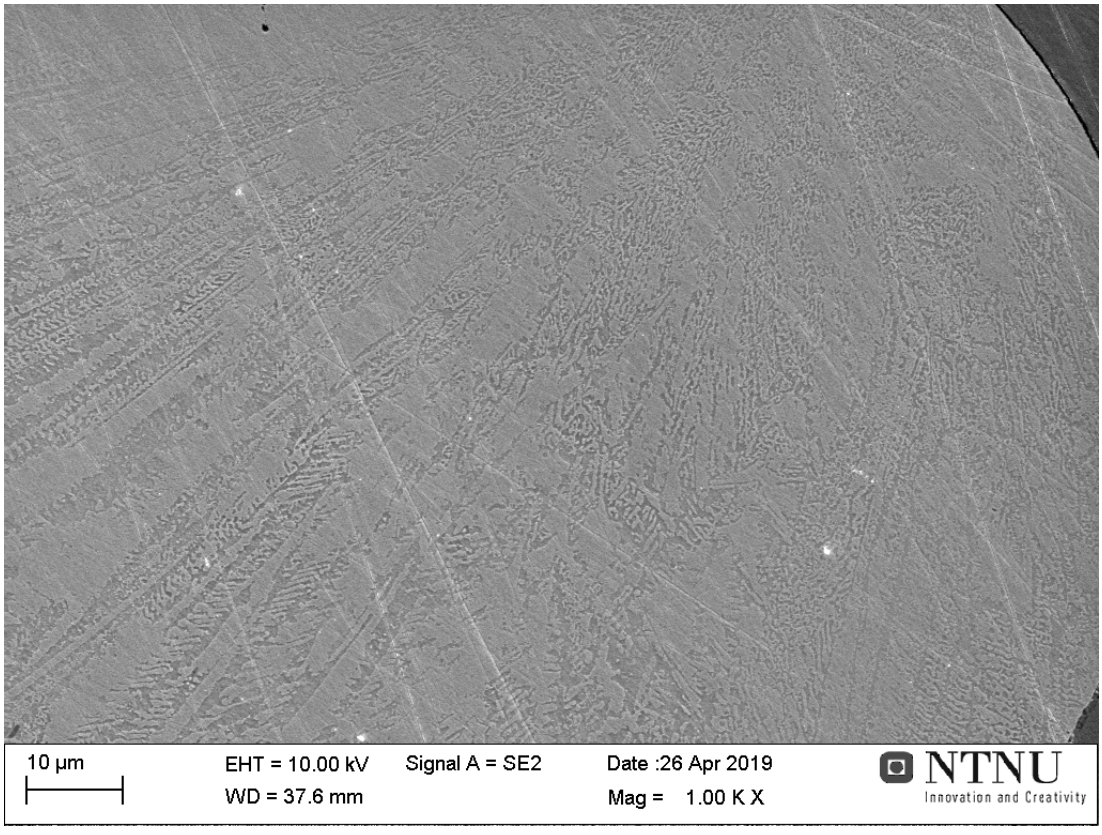

Figure 4.3.3.7: Metal of sample 10, magnified 1000 times

Table 4.3.3.1 lists the composition of the slag measured by SEM and EPMA, and the composition of the metal calculated from the slag composition measured by SEM. The slag has a high MnO content while the metal has a low content of silicon. The results from the EPMA and the SEM analysis of the slag are similar, which is expected.

Table 4.3.3.1: Slag composition measured by SEM and EPMA for sample 10, and metal composition calculated from SEM results

Slag (measured)	**MnO**	**SiO_2**	**FeO**	**Al_2O_3**	**CaO**	**MgO**	**SO_3**
SEM [wt%]	29,04	38,54	0	11,14	14,52	4,17	2,60
EPMA [wt%]	31,08	41,17	0,10	9,49	14,10	3,93	1,67
Metal (calculated)	**Total**	**Mn**		**Si**		**Fe**	
[wt%]	100	75,35		4,16		20,49	
[g]	0,0226	0,0171		0,0009		0,0046	

Reduction degrees for test 10 are R_{Mn} = 0,518 and R_{Si} = 0,029

4.3.4 Test 6

The sixth test was run with coke pellet 6 and slag sample 1H, at 1600°C for 5 minutes. The slag sample melted at 1208°C. There was some activity through bubbling at 1250°C, and the activity increased some around 1350°C, with many bubbles and low volume expansion. Throughout the test, there was relatively low activity through bubbling, but there was some activity through particles scattering at the sides of the slag drop.

Figure 4.3.4.1 shows some pictures taken during test 6. The pictures show the slag sample before heating at 25°C, after melting at 1208°C, as the furnace reaches 1600°C, and after 5 minutes at 1600°C. The figure shows that the changes in the slag drop were rather small during the 5 minutes of reduction time, and that there were some coke particles at the slag drop surface at the end of the test.

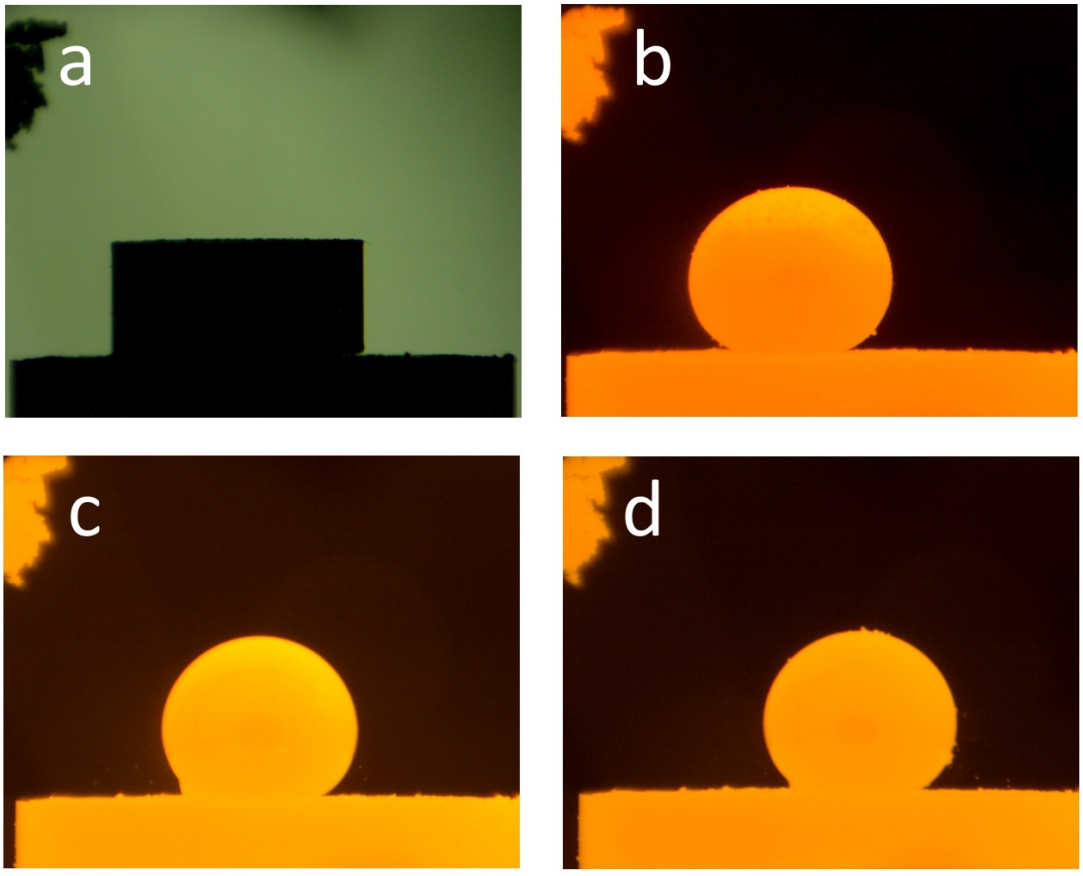

Figure 4.3.4.1: Pictures taken during test 6; a - before heating at 25°C; b - after melting at 1208°C; c - as furnace reaches 1600°C; d - after 5 minutes at 1600°C

Figure 4.3.4.2 shows pictures taken of the slag drop and coke pellet after test 6. The figure shows that the slag drop came loose from the coke pellet after the test, that the slag drop was observed to have a transparent orange color on the top, and a pale green non-transparent color at the bottom, and that there were some metal drops at the bottom of the slag drop, where the slag drop was connected to the coke pellet.

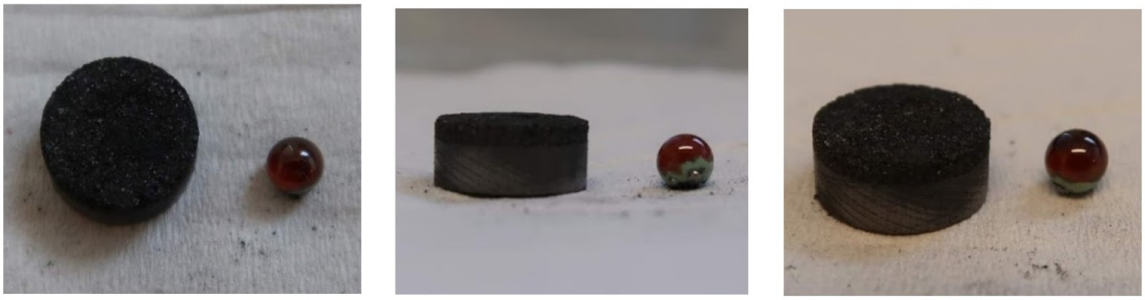

Figure 4.3.4.2: Pictures of slag drop and coke pellet after test 6

Figure 4.3.4.3 shows the development of contact angle and temperature for test 6, while figure 4.3.4.4. shows the development of relative volume and temperature for test 6. The figures show that the contact angle only has small changes during the test, and that the relative volume fluctuates some, likely due to gas trapped in the slag drop, and only has small changes.

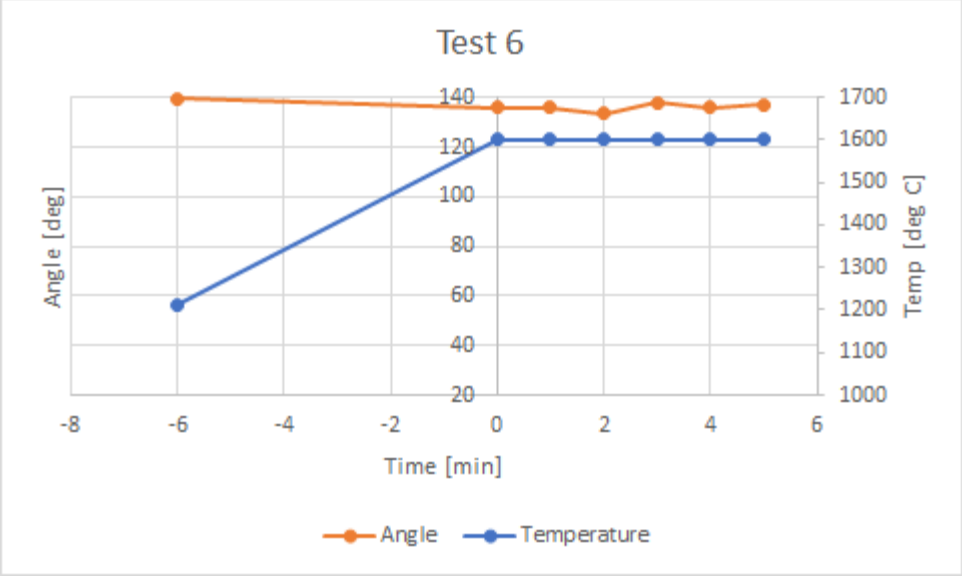

Figure 4.3.4.3: Contact angle and temperature development for test 6

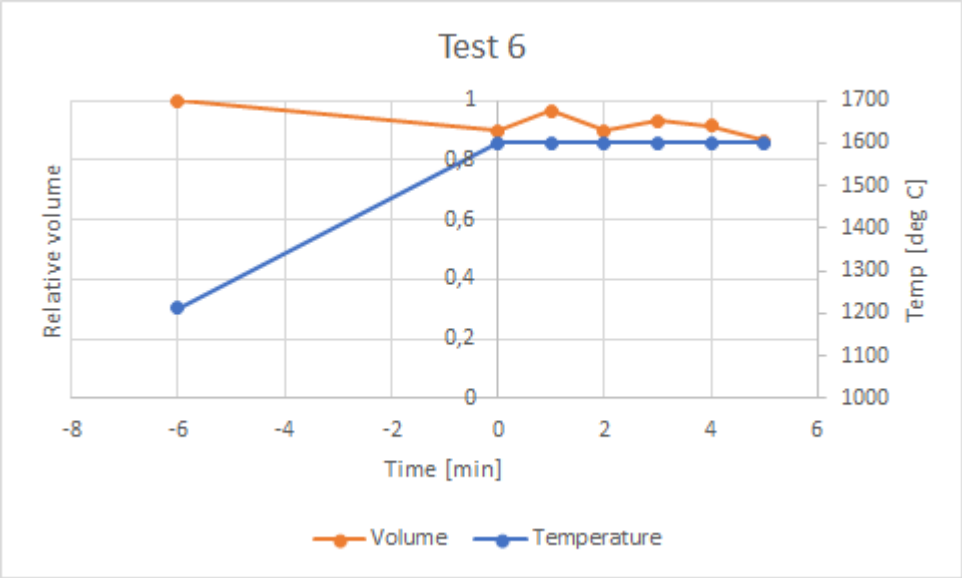

Figure 4.3.4.4: Relative volume and temperature development for test 6

Figure 4.3.4.5 shows an image of sample 6 taken in SEM. The figure shows that the sample has one metal droplet of considerable size at the surface. Figure 4.3.4.6 shows details of the slag magnified 1000 times, and show that the slag has areas with two-phase slag and areas with glassy slag, which is consistent with the visual observation of the slag drop having two colors shown in figure 4.3.4.2. Figure 4.3.4.7 shows details of the metal drop magnified 1000 times, andshows that the metal has structure at the surface.

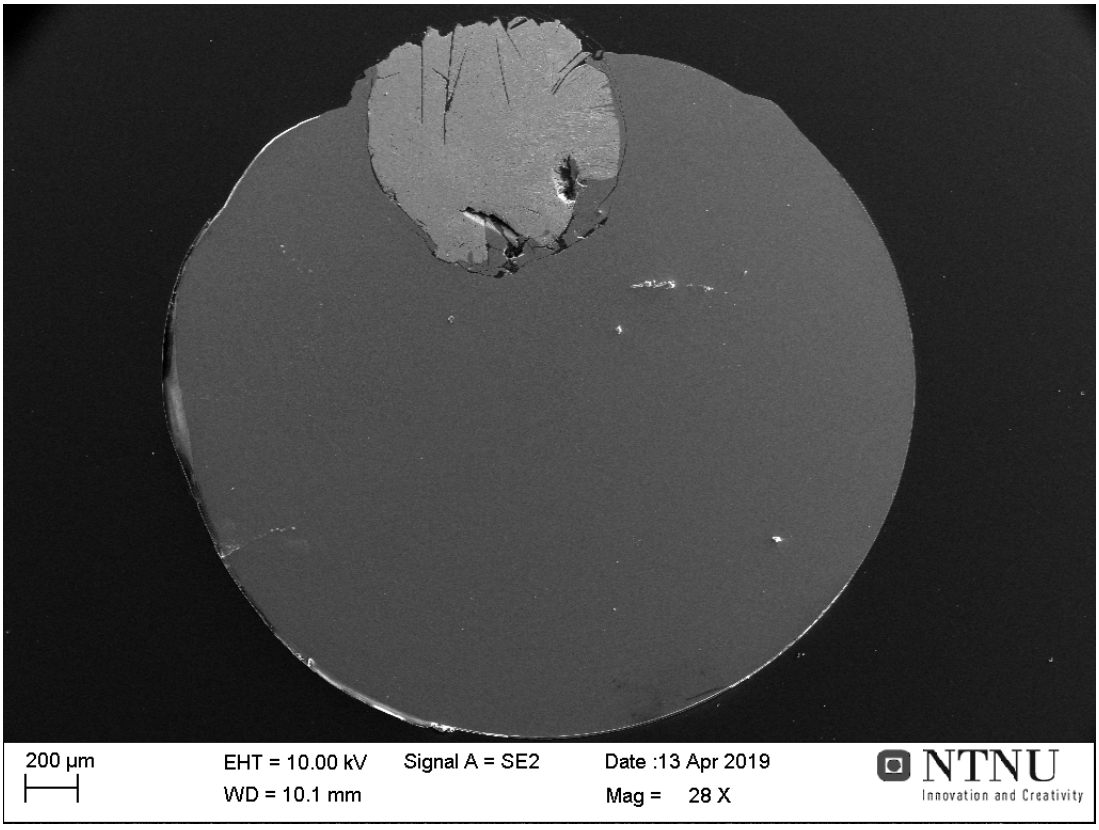

Figure 4.3.4.5: Image of sample 6 taken in SEM

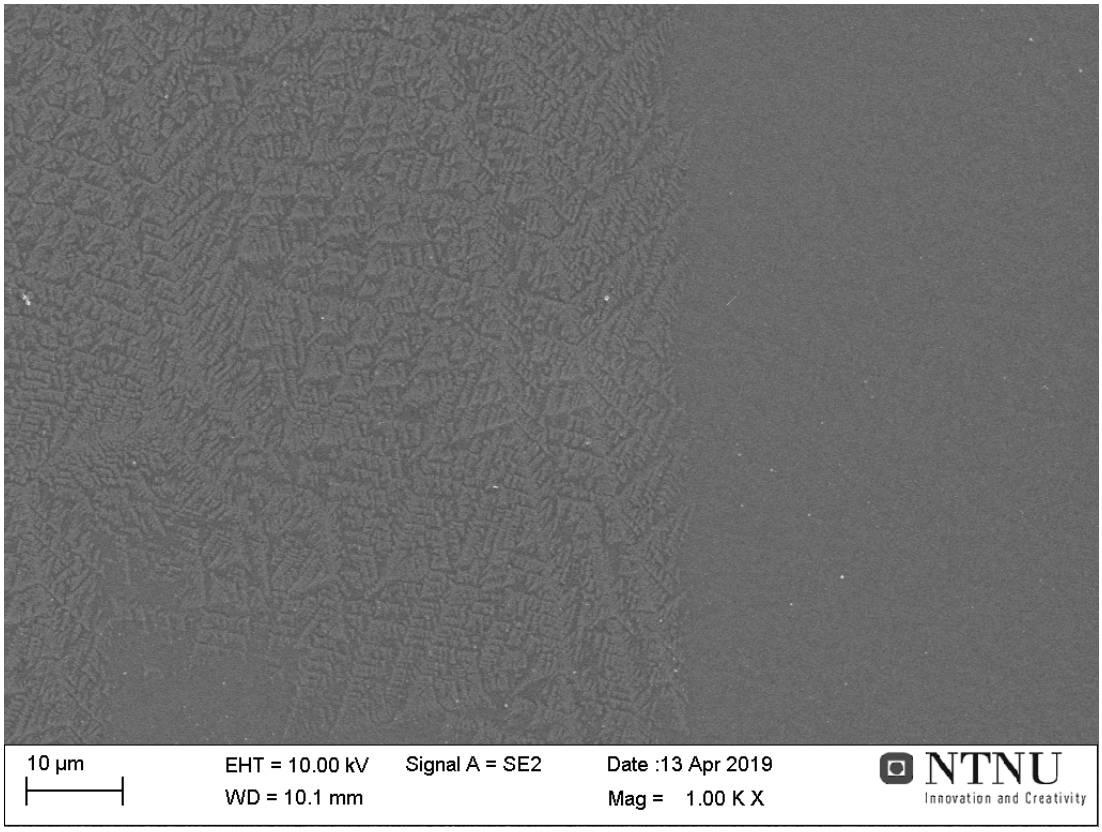

Figure 4.3.4.6: Details of sample 6, two-phase and glassy slag, magnified 1000 times

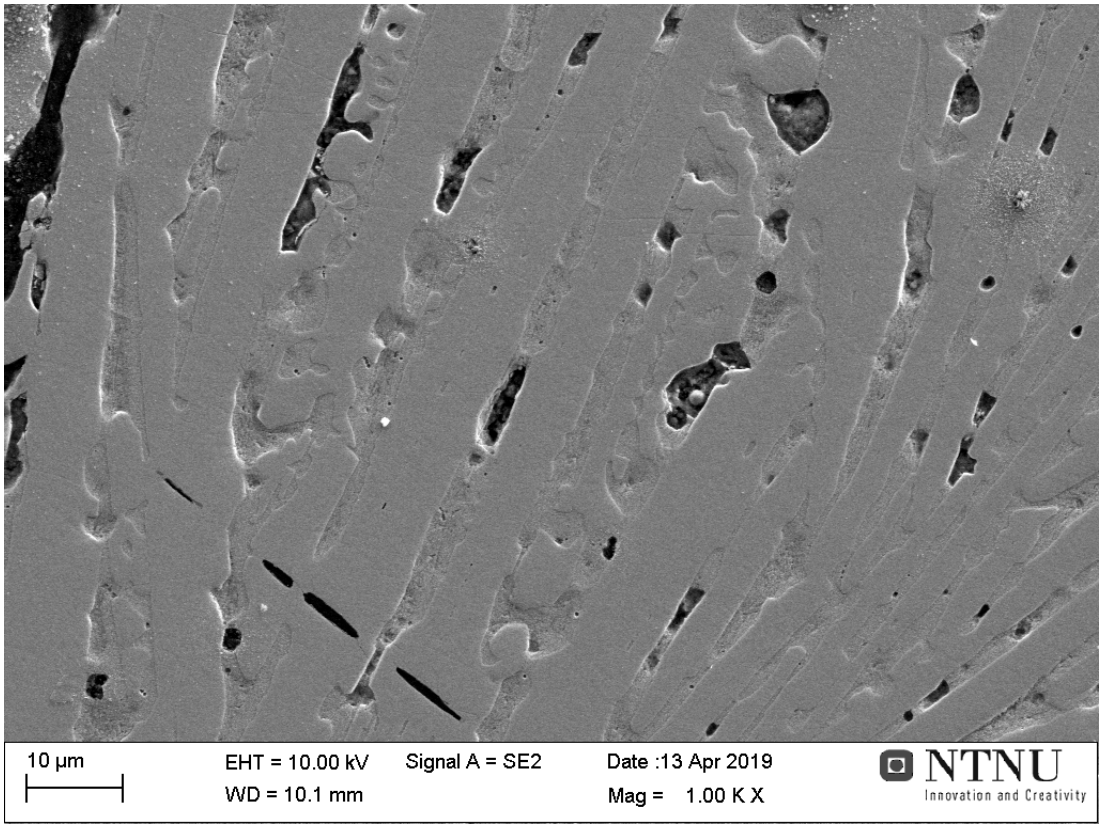

Figure 4.3.4.7: Details of metal droplet in sample 6 magnified 1000 times

Figure 4.3.4.8 shows an image taken of the coke pellet used in test 6 in SEM. The figure shows that the slag drop was located at the bottom right of the figure, and that the slag drop did not reduce much into the coke pellet. The rest of the pellet seems to be unaffected by the reduction.

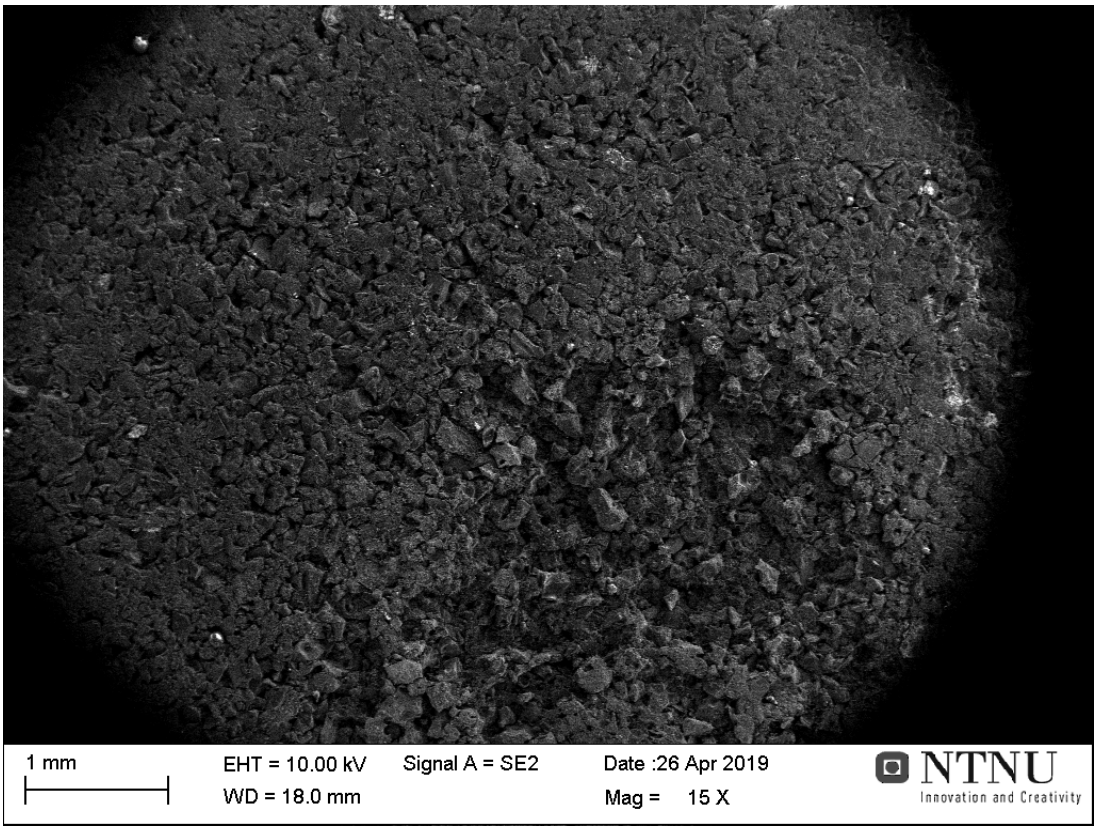

Figure 4.3.4.8: Image of coke pellet from test 6 taken in SEM

Table 4.3.4.1 lists the composition of the slag measured by SEM and EPMA and the composition of the metal calculated from the slag composition measured by SEM. The slag has high content of MnO, while the metal has very low content of silicon. The results from the SEM and EPMA analysis of the slag are similar, as is expected.

Table 4.3.4.1: Slag composition measured by SEM and EPMA for sample 6, and metal composition calculated from SEM results

Slag (measured)	**MnO**	**SiO_2**	**FeO**	**Al_2O_3**	**CaO**	**MgO**	**SO_3**
SEM [wt%]	38,20	33,70	0,05	9,60	12,48	3,71	2,26
EPMA [wt%]	38,92	35,19	0,15	8,72	12,70	3,45	1,53
Metal (calculated)	**Total**	**Mn**		**Si**		**Fe**	
[wt%]	100	61,94		5,60		32,46	
[g]	0,0141	0,0087		0,0008		0,0046	

Reduction degrees for test 6 are R_{Mn} = 0,267 and R_{Si} = 0,024

4.3.5 Test 7

The seventh test was run with coke pellet 7 and slag sample 1I, at 1600°C for 5 minutes. The slag drop acted a lot like in test 6, the slag melted at 1210°C, there was some activity at 1250°C, and the activity increased some as the temperature was increased, there was many bubbles and low volume expansion of the slag drop. There was also some activity through particle scattering at the sides of the slag drop.

Figure 4.3.5.1 shows some pictures taken during test 7. The pictures show the slag sample before heating at 25°C, after melting at 1210°C, as the furnace reaches 1600°C and after 5 minutes at 1600°C. The figure shows that the slag drop changes some during the test, and that there were some coke particles around the slag drop at the end of the test.

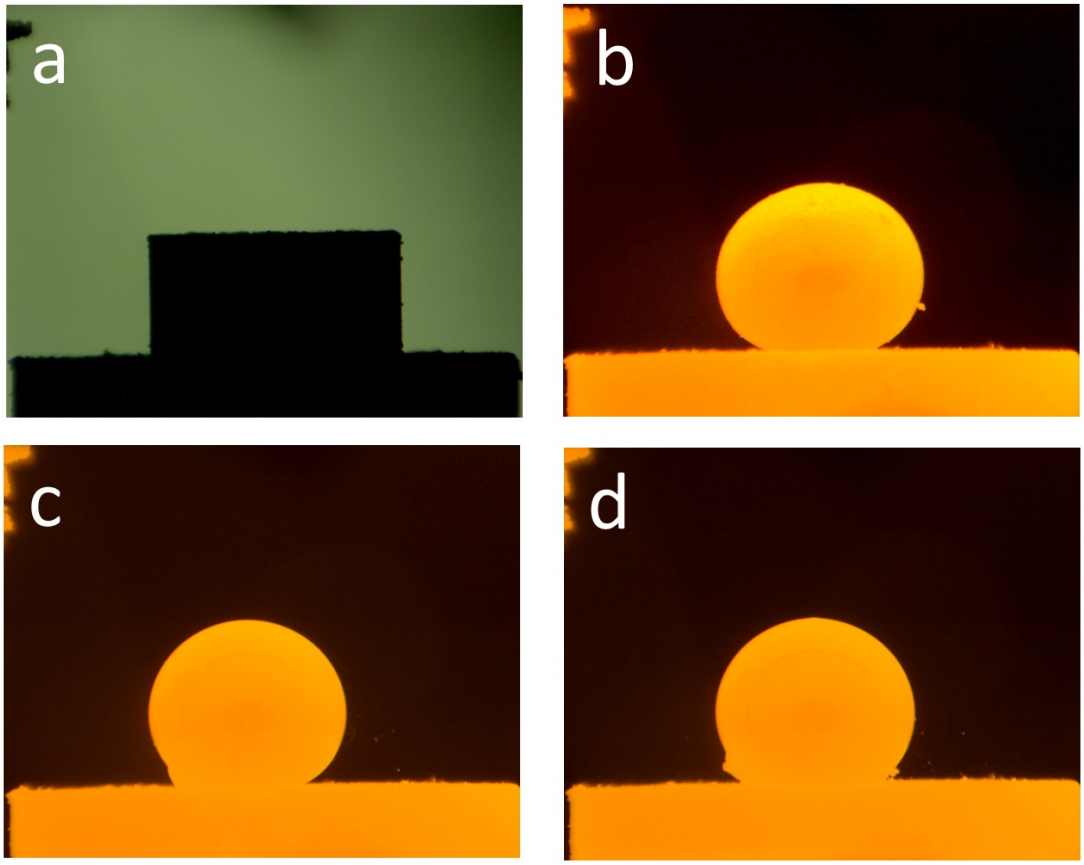

Figure 4.3.5.1: Pictures taken during test 7; a - before heating at 25°C; b - after melting at 1210°C; c - as furnace reaches 1600°C; d - after 5 minutes at 1600°C

Figure 4.3.5.2 shows pictures taken of the slag drop and coke pellet used in test 7 after the test was finished. The figure shows that the slag drop came loose after the test was finished. The slag drop is observed to have an orange transparent color at the top, and a pale non-transparent color at the bottom, in addition to having some visible metal droplets at the bottom of the slag drop.

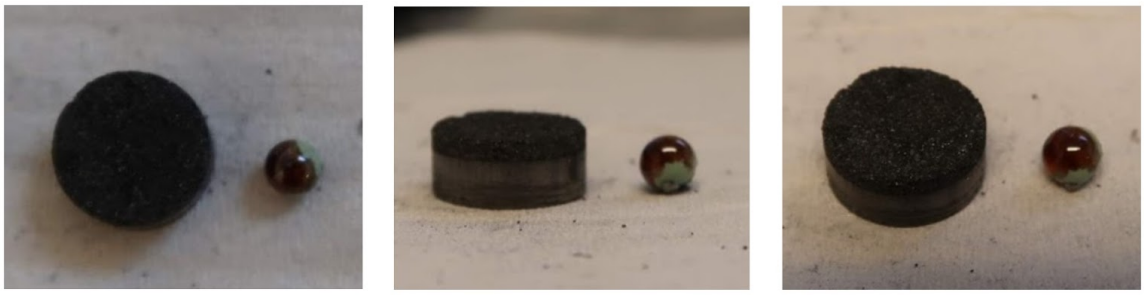

Figure 4.3.5.2: Pictures of slag drop and coke pellet from test 7

Figure 4.3.5.3 shows the development of contact angle and temperature of test 7, while figure 4.3.5.3 shows the development of relative volume and temperature of test 7. The figures show that the contact angle changes little during the test, and that the relative volume also changes little during the test, but has some fluctuations likely due to gas being trapped in the slag drop.

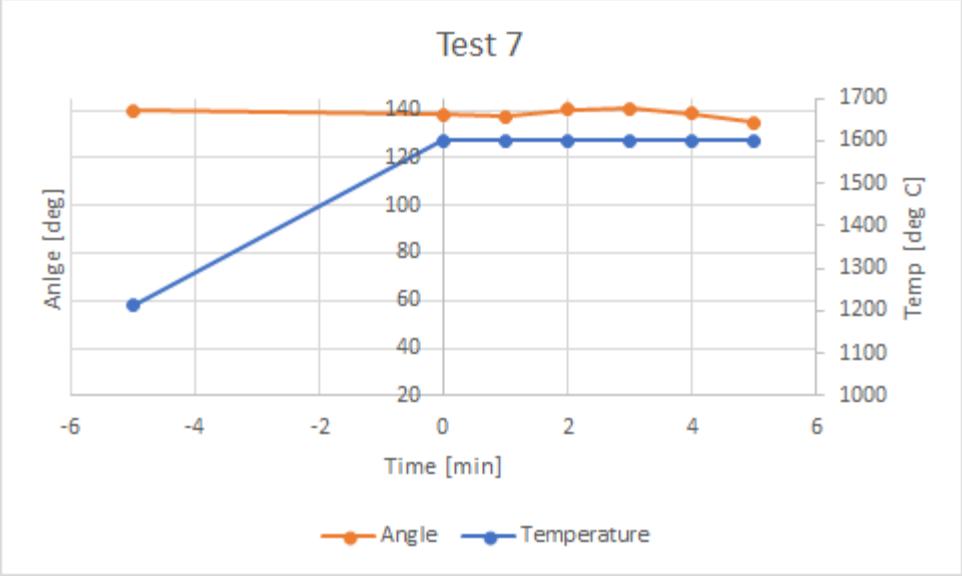

Figure 4.3.5.3: Contact angle and temperature development for test 7

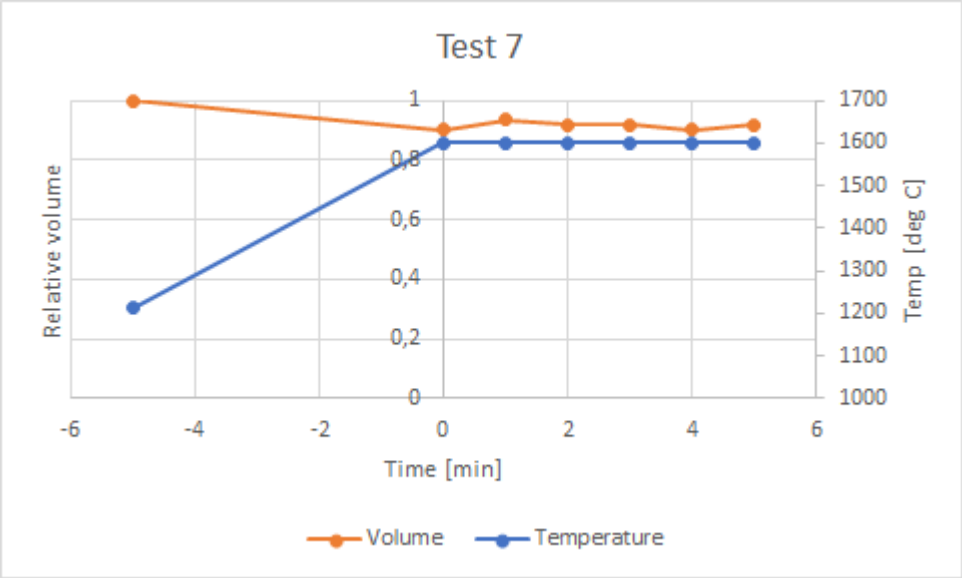

Figure 4.3.5.4: Relative volume and temperature development for test 7

Figure 4.3.5.5 shows an image taken in the SEM of sample 7. The figure shows that there are four metal droplets of considerable size, and that some coke particles can be made out at the upper side of the slag drop in the figure. Figure 4.3.5.6 and shows details of the two-phase slag magnified 1000 times. The figure show that the size and pattern of the slag varies in the sample. Figure 4.3.5.8 shows details of the glassy slag in the sample magnified 1000 times. Figure 4.3.5.9 shows details of a metal droplet, and shows that there is some structure at the surface of the slag.

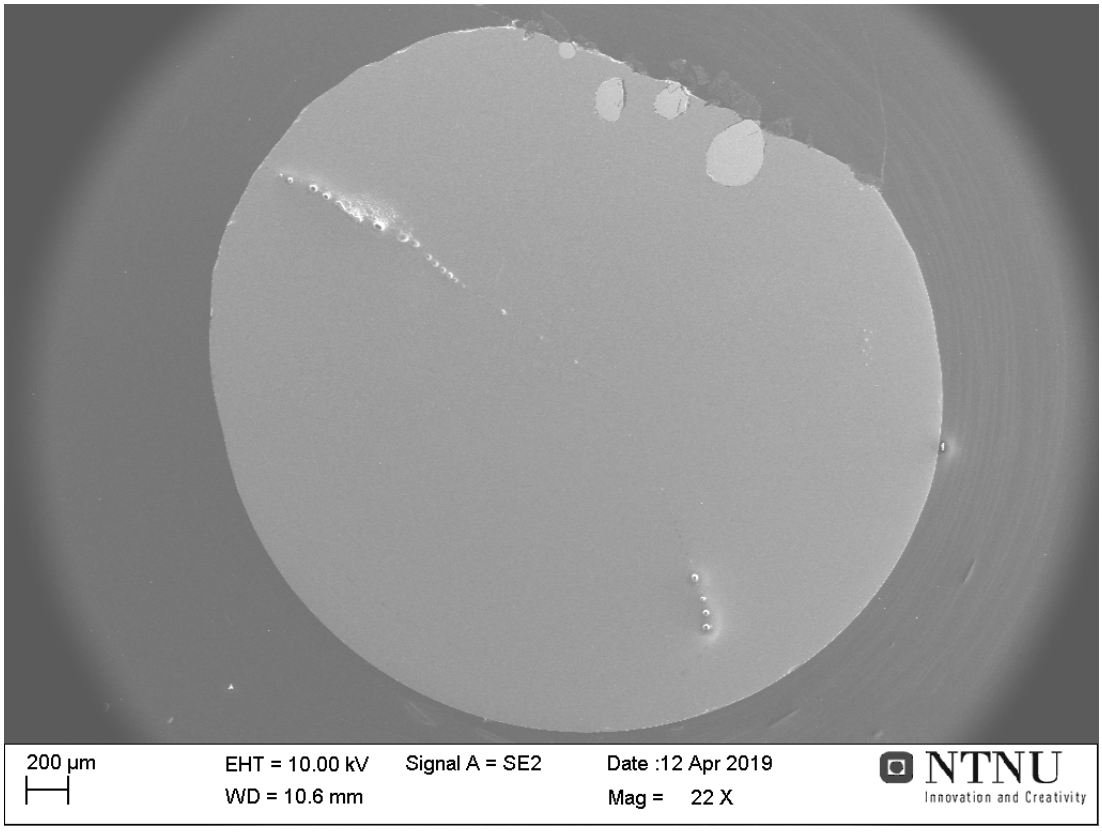

Figure 4.3.5.5: Image of sample 7 from SEM

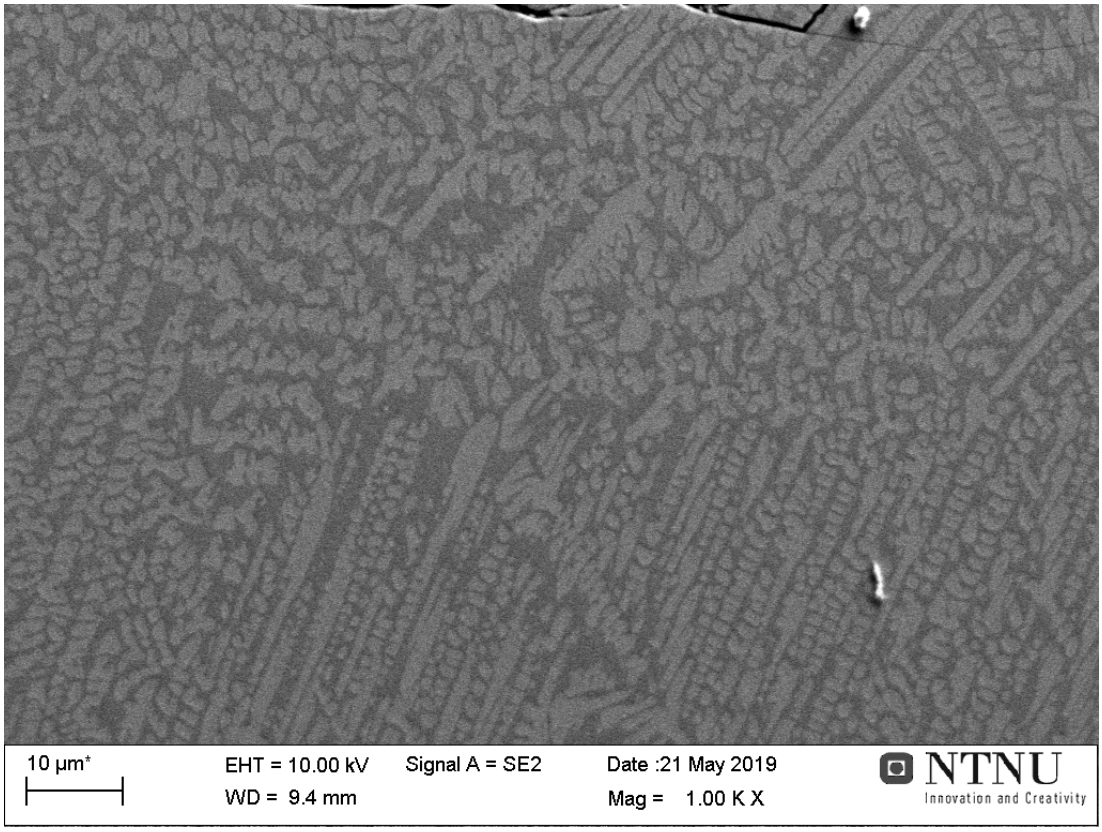

Figure 4.3.5.6: Two-phase slag of sample 7 magnified 1000 times

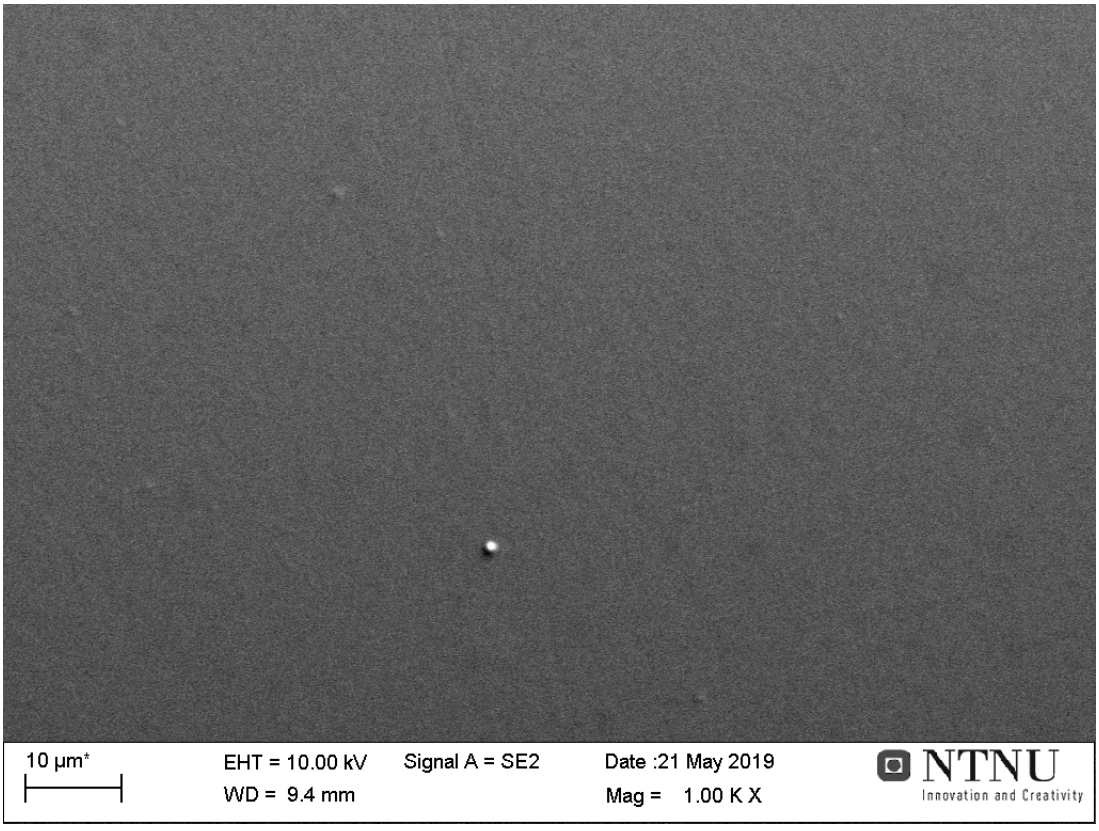

Figure 4.3.5.7: Details of glassy slag in sample 7 magnified 1000 times

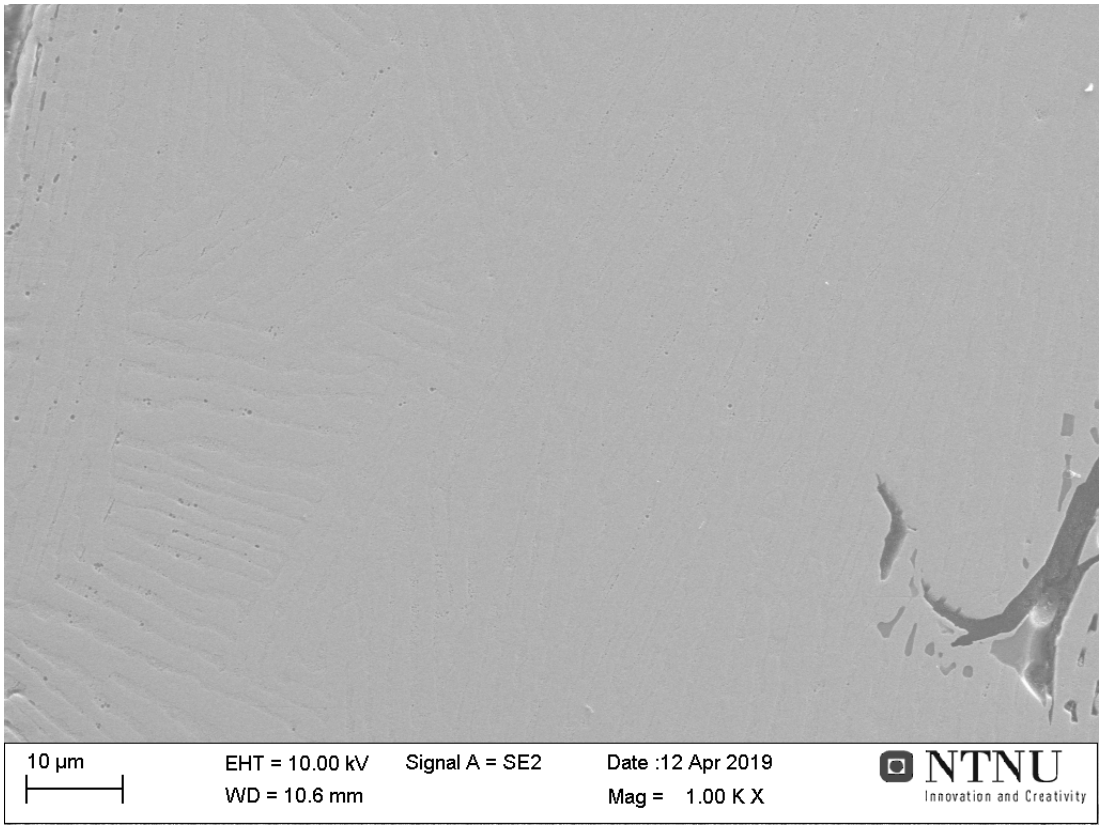

Figure 4.3.5.8: Details of metal in sample 7 magnified 1000 times

Figure 4.3.5.9 shows an image of the coke pellet used in test 7 taken in SEM. The figure shows that the slag drop was located at the lower right side in the figure, as the largest crater on the pellet is located here. The surrounding area is a bit structured, which could indicate that it has been affected during reduction, while the areas further away were not affected. There can be seen several small light spots on the surrounding area of the crater, when magnified, these spots resembled micro metal droplets. This could be a result of the activity at the sides of the slag drop that was observed for this test.

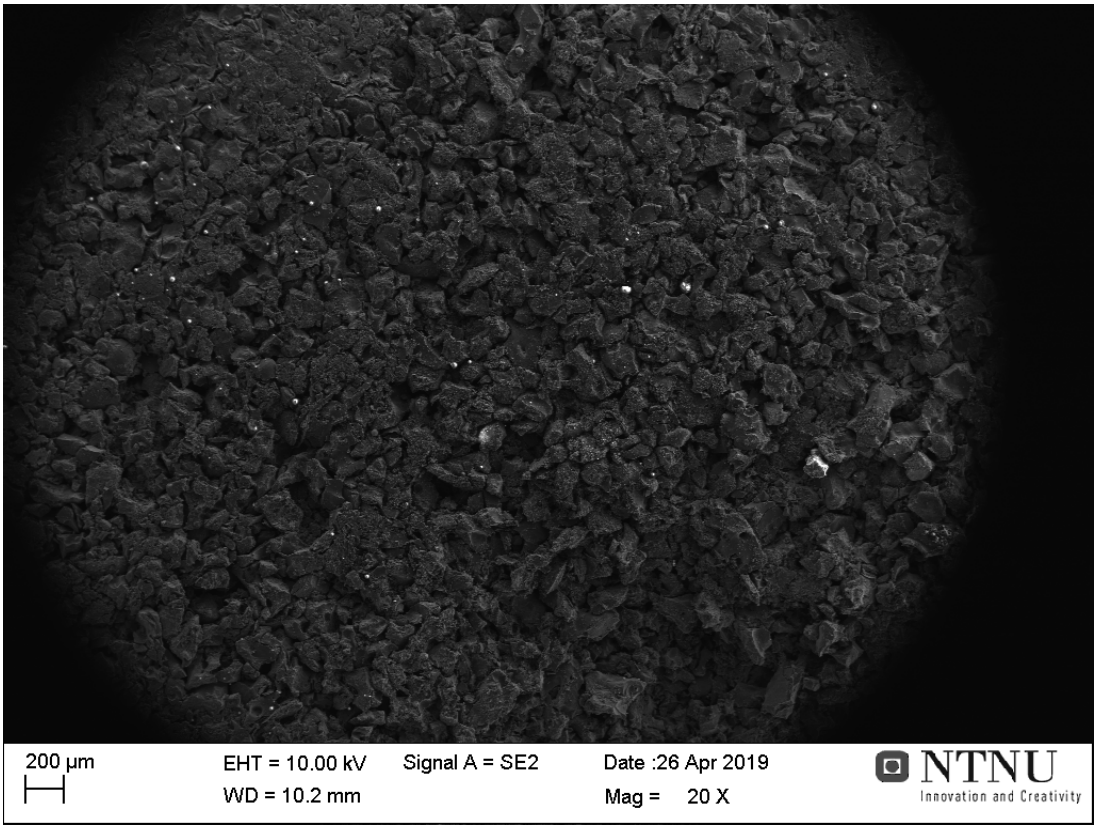

Figure 4.3.5.9: Image taken in SEM of coke pellet used in test 7

Table 4.3.5.1 lists the composition of the slag measured by SEM and EPMA, and the composition of the metal calculated from the slag composition measured by SEM. The MnO content in the slag is high, while the silicon content in the metal is low, and only half of the desired 18%. The results of SEM and EPMA analysis for the slag are similar, which is expected.

Table 4.3.5.1: Slag composition measured by SEM and EPMA for sample 7, and metal composition calculated from SEM results

Slag (measured)	**MnO**	**SiO_2**	**FeO**	**Al_2O_3**	**CaO**	**MgO**	**SO_3**
SEM [wt%]	40,29	32,23	0	9,69	12,18	3,54	2,06
EPMA [wt%]	39,92	34,56	0,15	8,69	12,56	3,35	1,44
Metal (calculated)	**Total**	**Mn**		**Si**		**Fe**	
[wt%]	100	53,94		9,10		35,96	
[g]	0,0135	0,00741		0,0012		0,0049	

Reduction degrees for test 7 are R_{Mn} = 0,215 and R_{Si} = 0,036

4.4 Test run with coke and slag 2

Test 14, 19, 12, 17, 22 and 13 were run with slag 2 towards coke. Table 4.4.1 shows the weight measurements of the slag pellet and charcoal pellet before the test, and the weight measurement of the slag and charcoal after the test, in addition to the weight loss.

Table 4.4.1: Weight measurement of tests run with coke and slag 2

	Time [min]	**Coke weight [g]**	**Slag weight [g]**	**Total weight before [g]**	**Weight after [g]**	**Weight loss [g]**	**Weight loss [%]**
14	30	0,1847	0,1002	0,2849	0,2116	0,0733	25,73
19	15	0,1842	0,1084	0,2926	0,2623	0,0303	10,36
12	5	0,1755	0,0952	0,2707	0,2454	0,0253	9,35
17	4	0,1823	0,1048	0,2871	0,2513	0,0358	12,47
22	2,5	0,1855	0,1021	0,2876	0,2371	0,0505	17,56
13	0	0,1786	0,0998	0,2784	0,2624	0,0160	5,75

The table shows that the test that had the highest reduction time has the highest percentage weight loss, as expected. The tests run for 2,5 and 4 minutes has the second and third highest weight loss, this was not expected. The tests run for 15 minutes and 5 minutes has almost the same weight loss, the difference between these two was expected to be higher. Test 13 that did not reach 13 minutes has a low weight loss as expected.

4.4.1 Test 14

The fourteenth test was run with coke pellet 11 and slag pellet 2D at 1600°C for 30 minutes. The coke pellet was observed to swell at around 450°C. The slag drop melted at 1202°C, and around 1250°C there was some activity with some bubbles and medium volume expansion, and small movements of the slag drop was observed. Around 1550°C some particle scattering around the slag drop was observed, and little bubbling. The amount of particle scattering increased some as hold temperature was reached, and the activity maintained the same level for the first 10 minutes, with some bubbles, low volume expansion, and particle scattering. Around 11 minutes the amount of particle scattering increased, while the amount of bubbles increased after 14 minutes at hold temperature. The volume expansion increased after 16 minutes, and the activity was high. The activity decreased after about 27 minutes at hold temperature. A lot of coke particles were observed at the slag drop surface at the end of test.

Figure 4.4.1.1 shows photographs captured from the furnace during test 14. The pictures shows the slag drop and coke pellet before heating, after the salg drop has melted, as the furnace temperature reaches 1600°C, and after 5, 15 and 30 minutes at 1600°C. The figure shows that the coke pellet changed during heating, that the slag drop changed contact angle during the test and that the slag drop had coke particles at the surface at the end of the test.

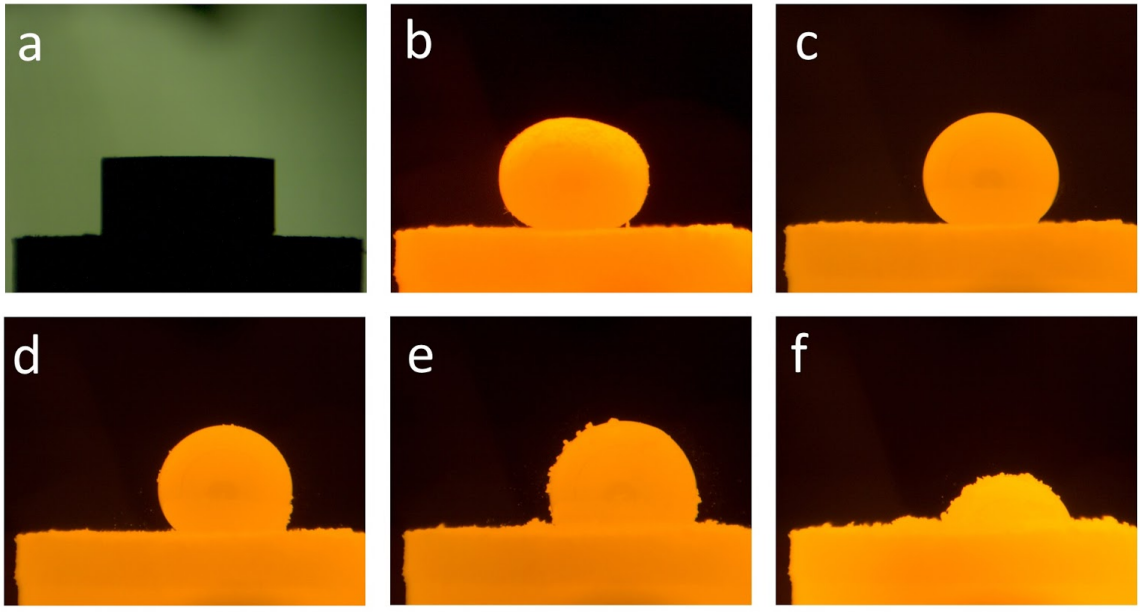

Figure 4.4.1.1: Photos taken during test 14; a - before heating, at 25°C; b - after melting at 1202°C; c - after furnace reaches 1600°C; d - after 5 minutes at 1600°C; e - after 15 minutes; f - after 30 minutes

Figure 4.4.1.2 shows pictures of the slag drop and coke pellet after test 14. The figure shows that the slag drop had a pale green non-transparent color after the test, and that there was quite a lot of coke particles at the slag drop surface.

Figure 4.4.1.2: Pictures of slag drop and coke pellet after test 14

Figure 4.4.1.3 shows the development of contact angle and temperature of test 14, while figure 4.4.1.4 shows the development of relative volume and temperature of test 14. The figures show that the contact angle decreases with time during the test, while the relative volume decreases some for the first 10 minutes, then increase likely due to gas being trapped in the slag drop at 15 minutes, before it decreases with time to the end of the test.

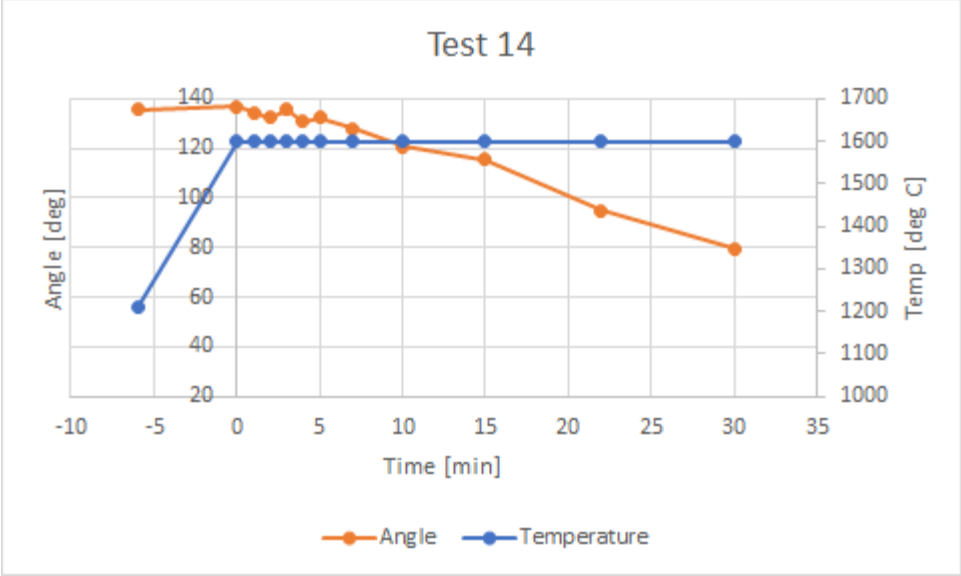

Figure 4.4.1.3: Contact angle and temperature development of test 14

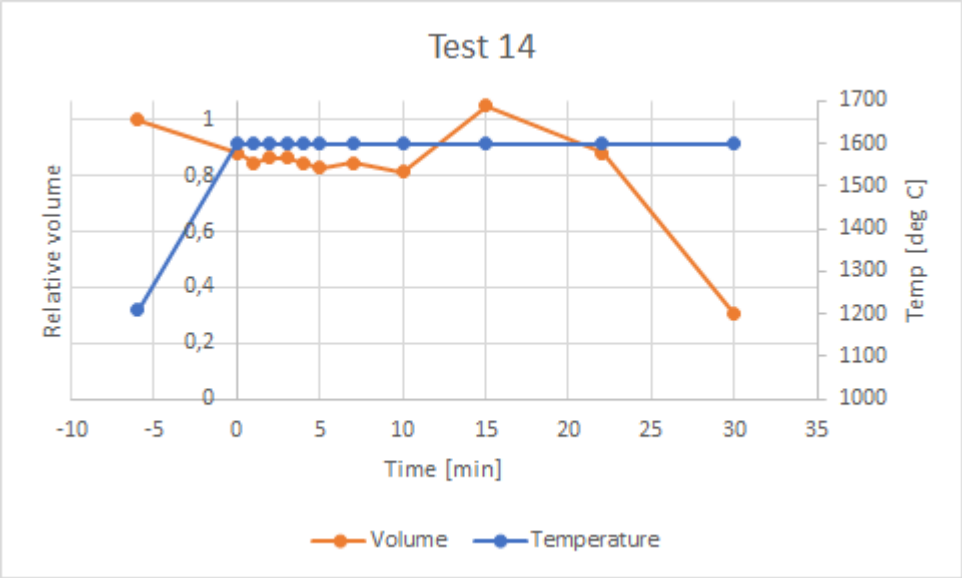

Figure 4.4.1.4: Relative volume and temperature development for test 14

Figure 4.4.1.5 shows an image of sample 14 taken in SEM. The figure shows that there are five metal droplets of considerable size at the sample surface. Figure 4.4.1.6 shows details of the slag phase magnified 1000 times, which shows that there are some contaminations on the surface and that the slag is glassy. Figure 4.4.1.7 shows details of the largest metal droplet magnified 1000 times, while sample 4.4.1.8 shows details of the metal drop at the bottom of figure 4.4.1.5 magnified 1000 times. The figures show that the metal droplets has a pattern in the surface, and that the pattern is larger in the large metal droplet.

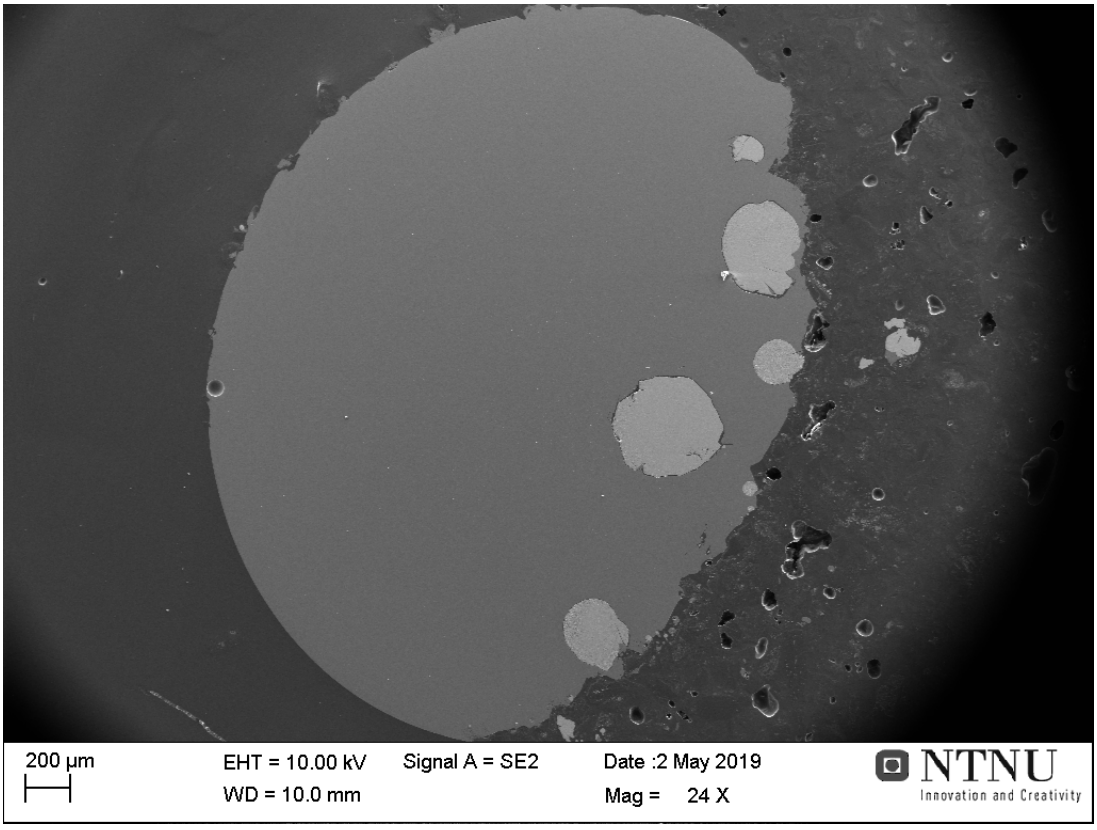

Figure 4.4.1.5: Image of sample 14 taken in SEM

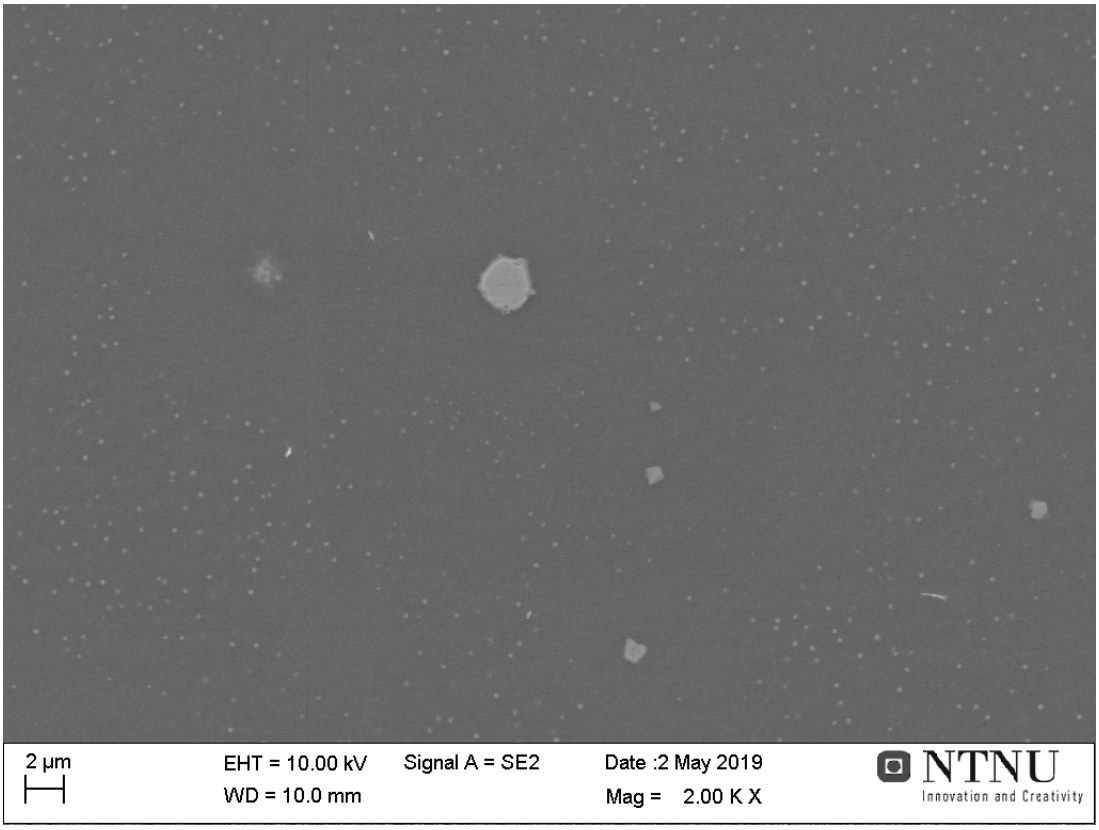

Figure 4.4.1.6: Slag phase of sample 14 magnified 2000 times

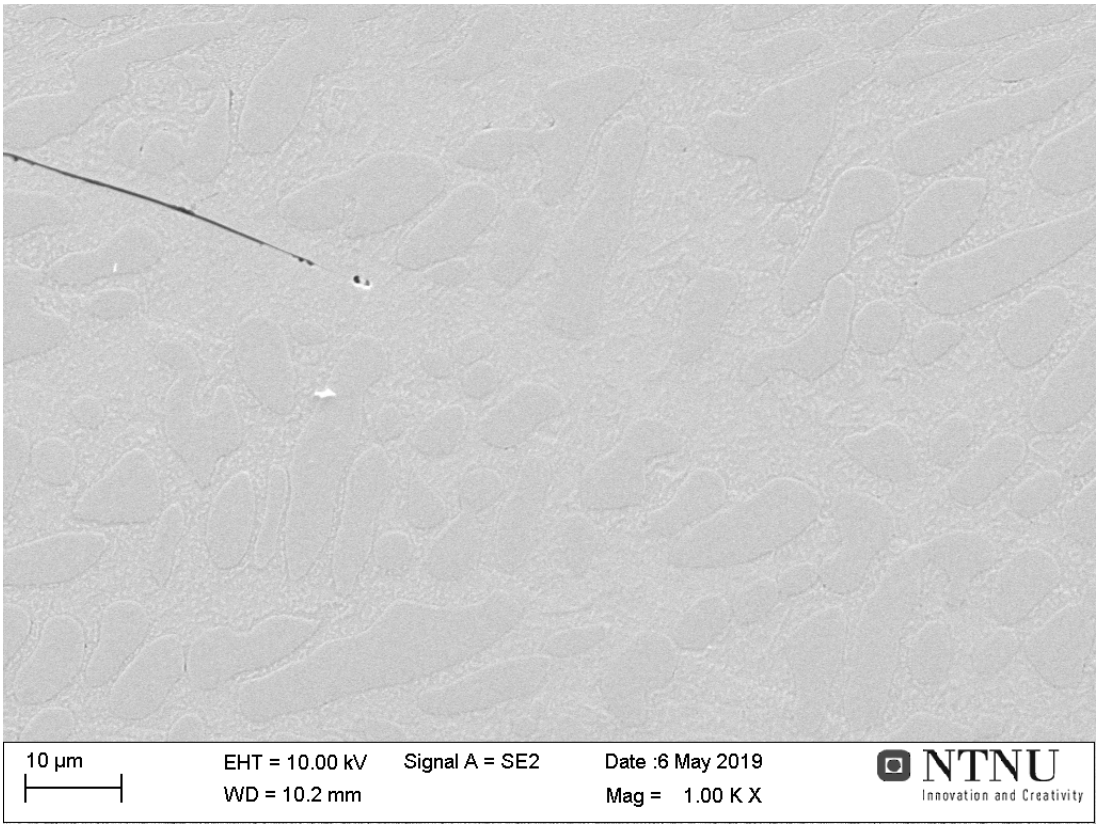

Figure 4.4.1.7: The largest metal droplet of sample 14 magnified 1000 times

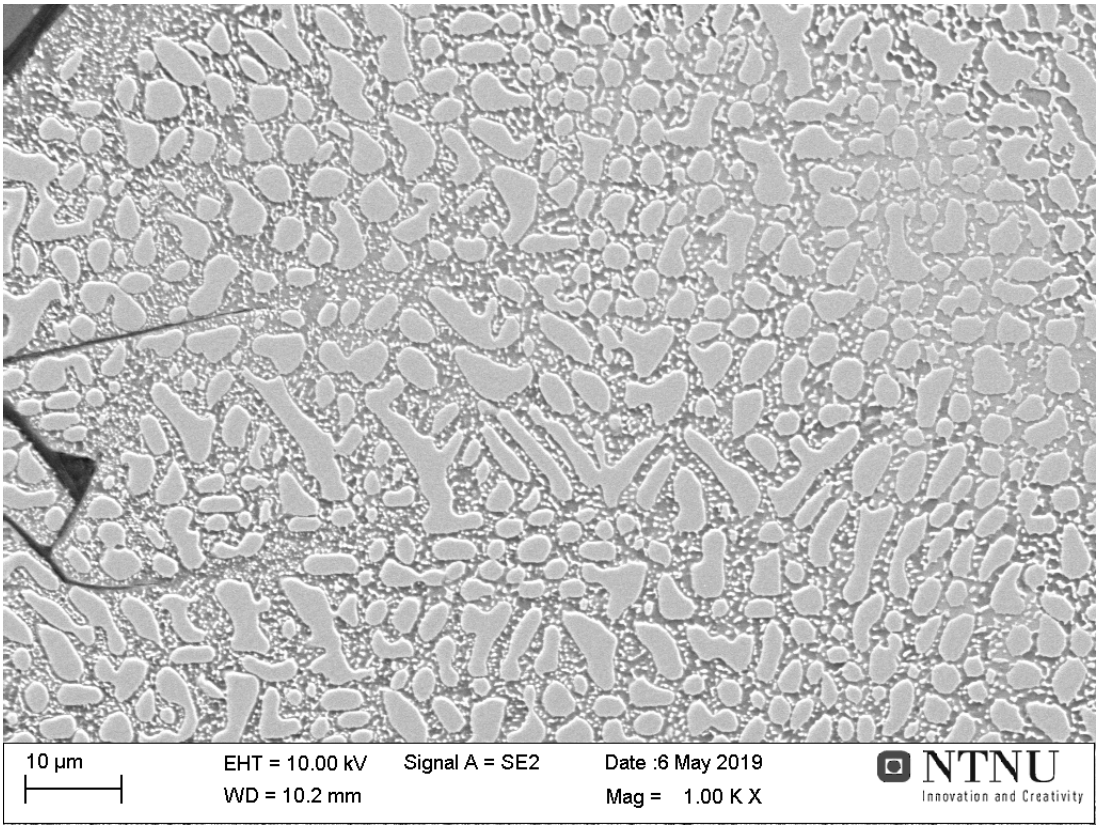

Figure 4.4.1.8: Smaller metal droplet in sample 14 magnified 1000 times

Table 4.4.1.1 lists the composition of the slag measured by SEM and EPMA, and the composition of the metal calculated from the slag composition measured by SEM. The MnO content in the slag is a higher than the desired 5%, while the silicon content in the metal is lower than the desired 18%. The results of the SEM and EPMA analysis of the slag are similar, as is expected.

Table 4.4.1.1: Slag composition measured by SEM and EPMA for sample 14, and metal composition calculated from SEM results

Slag (measured)	**MnO**	**SiO_2**	**FeO**	**Al_2O_3**	**CaO**	**MgO**	**SO_3**
SEM [wt%]	15,59	48,99	0	13,63	16,31	5,31	0,17
EPMA [wt%]	15,22	50,75	0,03	12,67	17,08	4,81	1,42
Metal (calculated)	**Total**	**Mn**		**Si**		**Fe**	
[wt%]	100	74,57		8,41		17,02	
[g]	0,0399	0,0298		0,0034		0,0068	

Reduction degrees for test 14 are R_{Mn} = 0,844 and R_{Si} = 0,095

4.4.2 Test 19

The nineteenth test was run with coke pellet 13 and slag sample 2I at 1600°C for 15 minutes. Around 400°C the coke pellet was observed to swell. The slag melted at 1201°C and the activity increased as the temperature was increased to 1300°C. The activity was then moderate until hold temperature was reached, the activity was then observed to increase through particle scattering and some bubbling. For the first 10 minutes at hold temperature there was little activity through bubbling and increasing activity through particle scattering. The slag drop was observed to have coke on the surface for the last part of the test.

Figure 4.4.2.1 shows some pictures captured from the furnace during test 19. The pictures show the slag drop and coke pellet before heating, after slag drop has melted, as the furnace temperature reaches 1600°C, and after 5 and 15 minutes at 1600°C. The figure shows that the coke pellet swell during heating, that the slag drop contact angle changed during the test, and that there was a lot of coke particles at the slag drop surface towards the end of the test.

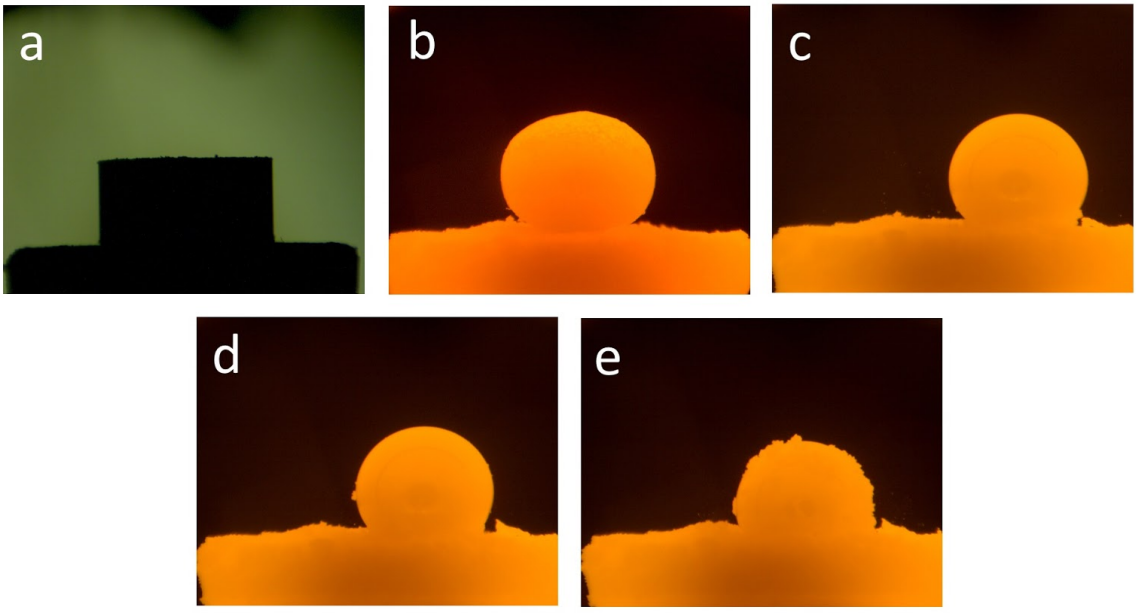

Figure 4.4.2.1: Pictures from test 19; a - before heating at 25°C; b - after melting at 1201°C; c - after furnace reached 1600°C; d - after 5 minutes at 1600°C; e - after 15 minutes

Figure 4.4.2.2 shows pictures taken of the slag drop and coke pellet after test 19. The figure shows that the coke pellet crumbled after the test, which made the slag drop loosen from the pellet. The slag drop had a transparent orange color as the figure shows, and there were some metal droplets at the bottom of the slag drop.

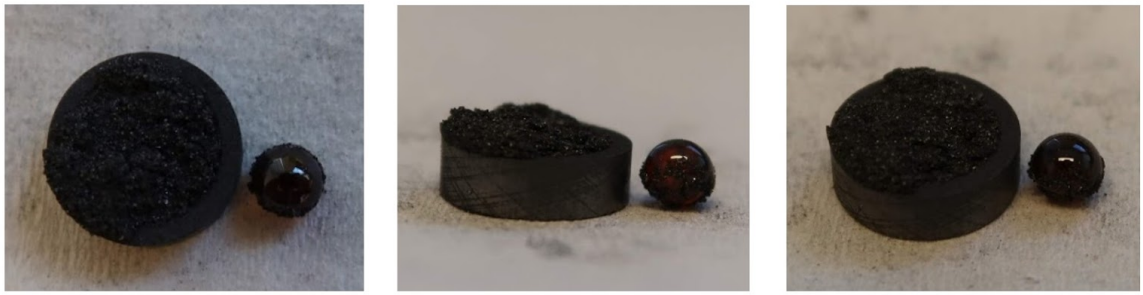

Figure 4.4.2.2: Pictures of slag drop and coke pellet after test 19

Figure 4.4.2.3 shows the development of contact angle and temperature for test 19, while figure 4.4.2.4 shows the development of relative volume and temperature for test 19. The figures show that the contact angle decreases moderately with time, and that the relative volume has a decreasing trend with time, and has some fluctuations likely caused by gas being trapped inside the slag drop.

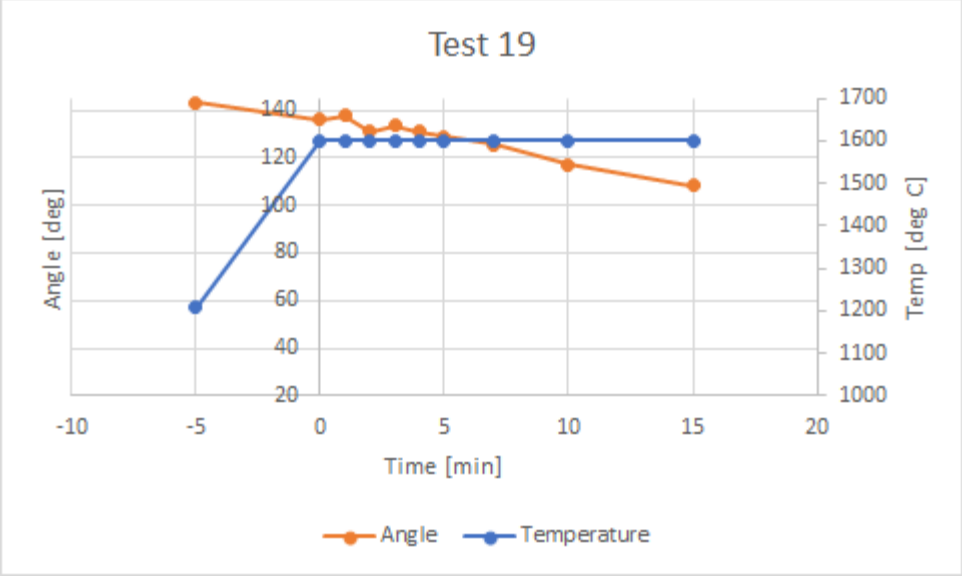

Figure 4.4.2.3: Contact angle and temperature development of test 19

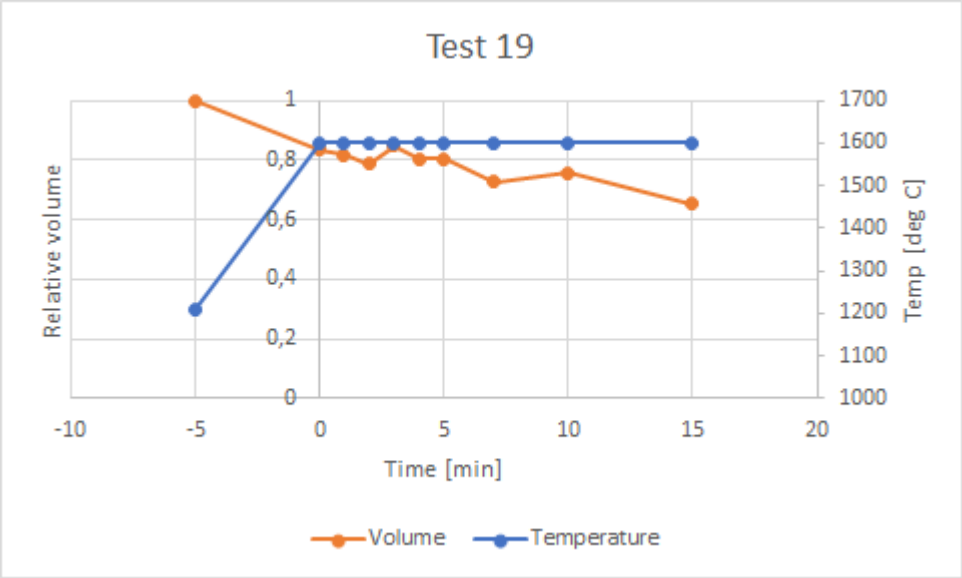

Figure 4.4.2.4: Relative volume and temperature development of test 19

Figure 4.4.2.5 shows an image of sample 19 taken in SEM. The figure shows that there are two metal droplets of considerable size in the sample. Figure 4.4.2.6 shows details of the slag in sample 19 magnified 2000 times, which shows that the slag is glassy. Figure 4.4.2.7 shows details of the larger metal droplet magnified 1000 times, which shows that the metal has a structured surface. The smaller metal droplet was observed to have smaller structure than the larger metal droplet.

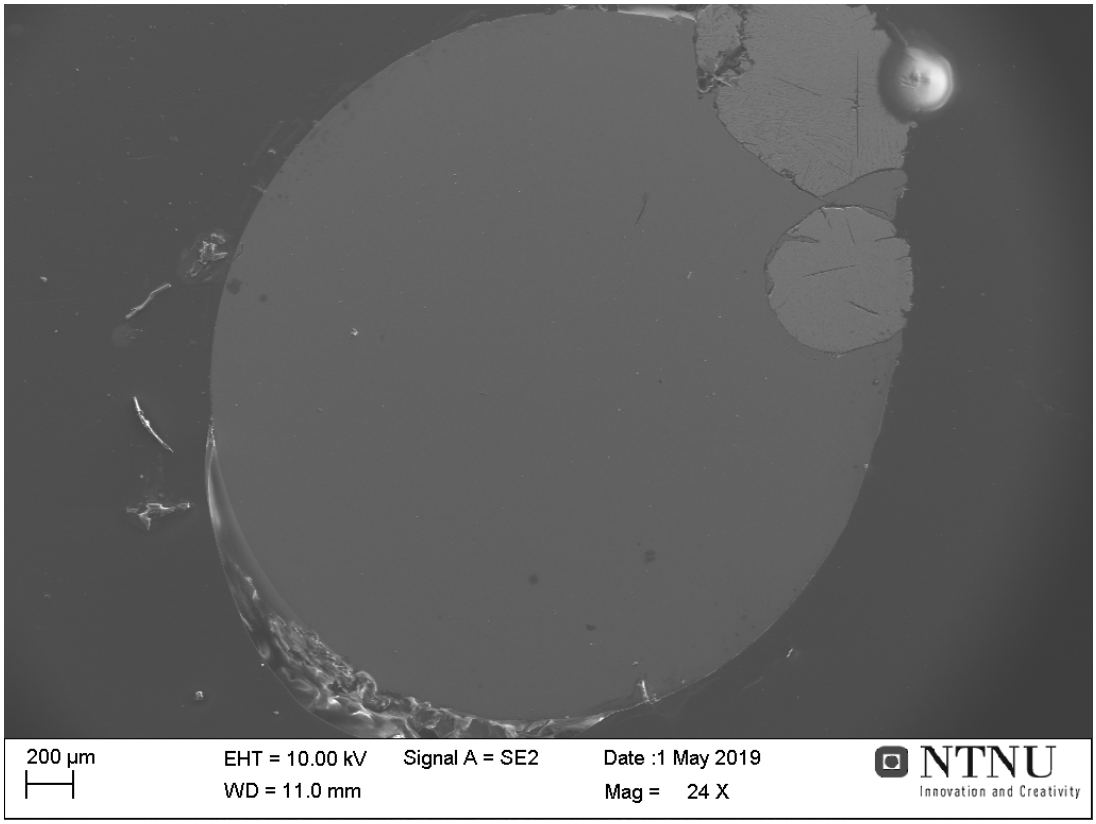

Figure 4.4.2.5: Image of sample 19 taken in SEM

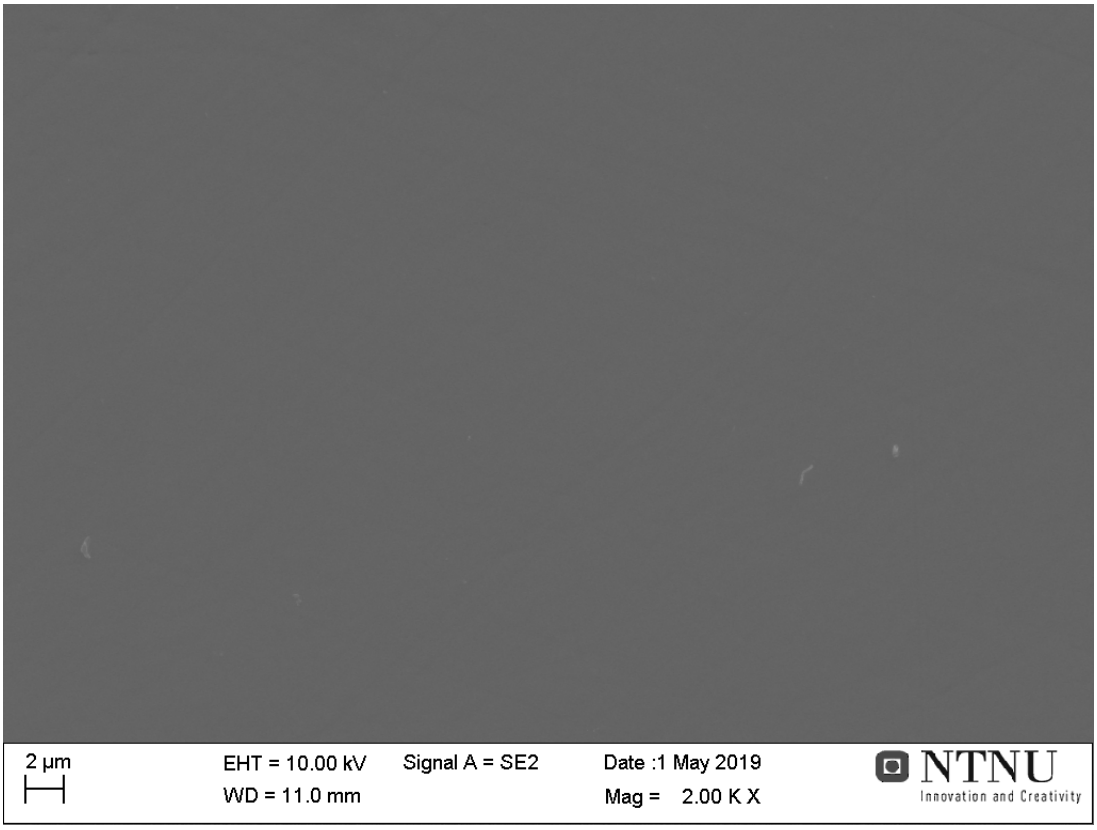

Figure 4.4.2.6: Details of the slag in sample 19 magnified 2000 times

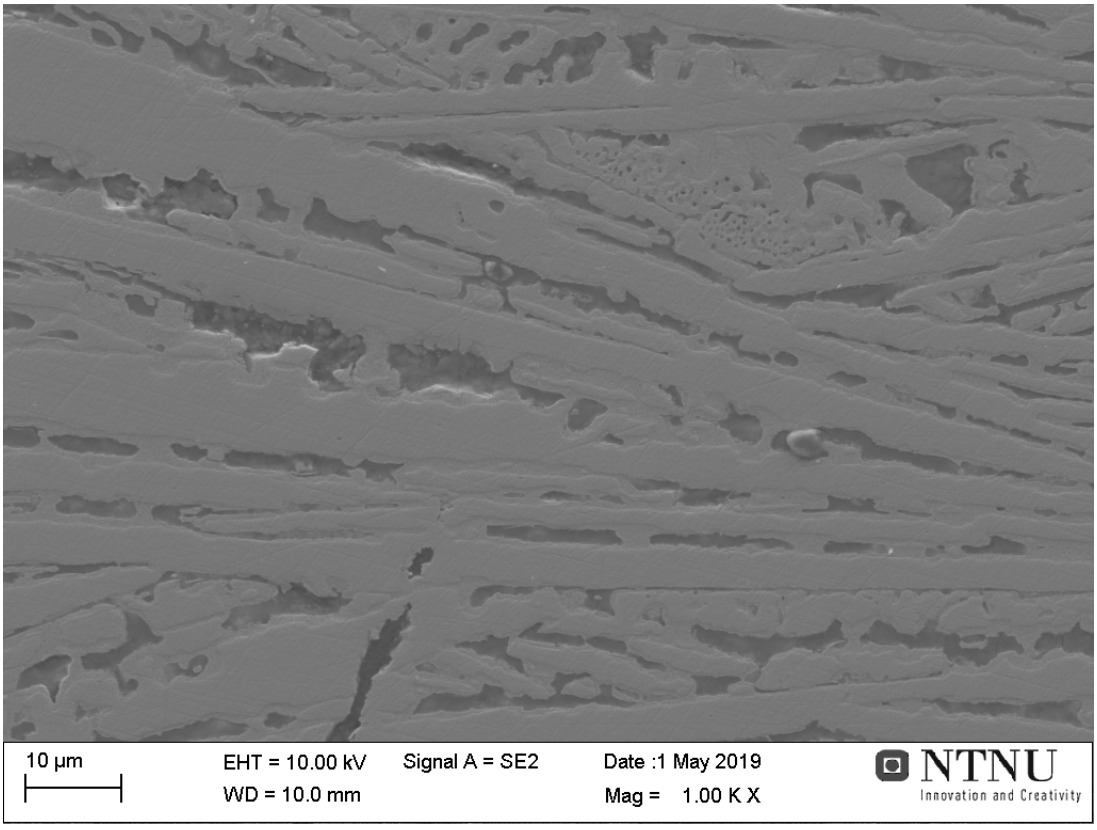

Figure 4.4.2.7: Details of metal in sample 19 magnified 1000 times

Table 4.4.2.1 lists the composition of the slag measured by SEM and EPMA, and the composition of the metal calculated from the slag composition measured by SEM. The content of MnO in the slag is high, while the silicon content in the metal is very low. The results of the SEM and EPMA analysis of the slag are similar, as is expected.

Table 4.4.2.1: Slag composition measured by SEM and EPMA for sample 19, and metal composition calculated from SEM results

Slag (measured)	**MnO**	**SiO_2**	**FeO**	**Al_2O_3**	**CaO**	**MgO**	**SO_3**
SEM [wt%]	37,60	40,01	0	8,31	10,65	3,43	0
EPMA [wt%]	37,27	40,54	0,13	7,44	10,49	2,98	1,83
Metal (calculated)	**Total**	**Mn**		**Si**		**Fe**	
[wt%]	100	66,74		1,77		31,49	
[g]	0,0233	0,0156		0,0004		0,0074	

Reduction degrees for test 19 are R_{Mn} = 0,408 and R_{Si} = 0,011

4.4.3 Test 12

The twelfth test was run with coke pellet 9 and slag sample 2B, at 1600°C for 5 minutes. The slag melted at 1204°C, and there was some activity at 1250°C. Around 1280°C the activity through bubbling was high. As the temperature was increased further there were more activity through particle scattering and less bubbling. The test was stopped after 5 minutes as the slag drop moved close to the edge of the coke pellet.

Figure 4.4.3.1 shows some photographs captured of the slag drop and coke pellet in the furnace. The pictures show the situation before heating, after the slag drop has melted, as the furnace temperature reaches 1600°C, and after 5 minutes at 1600°C. The figure shows that the coke pellet changed some during heating, and that the slag drop moved towards the edge of the coke pellet during the test.

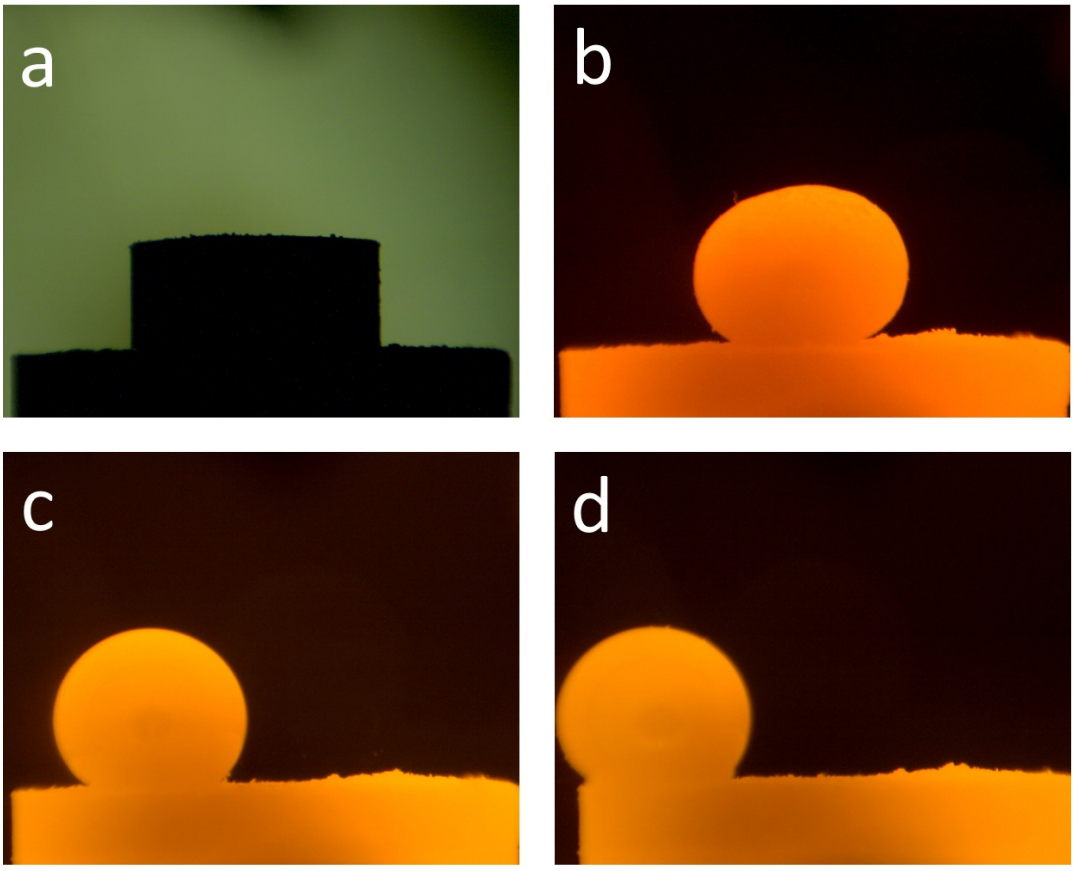

Figure 4.4.3.1: Pictures taken during test 12; a - before heating at 25°C; b - after melting at 1204°C; c - as furnace reaches 1600°C; d - after 5 minutes at 1600°C

Figure 4.4.3.2 shows pictures taken of the slag drop and coke pellet after test 12. The figure show that the coke was damaged on one side (right side in the pictures), which happened when the sample was wrapped and/or unwrapped and stored between the test and the weighing. The figure further shows that the slag drop had an orange transparent color on the top and a pale green color on the bottom, in addition to some visible metal droplets at the bottom of the slag drop.

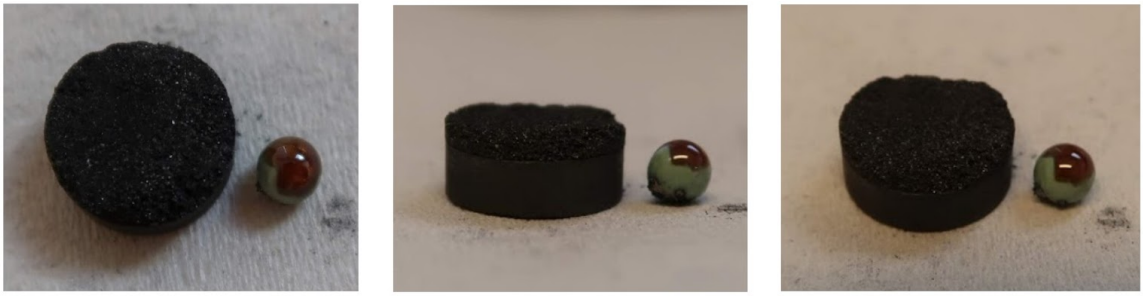

Figure 4.4.3.2: Pictures of slag drop and coke pellet after test 12

Figure 4.4.3.3 shows the development of contact angle and temperature for test 12, while figure 4.4.3.4 shows the development of relative volume and temperature for test 12. The figures show that the contact angle changes little during the test, and that the relative volume decreases some during the test.

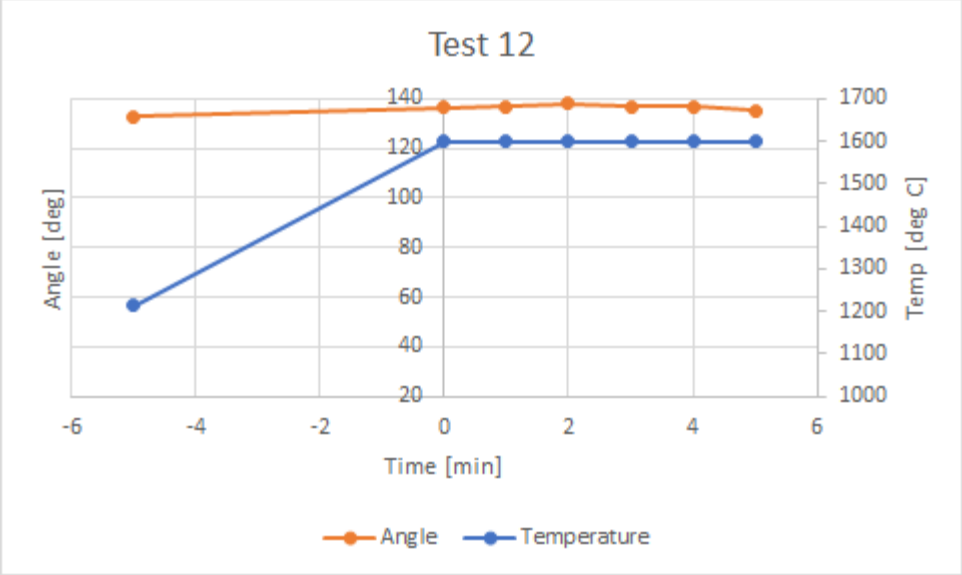

Figure 4.4.3.3: Contact angle and temperature development of test 12

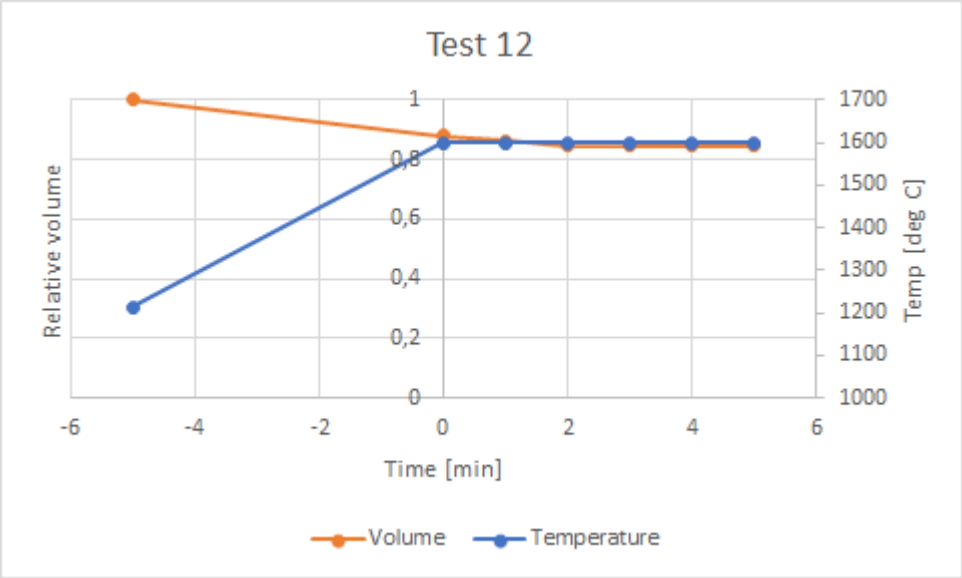

Figure 4.4.3.4: Relative volume and temperature development for test 12

Figure 4.4.3.5 shows an image of sample 12 taken in SEM. The sample has two metal droplets of considerable size. Figure 4.4.3.6 shows details of the slag phase magnified 1000 times, while figure 4.4.3.7 shows an overview of the two-phase slag magnified 215 times. The figures show that the size and pattern of the slag varies in the sample. Figure 4.4.3.8 shows the glassy slag in sample 12 magnified 1000 times. Figure 4.4.3.9 shows details of the large metal droplet in the sample magnified 1000 times. The figure shows that there is some structure at the surface of the metal.

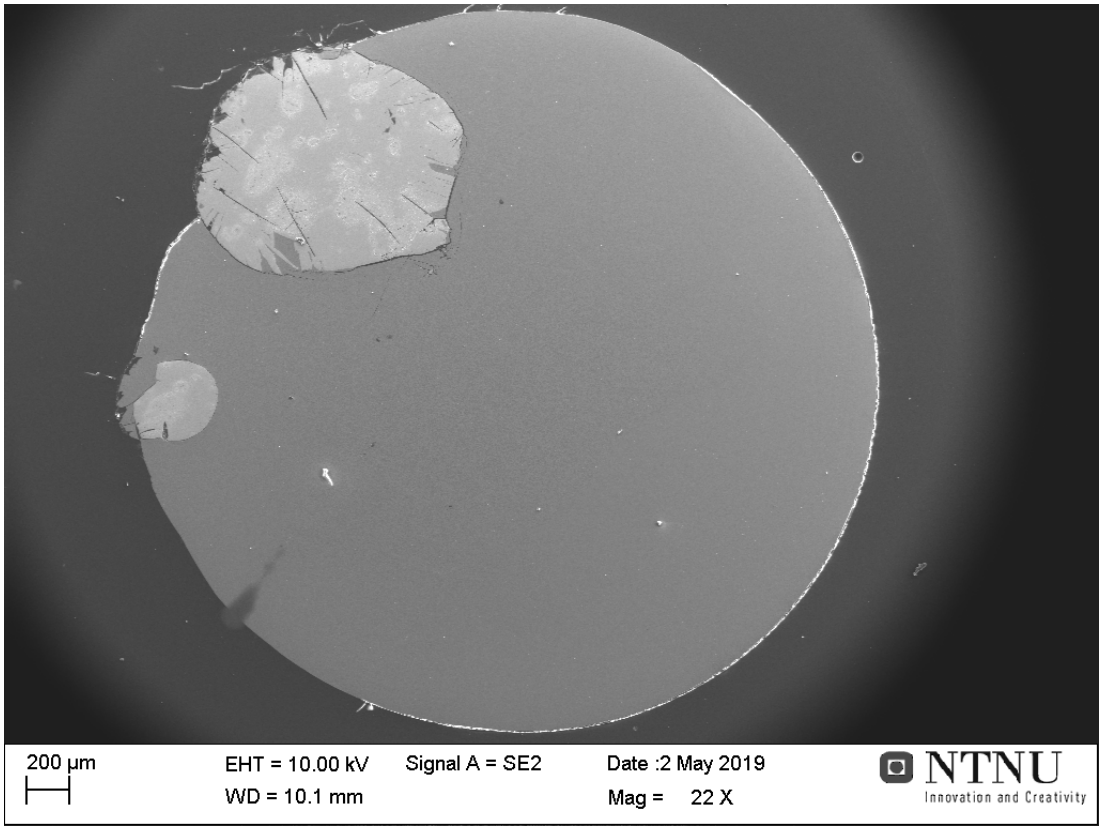

Figure 4.4.3.5: Image of sample 12 captures in SEM

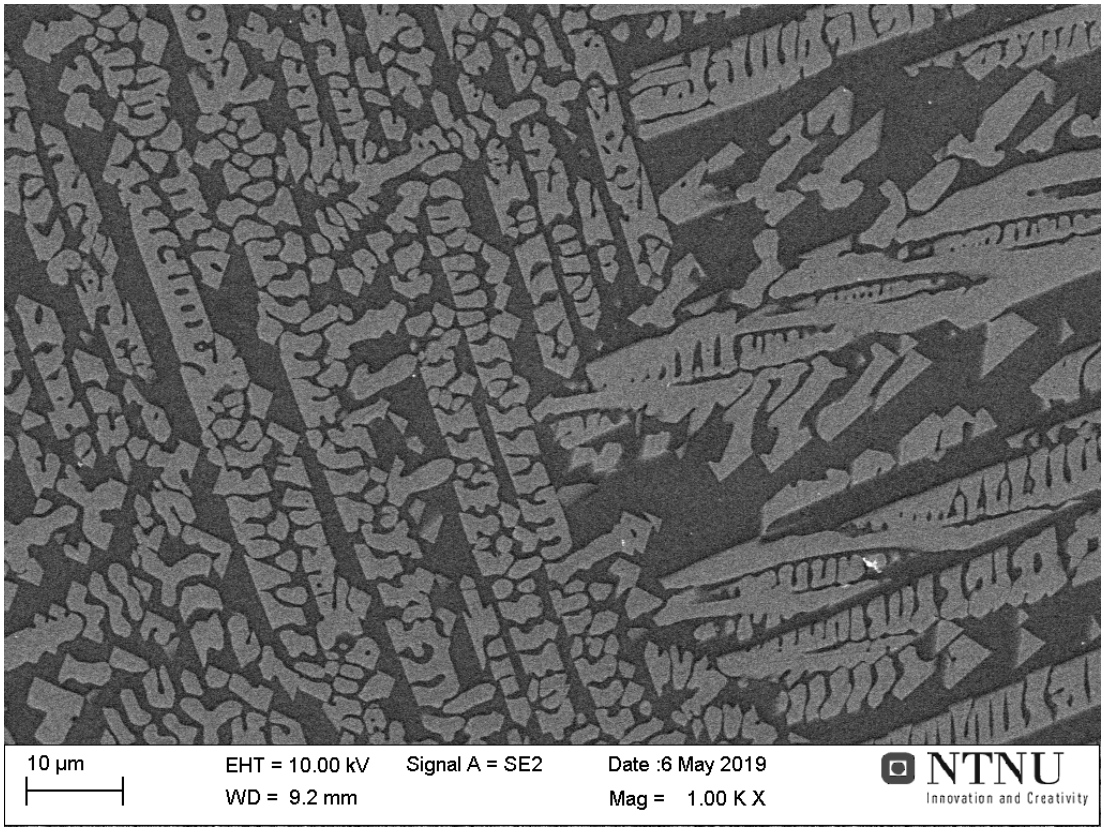

Figure 4.4.3.6: Details of slag phase of sample 12 magnified 1000 times

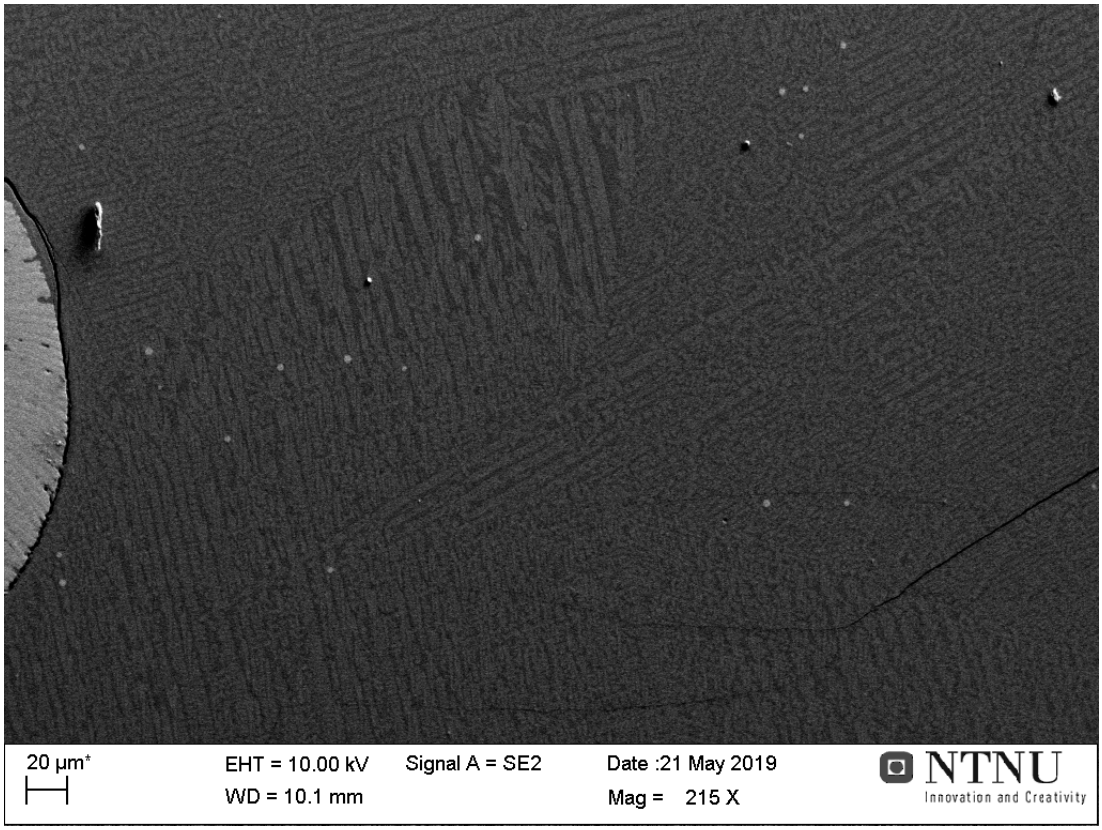

Figure 4.4.3.7: Details of slag phase of sample 12 magnified 215 times

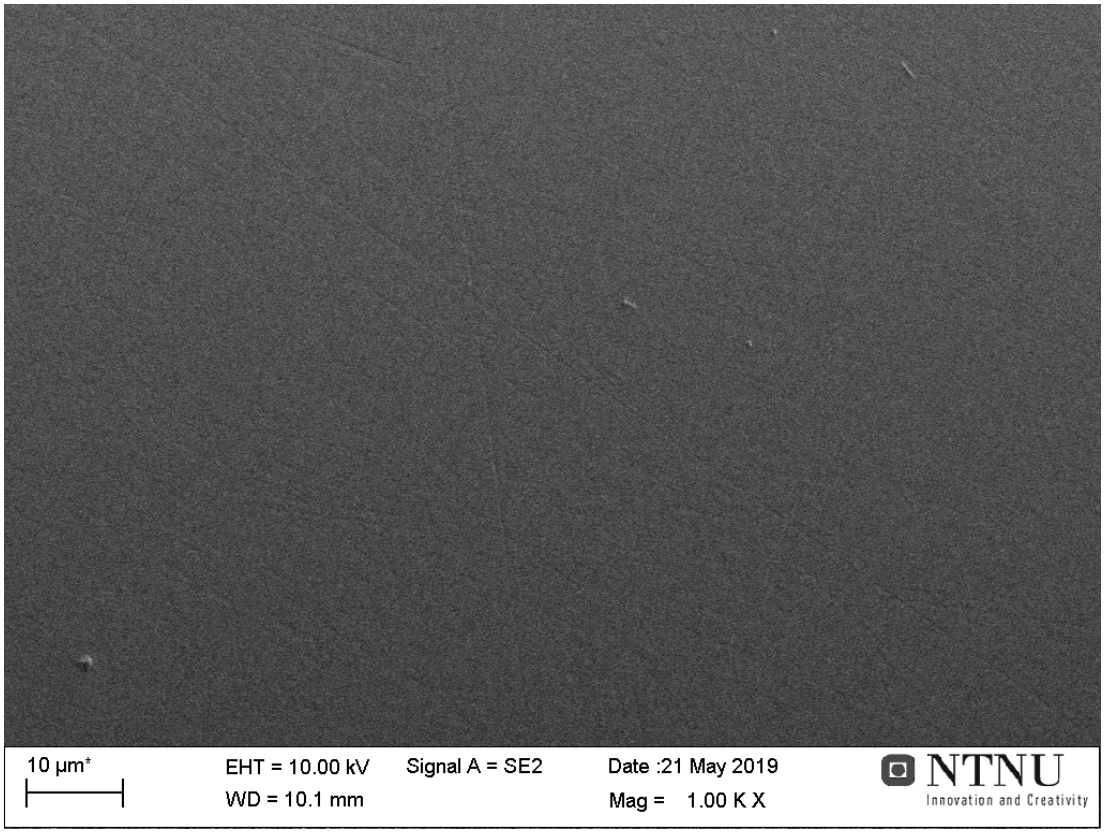

Figure 4.4.3.8: Details of glassy slag of sample 12 magnified 1000 times

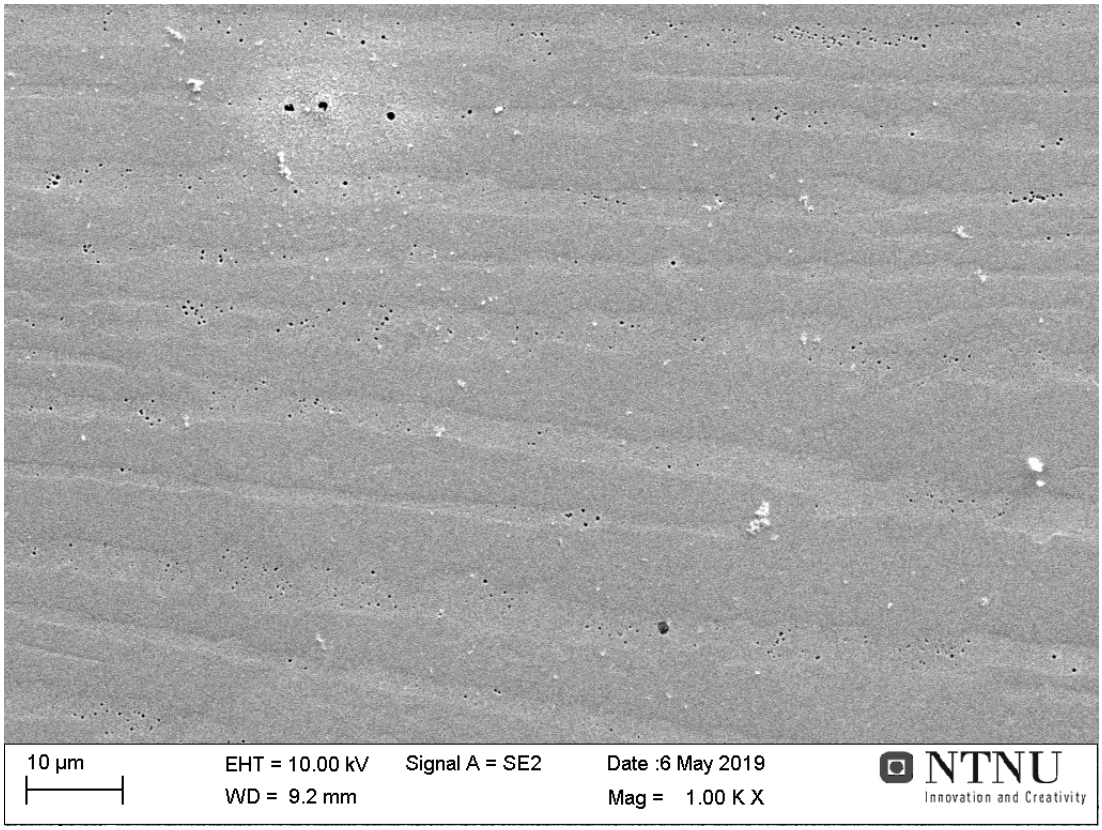

Figure 4.4.3.9: Details of the large metal droplet in sample 12 magnified 1000 times

Figure 4.4.3.10 shows an image of the coke pellet from test 12 taken in SEM. The figure shows a crater at the upper left side where the slag drop was located. There is also structure in the right upper side, which indicates that the slag drop moved some or affected this side some other way during reduction. The lower side of the coke pellet is unaffected.

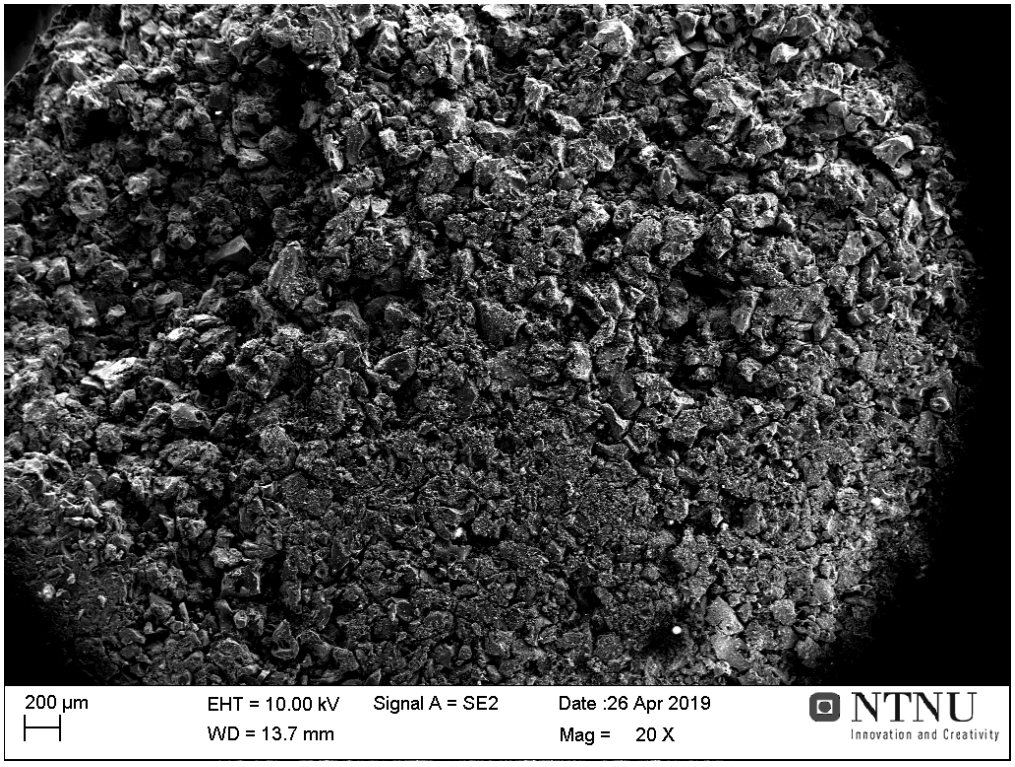

Figure 4.4.3.10: Image of coke sample used in test 12 taken in SEM

Table 4.4.3.1 lists the composition of the slag measured by SEM and EPMA, and the composition of the metal calculated from the slag composition measured by SEM. The MnO content of the slag is high, while the calculated silicon content in the metal is negative, which is not possible. The results of the SEM and EPMA analysis are similar, as is expected.

Table 4.4.3.1: Slag composition measured by SEM and EPMA for sample 12, and metal composition calculated from SEM results

Slag (measured)	**MnO**	**SiO_2**	**FeO**	**Al_2O_3**	**CaO**	**MgO**	**SO_3**
SEM [wt%]	47,66	33,95	0	7,13	8,73	2,54	0
EPMA	44,75	36,24	0,18	6,79	9,48	2,51	1,63
Metal (calculated)	**Total**	**Mn**		**Si**		**Fe**	
[wt%]	100	31,26		-0,63		69,37	
[g]	0,0093	0,0029		-0,00006		0,0065	

Reduction degrees for test 12 are R_{Mn} = 0,087 and R_{Si} = -0,002. The calculated negative silicon content in the metal gives a negative reduction degree for silicon.

4.4.4 Test 17

The seventeenth test was run with coke pellet 12 and slag sample 2G at 1600°C for 4 minutes. Around 400°C, the coke pellet was observed to swell. The slag melted at 1208°C, and there was little activity until 1250°C. Around 1300°C the activity increased, and there were many bubbles with low volume expansion. As hold temperature was reached, there were more activity through particle scattering and less activity through bubbling. The test was stopped after four minutes as the slag drop moved close to the edge of the coke pellet.

Figure 4.4.4.1 shows some photographs captured from the furnace during test 17. The pictures show the slag sample and coke pellet before heating, after the slag sample has melted, as the furnace temperature reached 1600°C, and right before the test was stopped after 4 minutes at 1600°C. The figure shows that the coke pellet swelled during heating, which resulted in an uneven surface of the coke pellet. It also shows that the slag drop moved during the test, and that the contact angle changed some during the test.

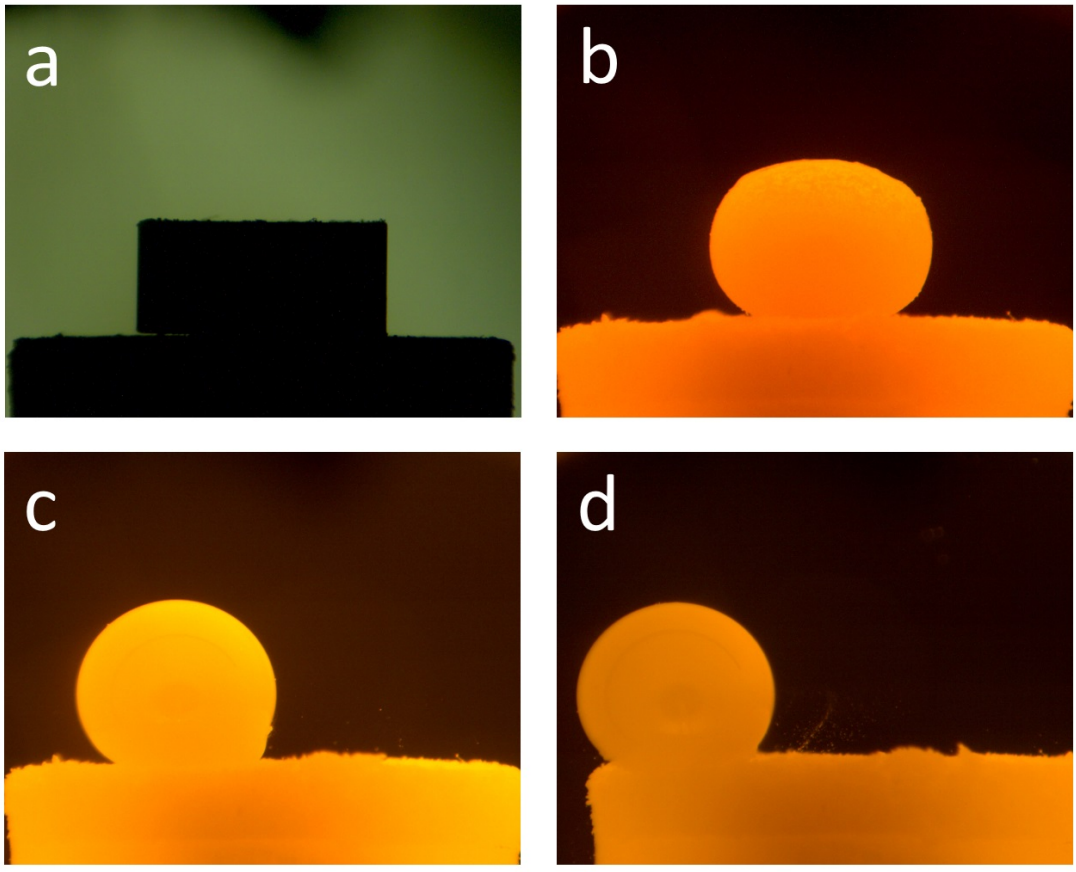

Figure 4.4.4.1: Pictures from test 17; a - before heating at 25°C; b - after melting at 1208°C; c - as furnace reaches 1600°C; d - after 4 minutes at 1600°C

Figure 4.4.4.2 shows pictures taken of the slag drop and coke pellet after test 17. The slag drop and was attached to the coke pellet after the test, but as the figure shows, the slag drop came loose as the coke pellet crumbled during wrapping and/or storage. The figure shows that the slag drop had a pale green non-transparent color, with a clear metal drop at the bottom of it.

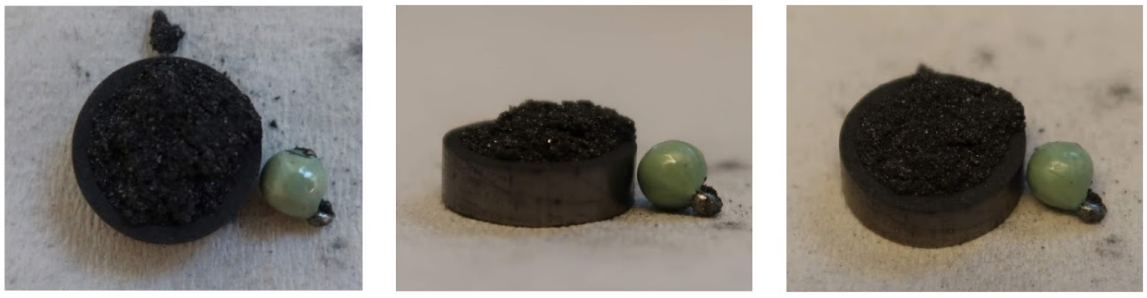

Figure 4.4.4.2: Pictures of slag drop and coke pellet after test 17

Figure 4.4.4.3 shows the development of contact angle and temperature for test 17, while figure 4.4.4.4 shows the development of relative volume and temperature for test 17. The figures show that the contact angle fluctuates some, but does not change much during the test, and that the relative volume decreases for the first two minutes of the test, and then increases for the last two minutes of the test.

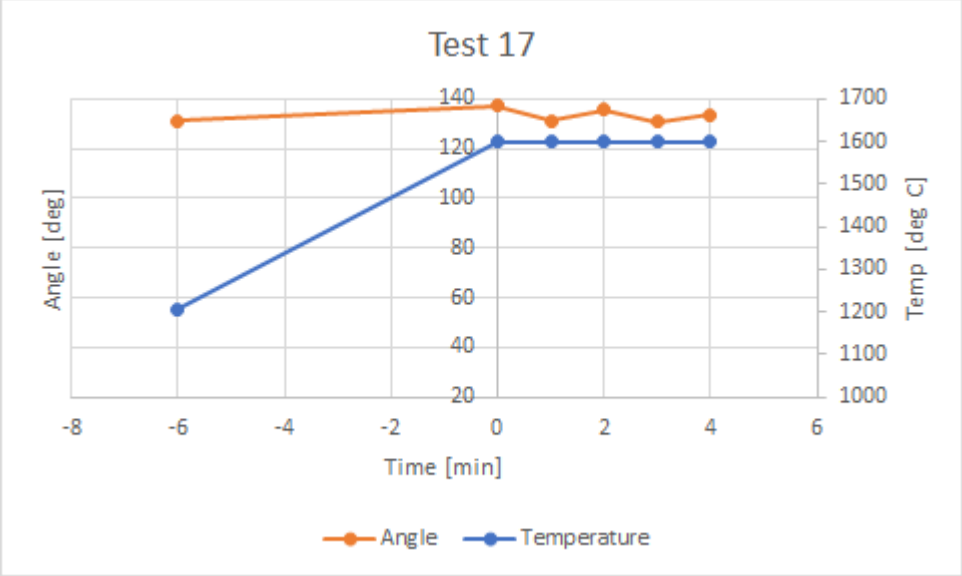

Figure 4.4.4.3: Contact angle and temperature development of test 17

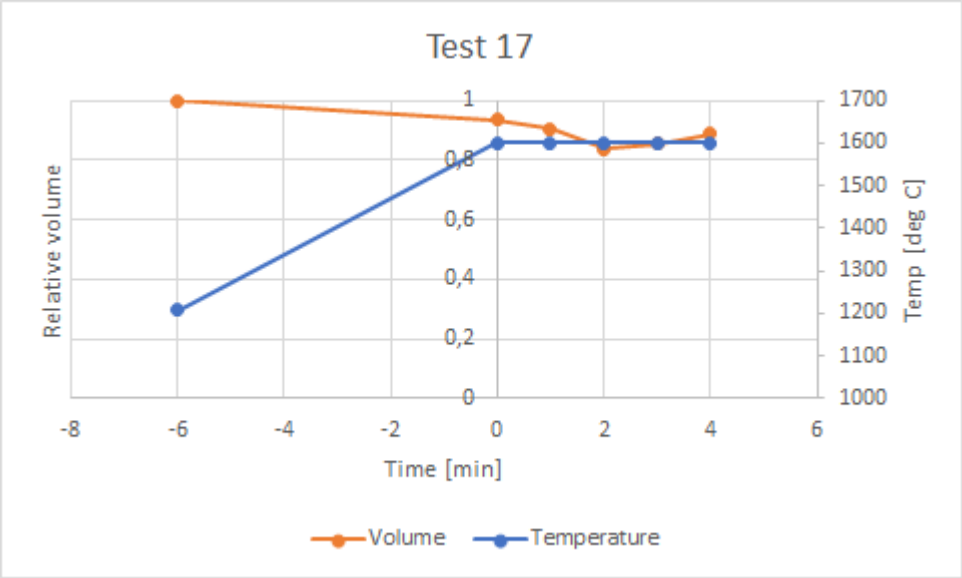

Figure 4.4.4.4: Relative volume and temperature development for test 17

Figure 4.4.4.5 shows an image of sample 17 taken in SEM. The figure shows that there are some cracks in the slag drop surface, and that there are two metal droplets of considerable size, one at the right bottom and one on the left side right above the crack. Figure 4.4.4.6 shows details of the slag, it shows that the slag is two-phase with varying size of the pattern. Figure 4.4.4.7 shows details of the metal phase, and it shows that the metal has some surface structure.

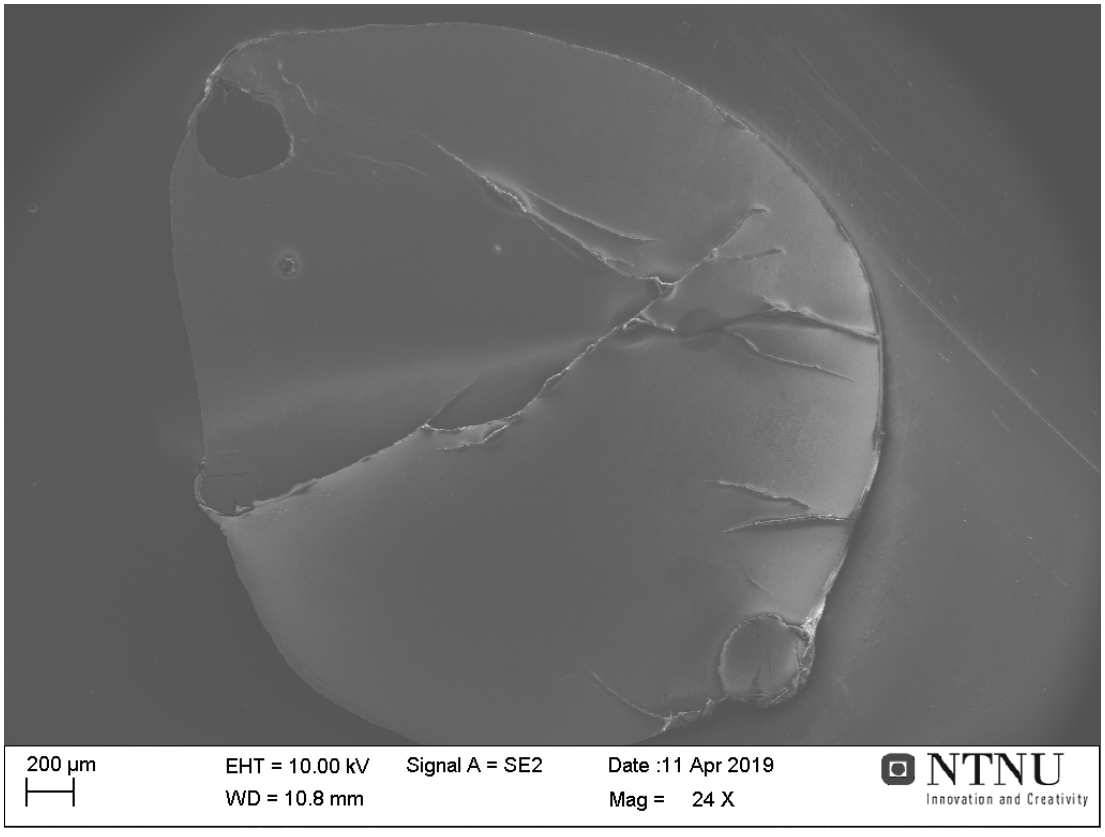

Figure 4.4.4.5: Image of sample 17 taken in SEM

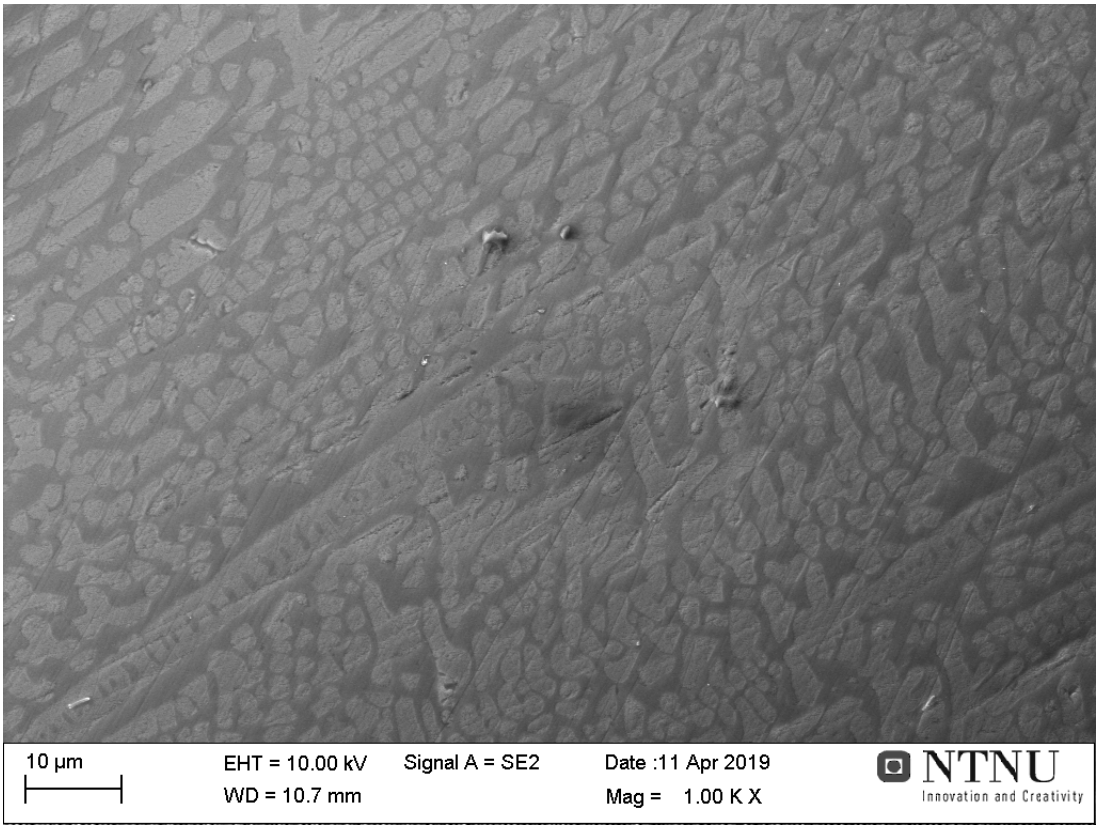

Figure 4.4.4.6: Details of two-phased slag of sample 17 magnified 1000 times

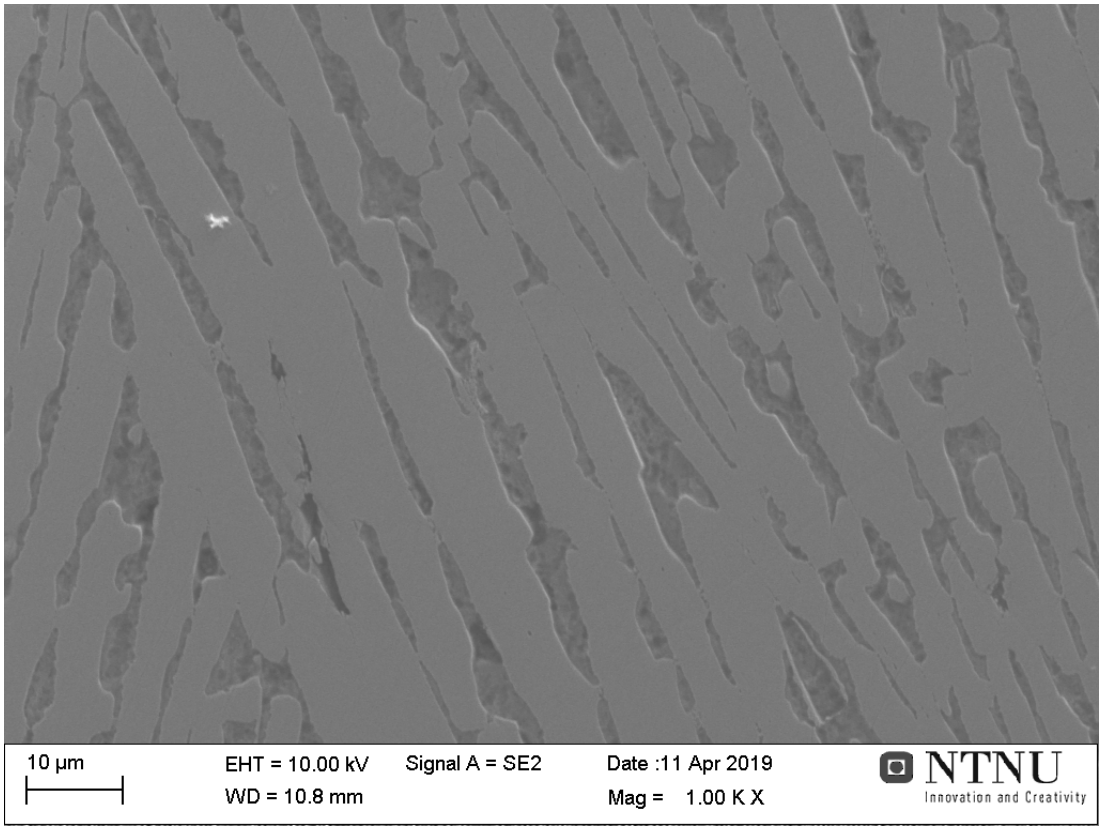

Figure 4.4.4.7: Details of metal of sample 17 magnified 1000 times

Table 4.4.4.1 lists the composition of the slag measured by SEM and EPMA, and the composition of the metal calculated from the slag composition measured by SEM. The slag has a MnO content higher than the desired 5%, while the metal has a lower content of silicon than the desired 18%. The results of the SEM and EPMA analysis of the slag are similar, as is expected.

Table 4.4.4.1: Slag composition measured by SEM and EPMA for sample 17, and metal composition calculated from SEM results

Slag (measured)	**MnO**	**SiO_2**	**FeO**	**Al_2O_3**	**CaO**	**MgO**	**SO_3**
SEM [wt%]	42,27	35,97	0	7,42	9,17	3,20	1,99
EPMA [wt%]	45,37	35,33	0,17	7,39	9,42	2,31	1,63
Metal (calculated)	**Total**	**Mn**		**Si**		**Fe**	
[wt%]	100	72,08		10,96		16,96	
[g]	0,0164	0,0091		0,0002		0,0071	

Reduction degrees for test 17 are R_{Mn} = 0,247 and R_{Si} = 0,004

4.4.5 Test 22

Test 22 was run with coke pellet 14 and slag sample 2L, at 1600°C for 2,5 minutes. Around 400°C the coke pellet was observed to swell. The slag drop melted at 1200°C, and there was some activity through bubbling from the slag drop, which increased as the temperature was increased. The test was stopped after 2,5 minutes as the slag drop moved close to the coke pellet edge.

Figure 4.4.5.1 shows some photographs from the furnace captured during test 22. The pictures shows the slag drop and coke pellet before heating, after slag drop melts, as the furnace temperature reaches 1600°C, and after 2.5 minutes at 1600°C. The figure shows that the coke pellet swelled during heating, which gave it an uneven surface. The figure also shows that the slag drop moved close to the edge during the test, which resulted in a shorter hold time than planned.

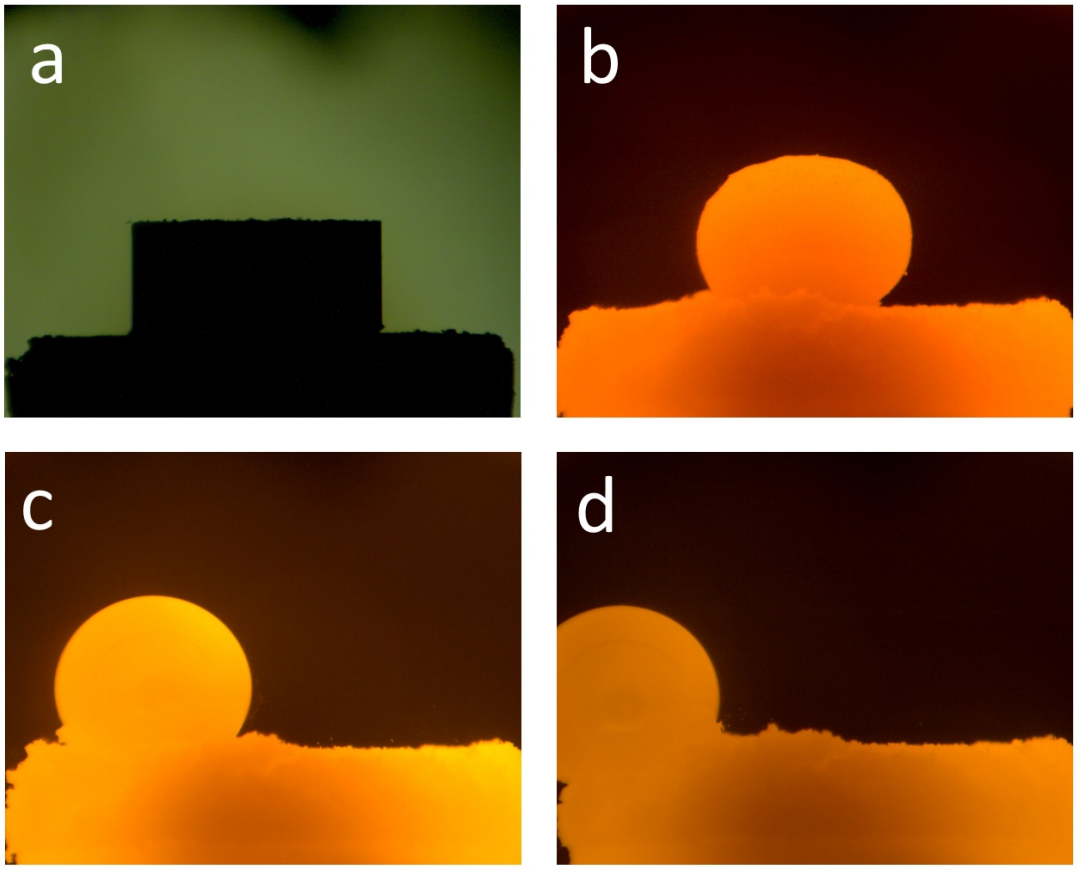

Figure 4.4.5.1: Pictures from test 22; a - before heating at 25°C; b - after melting at 1200°C; c - as furnace reaches 1600°C; d - after 2.5 minutes at 1600°C

Figure 4.4.5.2 shows pictures taken of the slag drop and coke pellet after test 22. As the figure shows, the coke pellet had crumbled during storage and/or wrapping, and that the slag drop was not attatched to the pellet. The slag drop had a pale green non-transparent color with some coke at the surface, and some metal could be observed at the bottom of the slag drop.

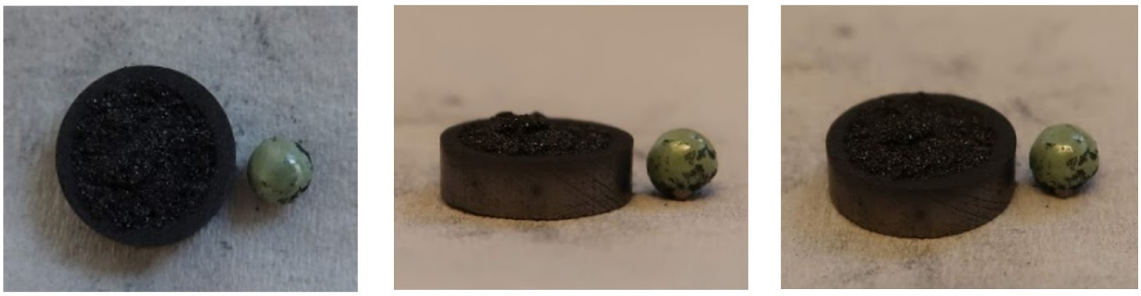

Figure 4.4.5.2: Pictures of slag drop and coke pellet after test 22

Figure 4.4.5.3 shows the development of contact angle and temperature for test 22, while figure 4.4.5.4 shows the development of relative volume and temperature for test 22. The figures show that the contact angle does not change much during the test, while the relative volume decreases from melting to hold temperature, and only has small changes for the 2,5 minutes of the test.

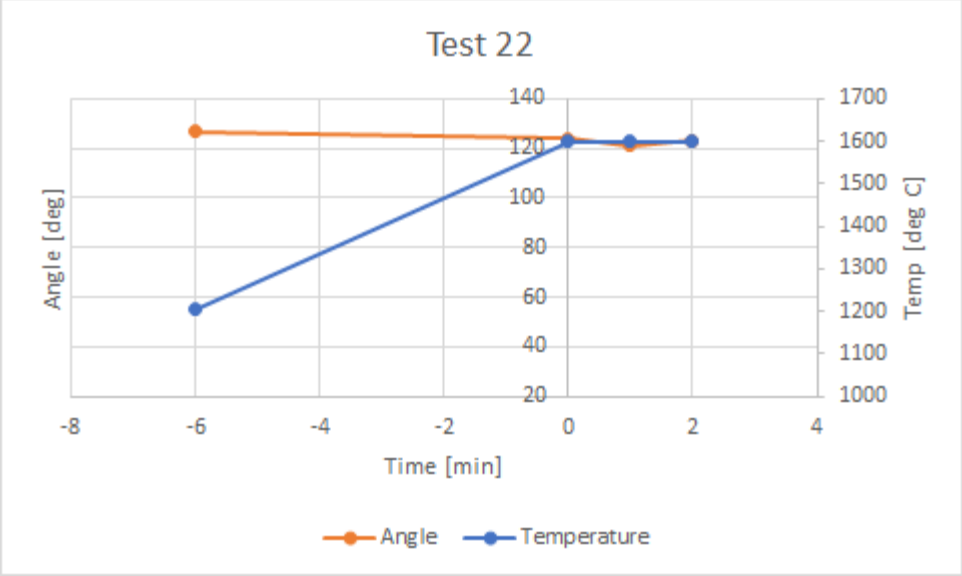

Figure 4.4.5.3: Contact angle and temperature development of test 22

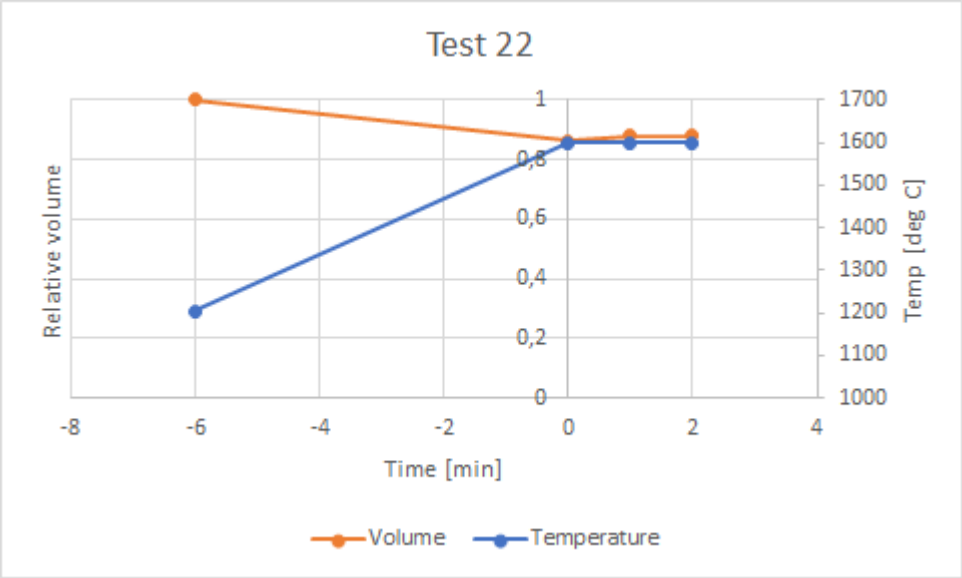

Figure 4.4.5.4: Relative volume and temperature development for test 22

Figure 4.4.5.5 shows an image of sample 22 taken in SEM. The figure shows that the sample has two metal droplets of considerable size, and that there were some particles on the sample surface. Figure 4.4.5.6 shows details of the slag magnified 1000 times, which shows that the slag has two phases. Figure 4.4.5.7 shows an overview of the slag magnified 100 times, which illustrates how the size and shape of the pattern in the slag varies. Figure 4.4.5.8 shows details of the metal magnified 1000 times, which shows that the metal has structure at the surface.

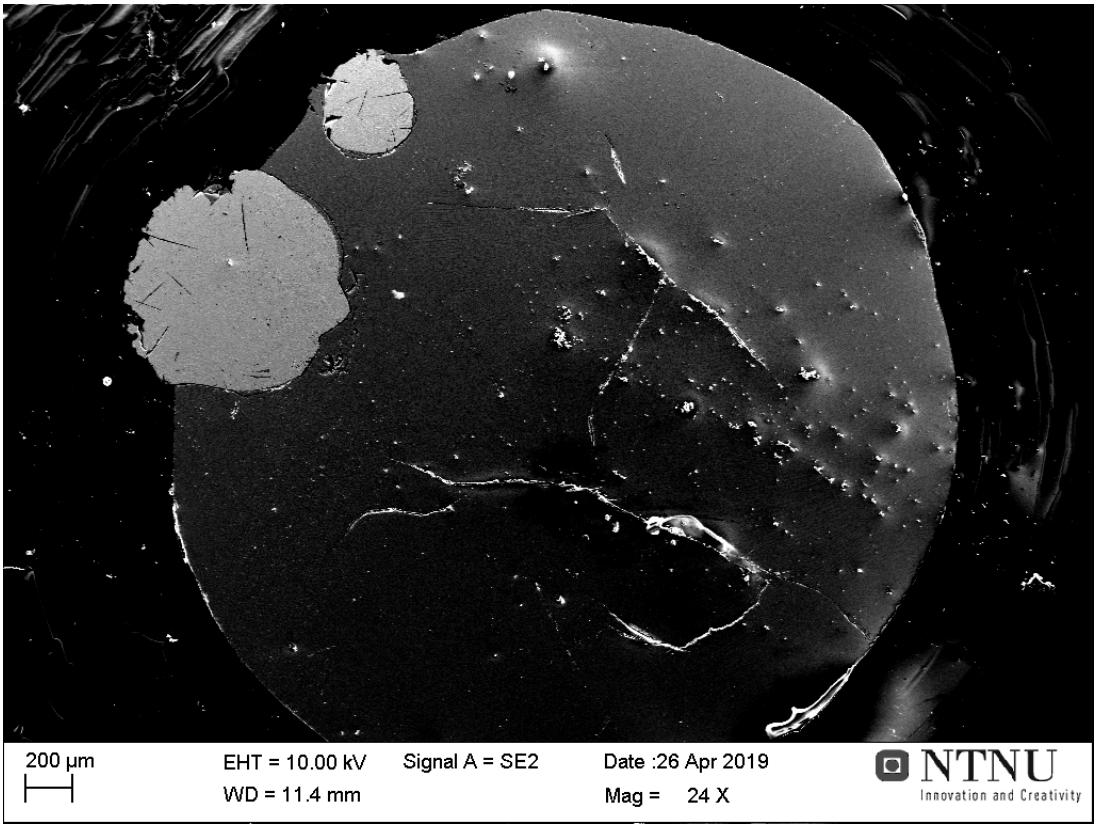

Figure 4.4.5.5: Image of sample 22 taken in SEM

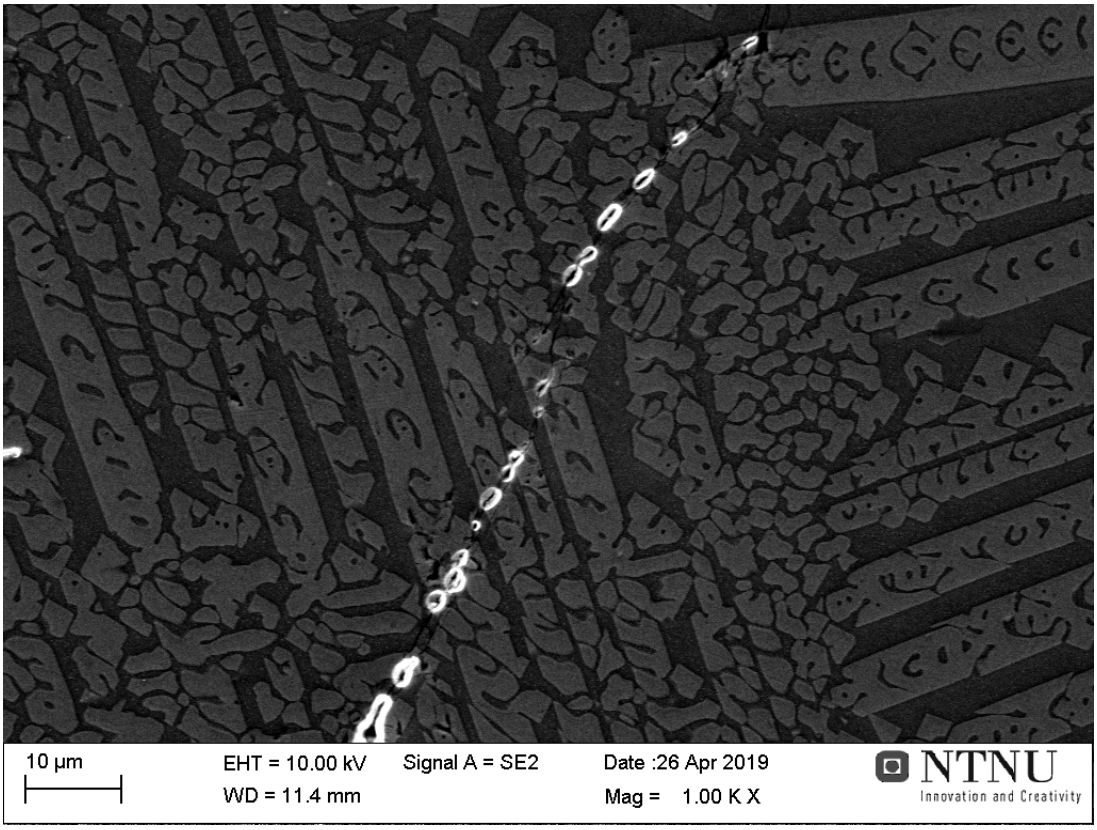

Figure 4.4.5.6: Details of the two-phased slag in sample 22 magnified 1000 times

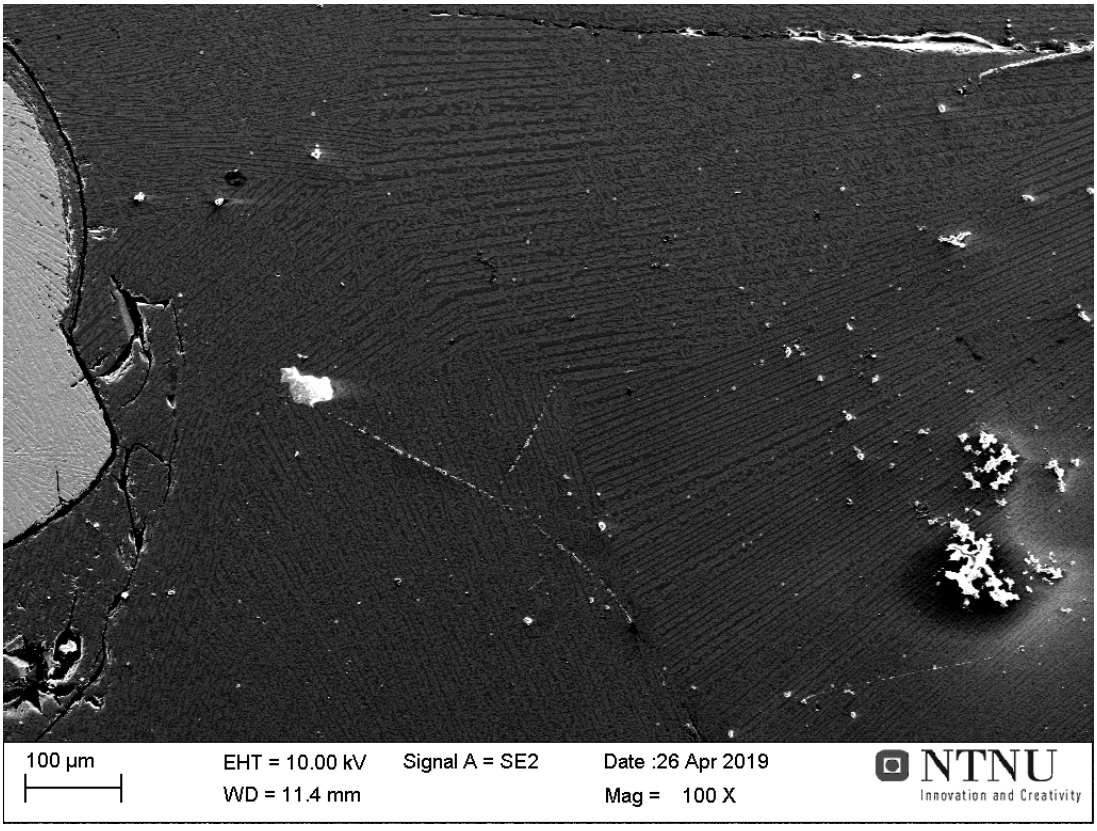

Figure 4.4.5.7: Overview of slag pattern magnified 100 times

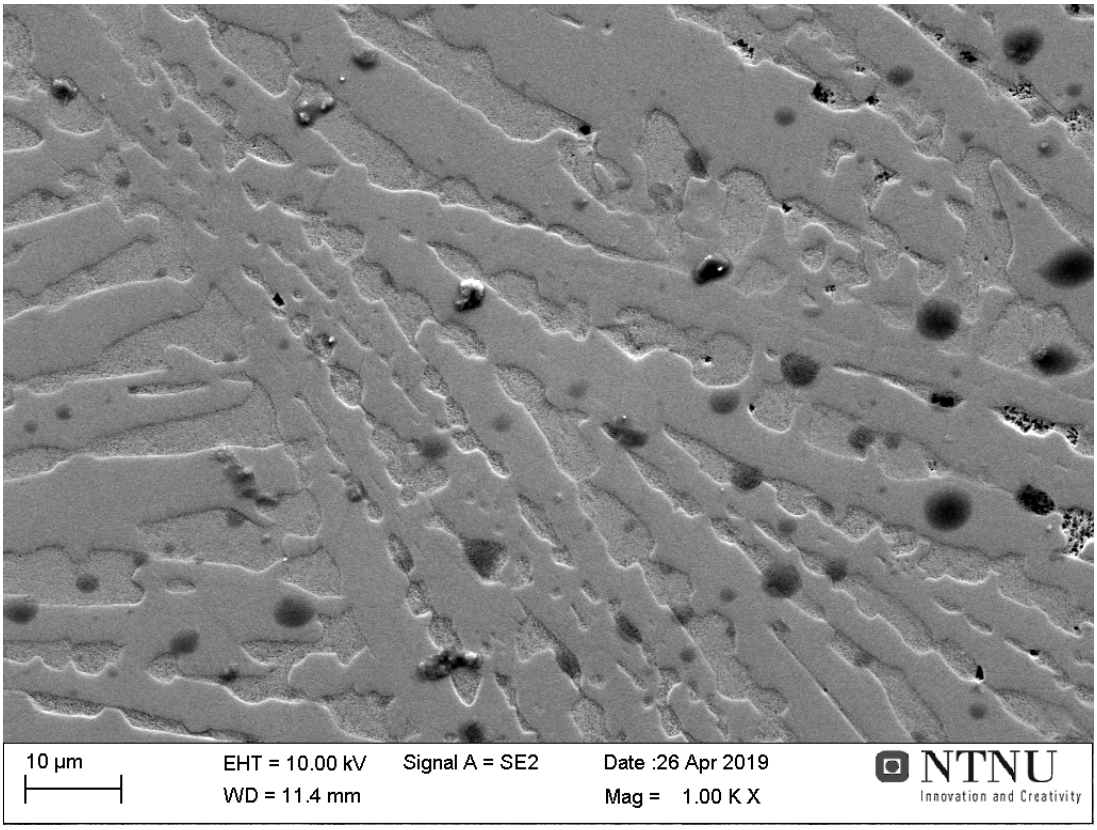

Figure 4.4.5.8: Details of metal in sample 22 magnified 1000 times

Table 4.4.5.1 lists the composition of the slag measured by SEM and EPMA, and the composition of the metal calculated from the slag composition measured by SEM. The MnO content in the slag is high, while the silicon content in the metal is low. The results of the SEM and EPMA analysis of the slag are similar, as is expected.

Table 4.4.5.1: Slag composition measured by SEM and EPMA for sample 22, and metal composition calculated from SEM results

Slag (measured)	**MnO**	**SiO_2**	**FeO**	**Al_2O_3**	**CaO**	**MgO**	**SO_3**
SEM [wt%]	45,08	32,71	0	7,67	9,57	2,63	2,35
EPMA [wt%]	46,40	34,57	0,21	6,97	9,25	2,35	1,60
Metal (calculated)	**Total**	**Mn**		**Si**		**Fe**	
[wt%]	100	46,20		9,36		44,43	
[g]	0,0156	0,0072		0,0015		0,0069	

Reduction degrees for test 22 are R_{Mn} = 0,200 and R_{Si} = 0,041

4.4.6 Test 13

The test was run with coke pellet 10 and slag sample 2C. Around 400°C the coke pellet was observed to swell, and at 1207°C the slag sample melted. When the temperature reached 1312°C the test was stopped as the slag drop moved close to the coke pellet edge.

Figure 4.4.6.1 shows some pictures captured during test 13. The pictures show the slag drop and coke pellet before the test is started, after the slag drop has melted, a picture between melting and the test was stopped taken at 1289°C, and the last picture captured before the test was stopped at 1312°C. The figure shows that the surface of the coke pellet swelled during heating, and that the slag drop moved during heating, resulting in the furnace temperature never reached 1600°C.

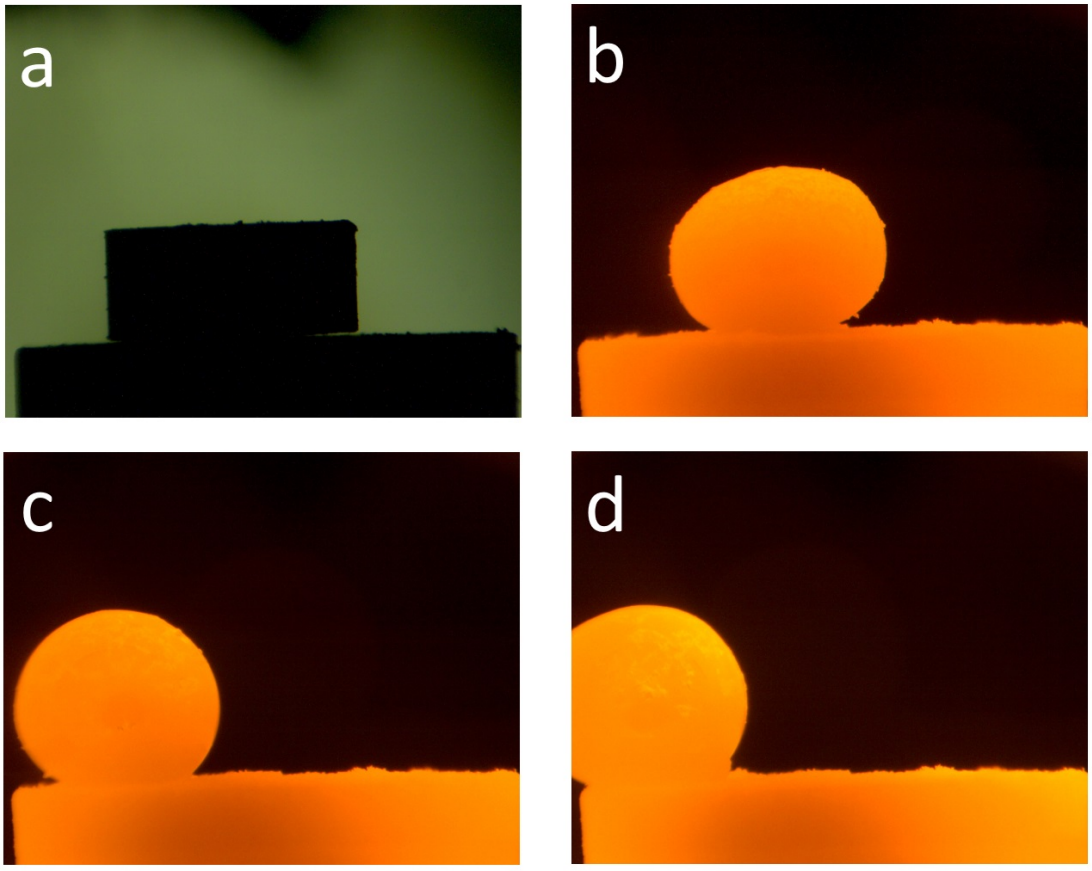

Figure 4.4.6.1: Pictures taken during test 13; a - before heating at 25°C; b - after melting at 1207°C; c - shortly before test was stopped at 1289°C; d - as test was stopped at 1312°C

Figure 4.4.6.2 shows pictures taken of the slag drop and coke pellet after test 13. The figure shows that the slag drop fell off the coke pellet as the test was stopped, and that the slag drop had a grey metallic color and no visible metal droplets.

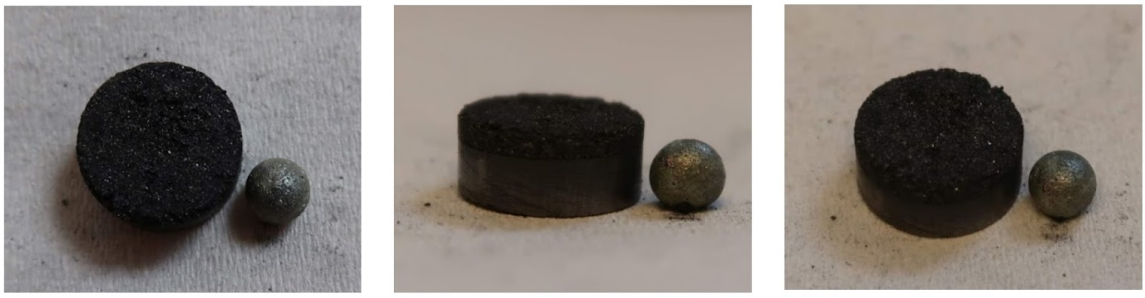

Figure 4.4.6.2: Pictures of slag drop and coke pellet after test 13

Figure 4.4.6.3 shows the development of contact angle and temperature for test 13, while figure 4.4.6.4 shows the development of relative volume and temperature for test 13. For these two figures the time is zero as the slag drop melted, since the furnace did not reach 1600°C. The figures show that the contact angle increased some as the temperature increased, and that the relative volume had a small decrease as the temperature increased.

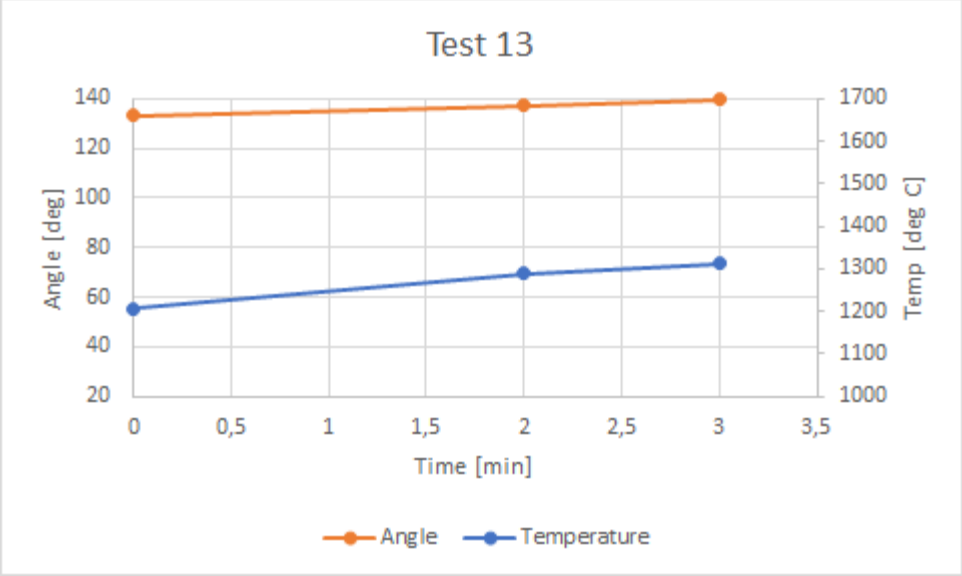

Figure 4.4.6.3: Contact angle and temperature development for test 13

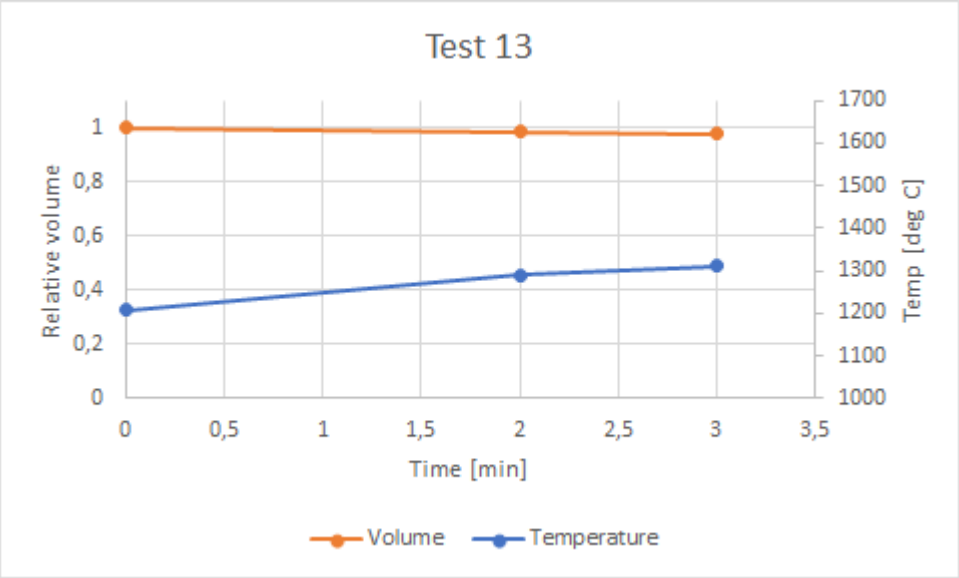

Figure 4.4.6.4: Relative volume and temperature development for test 13

Figure 4.4.6.5 shows an image of sample 13. The figure shows that the sample has some holes caused by gas being trapped in the sample as it solidified, and that the sample contained a little metal at the edge by the hole at the top of the figure and at the edge by the hole at the right lower side. Figure 4.4.6.6 shows details of the slag magnified 1000 times, which shows that the slag has two phases. Figure 4.4.6.7 shows metal and slag magnified 250 times. The figures show that the slag has larger pattern and a color difference between the phases that seems to be less than other samples with two-phased slag.

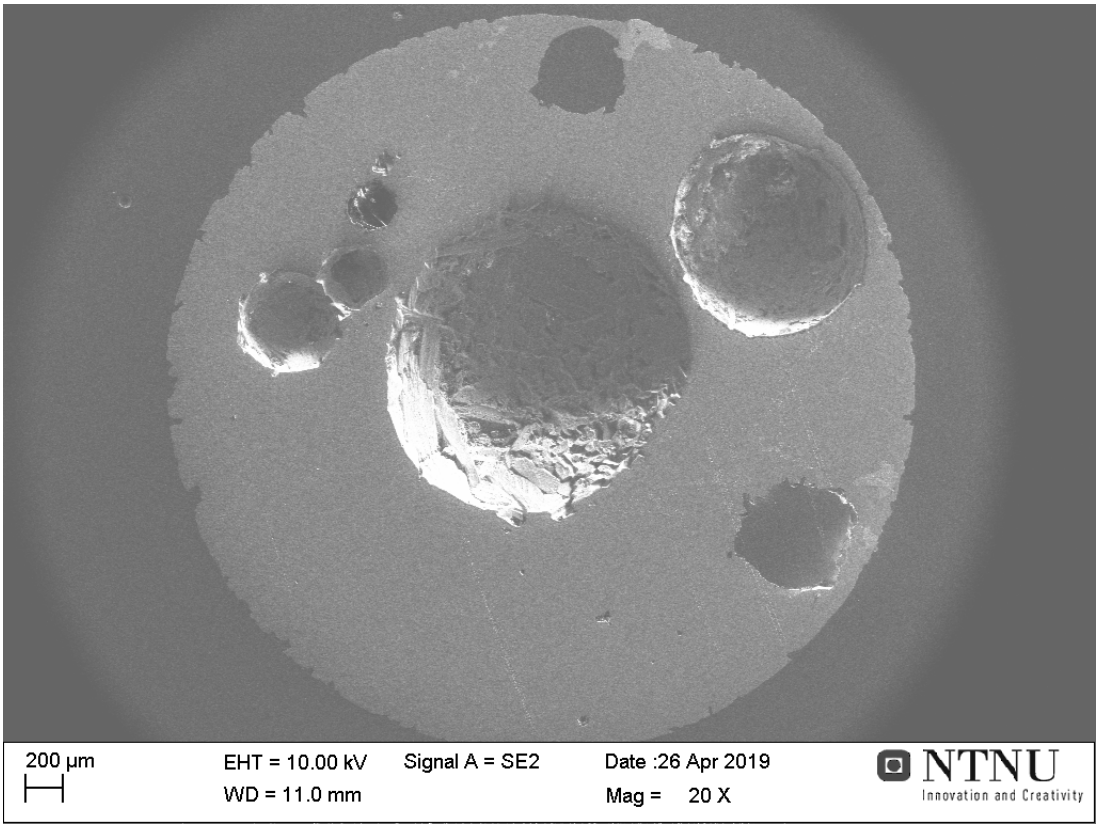

Figure 4.4.6.5: Image of sample 13 taken in SEM

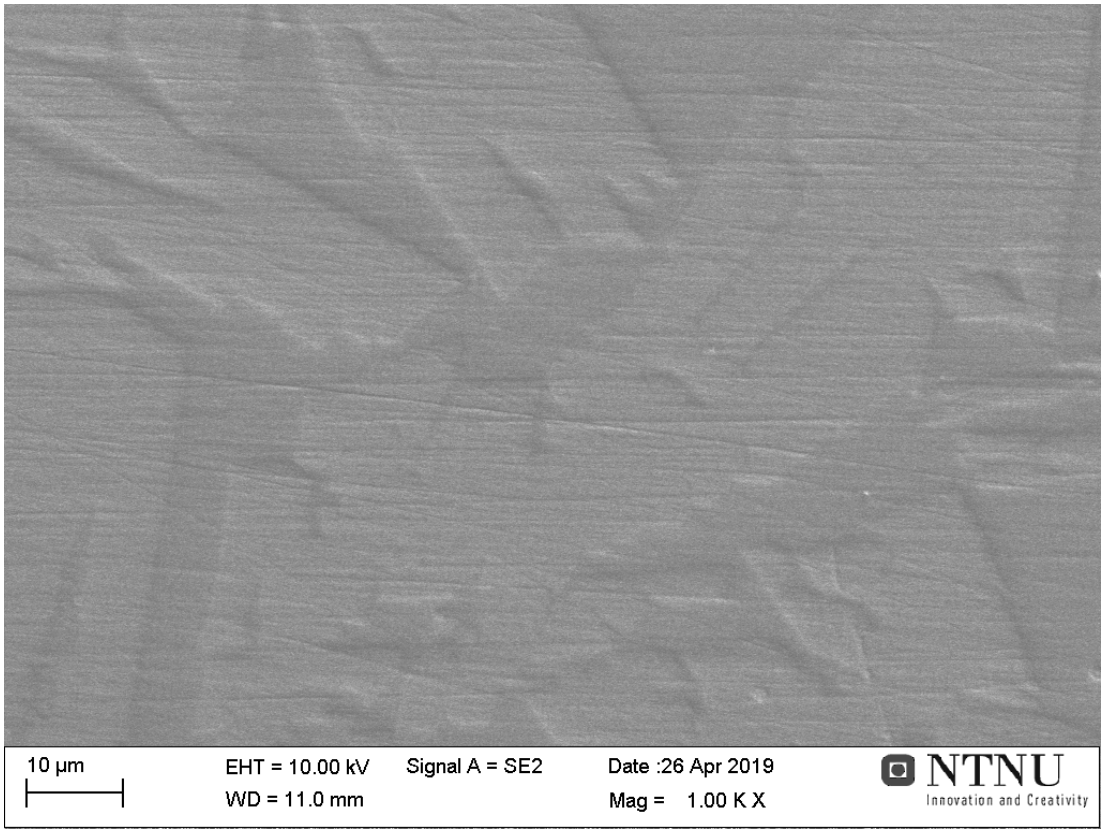

Figure 4.4.6.6: Details of the slag in sample 13 magnified 1000 times

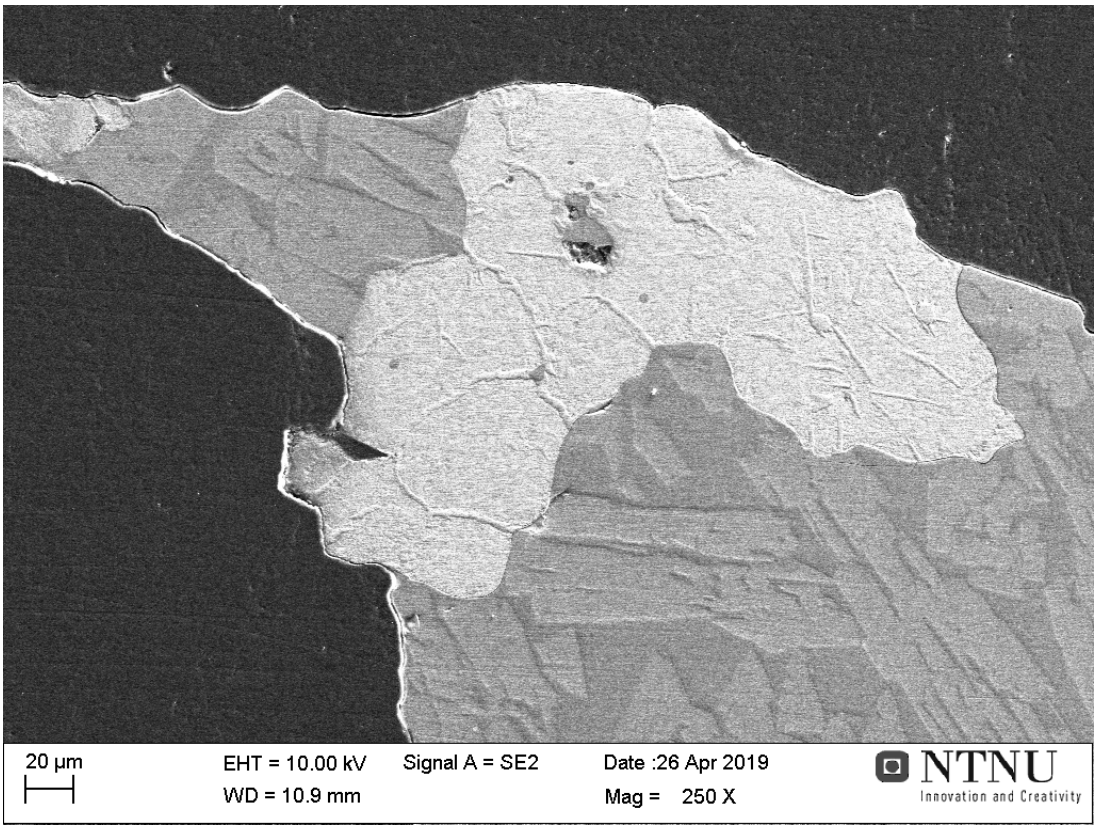

Figure 4.4.6.7: Metal and slag in sample 13 magnified 250 times

Figure 4.4.6.8 shows an image of the coke pellet used in test 13 taken in SEM. The figure shows that the slag drop moved towards the lower left side of the coke pellet before the test was stopped, and it seems like the slag drop broke of some coke particles from the pellet when falling off, leaving a crater close to the edge of the pellet. The other edges of the coke pellet are unaffected, while the center of the pellet is affected by the slag drop moving.

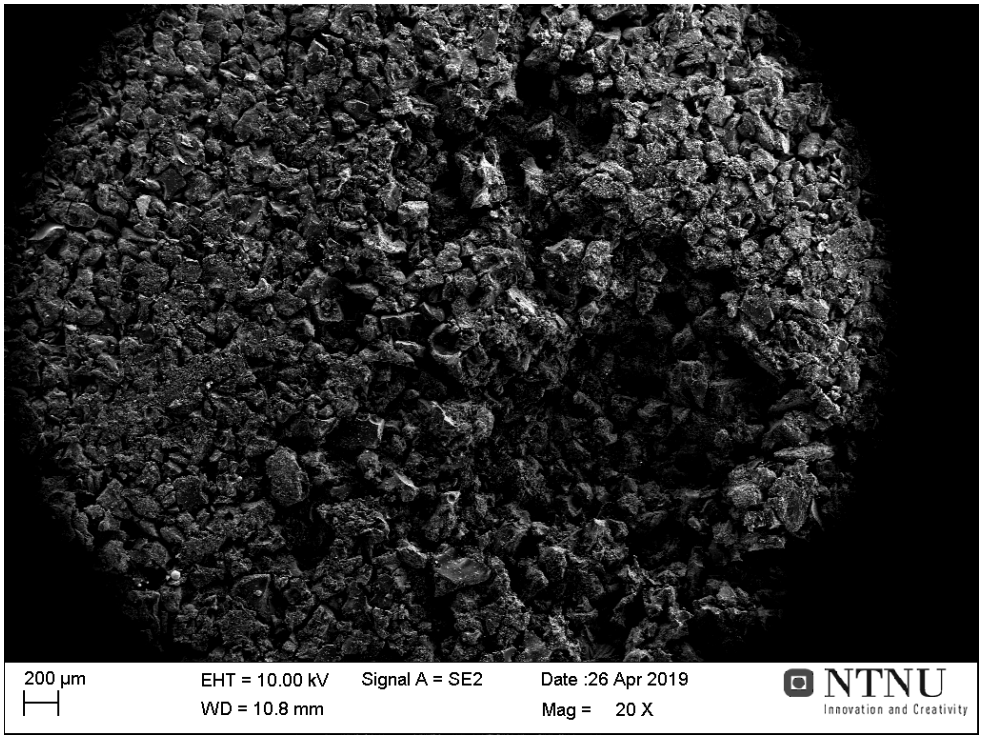

Figure 4.4.6.8: Image of the coke pellet used in test 13 taken in SEM

Table 4.4.6.1 lists the composition of the slag measured by SEM and EPMA, and the composition of the metal calculated from the slag composition measured by SEM. The slag has a high content of MnO, while the metal has a content that is close to the desired 18%, but has a low content of manganese. The results of the SEM and EPMA analysis for the slag are similar, which is expected.

Table 4.4.6.1: Slag composition measured by SEM and EPMA for sample 13, and metal composition calculated from SEM results

Slag (measured)	**MnO**	**SiO_2**	**FeO**	**Al_2O_3**	**CaO**	**MgO**	**SO_3**
SEM [wt%]	48,78	30,53	0	8,18	10,08	2,43	0
EPMA [wt%]	46,43	32,37	0,53	8,03	10,15	2,44	1,83
Metal (calculated)	**Total**	**Mn**		**Si**		**Fe**	
[wt%]	100	38,57		17,53		43,90	
[g]	0,0156	0,0072		0,0015		0,0069	

Reduction degrees for test 13 are R_{Mn} = 0,169 and R_{Si} = 0,077

5. Discussion

In this chapter the results presented in chapter 4 will be assessed and compared. Figures and tables that shows the differences and similarities between the tests will be presented. First, the quality of the results will be shortly discussed and possible sources of errors during measurements will be mentioned, then the results of the tests are assessed. Weight measurements, contact angles, volume development, visual appearance of slag, manganese oxide content of slag, silicon content of metal metal, and reduction degrees of manganese and silicon are presented.

5.1 Quality of results

Weight measurements: The scales used for measurement have some error margin, and the measurements of comparable weights, e.g. before and after drying, were therefore performed with the same scale. In addition, the weights of some samples after test may have been affected by some spoilage, considering that some charcoal and coke pellets were porous which resulted in some powder breaking off during storage and handling.

Contact angles: There are some things to consider in connection with measurement of contact angle. The contact angle was measured using the spherical measurements of the Fta32 software. Right after melting the slag drop could have more of an elliptical shape and not a complete spherical shape, which gave some uncertainty to the when the spherical measurement was used at this point. This was only an issue for the earliest measurements, and measurements from approximately 120 degrees were more accurate.

Another source of error was that the images used for measurement were selected manually. A number of images were assessed during selection, in order to find an image with the lowest volume of the slag drop. However, the results indicate that some of the selected images may be a slag drop which contained gas, which affected the measurement of contact angle. Where this was observed, it was often when the slag drop activity was very high and the increases and decreases in slag drop volume were frequent. At the beginning and end of the tests this was not an issue, but it was more difficult to select an image with no gas in the slag drop, when the activity was so high that the image with the lowest slag drop volume was not necessarily without gas. Where it was suspected that the slag drop contained gas at measurement, this was commented.

In addition, some SEM images show that the slag drop reduced down into the carbon pellet during the tests. In this case, the contact angle measurement would be affected, as the images from the furnace only show the part of the slag drop that is above the carbon pellet. This would be an issue for some of the tests that had long reduction times, as the tests with short reduction times likely did not have time to reduce into the carbon pellet.

However, the results can be used to show development and trends even though there are a few sources of error and the accuracy of the measurements may be decreased some.

Volume expansion: There are some error sources when measuring the volume of the slag drop, and these are the same as were described for contact angle measurement. Specially gas trapped in the slag drop and if the slag drop reduced its way into the carbon pellet will affect the volume measurement. From the results it seemed like the volume was affected more than the contact angle by these sources of error.

However, even if there are some sources of errors that reduce the accuracy of the measurements, the results can still be used to show development and trends of the volume.

Chemical analysis with SEM and with EPMA: The chemical analysis is done by EDS in SEM and WDS in EPMA. Both uses an electron beam and investigates the resulting wave that is emitted from the sample. The quality of these results are high. EDS identifies elements by using the energy of the waves that are emitted, while WDS identifies elements using the wavelength of the waves that are emitted. This makes the WDS more accurate, as the energy of the waves used in EDS can be more easily mixed together than the wavelengths. [30]

5.2 Carbon material pellets

The measurements of the carbon material pellets were presented in chapter 4. The differences between the charcoal pellets and the coke pellets were large, but the differences within charcoal or coke pellets were not so large. Highest, lowest and average values for moisture losses and densities for the charcoal and coke pellets are listed in table 5.2.1.

Table 5.2.1: Moisture loss and density values for coke and charcoal pellets

Material	**Value**	**Moisture loss [%]**	**Density [kg/m^3]**
Charcoal	High	23,87	599,3
Charcoal	Low	34,61	635,3
Charcoal	Average	28,95	618,7
Coke	High	6,59	1261,7
Coke	Low	0,0	1140,2
Coke	Average	2,65	1194,8

The lowest value for moisture loss in a coke pellet was 0 percent. This was unexpected, but the value did not stand out as the next lowest value for moisture loss in a coke pellet was 0,60 percent. The scale used for measurements before drying was the same as used after drying, and the pellets were not stored between pressing and drying, to increase the accuracy of the moisture loss measurements. However, varying amount of water was pressed out of both materials when using the uniaxial press to make pellets.

The table shows that the differences in high and low value for moisture loss are 10,74 percentage points for charcoal and 6,59 percentage points for coke, while the differences in high and low value for density are 36,0 kg/m^3 for charcoal and 121,5 kg/m^3 for coke. The variation in moisture loss is higher for charcoal than for coke, but the values of moisture loss are significantly higher for charcoal than for coke. In the same way the variation in density is higher for coke than for charcoal, but the values of density are higher for coke than for charcoal. All in all the variation in moisture loss for both materials are higher than expected, considering that the same method has been used when making all pellets. An explanation could be that the water was not homogeneously distributed in the pellet mix for both materials. The variation in density is lower than 10 percent of the average value, which is not disturbingly high.

Considering the average values for moisture loss and density between charcoal and coke, the differences are high. Coke has an average density value of 1194,8 kg/m^3 which is almost twice as high as charcoal which has an average density value of 618,7 kg/m^3. This is expected, considering the differences in density charcoal and coke has. Charcoal is a porous material with low volume weight compared to coke, and the table shows that this does not change when the materials are crushed and pressed into pellets. The high difference in

moisture loss, where charcoal has an average of 28,95 percentage while coke has an average of 2,65 percentage, is also expected considering that the charcoal pellet mix was added 60 wt% water, while the coke pellet mix was added 30 wt% water.

5.3 Weight measurements

All samples were weighed after testing. The weight loss after test was calculated by subtracting the weight after test from the sum of the weights of the carbon pellet used and the slag pellet used in the test. Figure 5.3.1 shows the weight loss in percentage for all tests, while figure 5.3.2 shows the weight loss in grams for all tests.

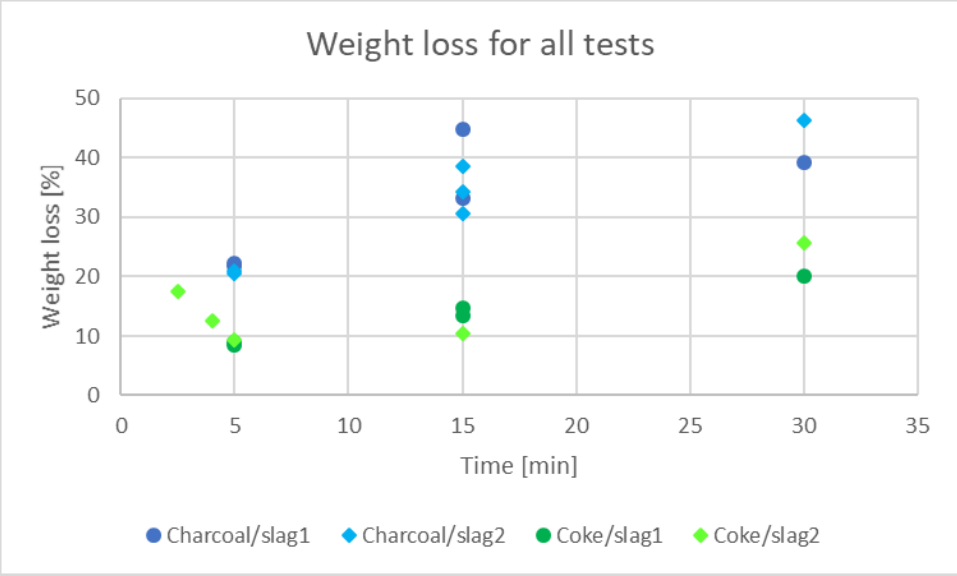

Figure 5.3.1: Weight loss in percentage for all tests

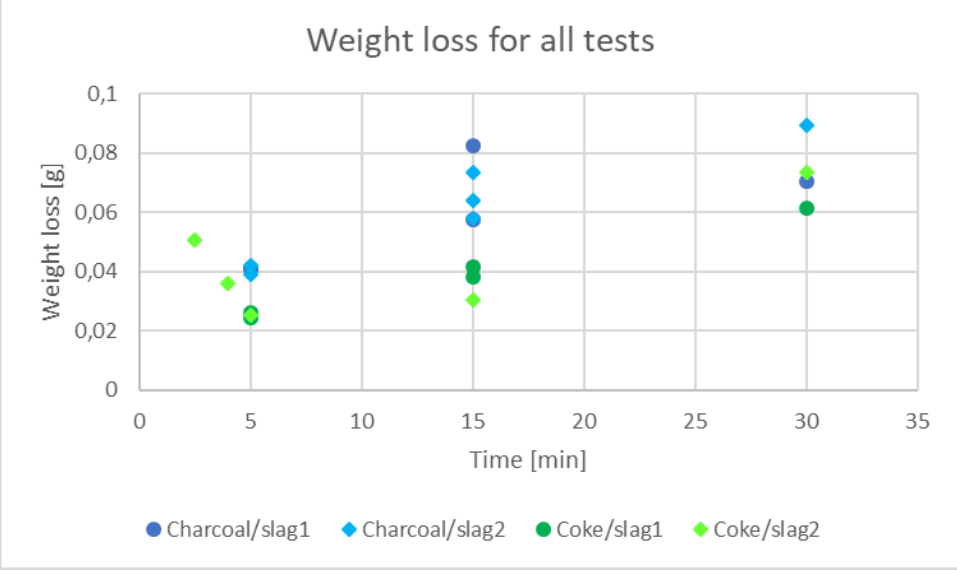

Figure 5.3.2: Weight loss in gram for all tests

The figures shows that the weight losses were higher for the tests run with charcoal for both slags, while the weight losses for the tests run with coke were lower, for both slags. The difference between weight loss for tests run with charcoal and tests run with coke was higher for the relative measurement in percent, this was because the coke pellets weighed more than the charcoal pellets. The figures indicates that the type of carbon pellet used in the test affected the weight loss more than which slag was used in the tests did.

There were some differences between slag 1 and slag 2. At 30 minutes the tests run with slag 2 had higher weight loss than the tests run with slag 1 for both charcoal and coke. However, at 15 minutes the tests run with slag 1 had higher weight loss than the tests run with slag 2, and at five minutes there was no clear difference between slag 1 and slag 2 for both charcoal and coke. A clear trend of weight loss between the slags could therefore not be observed, but it could seem like slag 1 had higher reduction rate and thus higher weight loss between 5-15 minutes, while slag 2 had higher weight loss after 30 minutes and thus produced more metal than slag 1. Considering the increased amount of manganese oxide and silicon oxide in slag 2, tests run with slag 2 were expected to produce more metal than tests run with slag 1.

The differences between charcoal (blue) and coke (green) were quite clear. The difference between the carbon materials in figure 5.3.2 varied from about 0,25 grams at 5 minutes, to about 0,2-0,4 grams at 15 minutes, to about 0,15 grams at 30 minutes. At all times the tests run with charcoal had higher weight loss than the tests run with coke, which indicates that the carbon material used in the tests has impact on the weight loss during the tests. Charcoal contains more volatiles than coke, which evaporates during heating in the furnace and accounts for some of the weight loss for the tests run with charcoal. However, higher weight loss could also indicate that the reduction of manganese oxide and silicon oxide is higher for tests run with charcoal than tests run with coke.

5.4 Wetting

Figure 5.4.1 shows the development of contact angles for the tests run with charcoal and slag 1. The figure shows that the development of the contact angles are similar for these tests, and that the contact angle decreases as the reduction time increases for all tests.

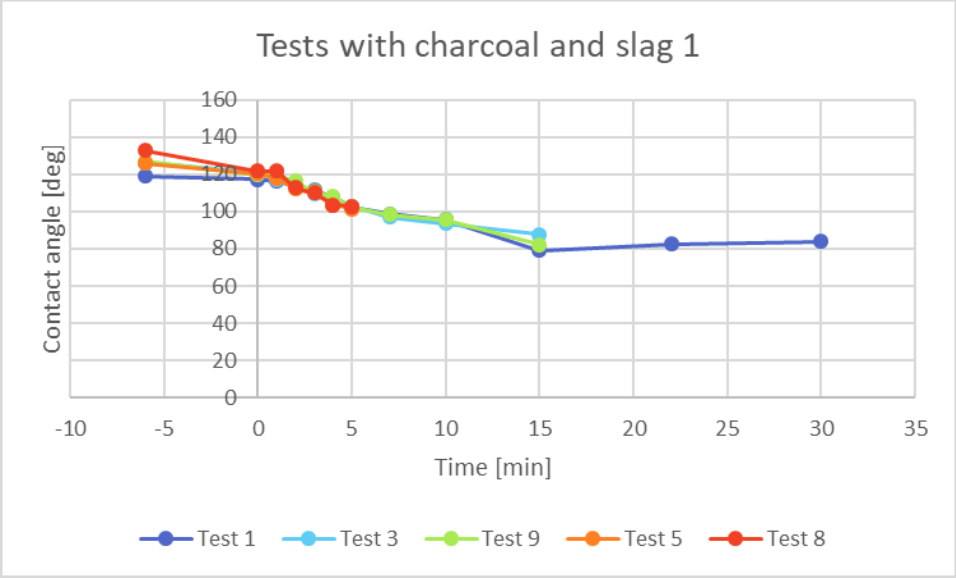

Figure 5.4.1: Development of contact angle for tests run with charcoal and slag 1

Figure 5.4.2 shows the development of contact angles for the tests run with charcoal and slag 2. The figure shows that the contact angle develops similarly for these test, but that the values vary some and that the variation in contact angles increase with time. At 15 minutes the variations are significant, however, test 20 does not follow the same trend as the other three tests between 10 and 15 minutes, and stands out. When omitting test 20, the remaining results follow a clear trend, where the contact angle decrease with increasing reduction time, and the decrease is highest between 10 and 15 minutes.

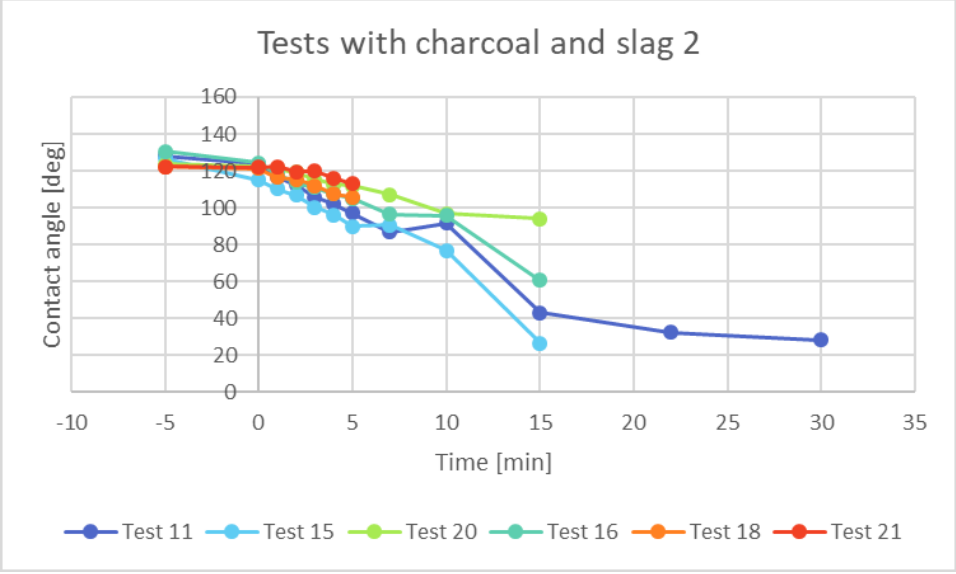

Figure 5.4.2: Development of contact angle for tests run with charcoal and slag 2

Figure 5.4.3 show the development of contact angles for the tests run with coke and slag 1. The figure shows that these tests have a similar development of the contact angle, with little deviation between the values. The contact angle decreases moderately with increasing reduction time.

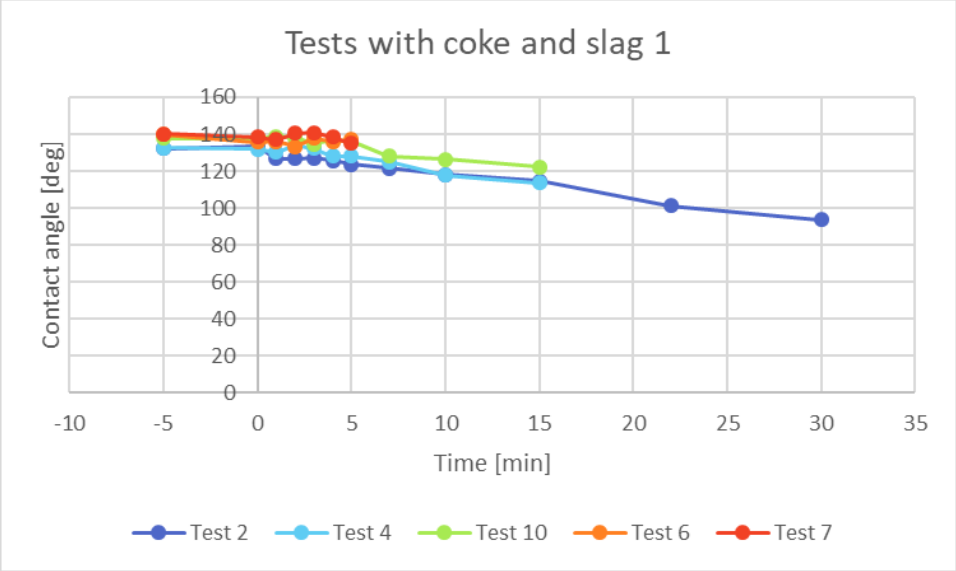

Figure 5.4.3: Development of contact angles for tests run with coke and slag 1

Figure 5.4.4 shows the development of the contact angles for tests run with coke and slag 2. The figure shows that the development is similar for all tests, with little variation in contact angle between the tests. The contact angle decreases moderately with increasing reduction time for these tests.

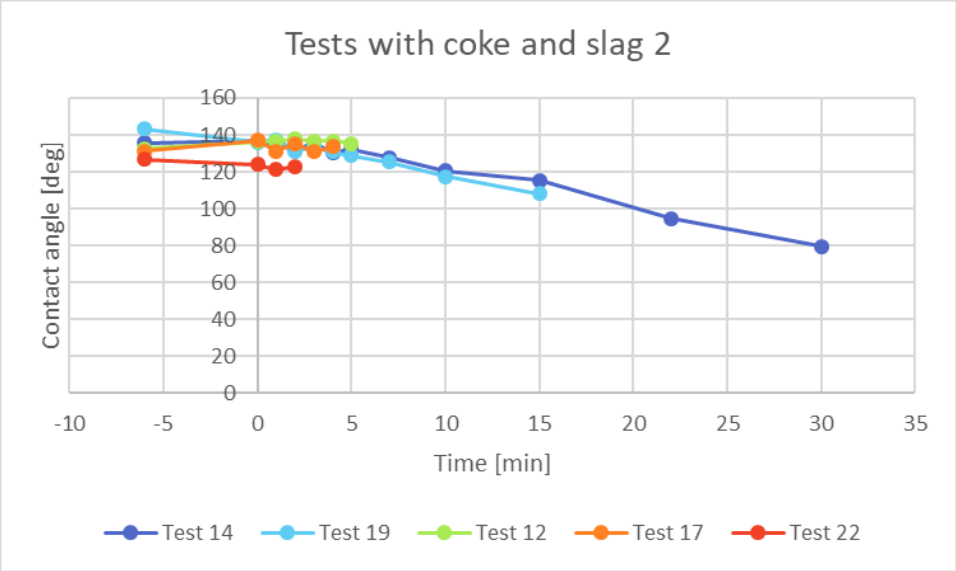

Figure 5.4.4: Development of contact angles for tests run with coke and slag 2

5.4.1 Comparison of contact angles for charcoal and coke

Figure 5.4.1.1 shows the contact angles for all tests run with slag 1, while figure 5.4.1.2 shows the contact angles for all tests run with slag 2. The tests run with charcoal has orange colors and crosses as point indicators, while tests run with coke has blue colors and pluses as point indicators, in both figures.

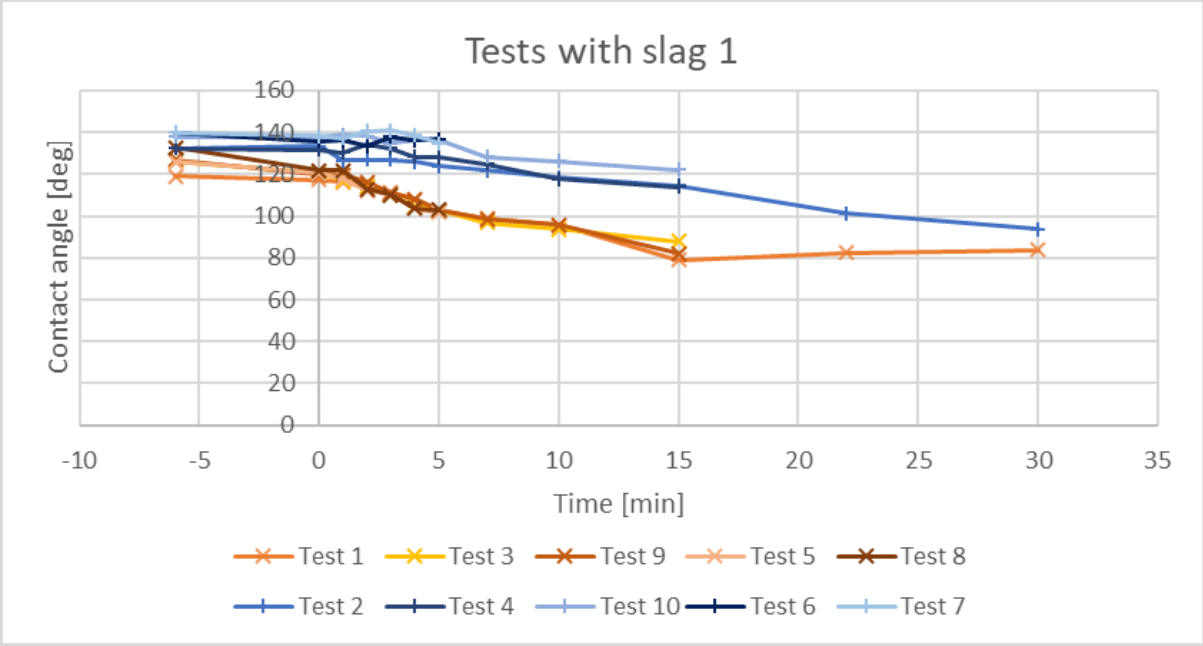

Figure 5.4.1.1: Wetting angles of all tests run with slag 1. Orange lines are tests run with charcoal, while blue lines are tests run with coke

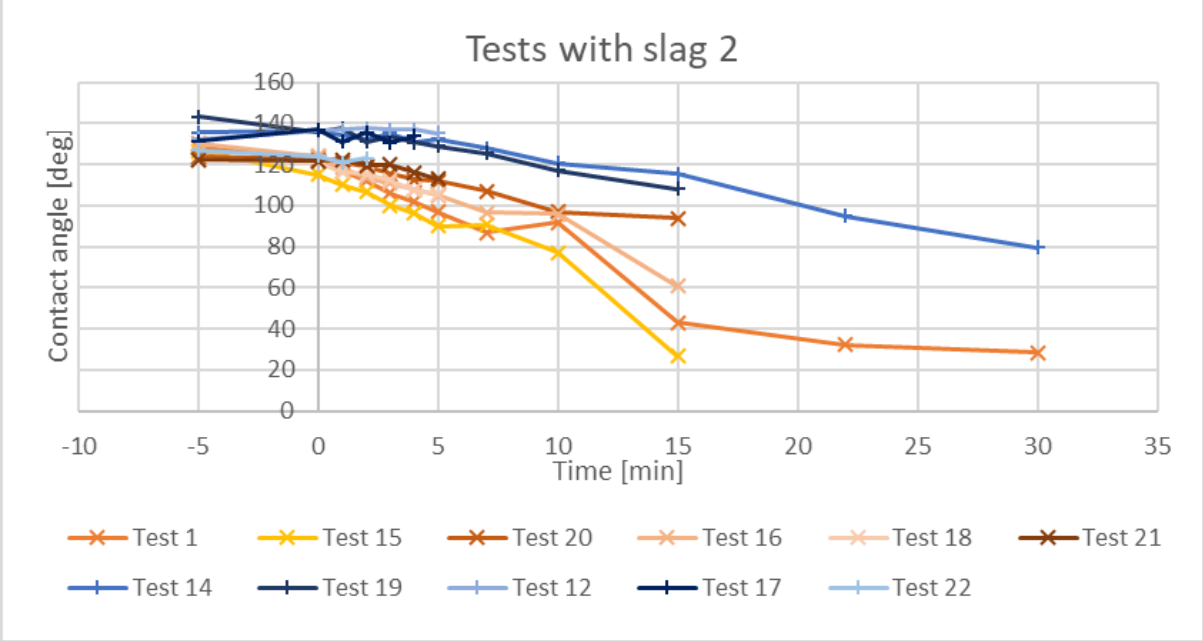

Figure 5.4.1.2: Wetting angles of all tests run with slag 2. Orange lines are tests run with charcoal, while blue lines are tests run with coke

Figure 5.4.1.1 shows that all tests have the same development in contact angle, it decrease with increasing reduction time. The tests run with charcoal generally has a steeper decrease than the tests run with coke, and the values for the tests run with charcoal are lower than the values for the tests run with coke at all times after hold temperature was reached. There is a clear trend of tests run with charcoal having lower contact angles than the tests run with coke when slag 1 is used.

Figure 5.4.1.2 shows that the tests run with charcoal has more varying development than the tests run with coke. Still, all tests run with charcoal has lower contact angle values than the tests run with coke at all times after hold temperature was reached. Even though test 20 run with charcoal stands out with high final contact angle value at 15 minutes, the trend is clear, the tests run with charcoal has lower contact angles than the tests run with coke when slag 2 is used.

Figure 5.4.1.1 and 5.4.1.2 shows that the tests run with charcoal has lower contact angle values than the tests run with coke when both slag 1 and slag 2 was used. This indicates that the charcoal is wetted better than the coke by both slag 1 and slag 2. The wetting is affected by the surface of the material, and the charcoal and coke used for the pellets were sieved to the same fraction. Charcoal is porous and coke is not, this could affect the wetting and result in better wetting for slag 1 and slag 2 towards charcoal than towards coke.

Another factor that affects the contact angle is whether the slag drop stays on top of the substrate or if it reduces its way down into the substrate. If the slag drop reduce into the substrate, some of the slag drop will be hidden from the camera, which affects the measurements of contact angle. When assessing the images captured in SEM, it seems as the time has more impact on if or how much the slag drop reduce into the carbon pellet, and it seemed like tests run with slag 2 reduced more into the carbon pellet than the tests run with slag 2 for both charcoal and coke. However, there was no clear difference between tests run with charcoal and coke. The contact angle of the tests run with charcoal and coke can therefore be assumed to have been equally accurately measured. Then the clear conclusion is that the contact angle is lower when charcoal is used than when coke is used, which may indicate that the reduction rate of manganese and silicon oxide is higher when charcoal is used than when coke is used.

5.4.2 Comparison of contact angles for slag 1 and slag 2

Figure 5.4.2.1 shows the contact angle for tests run with charcoal, while figure 5.4.2.2 shows the contact angle for tests run with coke. Tests run with slag 1 have orange colors and has crosses as point indicators, while tests run with slag 2 have blue colors and has pluses as point indicators, in both figures.

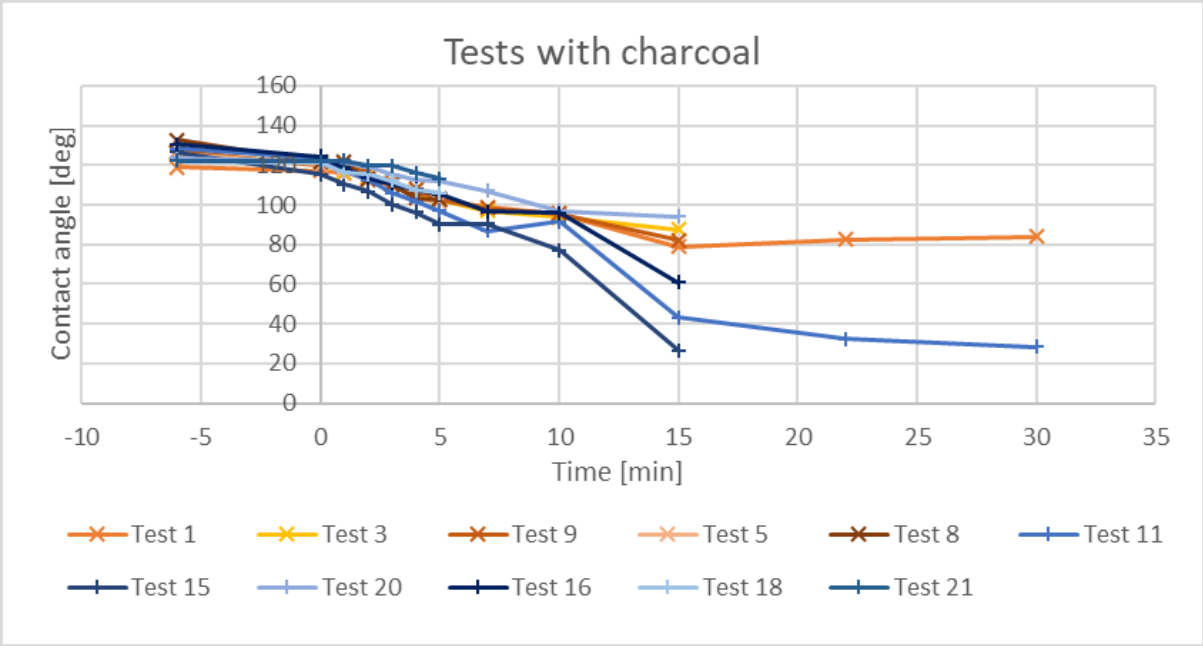

Figure 5.4.2.1: Contact angles for all tests run with charcoal. Orange lines are tests run with slag 1, while blue lines are tests run with slag 2

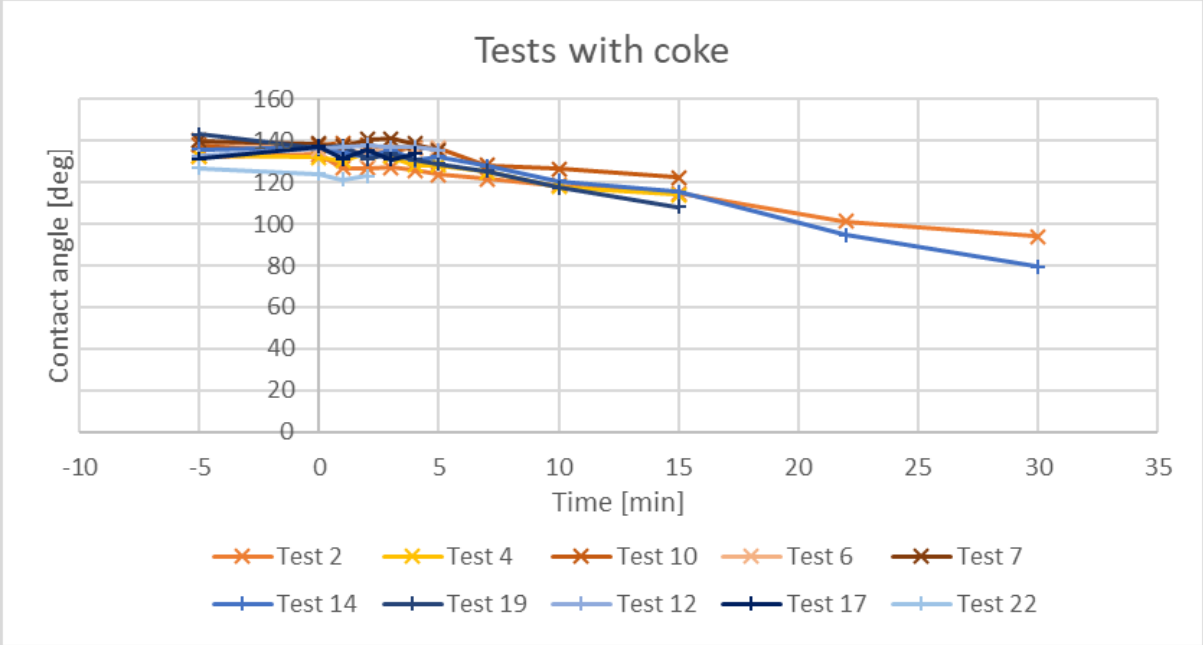

Figure 5.4.2.2: Contact angles for all tests run with coke. Orange lines are tests run with slag 1, while blue lines are tests run with slag 2

Figure 5.4.2.1 shows that for charcoal, the tests run with slag 1 has the same development, while the tests run with slag 2 have high difference in development and end values. Test 20 stands out from the rest of the tests run with slag 2 and has high end value for the contact angle. If this test is omitted, then the tests run with slag 2 are observed to have lower contact angle values than the tests run with slag 1.

Figure 5.4.2.2 shows that for coke, the tests run with slag 1 and the tests run with slag 2 has the same development. There is little difference between the two slag types, but the tests run with slag 2 has some lower values than the tests run with slag 1 at 15, 22 and 30 minutes. However, the difference between the two slags is low, and the conclusion is therefore that there are no significant difference in contact angle value between slag 1 and slag 2 for tests run with coke.

Figure 5.4.2.1 and 5.4.2.2 show that there was no difference in contact angles between slag 1 and slag 2 towards coke, while the contact angles for slag 1 was higher than the contact angles for slag 2 towards charcoal. Slag 2 contained more manganese oxide and silicon oxide than slag 1, which may have increased the reduction of these oxides in the tests run towards charcoal. Since the difference between slag 1 and slag 2 was not observed for tests run with coke, it indicates that the difference in slag composition had higher impact towards charcoal than towards coke. This could be a result of the different properties of charcoal and coke, that charcoal is porous and has lower density than coke.

5.5 Relative volume

Figure 5.5.1 shows the relative volume development for tests run with charcoal and slag 1. The figure shows that the tests has similar development of the relative volume. For the first five minutes the volume developments are almost the same, the volume then varies some at 7 and 10 minutes before it decreases significantly and the tests has similar values at 15 minutes. Test 1, with reduction time of 30 minutes has a final value of about 0,35.

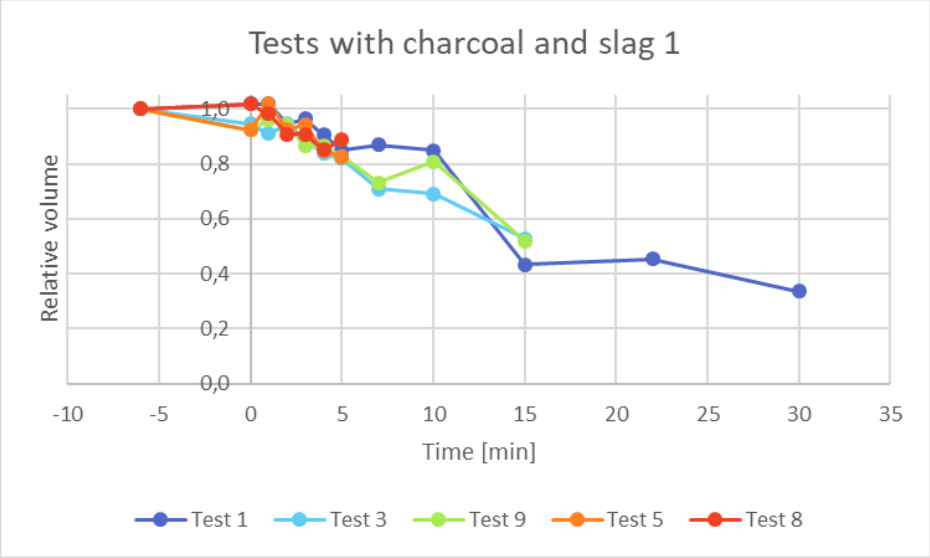

Figure 5.5.1: Relative volume development for tests run with charcoal and slag 1

Figure 5.5.2 shows the relative volume development for tests run with charcoal and slag 2. The figure shows that the development of the volume are similar for the tests, but with varying values. The volume decreases moderately for all tests the first minutes, and from 10 to 15 minutes the volume decrease significantly, except for test 20 that stands out. After 15 minutes there is a mild decrease and test 11 that has reduction time of 30 minutes has a final value close to zero. Test 11 and 15 has very low final values, and it is likely that the slag drop reduced down into the pellet, and actually has higher volume than measured for these tests.

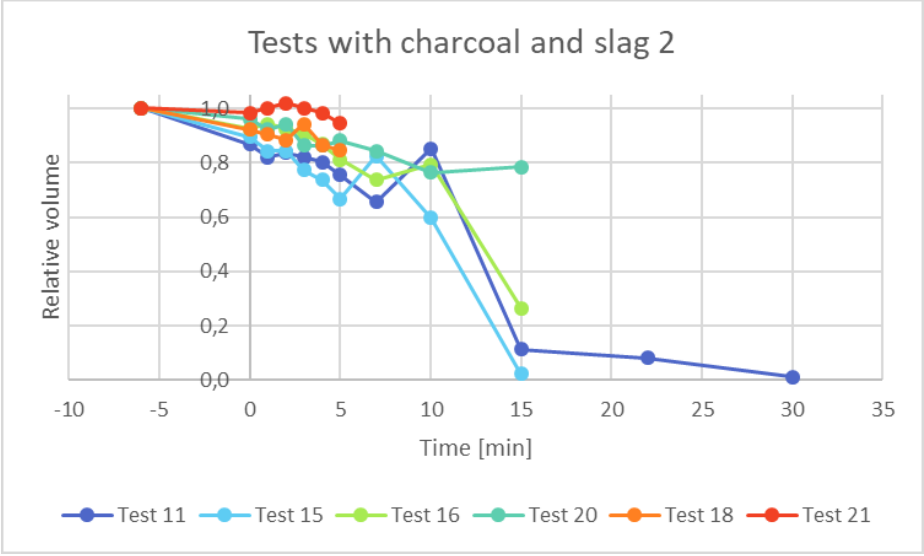

Figure 5.5.2: Relative volume development for tests run with charcoal and slag 2

Figure 5.5.3 shows the relative volume development for tests run with coke and slag 1. The figure show that the tests has similar development. The volume decreases for all tests from melting to hold temperature, and then the volume does not change much in the 15 first minutes. For some of the tests the volume increases some, likely due to gas being trapped in the slag drop during measurement. After 15 minutes the volume decreases significantly and the final value of tests 2 that has 30 minutes reduction time is around 0,50.

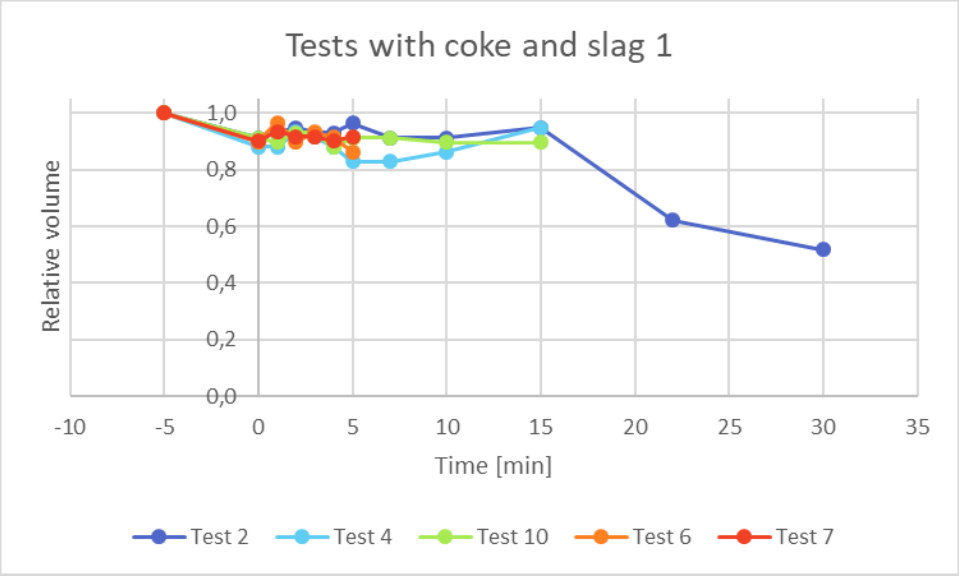

Figure 5.5.3: Relative volume development for tests run with coke and slag 1

Figure 5.5.4 shows the relative volume development for tests run with coke and slag 2. The figure shows that all samples has a decreasing trend except test 14 where the volume increase from 10 to 15 minutes before it decrease for the rest of the test. It is likely that the slag drop in test 14 contained gas for the measurement at 15 and 22 minutes. The final value for test 14 is about 0,30.

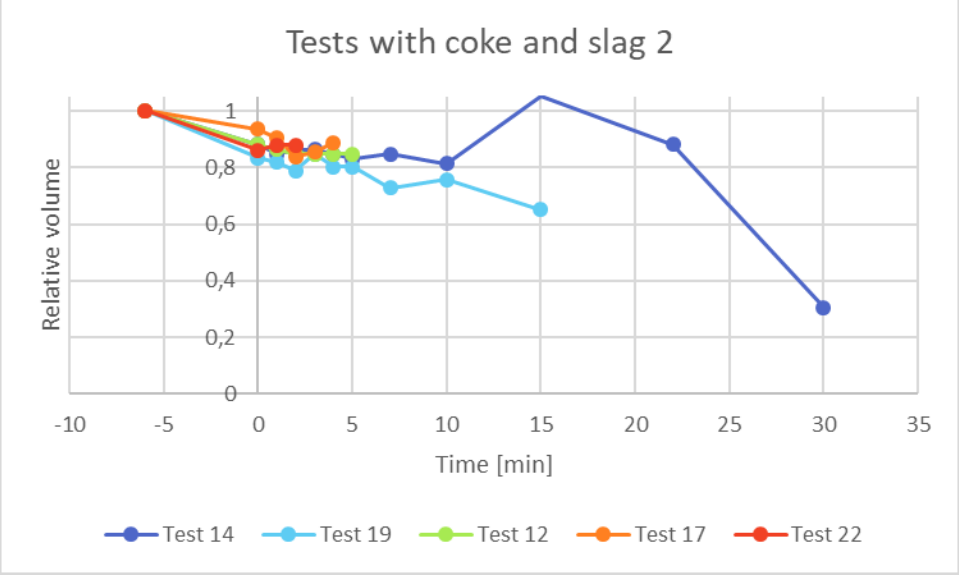

Figure 5.5.4: Relative volume development for tests run with coke and slag 2

5.5.1 Comparison of relative volume development for charcoal and coke

Figure 5.5.1.1 shows the relative volume development for all tests run with slag 1, while sample 5.5.1.2 shows the relative volume development for all tests run with slag 2. The tests run with charcoal have orange colors and crosses as point indicators while the tests run with coke have blue colors and pluses as point indicators, in both figures.

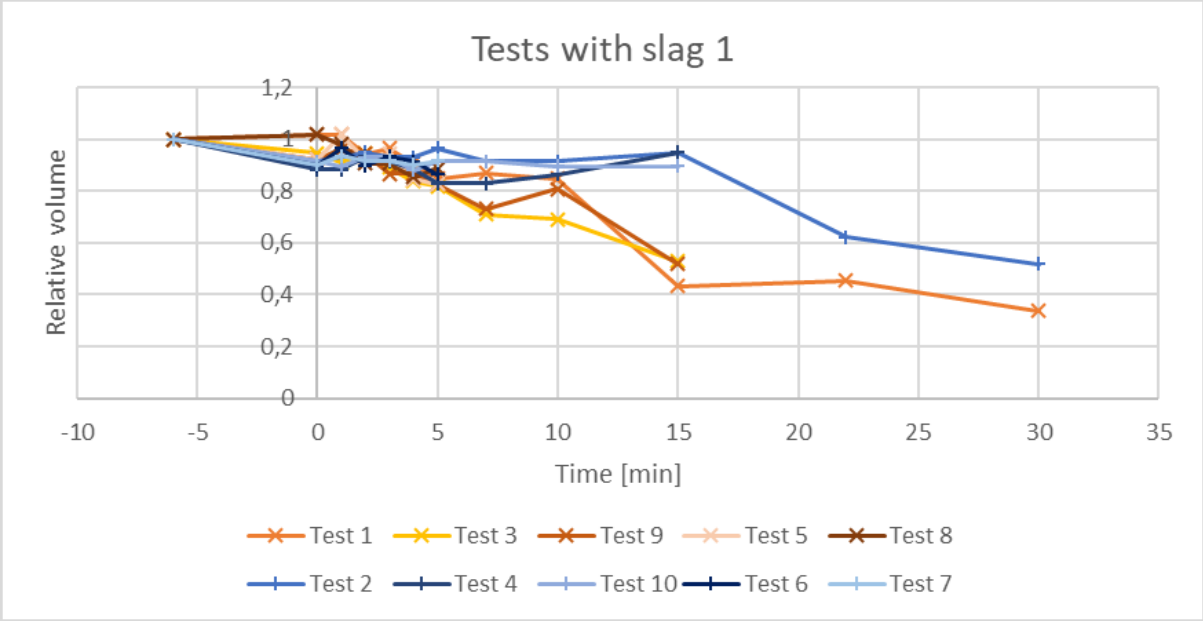

Figure 5.5.1.1: Relative volume development for all samples with slag 1. Orange lines are tests run with charcoal, blue lines are tests run with coke

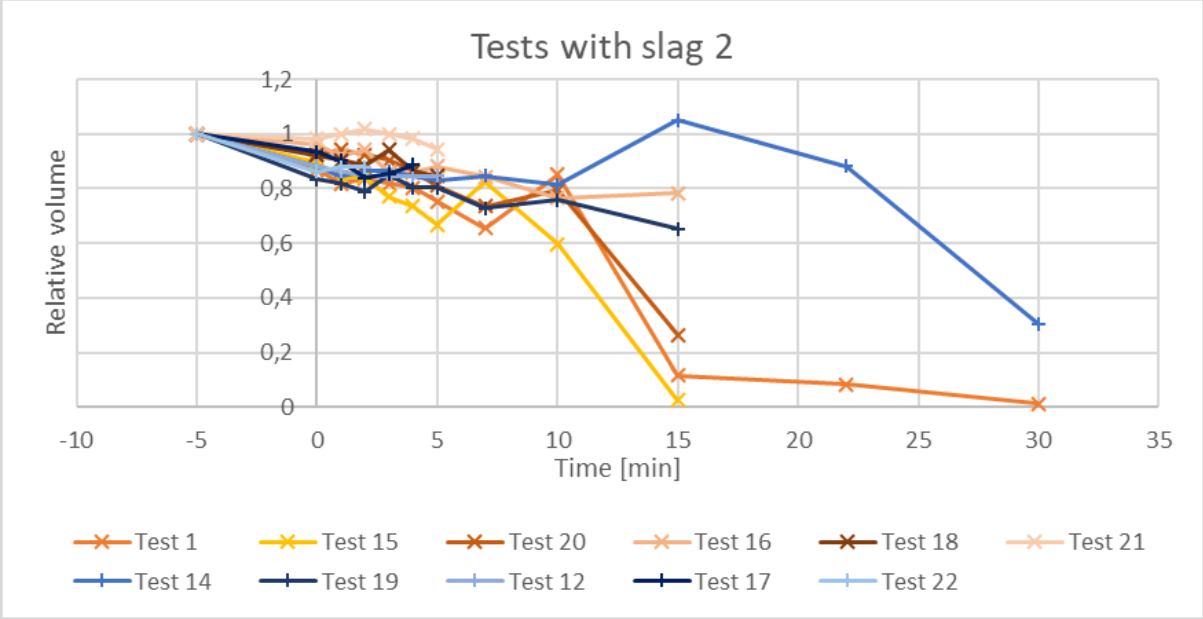

Figure 5.5.1.2: Relative volume development for all samples with slag 2. Orange lines are tests run with charcoal, blue lines are tests run with coke

Figure 5.5.1.1 shows that the relative volume develops similarly for the tests run with charcoal, and similarly for the tests run with coke, but that there is a difference between the tests run with charcoal and coke. The tests run with charcoal has lower relative volume than the tests run with coke at 10, 15, 22 and 30 minutes. The trend is therefore clear, the relative volume decreases more when charcoal is used as substrate, than when coke is used as substrate.

Figure 5.5.1.2 shows that the volume develops similarly for the tests run with charcoal, omitting test 16 that stands out at 15 minutes, and varies more for the tests run with coke. The measurements of test 14 shows an increase in volume from 10 to 15 minutes. This is not an actual increase, but faulty measurements as gas was trapped in the slag drop. There was likely gas in the slag drop for the measurements at boh 15 and 22 minutes for test 15. Test 11 and 15 has values close to zero at 15 minutes. The volume does not decrease to zero, but the low measurements are results of the slag drop reducing its way down into the carbon pellet. In this way, some of the slag drop volume is hidden in the carbon pellet, and is not measured with this technique. Considering these two sources of errors, the figure is more difficult to interpret, but taking the results between 5-10 minutes into consideration, it seems like the tests run with charcoal has lower relative volume than the tests run with coke. The trend is therefore that the relative volume decrease more when charcoal is used as substrate, than when coke is used as substrate.

Figure 5.5.1.1 and 5.5.1.2 show that the relative volume decreases more when charcoal is used than when coke is used for both slag 1 and slag 2. Large decrease in slag drop relative volume indicates that the reduction of manganese oxide and silicon oxide is high, and that higher amounts of oxygen are leaving the oxides in the sample as CO-gas, resulting in more produced metal. The results therefore indicates that the tests run with charcoal has higher reduction rates of manganese oxide and silicon oxide than the tests run with coke, for both slag 1 and slag 2.

The relative volume is also affected by whether or not the slag drop reduced its way down into the substrate. If this is the case, the carbon pellet hides some of the volume of the slag drop in the pellet, and the volume measured will be lower than the actual volume of the slag drop. When assessing the images taken in SEM, it seemed like the slag droplets in the tests run with slag 2 reduced more into the carbon pellets than the slag droplets in the tests run with slag 1. However, there was no significant difference between charcoal and coke regarding if and how much the slag drop reduced into the carbon pellet. Assuming that this had approximately the same impact on the majority of the measurements, the trend is clear. The reduction rate is higher when charcoal is used as substrate, than when coke is used as a substrate, for both slag 1 and slag 2.

5.5.2 Comparison of relative volume development for slag 1 and slag 2

Figure 5.5.2.1 shows the relative volume development for all tests run with charcoal, while figure 5.5.2.2 shows the relative volume development for all tests run with coke. The tests where slag 1 was used have orange colors and crosses as point indicators, and the tests where slag 2 was used have blue colors and pluses as point indicators, in both figures.

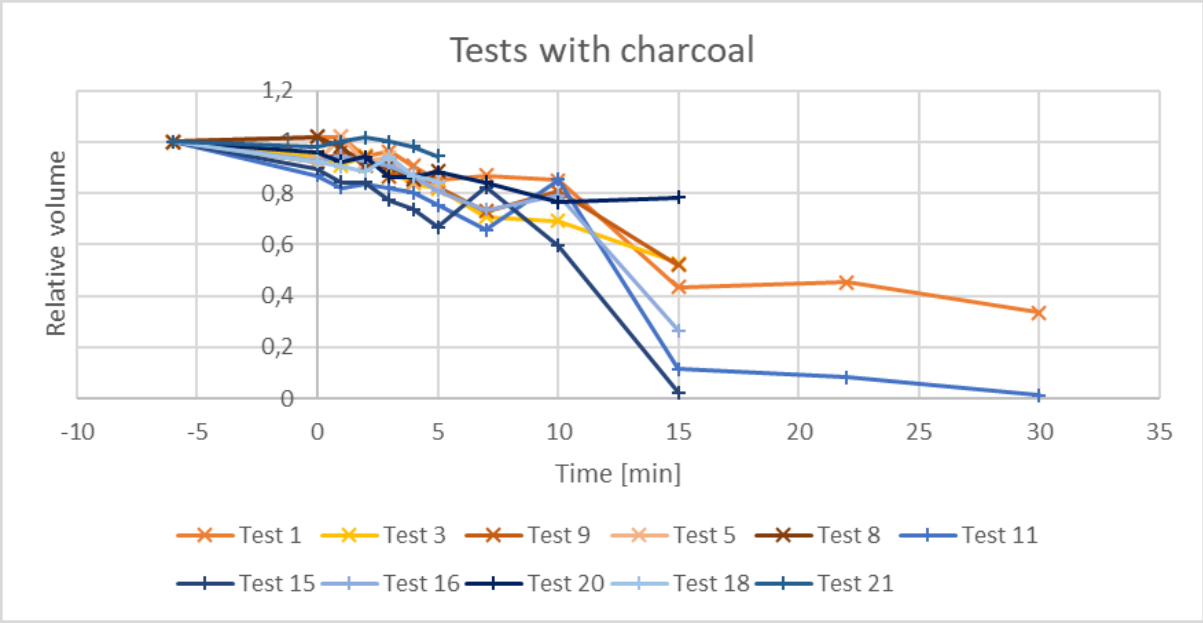

Figure 5.5.2.1: Relative volume development for all samples with charcoal. Orange lines are tests run with slag 1, blue lines are tests run with slag 2

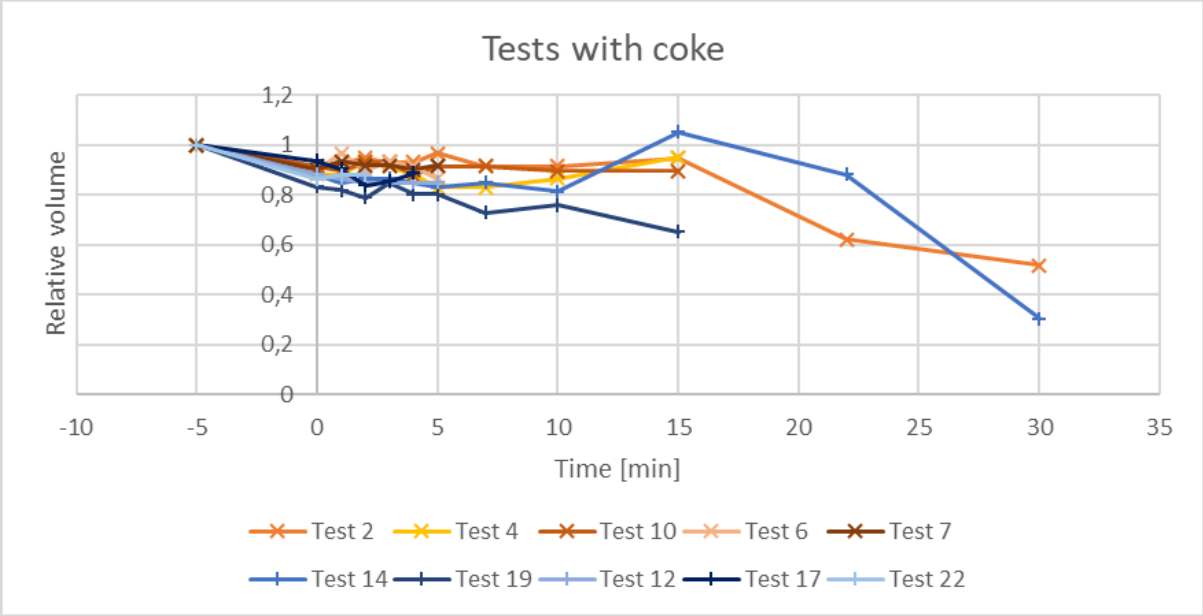

Figure 5.5.2.2: Relative volume development for all samples with coke. Orange lines are tests run with slag 1, blue lines are tests run with slag 2

Figure 5.5.2.1 shows that the tests run with slag 1 has similar developments of the relative volume, while the tests run with slag 2 has similar developments, if test 20 is omitted. There is a difference in relative volume development for the tests run with slag 1 and the tests run with slag 2, the tests run with slag 2 has lower values than the tests run with slag 1 at 15, 22 and 30 minutes.

Figure 5.5.2.2 shows that the tests run with slag 1 has a similar development of the relative volume while the tests run with slag 2 varies some. The high relative volume in test 14 at 15 and 22 minutes is likely caused by gas being trapped in the slag drop. When these high measurements are omitted, the difference between slag 1 and slag 2 is more clear. Slag 2 has lower values at 5, 7, 15 and 30 minutes than slag 1 has.

Figure 5.5.2.1 and 5.5.2.2 show that the tests run with slag 2 has lower relative volume values than the tests run with slag 1 for both charcoal and coke. Slag 2 contains more silicon oxide and manganese oxide than slag 1, which may be the reason for the higher volume decrease observed in the tests run with slag 2. Higher volume decrease indicates that more metal is produced for slag 2 than for slag 1 for both carbon materials, which is expected considering the increased content of manganese oxide and silicon oxide in slag 2.

5.6 Visual appearance and SEM imaging

Images of the samples taken after test and images from the SEM were presented in chapter 4. These images showed the visual appearance of the slag droplets, and the slag phase and metal phase magnified 1000 times in the SEM. The differences and similarities between visual appearance and appearance in SEM images are discussed in this section.

Table 5.6.1 lists an overview of the tests run and the observations from the tests. Visual observation can be transparent orange color (t.o.), pale green color (p.g.) or the sample has areas of both (both). The SEM results can be glassy slag (gl), two-phase slag (2ph) or both (both). The carbon materials are either charcoal (ch) or coke (co).

Table 5.6.1: Overview of observations of all tests. Abbreviations: t.o - transparent orange, p.g - pale green, gl - glassy slag, 2ph - two phase slag, ch - charcoal, co - coke

Nr	**Time**	**Visual**	**SEM**	**C-mat**	**Slag**	***Nr***	**Time**	**Visual**	**SEM**	**C-mat**	**Slag**
1	30	t.o.	gl	ch	1	*2*	30	p.g.	gl	co	1
3	15	t.o.	gl	ch	1	*4*	15	t.o.	gl	co	1
9	15	t.o.	gl	ch	1	*10*	15	t.o.	gl	co	1
5	5	both*	2ph	ch	1	*6*	5	both	both	co	1
8	5	both	both	ch	1	*7*	5	both	both	co	1
Nr	**Time**	**Visual**	**SEM**	**C-mat**	**Slag**	***Nr***	**Time**	**Visual**	**SEM**	**C-mat**	**Slag**
11	30	t.o.	gl	ch	2	*14*	30	p.g.	gl	co	2
15	15	t.o.	gl	ch	2	*19*	15	t.o.	gl	co	2
16	15	t.o.	gl	ch	2	*12*	5	both	both	co	2
20	15	t.o.	gl	ch	2	*17*	4	p.g.	2ph	co	2
18	5	p.g.	2ph	ch	2	*22*	2,5	p.g.	2ph	co	2
21	5	p.g.	2ph	ch	2	*13*	0	p.g.	2ph	co	2

*Sample 5 only had little orange color in the slag drop, mostly pale green

Table 5.6.1 shows that all samples that had transparent orange color were observed to have glassy slag, while the samples that had pale green non-transparent color were observed to have two-phase slag. The samples that had both orange transparent and pale green color of the slag drop had both glassy and two-phase slag, and there was observed a transition from two-phase to glassy slag where the size of the pattern in the two-phase slag decreased closer to the glassy slag, and increased further away from the glassy slag.

The table also shows that all samples that had a reduction time of 30 and 15 minutes had glassy slag. These samples had transparent orange color, except for the two samples run with coke for 30 minutes, which had pale green non-transparent color. Four samples run with five minutes hold time had both glassy and two-phase slag. Of these samples, two were run with coke and slag 1, one with coke an slag 2 and one with charcoal and slag 1. This could indicate that 5 minutes reduction time is in the transition between two-phase slag and glassy slag. The last samples, three with coke and slag 2 with less than 5 minutes reduction time, two with charcoal and slag 2 with reduction time of 5 minutes and one with charcoal and slag 1 with 5 minutes reduction time, had pale green color and two-phase slag.

These results indicate that the tests run with charcoal have a transition area between two-phase and glassy slag between 5 and 15 minutes, a bit sooner for slag 2 than for slag 1. The tests run with coke is indicated to have a transition area between two-phase and glassy slag around 5 minutes hold time for both slag 1 and slag 2. The tests run with slag 1 indicate that the transition area between two-phase and glassy slag is around five minutes, and that it starts a bit sooner with coke than with charcoal. The tests run with slag 2 indicate that the transition area between two-phase and glassy slag is around five minutes for coke and a bit later for charcoal.

The results overall indicate that the transition between the two-phase and glassy slag starts sooner for tests run with coke than for tests run with charcoal for both slags, and that the transition starts sooner with slag 1 than with slag 2 towards charcoal, while there is no clear difference between slag 1 and slag 2 towards coke. Faster transition to glassy slag could indicate that the reduction rate is initially high. This could mean that the reduction rate is initially higher on coke than on charcoal and initially higher for slag 1 than for slag 2 on charcoal. An attempt at visualising the difference in colors and the transition area for tests run with coke and charcoal is shown in figure 5.6.1, where green indicates pale green color, striped indicates both colors and orange indicates transparent orange color of the samples.

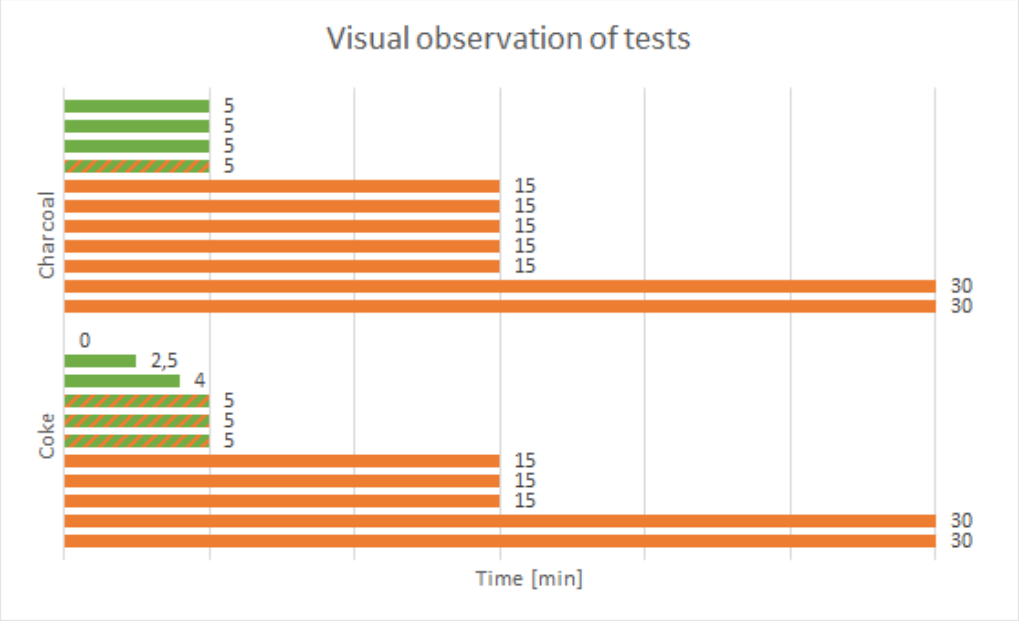

Figure 5.6.1: Difference between visual observation for tests run with charcoal and tests run with coke. Indicates if samples had pale green, transparent orange or both colors

5.7 Slag and metal composition

The content of manganese oxide in the slag and the content of silicon in the metal are used to gain information about the reduction of manganese oxide and silicon oxide. In this section, the MnO content in the slag and the Si content in the metal is compared for the two carbon materials and for the two slags.

5.7.1 Comparison of MnO and Si content for charcoal and coke

Figure 5.7.1.1 shows the content of manganese oxide in the slag for all tests run with slag 1, while figure 5.7.1.2 shows the manganese oxide content in the slag for all tests run with slag 2 Tests run with charcoal have blue point indicators and tests run with coke have orange point indicators in both figures.

Figure 5.7.1.1: MnO content in slag for all tests run with slag 1

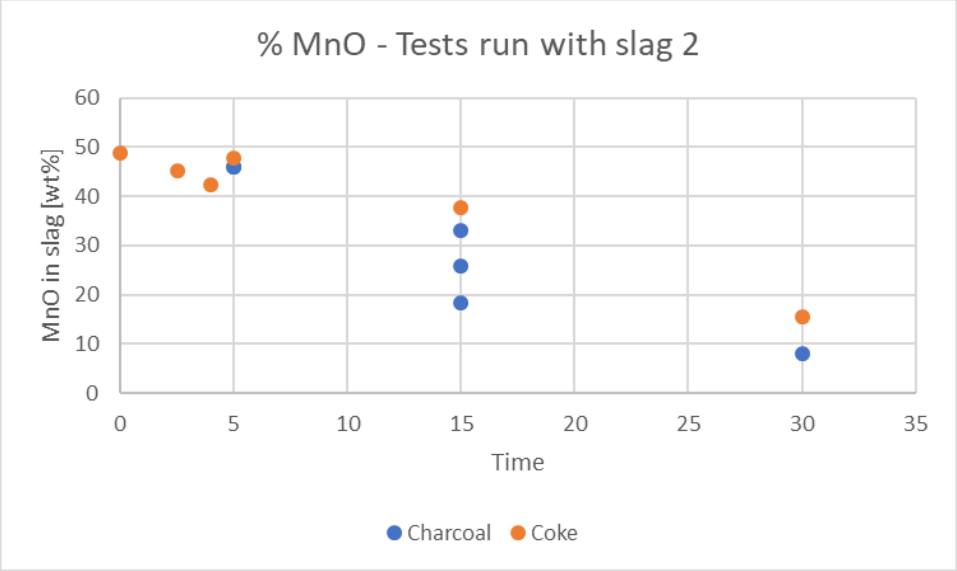

Figure 5.7.1.2: MnO content in slag for all tests run with slag 2

Figure 5.7.1.1 shows that both carbon materials have a decreasing content of manganese oxide in the slag with increasing time. The difference between the tests run with charcoal and the tests run with coke is low at 5 and 30 minutes, while the difference is higher at 15 minutes. Tests run with charcoal has lower content of manganese oxide in the slag at 15 minutes than the tests run with coke, which indicates that the reduction rate of manganese oxide is higher towards charcoal than towards coke for slag 1 at 15 minutes. However, as there is little difference at 30 minutes, no clear trend can be observed between charcoal and coke as reducing agent for slag 1.

Figure 5.7.1.2 shows that the content of manganese oxide in the slag decrease with time for both charcoal and coke, and that the content of manganese oxide is lower for the tests run with charcoal than for the tests run with coke at both 15 and 30 minutes reduction time. This indicates that the reduction rate of manganese oxide is higher towards charcoal than towards coke for slag 2.

The figures show that the reduction rate of manganese oxide is higher when charcoal is used as substrate than when coke is used as substrate, at 15 minutes for slag 1, and at 15 and 30 minutes for slag 2. This could indicate that charcoal is a better reducing agent for manganese oxide in both the silicomanganese slags, however, the trend is not clear for slag 1. In the specialisation project [25] coke was found to be a better reducing agent for silicomanganese slag than charcoal, which is the opposite results as what is presented here. This is unexpected considering that the experimental work has been performed similarly in the two projects, but there are some things that are different between the projects that can explain the results.

Two cokes and two charcoals were used in the specialisation project while only one of the cokes was used in this project, and the hold times varied between charcoal and coke in the specialisation project while the same hold times were achieved in this project. This, in addition to not all results from the coke experiments being plotted in the specialisation project made the results a bit difficult to assess, and the amount of experiments was also lower.

The experiments in this project were performed with two slags. Slag 1 was the same slag that was used in the specialisation project, and the results shown in figure 5.7.1.1 does not show a clear trend regarding the difference between charcoal and coke as reducing agent. Slag 2, that was only used in this project shows a clear trend of charcoal being a better reducing agent than coke. This could indicate that the increased content of manganese oxide and silicon oxide in slag 2 increased the difference between charcoal and coke as reducing agent. The results found for slag 2 in this project confirms the results of Safarian in 2007 and 2008, and the findings of Tranell et al in 2007. However, these three studies were performed with HC FeMn slag, and without pelletising the carbon substrates.

Figure 5.7.1.3. shows the calculated silicon content in the metal for all tests run with slag 1, while figure 5.7.1.4 shows the calculated silicon content in the metal for all tests run with slag 2. The tests run with charcoal has blue point indicators and the tests run with coke has orange point indicators in both figures.

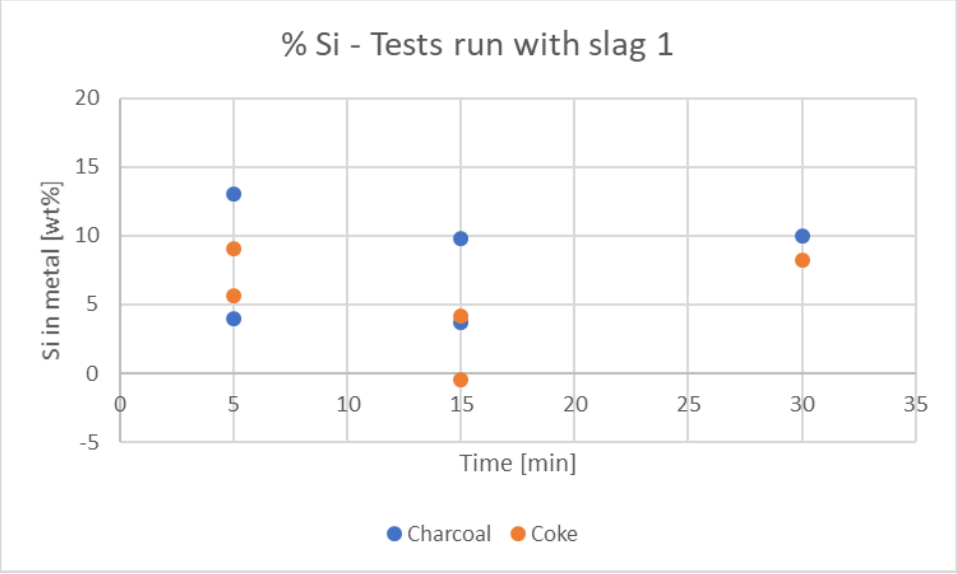

Figure 5.7.1.3: Calculated Si content in metal for all tests run with slag 1

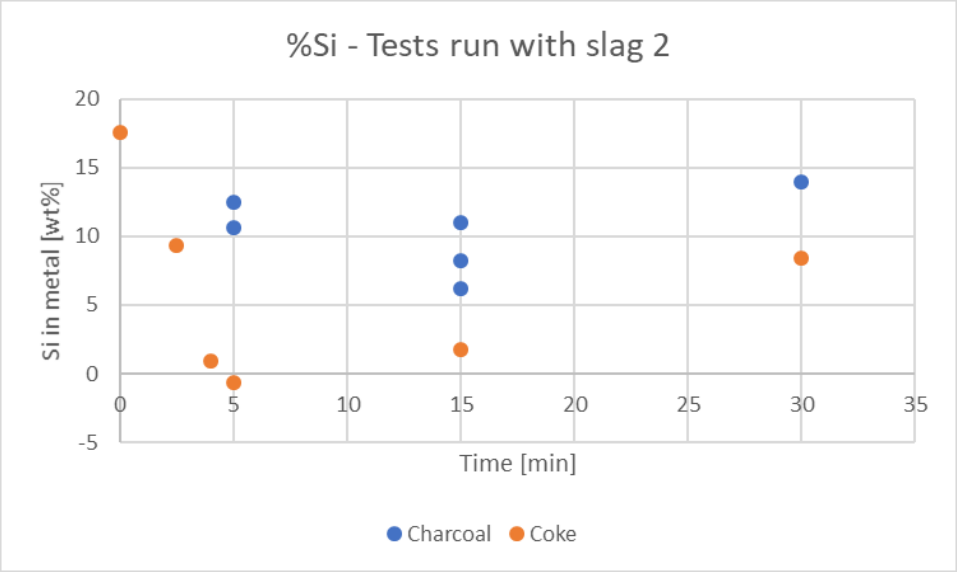

Figure 5.7.1.4: Calculated Si content in metal for all tests run with slag 2

Figure 5.7.1.3 shows that there is high variation between the measurements of silicon in the metal for tests that had the same reduction time and same carbon material. In addition, one of the tests run with coke for 5 minutes has negative calculated silicon content, which is a false measurement. It is assumed that this sample has a low positive content of silicon in the metal. The silicon content in the metal should increase with increasing reduction time, which does not seem to be the case for the results in figure 5.7.1.3. The tests run with charcoal has higher content of silicon in the metal than tests run with coke at 15 and 30 minutes, which could indicate that the reduction rate of silicon oxide from slag 1 is higher when charcoal is used as reduction agent than when coke is used as reduction agent.

Figure 5.7.1.4 shows that there is lower variation between the measurements of silicon in the metal for tests that had the same reduction time and same carbon material when slag 2 was used than when slag 1 was used. One of the tests run with coke and 5 minutes hold time has negative calculated silicon content in the metal, this is a false measurement. The test is assumed to have low positive silicon content in the metal. The silicon content in the metal increase with time when coke is used, and from 15 to 30 minutes when charcoal is used. The tests run with charcoal has higher content of silicon in the metal than the tests run with coke at 5, 15 and 30 minutes reduction time. This indicates that the reduction of silicon oxide is higher when charcoal is used as substrate than when coke is used as substrate for tests run with slag 2.

The figures show that the tests run with charcoal has higher content of silicon in the metal than the tests run with coke for both slags, which could indicate that the reduction rate of silicon oxide is higher when charcoal is used as reduction agent than when coke is used as reduction agent. The results of the specialisation project [25] showed that the tests run with coke had higher content of silicon in the metal than the tests run with charcoal, which is the opposite of what is found in this project. Some of the differences between the two projects were mentioned earlier, and could contribute to the different results obtained. The silicon content in the metal is also a difficult variable to assess, as it is affected by the manganese content in the metal which is also changing with time. This can be seen in figures 5.7.1.3 and 5.7.1.4, where the expected trend of the silicon content increasing with time for all tests is not present in either figure.

5.7.2 Comparison of MnO and Si content for slag 1 and slag 2

Figure 5.7.2.1 shows the content of manganese oxide in the slag for all tests run with charcoal, while figure 5.7.2.2 shows the content of manganese oxide in the slag for all tests run with coke. The tests run with slag 1 have blue point markers and the tests run with slag 2 have orange point markers in both figures.

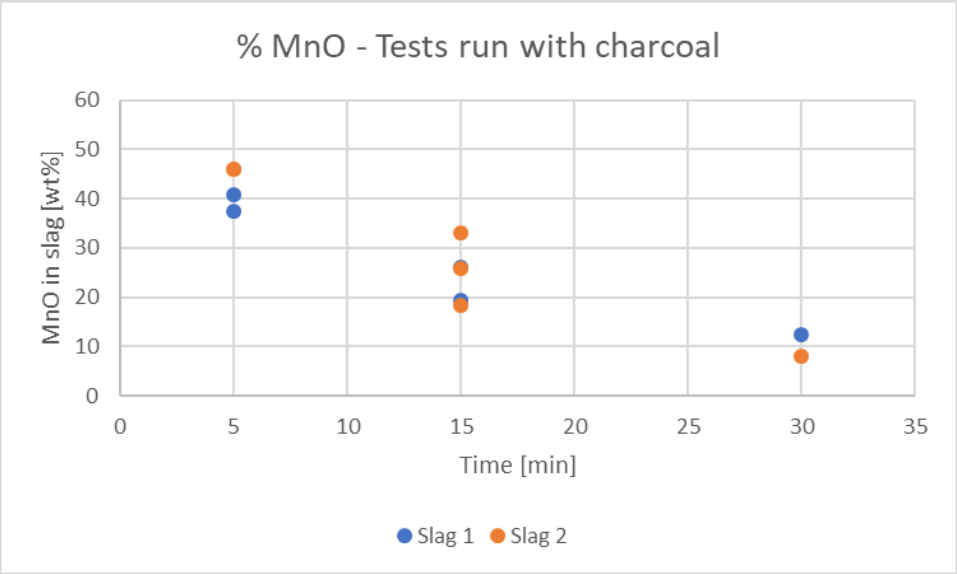

Figure 5.7.2.1: MnO content in slag for all tests run with charcoal

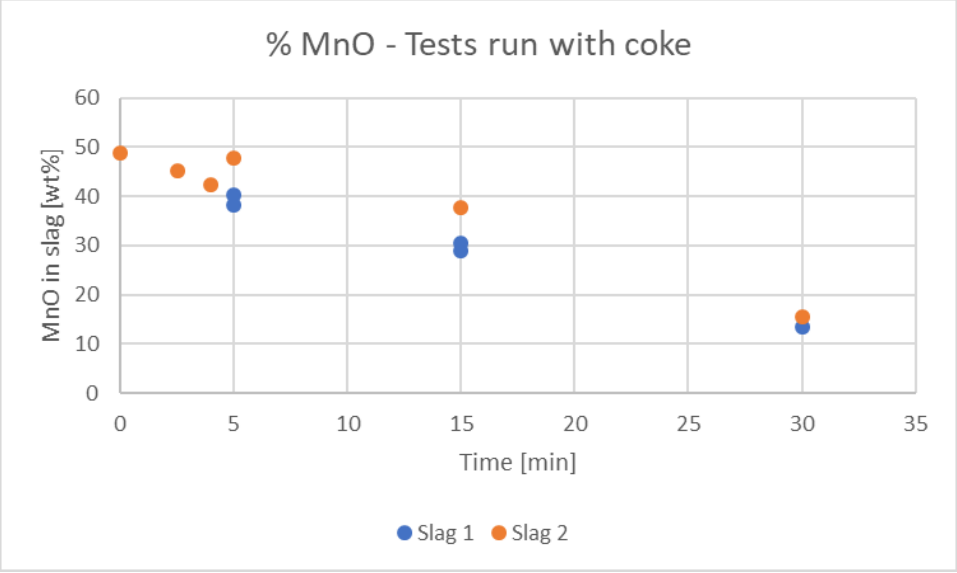

Figure 5.7.2.2: MnO content in slag for all tests run with coke

Figure 5.7.2.1 shows that there is little variation in manganese oxide content in the slag between the tests run with slag 1 and the tests run with slag 2 at 15 minutes, while slag 1 has lower content at 5 minutes and slag 2 has lower content at 30 minutes. The content of manganese oxide decrease with increasing reduction time for both slags, but there is no clear trend of one slag having lower content of manganese oxide for all reduction times when charcoal is used as reduction agent.

Figure 5.7.2.2 shows that the tests run with slag 1 has lower content of manganese oxide in the slag than the tests run with slag 2 when coke is used as reducing agent. This indicates that the reduction rate of manganese oxide is higher for the tests run with coke and slag 1 than with coke and slag 2, but the difference is not so high.

The figures show that the difference in manganese oxide content in the slag between the tests run with slag 1 and the tests run with slag 2 is insignificant when charcoal is used as reducing agent, while the difference between tests run with slag 1 and tests run with slag 2 is significant when coke is used as reducing agent. This indicates that the reduction of manganese oxide is affected by which slag is used when coke is the reducing agent, but is not affected by which slag is used when charcoal is the reducing agent.

Figure 5.7.2.3 shows the calculated silicon content in the metal for all tests run with charcoal, while figure 5.7.2.4 shows the calculated silicon content in the metal for all tests run with coke. Tests run with slag 1 have blue point indicators and tests run with slag 2 have orange point indicators in both figures.

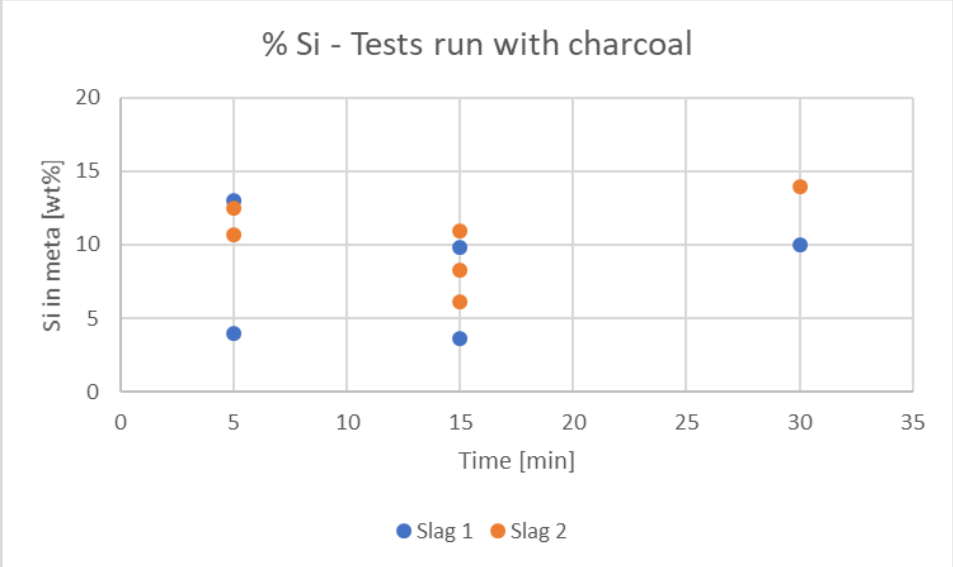

Figure 5.7.2.3: Calculated Si content in metal for all tests run with charcoal

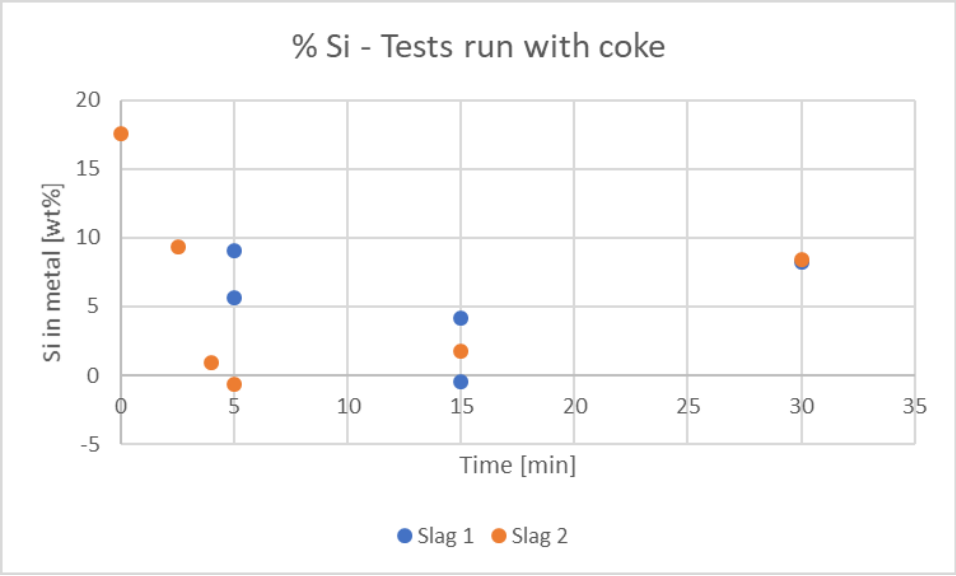

Figure 5.7.2.4: Calculated Si content in metal for all tests run with coke

Figure 5.7.2.3 shows that the variation in calculated silicon content is high between the two tests run with slag 1 and 5 minutes hold time, and between the two tests run with slag 1 and 15 minutes hold time. The tests run with slag 2 also has some variation at the same reduction times, but the variation is lower. It is difficult to observe a clear trend in this figure, but the tests run with slag 2 has highest silicon content in the metal at 15 and 30 minutes, which could indicate that the reduction rate of silicon oxide towards charcoal is higher when slag 2 is used than when slag 1 is used.

Figure 5.7.2.4 shows the calculated silicon content in the metal for tests run with coke. A test run with slag 2 and 5 minutes reduction time and a tests run with slag 1 and 15 minutes reduction time have negative silicon content, which are false measurements. These tests are assumed to have low positive content of silicon in the metal. It is difficult to observe a trend from figure 5.7.2.4, it is expected that the silicon content increase with time from start, which does not seem to be the case in this figure. The tests run with slag 1 has higher content of silicon in the metal at 5 and 15 minutes, which could indicate that the reduction rate of silicon oxide was higher towards coke when slag 1 was used than when slag 2 was used.

The figures shows that the development of silicon content in the metal does not necessarily follow the expected trend, and that this is a difficult variable to assess. The results that can be observed from the figures are that the tests run with charcoal has higher content of silicon when slag 2 is used than when slag 1 is used, and that the tests run with coke seems to have higher silicon content when slag 1 is used than when slag 2 is used. Considering the increased content of silicon oxide in slag 2, the silicon content is expected to be higher for tests run with slag 2 than for tests run with slag 1. This was the case when charcoal was used as reducing agent, but not when coke was used as reducing agent.

5.7.3 Weight of MnO and SiO_2 in the slag

The weight of manganese oxide and silicon oxide shows how the reduction develops isolated, as opposed to the weight percentage where the reduction of the other oxide affects the content of manganese oxide in the slag and content of silicon in the metal.

Figure 5.7.3.1 shows the weight of MnO and SiO_2 in the slag for tests run with charcoal and slag 1, figure 5.7.3.2 shows the weight of MnO and SiO_2 in the slag for tests run with charcoal and slag 2, figure 5.7.3.3 shows the weight of MnO and SiO_2 in the slag for tests run with coke and slag 1, and figure 5.7.3.4 shows the weight of MnO and SiO_2 in the slag for tests run with coke and slag 2. The blue point indicators shows the content of manganese oxide and the orange point indicators shows the content of silicon oxide in the slag, in all four figures.

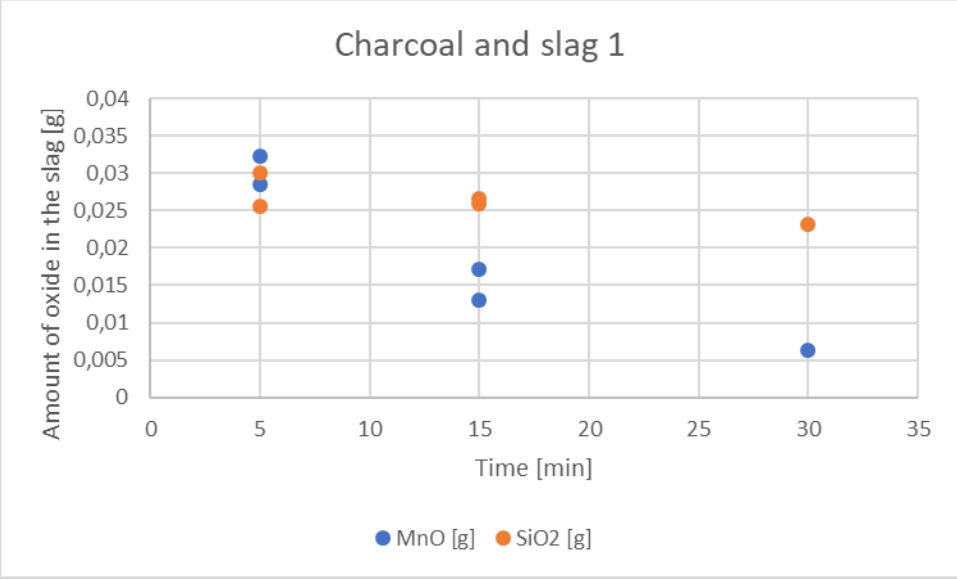

Figure 5.7.3.1: MnO and SiO_2 content in slag for tests run with charcoal and slag 1

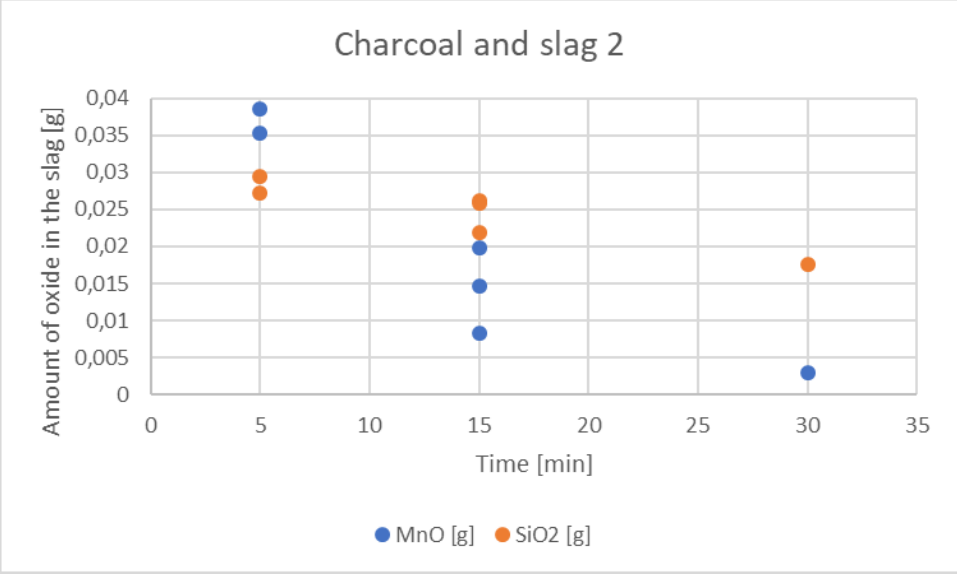

Figure 5.7.3.2: MnO and SiO_2 content in slag for tests run with charcoal and slag 2

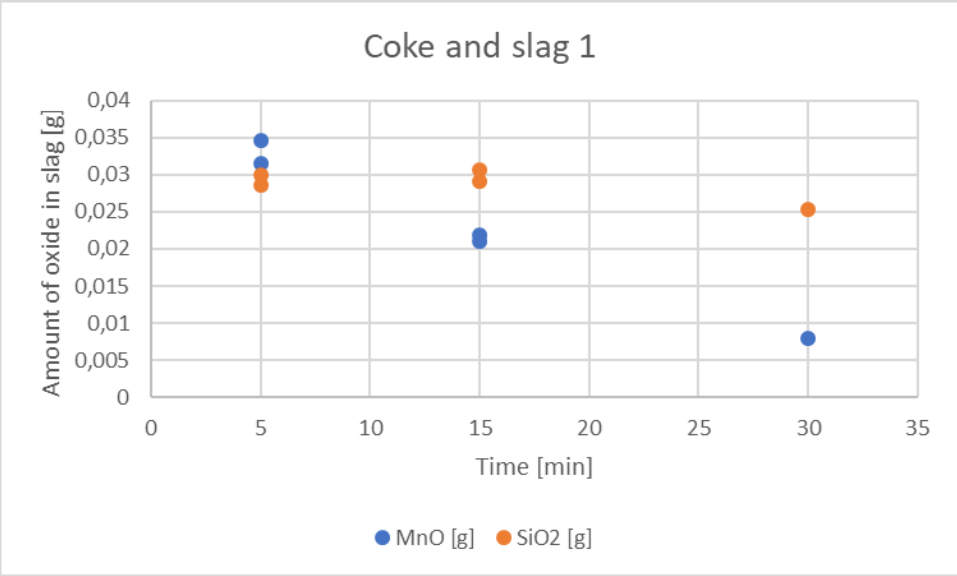

Figure 5.7.3.3: MnO and SiO_2 content in slag for tests run with charcoal and slag 1

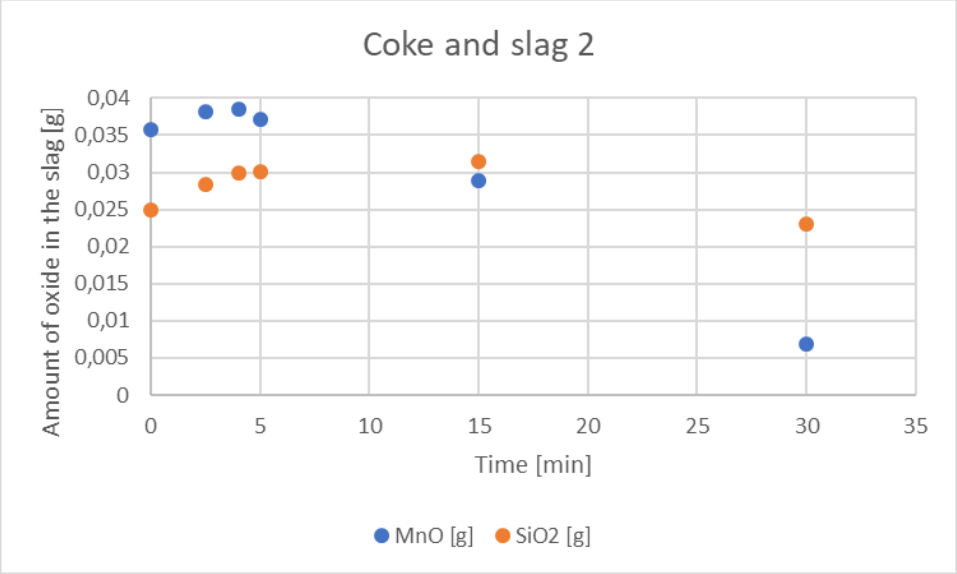

Figure 5.7.3.4: MnO and SiO_2 content in slag for tests run with charcoal and slag 2

The weights of manganese oxide and silicon oxide plotted in these figures are calculated from the slag analysis performed in EPMA. The figures show similar trends, the content of manganese oxide decreases with time for the whole reduction time. The tests run with coke has approximately the same slope throughout the tests for both slags, while the tests run with charcoal has a bit higher slope between 5 and 15 minutes than between 15 and 30 minutes for both slags. The manganese oxide is expected to decrease with time for the whole test, however the tests run with charcoal seems to have a higher initial reduction rate of manganese oxide than the tests run with coke.

The silicon oxide content has the same trend in the four figures, it only shows small variations from 5 to 15 minutes, and then decrease from 15 to 30 minutes. This indicates that the reduction of silicon oxide starts later than the reduction of manganese oxide. This may be because the reduction of SiO_2 occurs at higher temperatures than reduction of MnO.

Figure 5.7.3.5 shows the manganese oxide content for all tests and figure 5.7.3.6 shows the silicon oxide content for all tests. Tests run with charcoal and slag 1 has blue point indicators, tests run with charcoal and slag 2 has green point indicators, tests run with coke and slag 2 has orange point indicators and tests run with coke and slag 2 have yellow point indicators, in both figures.

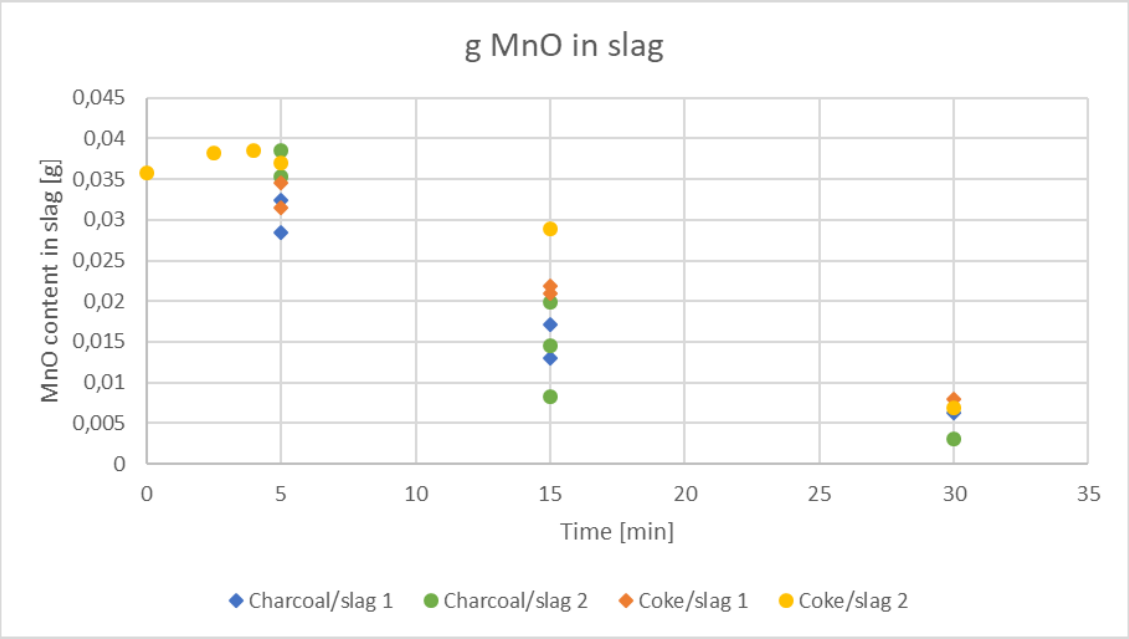

Figure 5.7.3.5: Manganese oxide content in slag for all tests

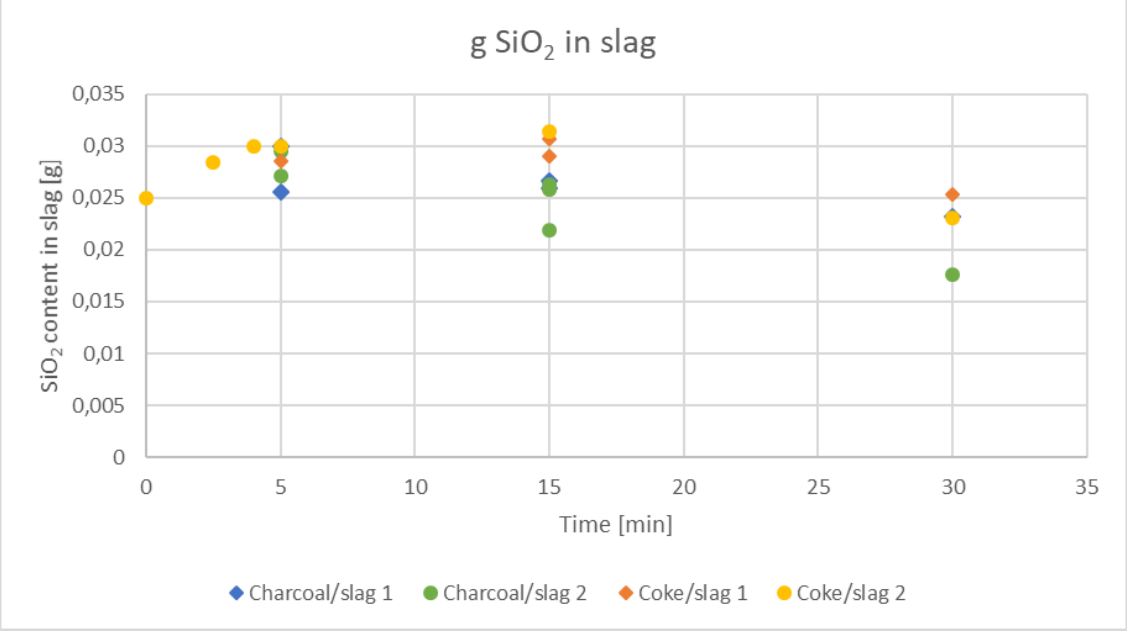

Figure 5.7.3.6: Silicon oxidde content in slag for all tests

Figure 5.7.3.5 shows that the tests run with charcoal and slag 2 has the highest decrease in manganese oxide content in the slag between 5 and 15 minutes, while the tests run with coke and slag 2 has the highest decrease in manganese oxide content between 15 and 30 minutes. In addition, the tests run with slag 2 has higher decrease in manganese oxide content from 5 to 30 minutes than the tests with slag 1 has. This indicates that the reduction

rate is higher for slag 2 than for slag 1 for both carbon materials, which is expected considering the increased content of manganese oxide in slag 2. The results also indicate that the reduction rate is initially higher when charcoal is used as reducing agent, from 5 to 15 minutes for both slags, and higher between 15 and 30 minutes when coke is used as reducing agent.

Figure 5.7.3.6 shows that tests run with slag 2 has higher decrease in silicon oxide content from 15 to 30 minutes than the tests run with slag 1. This is expected considering the increased content of silicon oxide in slag 2. The tests run with charcoal and slag 2 has the highest decrease in silicon oxide content throughout the test

The figures shows that the content of manganese oxide and silicon oxide decrease more when slag 2 is used than when slag 1 is used for both slags. This is likely due to the increased content of manganese oxide and silicon oxide in slag 2 compared to slag 1. The figures also shows that the reduction of manganese oxide is initially higher when charcoal is used as reducing agent, and higher between 15 and 30 minutes when coke is used as reducing agent. This indicates that the reduction of manganese oxide starts earlier for tests where charcoal is used, but then decrease some while the reduction increase for tests where coke is used. The total reduction of manganese oxide is similar when charcoal and coke is used, however, the reduction is higher when slag 2 is used than when slag 1 is used.

5.8 Reduction degrees for manganese and silicon

The reduction degrees for manganese and silicon for all tests are presented and discussed in this section. The reduction degree of manganese is defined as $R_{Mn} = wt_{Mn,red} / wt_{Mn,tot}$, and the calculated maximum values are $R_{Mn,max} = 0,954$ for slag 1 and $R_{Mn,max} = 0,964$ for slag 2. The reduction degree of silicon is defined as $R_{Si} = wt_{Si,red} / wt_{Mn,tot}$, and the calculated maximum values are $R_{Si,max} = 0,186$ for slag 1 and $R_{Si,max} = 0,224$ for slag 2.

5.8.1 Comparison of reduction degrees for charcoal and coke

Figure 5.8.1.1 shows the reduction degree of manganese for all tests run with slag 1, and figure 5.8.1.2 shows the reduction degree of manganese for all tests run with slag 2. The tests run with charcoal has blue point indicators and the tests run with coke has orange point indicators in both figures.

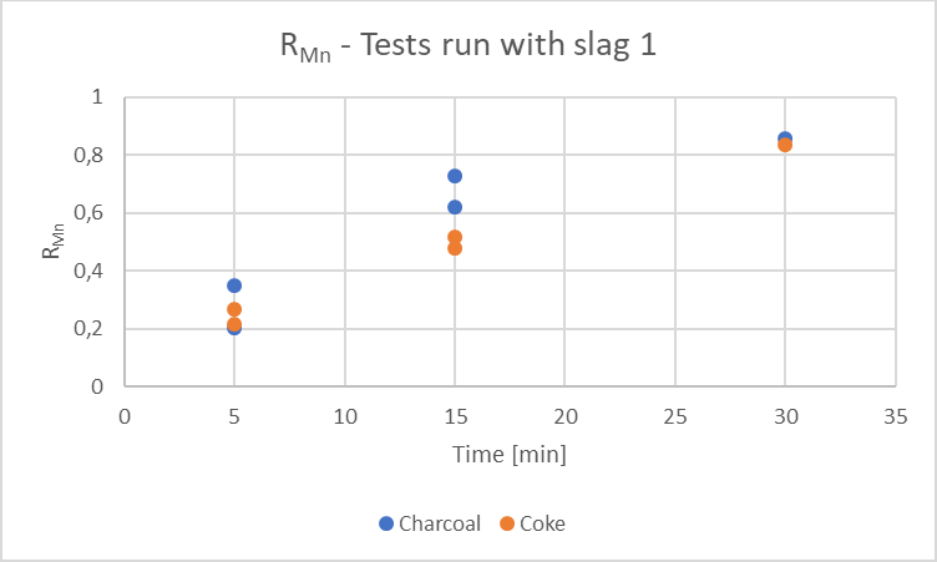

Figure 5.8.1.1: Reduction degree of manganese for all tests run with slag 1

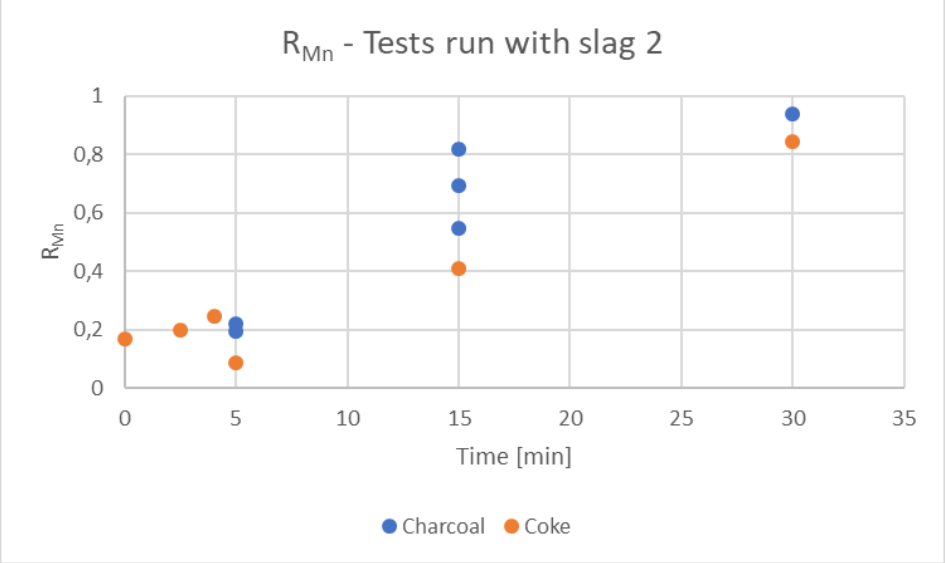

Figure 5.8.1.2: Reduction degree of manganese for all tests run with slag 2

Figure 5.8.1.1 shows that the reduction degree of manganese increase with time both for tests run with charcoal and tests run with coke when slag 1 is used, as is expected. The reduction degree of manganese is higher for the tests run with charcoal than for the tests run with coke at 5 and 15 minutes, while the reduction degree is similar for the test run with charcoal and the test run with coke for 30 minutes. This indicates that the reduction rate of manganese oxide is higher for the tests run with charcoal than the tests run with coke.

Figure 5.8.1.2 shows that the reduction degree of manganese increase with time for tests run with both charcoal and coke when slag 2 is used, as is expected. The reduction degree of manganese is significantly higher for the tests run with charcoal than for the tests run with coke at 15 and 30 minutes, which indicates that the reduction rate of manganese oxide is higher for the tests run with charcoal than the tests run with coke.

The figures shows that the reduction degree of manganese is higher for tests run with charcoal than for tests run with coke for both slags. The differences in reduction degree between tests with charcoal and tests with coke seems to be higher in figure 5.8.1.2 for slag 2 than in figure 5.8.1.1 for slag 1. The results indicates that charcoal is a better reducing agent than coke for both slags. This confirms the findings of Safarian in 2007 [17], Safarian et al. in 2008 [18], and the findings of Tranell et al. in 2007 [16]. However, these studies used high-carbon ferromanganese slag and did not pelletise the carbon material.

Figure 5.8.1.3 shows the reduction degree of silicon for all tests run with slag 1, while figure 5.8.1.4 shows the reduction degree of silicon for all tests run with slag 2. The tests run with charcoal has blue point markers and the tests run with coke has orange point markers, in both figures.

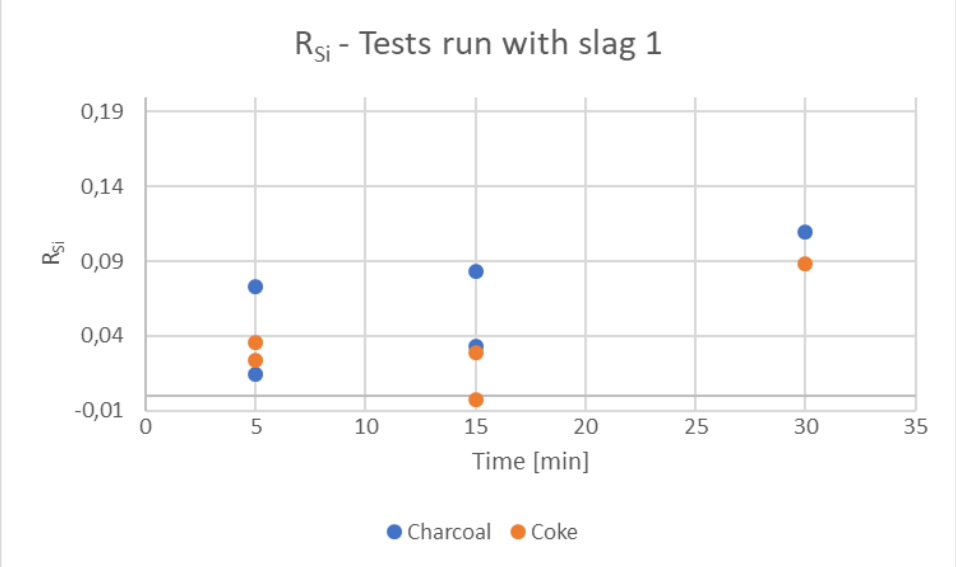

Figure 5.8.1.3: Reduction degree of silicon for tests run with slag 1

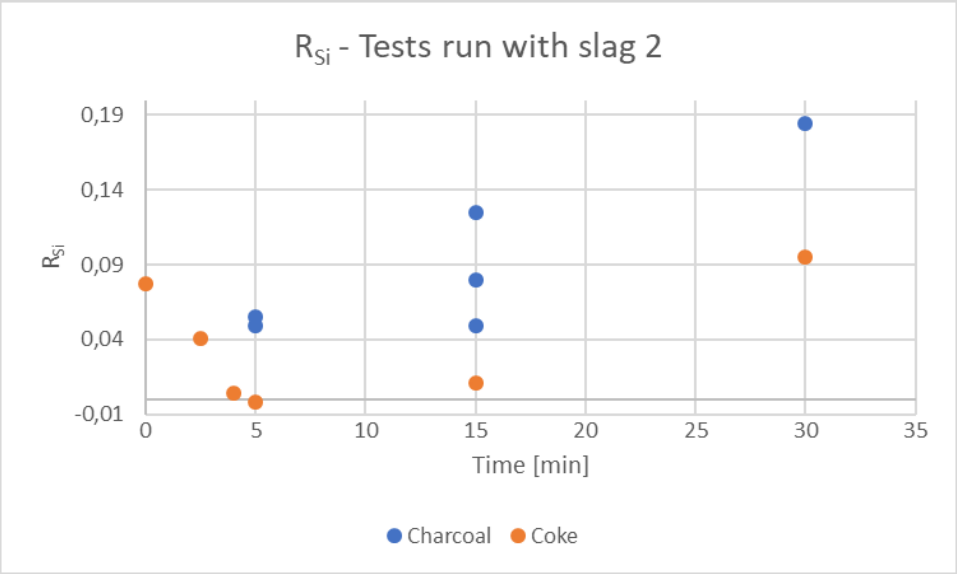

Figure 5.8.1.4: Reduction degree of silicon for tests run with slag 2

Figure 5.8.1.3 shows that one of the tests run with slag 1 and coke for 15 minutes has a negative reduction degree of silicon, which is a result of negative calculated silicon content in the metal. This test is therefore assumed to have a low positive reduction degree of silicon. The tests run with charcoal have higher reduction degrees of silicon at 5, 15 and 30 minutes than the tests run with coke has. This indicates that the reduction rate of silicon oxide from slag 1 is higher when charcoal is used as reducing agent, than when coke is used as reducing agent.

Figure 5.8.1.4 shows that one of the tests run with slag 1 and charcoal for 5 minutes has a negative reduction degree of silicon, which is caused by a negative calculated silicon content in the metal. This test is therefore assumed to have a low positive reduction degree of silicon. The tests run with charcoal has higher reduction degrees of silicon at 5, 15 and 30 minutes than the tests run with coke has. This indicates that the reduction rate of silicon oxide from slag 2 is higher when charcoal is used as a reducing agent than when coke is used as a reducing agent.

The figures shows that the reduction degree of silicon is higher for tests run with charcoal than for tests run with coke for both slags. The difference between tests with charcoal and tests with coke seems to be higher in figure 5.8.1.4 for slag 2 than in figure 5.8.1.3 for slag 1. The results indicates that charcoal is a better reducing agent than coke for both slags.

5.8.2 Comparison of reduction degrees for slag 1 and slag 2

Figure 5.8.2.1 shows the reduction degree of manganese for all tests run with charcoal, while figure 5.8.2.2 shows the reduction degree of manganese for all tests run with coke. The tests run with slag 1 has blue point indicators and the tests run with slag 2 has orange point indicators, in both figures.

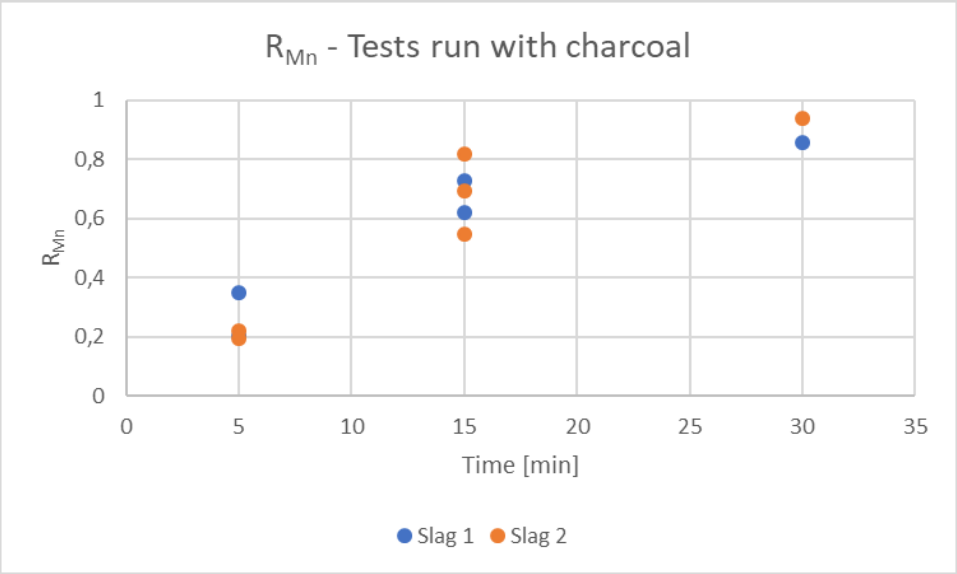

Figure 5.8.2.1: Reduction degree of manganese for tests run with charcoal

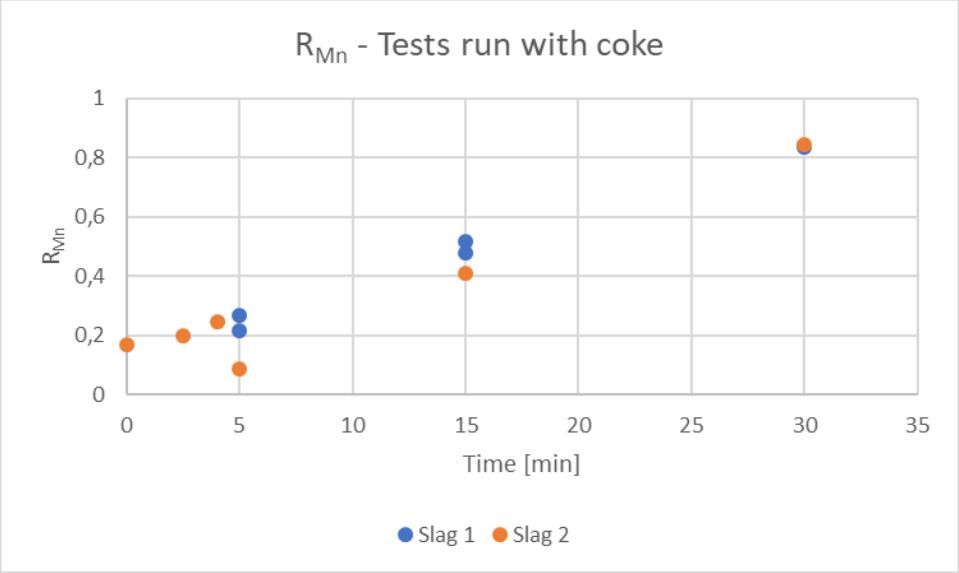

Figure 5.8.2.2: Reduction degree of manganese for tests run with coke

Figure 5.8.2.1 shows that the tests run with slag 1 has highest reduction degree of manganese at 5 minutes, and that the test run with slag 2 has highest reduction degree of manganese at 30 minutes. A clear trend of one slag having higher reduction degree of manganese than the other at all reduction times is not observed, however, the increase in reduction degree from 5 minutes reduction time to 30 minutes reduction time is higher for the tests run with slag 2 than for the tests run with slag 1.

Figure 5.8.2.2 shows that the reduction degree of manganese increase with time for both slags. The reduction degree of manganese is higher for the tests run with slag 1 than for the tests run with slag 2 at 5 and 15 minutes, but there is no significant difference between the test run with slag 1 and slag 2 at 30 minutes. The difference between the tests run with slag 1 and the tests run with slag 2 decrease with time. This indicates that the reduction rate of manganese oxide is higher towards coke when slag 1 is used than when slag 2 is used, but that the reduction degree of increases more from 5 to 30 minutes when slag 2 is used than when slag 1 is used.

The figures shows that the reduction degree of manganese increases more from 5 to 30 minutes when slag 2 is used than when slag 1 is used, for both charcoal and coke. This indicates that the initial reduction rate of manganese oxide is higher from slag 1 than from slag 2, but that the reduction rate from 5 to 30 minutes is higher when slag 2 is used than when slag 1 is used for both carbon materials.

Figure 5.8.2.3. shows the reduction degree of silicon for all tests run with charcoal, while figure 5.8.2.4 shows the reduction degree of silicon for all tests run with coke. The tests run with slag 1 has blue point indicators and the tests run with slag 2 has orange point indicators, in both figures.

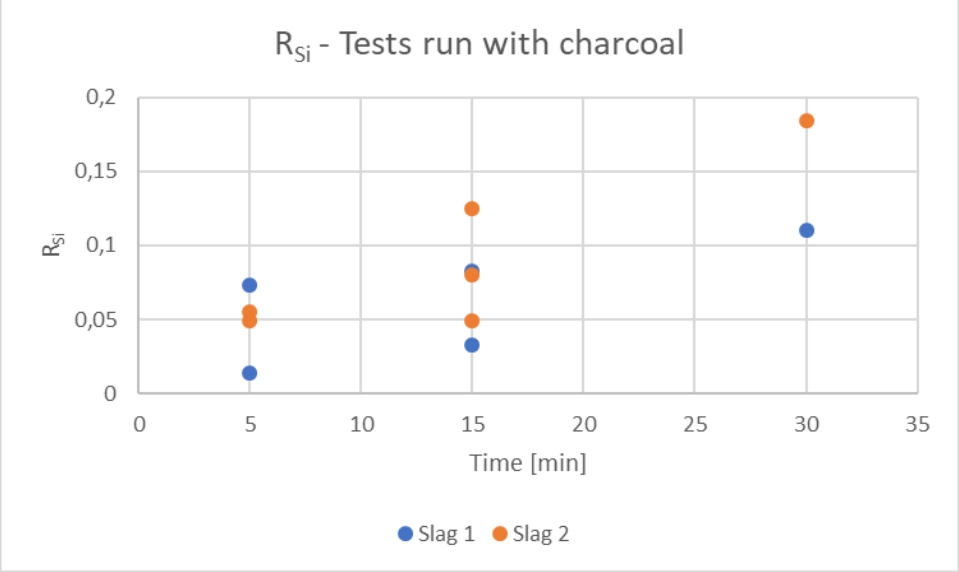

Figure 5.8.2.3: Reduction degree of silicon for tests run with charcoal

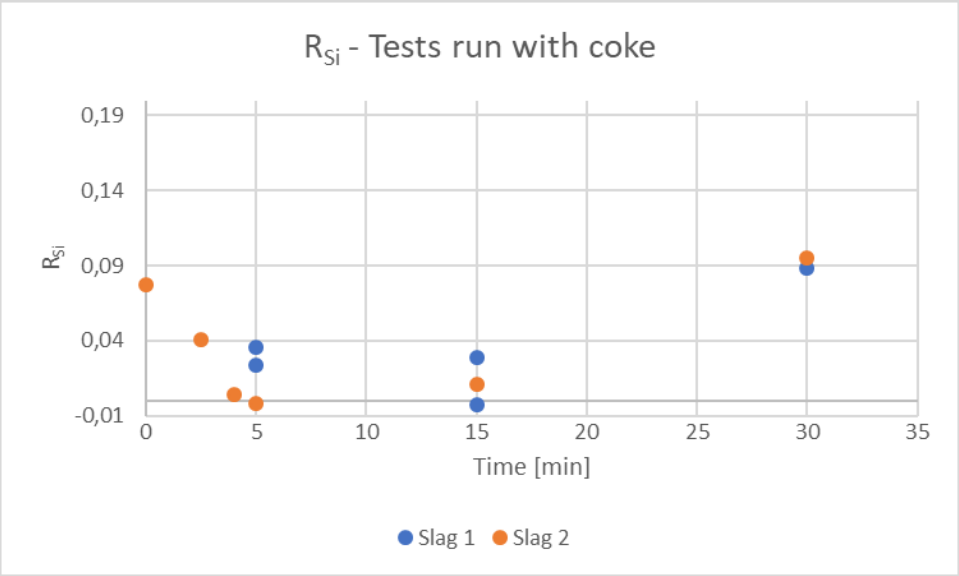

Figure 5.8.2.4: Reduction degree of silicon for tests run with coke

Figure 5.8.2.3 shows that the reduction degree of silicon increase with increasing reduction time, and that the tests run with slag 2 has significantly higher reduction degrees than the tests run with slag 1 at 15 and 30 minutes. This indicates that the reduction rate of silicon is higher towards charcoal for slag 2 than for slag 1. This is expected considering the increased content of silicon oxide in slag 2. This also indicates that the test run with slag 2 has higher content of silicon in the metal after 30 minutes than the test run with slag 1.

Figure 5.8.2.4 shows that a test run with slag 2 for 5 minutes and a test run with slag 1 for 15 minutes has negative reduction degrees of silicon. This is due to negative calculated silicon content in the metal, and these tests are therefore assumed to have low positive reduction degrees of silicon. The tests run with slag 1 has higher reduction degree of silicon at 5 and 15 minutes, while the tests run with slag 2 has higher reduction degree of silicon at 30 minutes. This could indicate that the reduction degree of silicon is initially higher for slag 1 and that it increases more with time for slag 2, but it is difficult to say for sure.

The figures show that the reduction degree of silicon is higher for slag 2 than for slag 1 when charcoal is used as reducing agent, and that the reduction degree of silicon seems to be initially higher for slag 1 than for slag 2 when coke is used as reducing agent. Further, that the reduction degree increases more with time for slag 2 than for slag 1 when coke is used. That slag 2 has higher reduction degree than slag 1 towards charcoal is expected considering the increased content of silicon oxide in slag 2. The difference in silicon oxide between the two slags could also explain why slag 2 seems to increase the reduction degree with time more than slag 1 towards coke.

6. Conclusions

The moisture loss and density of all charcoal and coke pellets that were made during the project were measured. The results showed that the charcoal pellets had higher moisture loss than the coke pellets, which was concluded to be due to the difference in water added to the pellet mix. The charcoal mix was added 60% water, while the coke pellet mix was added 30% water. The results of the density measurements showed that the coke pellets had almost twice as high density as the charcoal pellets, which was concluded to be due to the different density of the two materials used.

The weight loss was measured for all the 22 tests that were performed. The results showed that the weight loss of the slag drop and carbon pellet was higher for the tests run with charcoal than for the tests run with coke. This was concluded to be due to the increased content of volatile matters in charcoal compared to coke, and due to increased reduction of manganese oxide and silicon oxide when charcoal was used as reducing agent. There was no clear difference between tests run with slag 1 and tests run with slag 2 for either carbon material.

The contact angle development was measured for all tests. The results showed that the contact angle was higher when coke was used as reducing agent than when charcoal was used as reducing agent, and the wetting of both slags was therefore concluded to be better towards charcoal than towards coke. For the tests run with charcoal, slag 2 had lower contact angle than slag 1, and slag 2 wetted charcoal better than slag 1 did. There was no clear difference between slag 1 and slag 2 towards coke.

The relative volume development was also measured for all tests. The results showed that the tests run with charcoal had lower relative volume values than tests run with coke for both slags, which indicates that the reduction of manganese oxide and silicon oxide was higher for tests run with charcoal than for tests run with coke. However, two factors were found to impact the slag drop volume measurement and decrease the accuracy of the results. Gas trapped in the slag drop increased the measured volume, while craters in the carbon pellet caused by reduction decreased the measured volume. Tests run with slag 2 were found to have lower relative volume values than tests run with slag 1, which was concluded to be due to the increased content of manganese oxide and silicon oxide in slag 2.

The visual appearance of the slag samples and the observations from SEM analysis were compared. This showed that pale green colored slag was two-phase and that the orange transparent colored slag was glassy. The transition area between two-phase and glassy slag was concluded to be at five minutes for tests run with coke, and a bit later for tests run with charcoal.

The content of manganese oxide in the slag was assessed for the tests. The results showed that the manganese oxide content of the slag was lower for tests run with charcoal than for tests run with coke and that the silicon content in the metal was higher for tests run with charcoal than for tests run with coke, for both slags. This was concluded to be due to higher

reduction rate of manganese oxide and silicon oxide when charcoal was used as reducing agent than when coke was used as reducing agent.

The results also showed that the manganese oxide content in the slag decreased faster when slag 2 was used than when slag 1 was used for both carbon materials, which was concluded to be due to the increased content of manganese oxide in slag 2. The silicon content in the metal was higher when slag 2 was used for charcoal, but not for coke. The silicon content in the metal was concluded to be difficult variable to assess.

The development of manganese oxide and silicon oxide on weight basis in the tests showed that the reduction of both oxides were higher when slag 2 was used than when slag 1 was used. This was concluded to be due to the difference in manganese oxide and silicon oxide content in the two slags. In addition, the initial reduction of manganese oxide between 5 and 15 minutes was observed to be higher when charcoal was used, however the total reduction was similar, and the reduction was higher from 15 to 30 minutes when coke was used.

The reduction degrees of manganese and silicon were calculated for the tests. The results showed that the reduction degree of manganese was higher for tests run with charcoal than for tests run with coke for both slags, and that the reduction degree of silicon was higher for tests run with charcoal than for tests run with coke. Charcoal was therefore concluded to be a better reducing agent than coke for both slags.

The results also showed that the reduction degree of manganese increased more when slag 2 was used than when slag 1 was used for both charcoal and coke. The reduction degree of silicon was higher for slag 2 than for slag 1 when charcoal was used as reducing agent, and the reduction degree of silicon increased more for slag 2 than for slag 1 when coke was used. This was concluded to be due to the increased content of silicon oxide in slag 2.

An objective of the master thesis was to see if a standard silicomanganese alloy could be produced. The content of silicon in the metal after 30 minutes reduction time was observed to be higher when slag 2 was used then when slag 1 was used, however, none of the tests reached a silicon content of the desired 18 wt%. A standard silicomanganese alloy was therefore not observed to be produced under the conditions applied in this project.

The main objective was to compare the reactivity of silicomanganese slag towards charcoal and towards coke. When considering all the results found in this study, the conclusion is that charcoal is a better reducing agent than coke, as the reduction rate of manganese oxide and silicon oxide from both silicomanganese slags are higher when charcoal is used as reducing agent. The reactivity of silicomanganese slag was higher towards charcoal than the reactivity towards coke was, for both slags.

7. References

[1] European Commission, “The Sustainable Development Goals,” *International Cooperation and Development - European Commission*, 22-Nov-2016. [Online]. Available: https://ec.europa.eu/europeaid/policies/sustainable-development-goals_en. [Accessed: 26-Sep-2018].

[2] European Commission, “Paris Agreement,” *Climate Action - European Commission*, 23-Nov-2016. [Online]. Available: https://ec.europa.eu/clima/policies/international/negotiations/paris_en. [Accessed: 26-Sep-2018].

[3] Miljøstatus i Norge, “Parisavtalen.” [Online]. Available: http://www.miljostatus.no/tema/klima/internasjonal-klimapolitikk/parisavtalen/. [Accessed: 26-Sep-2018].

[4] Royal Society of Chemistry, “Manganese - Element information, properties and uses,” *Periodic Table*, 2019. [Online]. Available: http://www.rsc.org/periodic-table/element/25/manganese. [Accessed: 07-Feb-2019].

[5] M. Tangstad, *Metal Production in Norway*. Trondheim: Akademika Publishing, 2013.

[6] S. E. Olsen, S. Olsen, M. Tangstad, and T. Lindstad, *Production of Manganese Ferroalloys*. Tapir Academic Press, 2007.

[7] S. E. Olsen and M. Tangstad, “Silicomanganese Production – Process Understanding,” in *Tenth International Ferroalloys Congress*, Cape Town, South Africa, 2004, p. 8.

[8] P. M. Craven, J. W. Waudby, and D. B. Wellbeloved, “Ferrous Metals,” in *Handbook of Extractive Metallurgy*, F. Habashi, Ed. Germany: Wiley-VCH, 1997, pp. 420–427.

[9] T. Årtun and N. Nesse, “koks,” *Store norske leksikon*. 20-Feb-2018.

[10] B. Monsen and M. Syvertsen, “Trekull - egenskaper, produksjon, marked og pris,” SINTEF Materialer og Kjemi, Technical report A8970, 2008.

[11] B. Monsen, M. Tangstad, and H. Midtgaard, “Use of Charcoal in Silicomanganese Production,” in *Tenth International Ferroalloys Congress*, Cape Town, South Africa, 2004, p. 14.

[12] B. Monsen, M. Tangstad, I. Solheim, M. Syvertsen, R. Ishak, and H. Midtgaard, “CHARCOAL FOR MANGANESE ALLOY PRODUCTION,” presented at the INFACON XI: Innovations in Ferro Alloy Industry, 2007, p. 14.

[13] S. Gaal, K. Berg, G. Tranell, S. E. Olsen, and M. Tangstad, “An investigation into aspects of liquid phase reduction of manganese and silica containing slag,” presented at the VII International Conference on Molten Slags Fluxes and Salts, South African Institute of Mining and Metallurgy, 2004, p. 8.

[14] B. Nadir, “Mn alloys production with the use of natural gas.,” Master Thesis, NTNU, Trondheim, 2015.

[15] S. Jayakumari and M. Tangstad, “Carbon Materials for Silicomanganese reduction,” in *The Fourteenth International Ferroalloys Congress*, Kiev, Ukraine, 2015, p. 8.

[16] G. Tranell, S. Gaal, D. Lu, M. Tangstad, and J. Safarian, “REDUCTION KINETICS OF MANGANESE OXIDE FROM HC FeMn SLAGS,” presented at the INFACON XI: Innovations in Ferro Alloy Industry, 2007, p. 11.

[17] J. Safarian, “Kinetics and Mechanisms of Reduction of MnO- Containing Silicate Slags by Selected Forms of Carbonaceous Materials,” Doctorial, NTNU, Trondheim, 2007.

[18] J. Safarian, G. Tranell, L. Kolbeinsen, M. Tangstad, S. Gaal, and J. Kaczorowski, “Reduction Kinetics of MnO from High-Carbon Ferromanganese Slags by Carbonaceous Materials in Ar and CO Atmospheres,” *Metall. Mater. Trans. B*, vol. 39, no. 5, pp. 702–712, Oct. 2008.

[19] J. Safarian and L. Kolbeinsen, “Kinetic of Carbothermic Reduction of MnO from

High-carbon Ferromanganese Slag by Graphite Materials," *ISIJ Int.*, vol. 48, no. 4, pp. 395–404, 2008.
[20] J. Safarian, L. Kolbeinsen, M. Tangstad, and G. Tranell, "Kinetics and Mechanism of the Simultaneous Carbothermic Reduction of FeO and MnO from High-Carbon Ferromanganese Slag," *Metall. Mater. Trans. B*, vol. 40, no. 6, pp. 929–939, Dec. 2009.
[21] H. Sun, M. Y. Lone, S. Ganguly, and O. Ostrovski, "Wettability and Reduction of MnO in Slag by Carbonaceous Materials," *ISIJ Int.*, vol. 50, no. 5, pp. 639–646, 2010.
[22] J. Safarian and M. Tangstad, "SLAG-CARBON REACTIVITY," in *The Twelfth International Ferroalloys Congress*, Helsinki, Finland, 2010, p. 12.
[23] P. P. Kim and M. Tangstad, "Kinetic Investigations of SiMn Slags From Different Mn Sources," *Metall. Mater. Trans. B*, vol. 49, no. 3, pp. 1185–1196, Jun. 2018.
[24] X. Li and M. Tangstad, "The Influence of Sulfur Content on the Carbothermal Reduction of SiMn Slag," *Metall. Mater. Trans. B*, Aug. 2018.
[25] I. M. Haugli, "Reactivity of silicomanganese slag of charcoal compared to coke," NTNU, Trondheim, Specialisation project, Fall 2018.
[26] C. Dwivedi *et al.*, "Chapter 9 - Electrospun Nanofibrous Scaffold as a Potential Carrier of Antimicrobial Therapeutics for Diabetic Wound Healing and Tissue Regeneration," in *Nano- and Microscale Drug Delivery Systems*, A. M. Grumezescu, Ed. Elsevier, 2017, pp. 147–164.
[27] K. Kles, "Contact Angles," *Chemistry LibreTexts*, 06-Mar-2019. [Online]. Available: https://chem.libretexts.org/Bookshelves/Physical_and_Theoretical_Chemistry_Textbook_Maps/Supplemental_Modules_(Physical_and_Theoretical_Chemistry)/Physical_Properties_of_Matter/States_of_Matter/Properties_of_Liquids/Contact_Angles. [Accessed: 05-Jun-2019].
[28] S. Bradbury, B. J. Ford, and D. C. Joy, "Scanning Electron Microscopy," *Nanoscience Instruments*, 2019. [Online]. Available: https://www.nanoscience.com/techniques/scanning-electron-microscopy/. [Accessed: 01-Apr-2019].
[29] "Scanning electron microscope | instrument," *Encyclopedia Britannica*. [Online]. Available: https://www.britannica.com/technology/scanning-electron-microscope. [Accessed: 04-Jun-2019].
[30] "Tech Note: WDS vs EDS," *McSwiggen & Associates*, 2005. [Online]. Available: http://www.mcswiggen.com/TechNotes/WDSvsEDS.htm. [Accessed: 01-Apr-2019].
[31] J. Goodge, "Electron probe micro-analyzer (EPMA)," *Geochemical Instrumentation and Analysis*, 16-May-2017. [Online]. Available: https://serc.carleton.edu/research_education/geochemsheets/techniques/EPMA.html. [Accessed: 07-Dec-2018].
[32] Encyclopedia Britannica, "Electron-probe microanalyzer | instrument," *Encyclopedia Britannica*. [Online]. Available: https://www.britannica.com/technology/electron-probe-microanalyzer. [Accessed: 07-Dec-2018].

Appendix

A.1 Analysis results of slag from SEM

TEST 1	O	Mn	Si	Fe	Al+Br	Ca	Mg+Dy	S + Pb	SUM
	42,68	9,49	20,07	0,00	8,56	14,58	3,31	0,50	99,19
	42,94	9,77	20,25	0,00	8,90	14,47	3,30	0,37	100,00
	42,69	9,33	20,42	0,15	9,19	14,32	3,34	0,57	100,01
Average	42,77	9,53	20,25	0,05	8,88	14,46	3,32	0,48	99,73

TEST 2	O	Mn	Si	Fe	Al+Br	Ca	Mg+Dy	S+Pb	SUM
	42,36	9,45	20,74	0,00	7,35	13,08	5,87	0,79	99,64
	42,38	10,11	20,62	0,16	8,52	13,39	3,19	1,04	99,41
	42,79	9,42	21,35	0,00	9,45	13,30	3,06	0,63	100,00
	41,88	11,50	20,11	0,00	8,54	13,19	3,17	1,02	99,41
	42,04	11,53	20,80	0,00	7,96	13,39	3,56	0,71	99,99
	41,36	10,96	20,58	0,00	7,95	13,56	3,40	0,83	98,64
Average	42,14	10,50	20,70	0,03	8,30	13,32	3,71	0,84	99,52

TEST 3	O	Mn	Si	Fe	Al+Br	Ca	Mg+Dy	S+Pb	SUM
	36,86	22,89	18,34	0,00	6,37	11,58	2,92	0,00	98,96
	39,35	18,09	17,75	0,00	7,76	11,95	3,06	0,89	98,85
	38,21	20,48	18,02	0,00	6,06	12,39	2,94	0,67	98,77
	38,82	20,34	17,52	0,23	7,68	11,18	2,72	0,71	99,20
	39,24	20,12	17,73	0,00	7,11	11,78	2,73	0,65	99,36
Average	38,50	20,38	17,87	0,05	7,00	11,78	2,87	0,58	99,03

TEST 4	O	Mn	Si	Fe	Al+Br	Ca	Mg+Dy	S+Pb	SUM
	46,53	18,85	15,22	0,00	4,56	7,95	2,02	0,00	95,13
	46,22	19,26	15,45	0,00	4,62	7,94	2,00	0,00	95,49
	46,07	19,38	15,30	0,00	4,65	7,94	2,16	0,00	95,50
	46,01	18,65	15,12	0,00	4,73	7,82	2,40	0,00	94,73
	46,09	19,33	15,29	0,00	4,64	7,91	2,22	0,00	95,48
	46,31	19,02	15,20	0,00	4,56	7,90	2,10	0,00	95,09
Average	46,21	19,08	15,26	0,00	4,63	7,91	2,15	0,00	95,24

TEST 5	O	Mn	Si	Fe	Al+Br	Ca	Mg+Dy	S+Pb	SUM
	36,63	28,60	15,01	0,27	5,97	9,30	2,30	0,82	98,90
	38,18	23,79	16,13	0,00	7,55	11,63	1,78	0,00	99,06
	37,11	28,81	15,10	0,07	6,21	9,26	2,10	0,00	98,66
Average	36,87	28,71	15,06	0,17	6,09	9,28	2,20	0,41	98,78

TEST 6	O	Mn	Si	Fe	Al+Br	Ca	Mg+Dy	S+Pb	SUM
	36,98	29,56	15,62	0,00	4,80	8,77	2,30	0,92	98,95
	37,19	29,10	15,36	0,16	5,57	8,63	2,05	0,84	98,90
	36,85	29,78	15,61	0,00	4,73	8,79	2,34	0,85	98,95
	37,17	28,74	15,81	0,00	5,02	9,15	2,17	0,98	99,04
Average	37,05	29,30	15,60	0,04	5,03	8,84	2,22	0,90	98,96

TEST 7	O	Mn	Si	Fe	Al+Br	Ca	Mg+Dy	S+Pb	SUM
	36,01	30,63	15,37	0,00	5,35	9,10	2,05	0,94	99,45
	35,76	32,15	14,94	0,00	4,97	8,42	2,24	0,72	99,20
Average	35,89	31,39	15,16	0,00	5,16	8,76	2,15	0,83	99,33

TEST 8	O	Mn	Si	Fe	Al+Br	Ca	Mg+Dy	S+Pb	SUM
	43,04	24,87	12,97	0,00	4,45	7,20	2,04	0,00	94,57
	43,52	25,99	12,87	0,00	3,84	6,94	1,76	0,00	94,92
	43,34	26,41	13,06	0,00	3,98	7,04	1,87	0,00	95,70
	43,04	26,55	13,11	0,00	4,04	7,14	1,91	0,00	95,79
Average	43,24	25,96	13,00	0,00	4,08	7,08	1,90	0,00	95,25

TEST 9	O	Mn	Si	Fe	Al+Br	Ca	Mg+Dy	S+Pb	SUM
	49,36	11,80	16,57	0,00	5,45	9,39	2,38	0,00	94,95
	49,81	11,35	16,64	0,00	5,67	8,90	2,56	0,00	94,93
	49,78	11,27	16,65	0,00	5,54	9,16	2,65	0,00	95,05
	49,83	11,69	16,02	0,00	5,54	9,19	2,61	0,00	94,88
	50,46	11,58	15,98	0,00	5,42	8,87	2,54	0,00	94,85
	50,13	11,99	16,03	0,00	5,54	8,91	2,47	0,00	95,07
Average	49,90	11,61	16,32	0,00	5,53	9,07	2,54	0,00	94,96

TEST 10	O	Mn	Si	Fe	Al+Br	Ca	Mg+Dy	S+Pb	SUM
	38,42	22,88	18,00	0,00	5,30	10,23	2,63	1,17	98,63
	38,26	23,10	17,70	0,00	6,13	10,04	2,35	1,19	98,77
	38,80	22,43	17,93	0,00	6,14	10,06	2,43	0,98	98,77
	37,66	22,34	18,16	0,00	5,54	11,05	2,69	1,28	98,72
	38,23	22,29	18,40	0,00	6,22	10,56	2,57	0,55	98,82
	38,12	22,30	18,21	0,00	6,14	10,51	2,48	1,10	98,86
Average	38,25	22,56	18,07	0,00	5,91	10,41	2,53	1,05	98,76

TEST 11	O	Mn	Si	Fe	Al+Br	Ca	Mg+Dy	S+Pb	SUM
	44,04	6,06	20,88	0,00	9,34	15,93	3,28	0,00	99,53
	43,57	6,17	20,87	0,00	9,58	15,81	3,38	0,00	99,38
	43,08	6,90	20,67	0,00	9,90	15,54	3,41	0,00	99,50
	44,26	5,94	21,14	0,00	9,82	15,47	3,36	0,00	99,99
	44,55	5,75	20,86	0,00	9,92	15,43	3,49	0,00	100,00
Average	43,90	6,16	20,88	0,00	9,71	15,64	3,38	0,00	99,68

TEST 12	O	Mn	Si	Fe	Al+Br	Ca	Mg+Dy	S+Pb	SUM
	41,52	29,89	13,21	0,00	3,23	5,13	1,11	0,00	94,09
	41,12	30,46	13,12	0,00	3,15	5,07	1,20	0,00	94,12
	40,56	30,28	13,12	0,00	3,14	5,26	1,41	0,00	93,77
	41,72	30,12	13,07	0,00	3,02	4,96	1,27	0,00	94,16
	41,28	30,91	13,02	0,00	2,94	5,04	1,20	0,00	94,39
	40,87	30,52	12,95	0,00	3,15	5,18	1,45	0,00	94,12
	41,08	30,73	13,03	0,00	3,14	5,34	1,18	0,00	94,50
Average	41,16	30,42	13,07	0,00	3,11	5,14	1,26	0,00	94,16

TEST 13	O	Mn	Si	Fe	Al+Br	Ca	Mg+Dy	S+Pb	SUM
	33,17	45,53	13,76	0,39	0,00	3,70	2,53	0,00	99,08
	32,83	45,59	13,67	0,69	0,00	3,51	2,76	0,00	99,05
	37,58	25,14	14,45	0,00	9,02	10,99	0,43	0,00	97,61
	37,57	24,10	14,04	0,00	10,17	10,89	0,43	0,00	97,20
	34,84	36,58	13,82	0,00	4,19	6,98	1,42	0,00	97,83
	38,32	22,34	14,72	0,00	10,22	11,26	0,43	0,00	97,29
	32,94	45,80	13,58	0,00	0,25	3,51	2,89	0,00	98,97
Average	34,84	36,58	13,82	0,00	4,19	6,98	1,42	0,00	97,83

* Average of area measurement, not point measurements

TEST 14	O	Mn	Si	Fe	Al+Br	Ca	Mg+Dy	S+Pb	SUM
	48,08	10,70	18,10	0,00	5,64	9,43	2,38	0,00	94,33
	48,19	10,04	18,41	0,00	5,83	9,44	2,62	0,00	94,53
	48,60	10,29	18,62	0,00	5,84	9,46	2,62	0,34	95,77
	48,02	9,49	18,49	0,00	5,91	9,26	2,81	0,00	93,98
	48,81	9,17	18,72	0,00	5,86	9,38	2,52	0,00	94,46
	48,89	8,89	18,78	0,00	5,94	9,59	2,59	0,00	94,68
Average	48,43	9,76	18,52	0,00	5,84	9,43	2,59	0,06	94,63

TEST 15	O	Mn	Si	Fe	Al+Br	Ca	Mg+Dy	S+Pb	SUM
	47,55	11,13	16,82	0,00	5,90	9,78	2,89	0,75	94,82
	48,34	11,57	17,13	0,00	5,87	10,07	2,65	0,00	95,63
	48,12	12,07	17,20	0,00	5,77	9,90	2,61	0,00	95,67
	49,39	11,43	16,62	0,00	5,55	9,67	2,55	0,00	95,21
	49,11	11,39	16,99	0,00	5,81	9,71	2,58	0,00	95,59
	49,52	11,52	16,89	0,00	5,74	9,64	2,45	0,00	95,76
Average	48,67	11,52	16,94	0,00	5,77	9,80	2,62	0,13	95,45

TEST 16	O	Mn	Si	Fe	Al+Br	Ca	Mg+Dy	S+Pb	SUM
	45,43	17,10	16,31	0,00	4,88	7,89	2,08		93,69
	45,32	17,42	16,39	0,00	4,94	8,04	2,04		94,15
	45,40	16,62	16,29	0,00	5,02	8,33	2,24		93,90
	46,01	15,78	16,91	0,00	4,94	8,19	2,10		93,93
	46,64	15,07	17,63	0,00	5,12	8,73	2,14	0,29	95,62
Average	45,76	16,40	16,71	0,00	4,98	8,24	2,12	0,29	94,26

TEST 17	O	Mn	Si	Fe	Al+Br	Ca	Mg+Dy	S+Pb	SUM
	39,42	29,52	16,10	0,00	4,53	6,89	1,52	0,00	97,98
	37,41	37,80	15,61	0,00	1,40	4,07	2,47	1,00	99,76
	40,11	26,52	16,48	0,00	5,32	7,82	1,54	1,28	99,07
Average	38,98	31,28	16,06	0,00	3,75	6,26	1,84	0,76	98,94

TEST 18	O	Mn	Si	Fe	Al+Br	Ca	Mg+Dy	S+Pb	SUM
	32,92	35,28	15,28	0,00	4,06	7,15	1,63	0,00	96,32
	32,87	34,65	14,78	0,00	3,94	6,91	1,14	0,00	94,29
	33,20	34,61	15,33	0,00	4,24	7,43	1,61	0,00	96,42
	33,44	34,27	15,51	0,00	4,15	7,42	1,50	0,00	96,29
Average	33,11	34,70	15,23	0,00	4,10	7,23	1,47	0,00	95,83

TEST 19	O	Mn	Si	Fe	Al	Ca	Mg	S	SUM
	37,71	28,33	17,70	0,00	4,25	7,09	1,97	0,00	97,05
	37,75	28,12	17,76	0,00	4,20	7,18	2,06	0,00	97,07
	37,77	27,24	17,81	0,00	4,31	7,33	2,08	0,00	96,54
	38,37	27,53	17,73	0,00	3,94	7,28	1,63	0,00	96,48
	37,81	27,26	17,94	0,00	4,23	7,31	2,11	0,00	96,66
Average	37,88	27,70	17,79	0,00	4,19	7,24	1,97	0,00	96,76

TEST 20	O	Mn	Si	Fe	Al	Ca	Mg	S	SUM
	37,94	25,09	18,37	0,00	4,78	8,77	2,14	0,00	97,09
	38,31	24,84	18,71	0,00	4,90	8,87	2,19	0,00	97,82
	37,96	25,30	18,64	0,00	4,72	9,03	1,94	0,00	97,59
	37,62	25,36	18,65	0,00	4,99	9,11	2,35	0,00	98,08
	38,20	24,41	18,84	0,00	4,74	8,75	2,09	0,00	97,03
	38,55	24,16	19,48	0,00	4,66	8,93	1,78	0,00	97,56
	38,15	25,01	18,71	0,00	4,79	8,78	2,09	0,00	97,53
Average	38,10	24,88	18,77	0,00	4,80	8,89	2,08	0,00	97,53

TEST 21*	O	Mn	Si	Fe	Al+Br	Ca	Mg+Dy	S+Pb	SUM
	35,03	35,12	15,00	0,00	4,13	7,05	1,80	0,96	99,09
	34,81	36,28	14,79	0,00	3,94	6,71	1,77	0,77	99,07
Average	34,92	35,70	14,90	0,00	4,04	6,88	1,79	0,87	99,08

*Only area measurements are included for test 21 and test 22

TEST 22*	O	Mn	Si	Fe	Al+Br	Ca	Mg+Dy	S+Pb	SUM
	35,12	35,25	15,08	0,00	3,97	6,73	1,62	0,98	98,75
	35,72	34,19	15,33	0,00	4,10	6,87	1,54	0,89	98,64
Average	35,42	34,72	15,21	0,00	4,04	6,80	1,58	0,94	98,70

A.2 Average analysis results of metal from SEM

The average analysis of metal for all samples are listed in the table below. In addition to the expected elements; manganese, iron, silicon and carbon, the measured amount of the most common disturbances; cobalt, fluorine and oxygen are included.

	Mn	Fe	Si	C	Co	F	O	Sum
Test 1	64,85	12,83	16,63	4,36	0,23	0,00	1,10	100,00
Test 2	76,68	1,34	16,37	2,73	0,00	0,00	2,88	100,00
Test 3	60,52	23,72	3,62	10,17	0,54	0,00	0,00	98,57
Test 4	75,44	0,00	7,15	11,23	0,00	0,00	7,35	101,17
Test 5	64,47	21,58	0,11	9,20	0,42	0,00	2,33	98,11
Test 6	32,18	51,05	1,27	9,82	0,27	4,60	0,00	99,19
Test 7	48,51	35,49	0,49	9,49	0,08	5,29	0,00	99,35
Test 8	34,44	49,24	0,00	16,32	0,00	0,00	0,00	100,00
Test 9	72,91	0,00	9,51	10,71	0,00	0,00	6,87	100,00
Test 10	51,15	32,83	4,46	9,35	0,52	1,09	0,00	99,40
Test 11	66,66	10,68	18,87	3,28	0,12	0,00	0,00	99,61
Test 12	26,75	53,41	1,38	16,20	0,00	1,76	0,00	99,50
Test 13	1,46	85,83	0,00	9,20	0,52	0,00	0,00	97,01
Test 14	65,54	0,00	15,32	10,39	0,00	0,00	8,75	100,00
Test 15	71,18	0,00	10,48	12,16	0,00	0,00	6,18	100,00
Test 16	62,88	7,83	9,18	12,11	0,00	0,00	7,55	99,55
Test 17	32,10	50,09	0,15	11,91	0,13	4,50	8,63	107,51
Test 18	46,22	37,39	0,25	13,29	0,00	0,00	2,49	99,64
Test 19	41,35	33,83	3,40	16,05	0,00	7,97	4,75	107,35
Test 20	75,99	6,62	8,09	8,70	0,00	4,07	0,00	103,47
Test 21	35,12	50,32	0,37	8,57	0,45	0,00	4,04	98,87
Test 22	27,45	56,55	0,47	9,91	0,42	0,00	5,20	100,00

A.3 Analysis result of slag from EPMA

The results of five measurements and calculated average is listed in the table for each test.

Test	MnO	SiO2	FeO	Al2O3	CaO	MgO	SO3	Total	Comment
1	12,53	46,64	0,03	13,93	20,93	5,36	1,08	100,50	
1	12,62	46,58	0,00	13,95	21,16	5,55	0,98	100,84	
1	12,87	46,64	0,01	13,95	20,83	5,49	1,12	100,91	
1	12,61	46,49	0,00	14,19	20,89	5,65	1,04	100,87	
1	12,90	46,67	0,04	14,06	20,72	5,55	1,06	100,99	
1	*12,71*	*46,60*	*0,02*	*14,02*	*20,90*	*5,52*	*1,06*	*100,82*	*Average*
2	14,36	46,95	0,00	13,37	19,15	5,21	1,69	100,73	
2	14,57	46,69	0,03	13,08	18,93	5,30	1,83	100,43	
2	14,64	46,74	0,02	13,08	18,86	5,31	1,92	100,57	
2	14,78	46,15	0,02	13,16	18,74	5,33	1,78	99,97	
2	14,64	46,69	0,08	13,08	18,84	5,36	1,70	100,38	
2	*14,60*	*46,65*	*0,03*	*13,15*	*18,90*	*5,30*	*1,78*	*100,41*	*Average*
3	26,85	41,57	0,12	10,89	16,20	4,44	1,44	101,50	
3	26,87	41,39	0,03	10,96	16,44	4,53	1,30	101,51	
3	26,61	41,66	0,08	10,93	16,28	4,45	1,31	101,32	
3	27,06	41,60	0,08	10,72	16,59	4,51	1,39	101,96	
3	26,64	41,45	0,05	10,70	16,28	4,46	1,35	100,94	
3	*26,81*	*41,53*	*0,07*	*10,84*	*16,36*	*4,48*	*1,36*	*101,44*	*Average*
4	28,87	41,77	0,03	10,17	15,03	4,19	1,84	101,90	
4	28,76	41,56	0,10	10,27	14,82	4,13	1,86	101,49	
4	28,09	41,93	0,05	10,13	15,20	4,17	1,77	101,32	
4	28,41	41,89	0,09	10,12	14,87	4,23	2,13	101,74	
4	28,53	41,71	0,12	10,04	15,01	4,12	1,79	101,32	
4	*28,53*	*41,77*	*0,08*	*10,14*	*14,98*	*4,17*	*1,88*	*101,55*	*Average*
5	39,19	34,49	0,16	9,03	13,01	3,81	1,15	100,83	Glassy
5	39,02	34,42	0,12	9,04	13,26	3,73	1,09	100,67	Glassy
5	38,98	34,47	0,06	9,06	13,19	3,71	1,15	100,61	Glassy
5	39,12	34,61	0,12	8,98	13,46	3,79	1,07	101,15	Glassy
5	39,51	34,41	0,12	8,91	12,95	3,85	1,09	100,83	Glassy
5	*39,16*	*34,48*	*0,11*	*9,00*	*13,17*	*3,78*	*1,11*	*100,82*	*Average*

Test	MnO	SiO2	FeO	Al2O3	CaO	MgO	SO3	Total	Comment
5	37,86	33,88	0,08	9,57	13,31	3,51	0,97	99,17	Two-phase
5	37,52	33,82	0,09	9,31	13,13	3,53	1,12	98,51	Two-phase
5	36,90	34,37	0,10	9,59	13,33	3,50	1,01	98,80	Two-phase
5	37,40	33,90	0,10	9,60	13,18	3,49	1,11	98,77	Two-phase
5	36,46	34,36	0,10	9,87	13,49	3,36	1,19	98,84	Two-phase
5	*37,23*	*34,07*	*0,09*	*9,59*	*13,29*	*3,48*	*1,08*	*98,82*	*Average*
6	38,64	35,43	0,17	8,41	12,86	3,58	1,47	100,56	Glassy
6	39,25	35,64	0,17	8,49	12,86	3,57	1,45	101,42	Glassy
6	39,54	34,86	0,14	8,61	12,95	3,54	1,50	101,14	Glassy
6	39,64	35,65	0,20	8,59	12,40	3,55	1,59	101,62	Glassy
6	39,55	35,12	0,13	8,48	12,37	3,50	1,47	100,61	Glassy
6	*39,32*	*35,34*	*0,16*	*8,52*	*12,69*	*3,55*	*1,49*	*101,07*	*Average*
6	37,47	34,55	0,15	9,08	12,35	3,26	1,61	98,48	Two-phase
6	39,09	34,97	0,11	8,95	12,79	3,34	1,47	100,73	Two-phase
6	38,58	35,60	0,13	9,09	12,87	3,30	1,49	101,06	Two-phase
6	38,86	34,96	0,21	8,64	12,74	3,46	1,57	100,43	Two-phase
6	38,62	35,10	0,12	8,84	12,86	3,39	1,66	100,59	Two-phase
6	*38,52*	*35,04*	*0,14*	*8,92*	*12,72*	*3,35*	*1,56*	*100,26*	*Average*
7	40,70	34,62	0,14	8,46	12,22	3,51	1,30	100,95	Glassy
7	39,36	34,91	0,17	8,44	12,79	3,50	1,45	100,63	Glassy
7	40,33	34,75	0,15	8,40	12,67	3,44	1,41	101,15	Glassy
7	40,92	34,15	0,21	8,50	12,37	3,35	1,32	100,81	Glassy
7	39,94	34,63	0,08	8,44	12,58	3,47	1,49	100,61	Glassy
7	*40,25*	*34,61*	*0,15*	*8,45*	*12,53*	*3,46*	*1,39*	*100,83*	*Average*
7	39,14	35,16	0,09	8,70	12,84	3,20	1,58	100,71	Two-phase
7	39,95	34,62	0,13	8,83	12,54	3,26	1,49	100,82	Two-phase
7	39,94	33,83	0,18	9,10	12,56	3,20	1,42	100,23	Two-phase
7	39,15	34,19	0,13	8,87	12,55	3,35	1,48	99,71	Two-phase
7	39,75	34,71	0,18	9,14	12,48	3,22	1,49	100,96	Two-phase
7	*39,59*	*34,50*	*0,14*	*8,93*	*12,60*	*3,24*	*1,49*	*100,49*	*Average*
8	38,44	35,45	0,09	8,93	13,28	3,58	1,16	100,91	Glassy
8	38,47	35,09	0,11	8,65	13,22	3,56	1,03	100,13	Glassy
8	38,05	35,59	0,06	8,68	13,27	3,69	1,17	100,51	Glassy

Test	MnO	SiO2	FeO	Al2O3	CaO	MgO	SO3	Total	Comment
8	38,28	35,90	0,10	8,68	13,10	3,63	1,07	100,75	Glassy
8	38,68	34,98	0,13	8,65	13,38	3,57	1,09	100,48	Glassy
8	38,38	35,40	0,10	8,72	13,25	3,60	1,10	100,56	Average
8	37,88	35,56	0,14	9,29	13,47	3,41	1,22	100,98	Two-phase
8	38,35	34,90	0,10	9,03	13,22	3,49	1,14	100,23	Two-phase
8	37,78	35,13	0,08	9,08	13,23	3,42	1,28	100,01	Two-phase
8	37,42	35,28	0,08	9,46	13,40	3,34	1,20	100,17	Two-phase
8	37,44	35,49	0,04	9,08	13,67	3,37	1,18	100,26	Two-phase
8	*37,77*	*35,27*	*0,09*	*9,19*	*13,40*	*3,41*	*1,20*	*100,33*	*Average*
9	22,28	43,49	0,02	11,94	17,80	4,91	1,41	101,85	
9	22,11	43,51	0,05	11,85	18,09	4,74	1,50	101,85	
9	22,02	43,58	0,05	11,77	17,96	4,81	1,26	101,47	
9	21,98	44,34	0,07	11,77	17,90	4,75	1,23	102,03	
9	21,49	44,31	0,04	11,77	18,15	4,83	1,36	101,96	
9	*21,98*	*43,85*	*0,05*	*11,82*	*17,98*	*4,81*	*1,35*	*101,83*	*Average*
10	30,78	41,12	0,09	9,60	14,23	3,94	1,70	101,46	
10	30,96	41,19	0,09	9,49	14,02	3,89	1,70	101,35	
10	31,39	40,91	0,12	9,48	14,18	4,04	1,77	101,89	
10	31,33	41,50	0,09	9,40	14,01	3,88	1,63	101,84	
10	30,92	41,13	0,10	9,51	14,08	3,89	1,56	101,18	
10	*31,08*	*41,17*	*0,10*	*9,49*	*14,10*	*3,93*	*1,67*	*101,54*	*Average*
11	7,77	48,40	0,05	15,57	22,91	5,60	0,46	100,76	
11	8,12	47,53	0,02	15,66	22,65	5,71	0,52	100,21	
11	8,30	47,20	0,03	15,43	22,82	5,59	0,64	100,01	
11	8,36	46,99	0,02	15,69	22,61	5,66	0,71	100,04	
11	8,39	47,90	0,00	15,40	22,67	5,61	0,65	100,61	
11	*8,19*	*47,60*	*0,02*	*15,55*	*22,73*	*5,63*	*0,60*	*100,33*	*Average*
12	45,02	35,81	0,17	6,61	9,33	2,51	1,66	101,11	Glassy
12	45,15	36,12	0,19	6,69	9,28	2,56	1,62	101,61	Glassy
12	45,60	36,06	0,20	6,59	9,39	2,61	1,45	101,90	Glassy
12	44,86	35,95	0,19	6,64	9,39	2,53	1,83	101,38	Glassy
12	45,22	36,08	0,22	6,54	9,46	2,51	1,55	101,59	Glassy
12	*45,17*	*36,01*	*0,19*	*6,61*	*9,37*	*2,54*	*1,62*	*101,52*	*Average*

Test	MnO	SiO2	FeO	Al2O3	CaO	MgO	SO3	Total	Comment
12	44,21	36,36	0,18	7,03	9,62	2,52	1,58	101,50	Two-phase
12	44,12	36,48	0,17	7,06	9,69	2,39	1,53	101,43	Two-phase
12	44,95	36,33	0,15	6,59	9,34	2,63	1,62	101,60	Two-phase
12	44,33	36,65	0,15	6,95	9,73	2,50	1,67	101,97	Two-phase
12	44,07	36,58	0,15	7,20	9,57	2,34	1,77	101,68	Two-phase
12	*44,33*	*36,48*	*0,16*	*6,97*	*9,59*	*2,47*	*1,63*	*101,64*	*Average*
13	58,06	32,11	0,56	0,36	4,95	4,60	0,07	100,71	Light phase
13	58,31	32,00	0,51	0,24	5,22	4,41	0,05	100,75	Light phase
13	58,17	31,88	0,52	0,32	5,16	4,42	0,01	100,48	Light phase
13	57,87	31,82	0,53	0,32	5,26	4,20	0,07	100,06	Light phase
13	58,46	31,59	0,56	0,42	5,09	4,64	0,03	100,79	Light phase
13	*58,17*	*31,88*	*0,54*	*0,33*	*5,13*	*4,45*	*0,05*	*100,56*	*Average*
13	34,04	33,03	0,50	15,91	15,38	0,41	3,95	103,22	Dark phase
13	35,62	32,45	0,59	15,29	14,86	0,47	3,33	102,60	Dark phase
13	35,00	31,99	0,52	16,27	15,02	0,41	3,60	102,81	Dark phase
13	34,10	33,49	0,51	15,63	15,22	0,45	3,70	103,10	Dark phase
13	34,68	33,38	0,53	15,55	15,35	0,38	3,46	103,34	Dark phase
13	*34,69*	*32,87*	*0,53*	*15,73*	*15,17*	*0,42*	*3,60*	*103,01*	*Average*
14	15,52	50,78	0,04	12,52	17,06	4,81	1,32	102,05	
14	15,23	51,09	0,00	12,62	16,99	4,80	1,61	102,34	
14	15,58	50,48	0,03	12,46	16,93	4,82	1,65	101,94	
14	15,00	50,83	0,04	12,80	17,22	4,74	1,44	102,07	
14	14,80	50,55	0,02	12,94	17,19	4,87	1,07	101,44	
14	*15,22*	*50,75*	*0,03*	*12,67*	*17,08*	*4,81*	*1,42*	*101,97*	*Average*
15	17,57	46,14	0,00	12,44	18,40	4,91	1,77	101,22	
15	18,20	46,22	0,04	12,44	18,45	4,87	2,02	102,24	
15	18,17	46,06	0,07	12,38	18,23	4,88	1,92	101,70	
15	17,41	45,83	0,02	12,33	18,09	4,81	1,67	100,16	
15	16,97	47,17	0,06	12,60	18,45	4,95	1,86	102,05	
15	*17,66*	*46,28*	*0,04*	*12,44*	*18,32*	*4,88*	*1,85*	*101,47*	*Average*
16	25,46	44,10	0,08	10,30	15,08	4,07	1,81	100,90	
16	25,27	44,64	0,07	10,44	14,87	4,07	1,80	101,14	
16	25,07	44,29	0,10	10,51	15,07	4,15	1,83	101,02	

Test	MnO	SiO2	FeO	Al2O3	CaO	MgO	SO3	Total	Comment
16	25,08	45,07	0,08	10,58	15,10	4,19	1,89	101,98	
16	25,02	45,28	0,07	10,45	15,03	4,11	1,63	101,60	
16	*25,18*	*44,68*	*0,08*	*10,45*	*15,03*	*4,12*	*1,79*	*101,33*	*Average*
17	45,98	35,06	0,19	7,20	9,40	2,35	1,54	101,71	
17	44,92	35,52	0,18	7,57	9,64	2,26	1,78	101,88	
17	45,15	35,39	0,19	7,53	9,44	2,27	1,71	101,68	
17	45,35	35,27	0,20	7,46	9,28	2,36	1,46	101,38	
17	45,46	35,43	0,11	7,21	9,34	2,33	1,65	101,53	
17	*45,37*	*35,33*	*0,17*	*7,39*	*9,42*	*2,31*	*1,63*	*101,64*	*Average*
18	45,466	33,992	0,134	7,197	9,748	2,592	1,334	100,463	
18	44,91	35,157	0,145	7,332	9,85	2,523	1,363	101,28	
18	45,675	34,961	0,136	7,002	9,775	2,617	1,224	101,39	
18	44,945	34,99	0,131	7,457	9,861	2,505	1,407	101,296	
18	44,958	34,948	0,208	7,208	9,826	2,498	1,242	100,888	
18	*45,1908*	*34,8096*	*0,1508*	*7,2392*	*9,812*	*2,547*	*1,314*	*101,0634*	*Average*
19	37,392	40,814	0,145	7,329	10,606	2,964	1,919	101,169	
19	37,339	40,323	0,076	7,475	10,451	2,897	1,832	100,393	
19	37,473	40,704	0,142	7,45	10,474	3,014	1,764	101,021	
19	37,253	40,188	0,131	7,46	10,425	3,035	1,886	100,378	
19	36,911	40,646	0,142	7,496	10,517	3,013	1,757	100,482	
19	*37,2736*	*40,535*	*0,1272*	*7,442*	*10,4946*	*2,9846*	*1,8316*	*100,6886*	*Average*
20	32,37	42,127	0,058	8,768	12,723	3,526	1,676	101,248	
20	32,107	42,222	0,116	8,718	13,236	3,469	1,723	101,591	
20	31,839	42,752	0,045	8,722	12,772	3,47	1,613	101,213	
20	32,048	42,262	0,063	8,64	12,614	3,442	1,614	100,683	
20	31,946	42,183	0,104	8,777	12,966	3,582	1,628	101,186	
20	*32,062*	*42,3092*	*0,0772*	*8,725*	*12,8622*	*3,4978*	*1,6508*	*101,1842*	*Average*
21	44,045	34,53	0,188	8,306	10,421	2,354	1,463	101,307	
21	45,318	34,678	0,181	8,016	9,975	2,46	1,258	101,886	
21	44,261	34,9	0,158	8,658	10,611	2,32	1,319	102,227	
21	45,32	34,212	0,161	7,658	9,725	2,491	1,317	100,884	
21	45,617	33,823	0,179	7,369	9,811	2,492	1,205	100,496	
21	*44,9122*	*34,4286*	*0,1734*	*8,0014*	*10,1086*	*2,4234*	*1,3124*	*101,36*	*Average*

Test	MnO	SiO2	FeO	Al2O3	CaO	MgO	SO3	Total	Comment
22	45,579	34,72	0,209	7,092	9,375	2,291	1,675	100,941	
22	45,704	34,381	0,176	7,388	9,501	2,249	1,722	101,121	
22	47,103	34,34	0,199	6,992	9,219	2,345	1,472	101,67	
22	46,283	34,954	0,21	6,667	9,124	2,419	1,522	101,179	
22	47,306	34,435	0,258	6,727	9,03	2,444	1,59	101,79	
22	*46,395*	*34,566*	*0,2104*	*6,9732*	*9,2498*	*2,3496*	*1,5962*	*101,3402*	*Average*

A.4 Analysis results of metal from EPMA

The table lists the metal results from the EPMA analysis. Three measurements were taken for each sample, for the samples that thad more than one metal droplet, two of them were analysed with three measurements. Which metal droplets that was analysed are indicated in the comments.

Test	Si	Mn	Fe	Total	Comment
1	12,70	45,01	42,73	100,44	Large metal
1	14,63	45,17	40,64	100,44	
1	13,10	42,91	44,49	100,50	
1	16,03	66,86	17,07	99,96	Small metal
1	15,27	67,28	17,37	99,92	
1	15,68	67,32	16,91	99,91	
2	15,57	79,51	4,65	99,73	Only one metal
2	15,40	79,92	4,99	100,32	
2	15,49	79,97	4,70	100,16	
3	4,13	46,42	46,66	97,21	Only one metal
3	4,18	45,65	47,78	97,61	
3	3,91	46,81	46,62	97,34	
4	7,52	82,84	5,94	96,29	Large metal
4	7,74	82,65	6,09	96,48	
4	7,79	82,13	6,19	96,10	
4	7,90	81,76	7,17	96,83	Small metal
4	7,84	82,30	7,36	97,49	
4	7,96	81,45	7,17	96,57	
5	0,00	39,10	56,40	95,49	Large metal
5	0,00	38,58	57,31	95,89	
5	0,00	39,05	56,00	95,05	
5	0,22	54,46	41,95	96,64	Small metal
5	0,09	54,81	38,23	93,13	
5	0,07	55,79	39,93	95,79	
6	0,16	24,14	71,44	95,74	Only one metal
6	0,25	23,75	72,43	96,42	
6	0,33	23,10	72,13	95,56	

Test	Si	Mn	Fe	Total	Comment
7	0,25	31,71	63,90	95,85	Large metal
7	0,20	31,87	64,66	96,74	
7	0,21	32,20	63,50	95,91	
7	0,20	31,70	63,34	95,24	Small metal
7	0,20	35,24	60,07	95,51	
7	0,26	27,45	67,17	94,88	
8	0,21	36,06	58,95	95,22	Only one metal
8	0,40	35,08	60,64	96,12	
8	0,38	35,34	61,11	96,83	
9	10,76	85,04	2,93	98,73	Large metal
9	10,70	85,54	2,83	99,07	
9	10,87	85,33	2,87	99,07	
9	10,88	85,73	2,42	99,03	Medium metal
9	11,06	85,83	2,49	99,38	
9	10,96	85,46	2,57	98,99	
10	3,46	33,84	59,86	97,17	Only one metal
10	3,06	34,63	59,62	97,31	
10	3,04	34,37	59,47	96,89	
11	19,13	80,08	2,29	101,50	Metal drop in slag
11	18,83	80,13	2,17	101,14	
11	18,96	79,65	2,24	100,84	
11	18,96	59,82	23,87	102,65	Large metal left
11	18,85	59,23	23,85	101,92	
11	18,67	59,83	23,44	101,93	
12	0,25	23,03	74,04	97,32	Large metal
12	0,23	23,56	72,88	96,67	
12	0,21	23,59	72,98	96,77	
12	0,29	22,68	74,04	97,01	Small metal
12	0,23	22,32	73,85	96,40	
12	0,27	22,63	73,37	96,27	
13	0,21	2,01	93,65	95,87	Only one metal
13	0,10	1,62	95,22	96,94	
13	0,12	1,65	92,88	94,65	

Test	Si	Mn	Fe	Total	Comment
14	19,41	78,90	2,38	100,68	Largest metal
14	17,26	80,83	2,37	100,46	
14	18,45	79,73	2,31	100,50	
14	18,30	78,96	2,28	99,54	Second largest
14	19,48	77,33	2,14	98,95	
14	18,56	78,31	2,30	99,17	
15	16,56	83,68	0,93	101,18	Large metal, left
15	15,28	84,42	0,89	100,60	
15	16,45	84,00	0,92	101,37	
15	15,37	82,87	3,21	101,45	Second largest metal, left
15	15,34	82,71	3,28	101,32	
15	15,30	82,72	3,18	101,20	
16	11,02	65,37	23,46	99,85	Large metal, left
16	10,93	65,67	23,46	100,06	
16	10,99	65,26	23,32	99,57	
16	10,89	72,65	15,73	99,27	Large metal, right
16	10,86	72,12	16,04	99,02	
16	10,79	73,27	15,74	99,81	
17	0,13	21,12	74,23	95,48	Metal, left
17	0,15	22,45	71,75	94,35	
17	0,15	21,64	74,21	96,00	
17	0,15	21,12	74,40	95,66	Metal, right
17	0,17	20,23	74,33	94,73	
17	0,18	21,14	73,86	95,19	
18	0,40	28,57	66,71	95,67	Only one metal
18	0,34	28,00	67,07	95,41	
18	0,33	28,74	66,31	95,38	
19	2,66	27,79	64,11	94,57	Large metal
19	2,29	29,12	62,74	94,15	
19	0,18	29,44	63,36	92,98	
19	2,77	35,98	58,70	97,45	Small metal
19	2,99	35,43	57,57	95,98	
19	3,63	33,92	58,54	96,09	

Test	Si	Mn	Fe	Total	Comment
20	6,63	58,96	31,33	96,92	Largest metal
20	6,66	58,62	30,89	96,17	
20	6,67	58,67	31,14	96,48	
20	8,23	82,95	4,83	96,00	Second largest metal, left
20	8,17	82,68	4,88	95,74	
20	8,22	82,58	4,80	95,60	
21	0,16	23,65	72,87	96,68	Only one metal
21	0,13	23,96	72,77	96,86	
21	0,15	24,05	72,06	96,26	
22	0,12	16,95	79,22	96,30	Large metal
22	0,16	17,32	80,12	97,60	
22	0,17	16,78	80,20	97,14	
22	0,19	20,03	75,92	96,13	Small metal
22	0,15	20,19	75,37	95,71	
22	0,22	19,86	75,57	95,65	

Ine Mariell Fagerbakk Haugli

Reactivity of silicomanganese slag towards carbon materials

NTNU
Norwegian University of
Science and Technology